Preparation, Characterization and potential Application of new low-molecular-weight Organogels

Dissertation

Zur Erlangung des Doktorgrades

Dr. rer. nat.

an der Fakultät für Chemie und Pharmazie

der Universität Regensburg

vorgelegt von

Eva-Maria Schön

aus Tirschenreuth

Regensburg 2013

Die Arbeit wurde angeleitet von: Prof. Dr. David Díaz Díaz

Promotionsgesuch eingereicht am: 13.12.2013

Promotionskolloquium am: 31.01.2014

Prüfungsausschuss: Vorsitz: Prof. Dr. Bernhard Dick
1. Gutachter: Prof. Dr. David Díaz Díaz
2. Gutachter: Prof. Dr. Burkhard König
3. Prüfer: Prof. Dr. Henri Brunner

Der experimentelle Teil der vorliegenden Arbeit wurde in der Zeit von Oktober 2010 bis Mai 2012 und von September 2012 bis September 2013 unter der Leitung von Herrn Prof. Dr. David Díaz Díaz am Institut für Organische Chemie der Universität Regensburg angefertigt.

Herrn Prof. Dr. David Díaz Díaz möchte ich herzlich für die Überlassung des äußerst interessanten Themas, die anregenden Diskussionen und seine stete Unterstützung während der Durchführung dieser Arbeit danken.

LIFE BEGINS AT THE END OF YOUR COMFORT ZONE

Neale Donald Walsch

Meinem Vater
Johann Schön
*13.01.1952 - †03.04.2012

Content

Abbreviations

1D	1-dimensional
2D	2-dimensional
3D	3-dimensional
ACN	acetonitrile
ACT	acetone
AFM	atomic force microscopy
[BMIM][PF_6]	1-butyl-3-methylimidazolium hexafluorophosphate
BN	benzonitrile
CHN	cyclohexanone
CuAAC	copper(I)-catalyzed azide -alkyne cycloaddition
d	day
DABCO	1,4-diazabicyclo[2.2.2]octane
DBC	*N,N′*-dibenzoyl-*L*-cystine
DEE	diethyl ether
DFS	differential frequency sweep
DMA	dimethylacetamide
DME	1,2-dimethoxyethane
DMF	*N,N′*-dimethylformamide
DMSO	dimethyl sulfoxide
DOX	1,4-dioxane
DSS	differential strain sweep
DSC	differential scanning calorimetry
DTS	differential time sweep
ee	enantiomeric excess
ETAC	ethyl acetate
FT-IR	fourier transform infrared spectroscopy
G	gel
G*	complex modulus
G′	storage modulus
G″	loss modulus
GC	gas chromatography
gv	MGS volume
h	hour
HPLC	high performance liquid chromatography
Im	vinylimidazole
LMWG	low molecular weight gelator
IPN	interpenetrating polymer networks
MBN	3-methylbutan-2-one
MEE	2-methoxyethyl ether
min	minute
MBA	*N,N′*-methylenebisacrylamide
MGC	minimum gelation concentration
MGS	multicomponent liquid organogelator system
MOF	metal-organic framework
NIPA	*N*-isopropylacrylamide
NM	nitromethane
NMP	*N*-methyl-2-pyrrolidone
NMR	nuclear magnetic resonance
PLO	pluronic lecithin organogel
PG	partial gel
RT	room temperature
s	second
S	solution
SAFIN	self-assembled fibrillar networks
SEM	scanning electron microscopy
SISN	semi-interpenetrating supramolecular network
TEM	transmission electron microscopy
T_d	Gel destruction temperature
T_{gel}	*sol-gel* transition temperature
T_{mix}	cooling bath temperature
THF	tetrahydrofuran
TOF	turnover frequency
wt.%	percent by weight

A Introduction

1. Definition and classification of gels

When a material seems to be between a liquid and solid state, because it is not flowing away like liquid, but is more flexible than solid matter, this material can be described as a gel or as jelly-like material.

Along the past century, scientists have made attempts to find a clear definition for the term gel. In 1926, Dorothy Jordon-Lloyd already recognized that “the colloidal condition, the gel, is one which is easier to recognize than to define“.[1] Almost 50 years later Paul John Flory presented a more adaptive suggestion to define a gel in his “Universal characteristics of a gel“ which is widely accepted in academia today. The one, almost universally identified property, is the solid-like behavior that also can be seen in rheological observation. If a material‘s dynamical mechanical properties do not have a storage modulus, G‘, which is clearly higher than G‘‘, the loss modulus, then the material is not a gel.[2] As a second requirement, at least for the duration of an experiment, the gel must possess a continuous structure with macroscopic dimensions.[3]

Gel materials play an important role in people‘s everyday lives. Right at the beginning of a human life gels give a big convenience to every family using disposable diapers for their babies. Besides a polyethylene film and cotton, the most important ingredient is a superabsorbent polymer. When the superabsorber gets in contact with urine, a hydrogel is formed that keeps the baby dry.[4]

In agriculture the hydrogels also have found an important role in water-saving applications. Not only countries with dry and hot climate can benefit from the fact that superabsorbers impound water like a sponge.[5]

A further outstanding product which benefits from the hydrogels are contact lenses. In 1960 the Czech chemist Otto Wichterle published an article about hydrophilic gels for biological use.[6] This was the beginning of the development of the soft hydrogel lenses as they are widely used today.

Hydrogels have enabled revolutionary application in medicine by their ability to act as wound management systems, among other properties. Repithel® for example is a polyacrylate-based hydrogel with incorporated hydrosomes.[7] The hydrogel dresses the wound without the need of gauzes and cotton and exhibits a wet climate which supports

wound healing because it removes necrotic tissues. Furthermore, the hydrosomes in the wound decompose into building blocks which then are used for the regeneration of the damaged tissue.

Also organogels have shown their applicability in different field. Since 1980, organogels have been used for art conservation and offered a new approach to the cleaning of painted surfaces. This avoids the necessity to apply organic solvents directly on the work of art.[8]

Furthermore, organogels are used in medicine. Pluronic lecithin organogel, PLO, is a drug delivery media for transdermal drug transport. PLO enhances skin permeation and transport of the drug molecules into and across the skin at the same time.[9]

The aforementioned examples provide just a tiny aspect of the broad spectrum where gels find their application and they only contain a small slice of the different classes of gels. What all gels have in common is that they consist of at least two parts. One part is called the gelator, which entraps the solvent as liquid part. The gelator is building up a 3D network which entraps the second part, the solvent. Most of the time, the liquid component provides the major part and the the gelator molecules immobilize up to 10^5 solvent molecules per gelator molecule. By a factor of 10^{10} the viscosity is scaled up and can respond to different external stimuli.[10,11] Not every molecule that seems to act as a good gelator at the first sight is evolving the ability to gel a solvent, because the gel state is a fine balance between dissolving and crystallization. When a compound is dissolved by heat whereupon the concentration of the compound is higher than the solubility limit at RT, three possible scenarios can appear. While the molecules start to condense, a highly ordered aggregation could result in a formation of crystals. The second possibility is a random aggregation which could provide amorphous precipitate. And the last alternative is an aggregation process between precipitation and crystallization, which finally leads to a gel material (Figure 1).[12]

It must be mentioned that the heating-cooling process is not the only way to obtain a gel. The major requirement for the gelation process is the pre-achievement of an isotropic solution of the gelator. In this regard, other non-thermal methods, such as sonication or pre-dissolution in a different solvent, can also be used to induce the formation of a gel.[13,14]

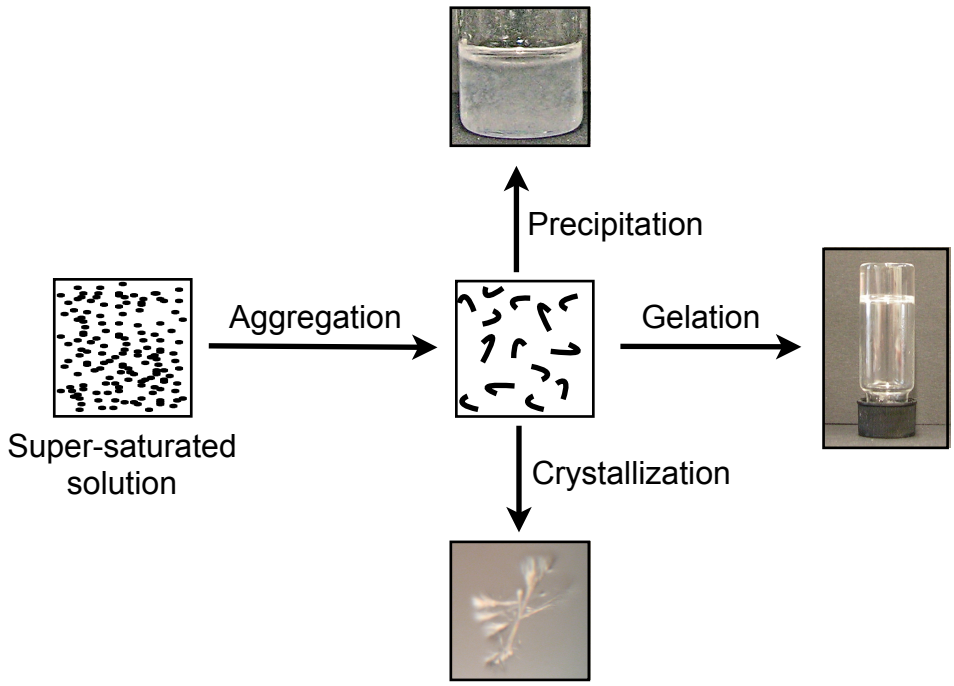

Figure 1: Illustration of aggregation modes.[12]

Gels can be classified by different criteria. One of the simplest methods is to categorize them by their solvent. When water is used as solvent it is called hydrogel.[15] If an organic solvent like ethanol, dichloromethane or toluene is used for preparation, it is called organogel instead.[16] Additionally, special cases exist where the solvent is a mixture of organic solvent and water, for example water-alcohol mixtures.[17] Aerogels can be obtained when the solvent in the gel is replaced by gas without shrinking of the gelator structure.[18] Xerogels show the same replacement of solvent by gas, but the difference is that their gelator structure is suffering from shrinking.[19]

Furthermore, the gels can be distinguished by a natural or artificial origin of the gelator. Like alginate, chitosan or gelatin, a huge number of natural gelators derived from plants and animals exists. Chitosan can be obtained from chitin,[20] gelatin from skin and bones of animals, like fish, pork or cattle.[21] Alginate is extracted from seaweed.[22] These materials are therefore cheap and sustainable compared to artificial gelators which were designed in laboratories. Often a time-consuming synthesis and screening with costly chemicals is required. However, the artificial gelators can be equipped with certain building blocks that offer various functionalities, for example an photoresponsive azobenzene residue. The incorporation of a functional group enables the gelator to form not only a gel, but also a smart material (Scheme 1).[23]

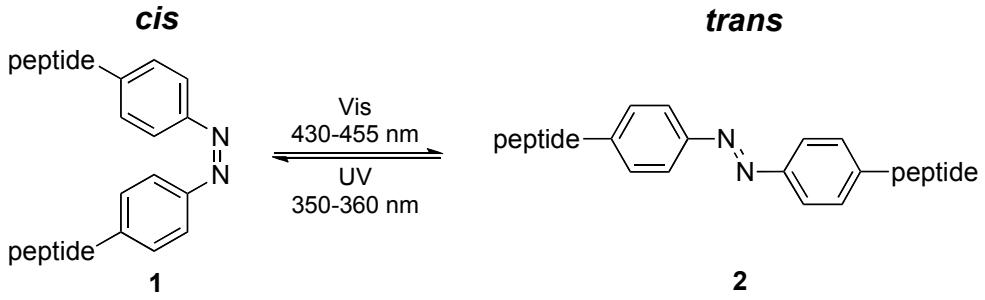

Scheme 1: *Cis-trans* conversion of an azobenzene-group by irradiation with light.[23]

A third way of distinguishing between gels is to analyze their driving force for molecular aggregation (Figure 2). Nature-derived gelators like the ones discussed above are mostly macromolecular and use H-bonding and other physical cross-linking to form gels.[12] Literature differentiates between two types of artificial gelator based gels, chemical and physical gels.

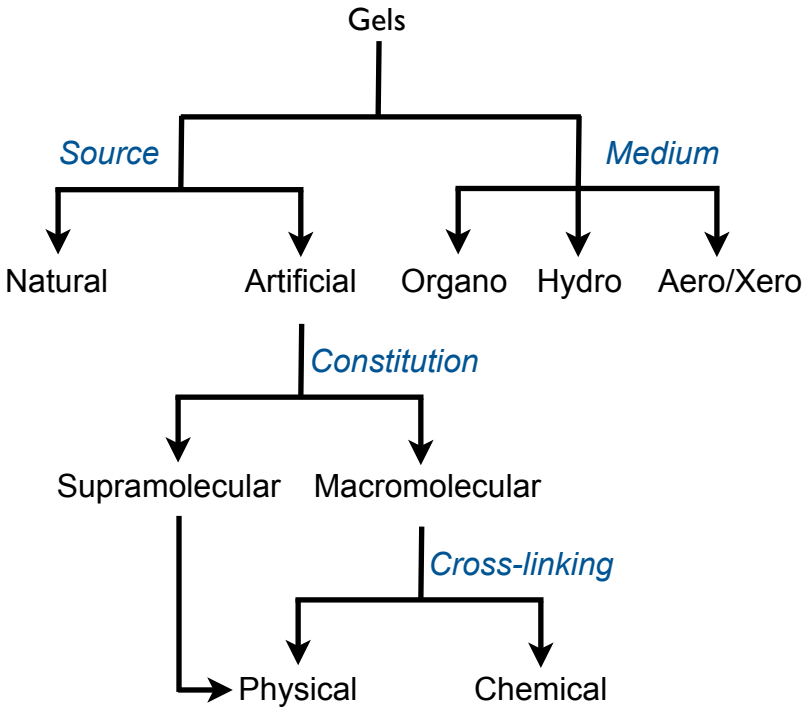

Figure 2: Classification of gels.[12]

Chemical gels are hold together by strong chemical bonds.[24,25] They are obtained by cross-linking macromolecular compounds, for example. Physical gels can be derived from macromolecules or low molecular mass compounds, called supramolecular gels.[12,26] Starting from entangled Self-Assembled Fibrillar Networks (SAFINs), the small gelator

molecules are able to self-aggregate by one or in combination of several non-covalent, but intermolecular interactions. H-bonding, van der Waals interactions, π-π stacking, dipole-dipole interactions, donor-acceptor interactions, metal coordination, solvophobic or hydrophobic forces are forming bonds which hold the gelator structure together (Figure 3). [27] Besides these, there are also systems which include both types of connections.[28,29]

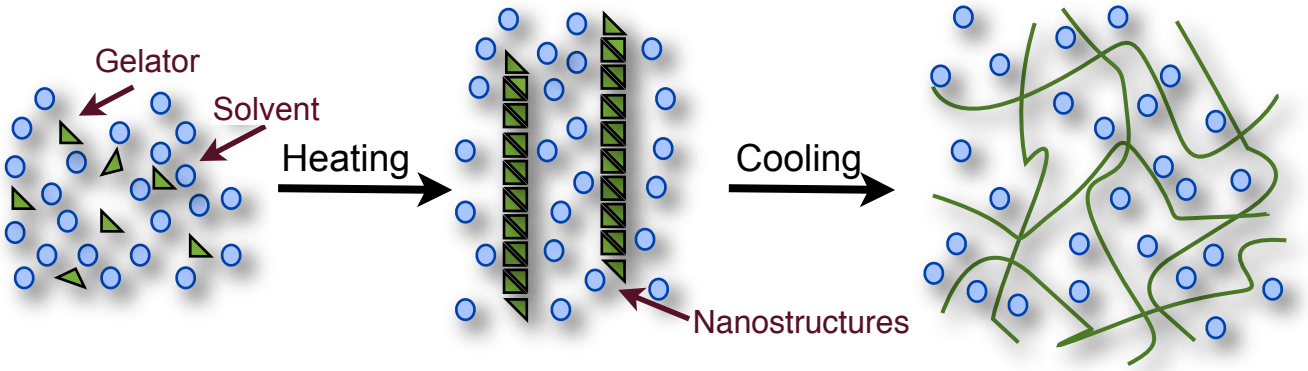

Figure 3: Schematic representation of the gelation process for supramolecular gels.[30]

The simplest way of clarifying the difference between physical and chemical gels is to compare their thermoreversibility. Most of the chemical gels cannot be re-dissolved due to their formation by chemical bonds. Physical gels consist of weaker non-covalent interactions which makes them often thermally reversible. They can be liquified by heating up to their *sol*-to-*gel* transition temperature T_{gel} which results in the collapsing of their 3D network and the re-forming of their 3D gelator structure upon cooling again.[12,31] This thermally reversible *gel*-to-*sol* transition is shown in Figure 4.

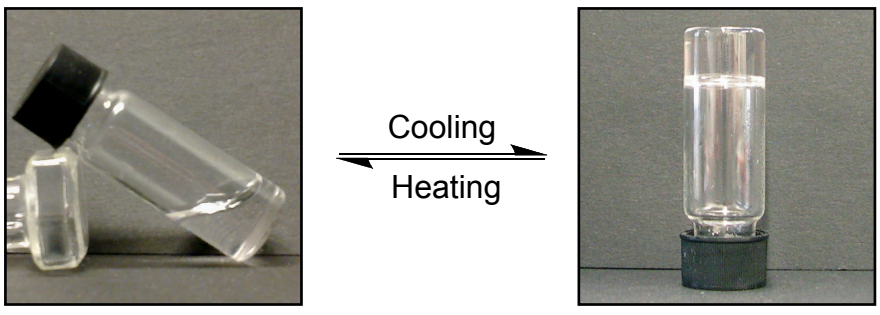

Figure 4: Example for heating-cooling cycle for thermoreversible supramolecular gels.

For scientists it is now possible to create gelators by rational design,[32-35] but in former times they were often found by serendipity as result of a failed crystallization attempt. The

variety of classes of gels leads to an enormous choice of properties and the possible applications where they can be used.

In Figure 5 only a tiny slice of gelator structures is shown, but it gives an outlook which gelators already exist and how diverse they are. Chitosan[20] is an example for bio-material, polyacrylamide and poly (vinylalcohol) are artificial building blocks which are further cross-linked or functionalized.[36,37] Wooley`s group has reported on polyethylene glycol functionalized by polypeptides.[38] Furthermore, dendritic,[39] sugar-based[40] and two-component gelator systems[41] are known.

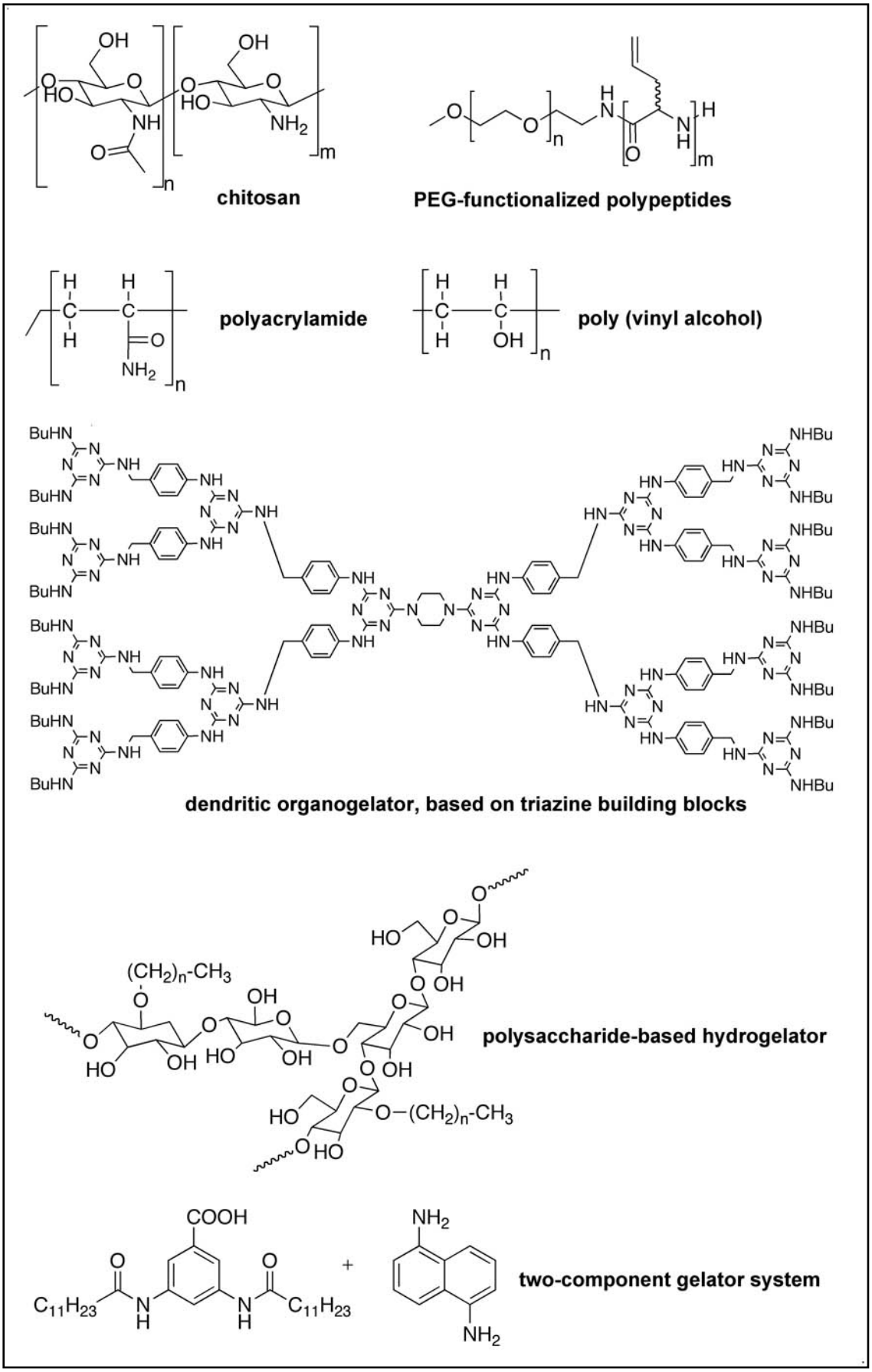

Figure 5: Variety of gelator structures.

For both types, chemical and physical gels, a potential use in other fields of chemistry is possible. As they are all providing 3D networks, they can act as reaction vessels and catalysts. Díaz Díaz and coworkers classified gels in low molecular weight and polymer gels. These polymer gels can construct their gel network either by non-covalent or covalent forces. The polymer gels were divided in three groups: electroactive hydrogels, acrylamide- and PVA-based hydrogels and biopolymer-based hydrogels. Hydrogels, organogels and metallogels form the three columns for the low molecular weight gels (Figure 6).[27]

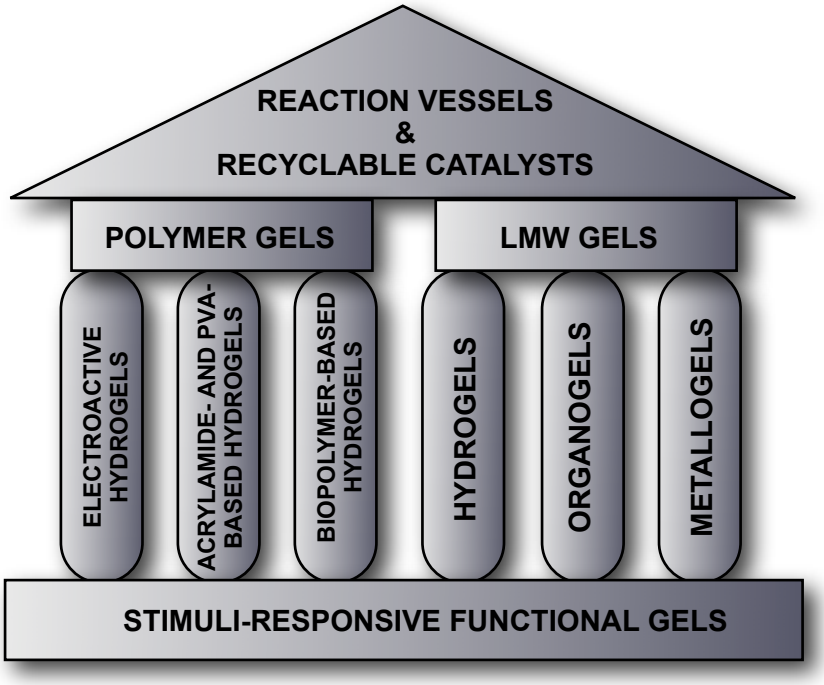

Figure 6: Classification of gels applied as reaction vessels and recyclable catalyst.[27]

Specific advantages of gels compared to homogeneous phase reactions are:

- Highly active surface[42,43]

  Compared to the solution phase, the high active surface of its fibrillar network allows to act as on-demand supplier of reagents.

- Diffusion-controlled processes within the gel[44,45]
- Control of product selectivity

  The confinement effect may cause the enhanced interaction of substrate and catalyst in comparison to reactions that were carried out in the homogeneous phase (Figure 7).

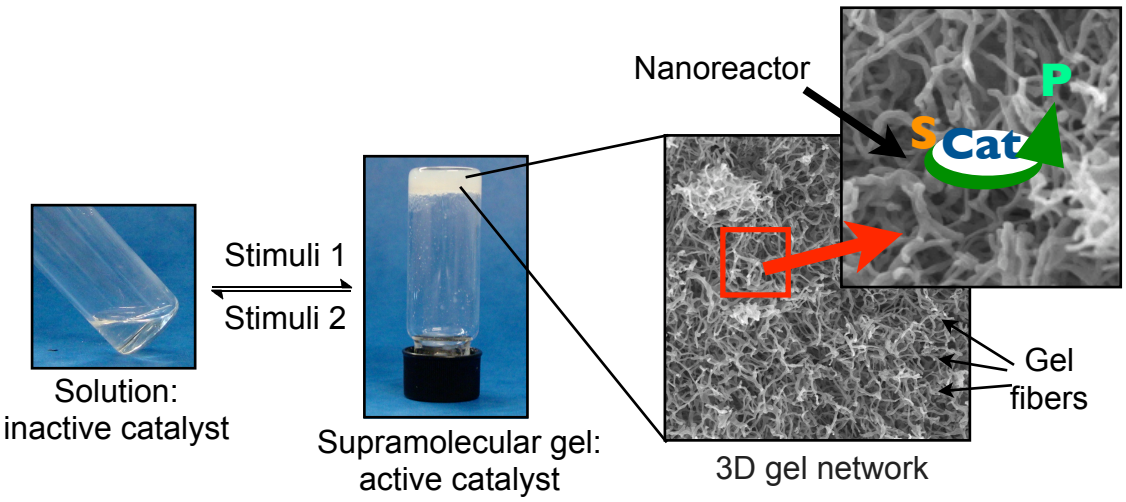

Figure 7: Potential use of gel materials as nanoreactors for selective synthetic transformations.

The confinement in gels can induce chirality in the product and also lead to an improvement in the product‘s stereoselectivity when compared to the reaction in solution. One example for the acrylamide polymer gel was reported in 2000 from Tanaka and coworkers. They created a smart polymer gel where the catalyst can be switched on and off.[46] The remarkably switchable catalytic activity can be controlled by the composition of the solvent, an ethanol-water mixture. The cross-linked gelator network consists of two different monomers, *N*-isopropylacrylamide **3** (NIPA), the major component and the monomer vinylimidazole **4** (Im). NIPA is responsible for the shrinking and swelling in dependence of the solvent and Im, the minor component, is the catalytic species. *N*,*N*′-methylenebisacrylamide **5** (MBA) serves as cross-linker (Figure 8).

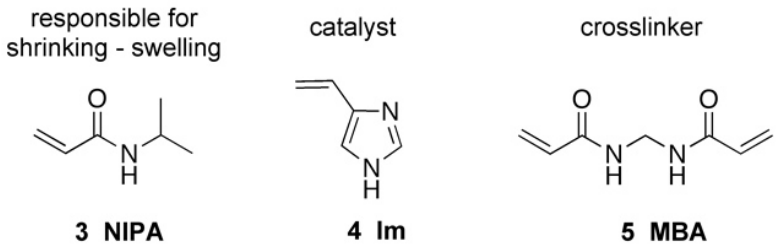

Figure 8: Components of gelator network.[46]

The catalytic hydrolysis of *p*-nitrophenyl caprylate **6** leads to the products *p*-nitrophenol **7** and carboxylic acid **8** (Scheme 2). When the gel was swollen the reaction rate was low in comparison to the reaction rate when the gel was shrunken. Compared to the catalytic

reaction in solution the reaction rate increased significantly: it was five times higher in the shrunken gel. The factor that the NIPA creates an hydrophobic environment in which the substrate could be absorbed would be one explanation for the excellent kinetics in the shrunken gel compared to the swollen state.

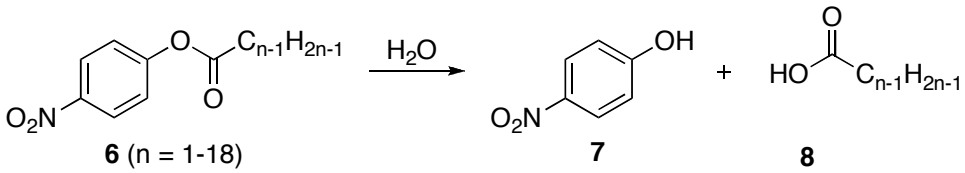

6 (n = 1-18) **7** **8**

Scheme 2: Hydrolysis of 4-nitrophenyl ester 6.[46]

Chitosan forms hydrogel beads with high catalytic activity and selectivity in Knoevenagel and Henry reaction compared to the reaction catalyzed by powdered chitosan. Unfortunately it turned out that the hydrogel beads did not act as a bio-nanoreactor, but as an immobilized base-catalyst.[47]

Bhat and Maitra successfully developed a LMW-hydrogel which was used as a photochemical nanoreactor. They described the formation of bile acid-based hydrogels (Figure 9, **9**-**12**) where photoactivated reactions can be carried out.[48]

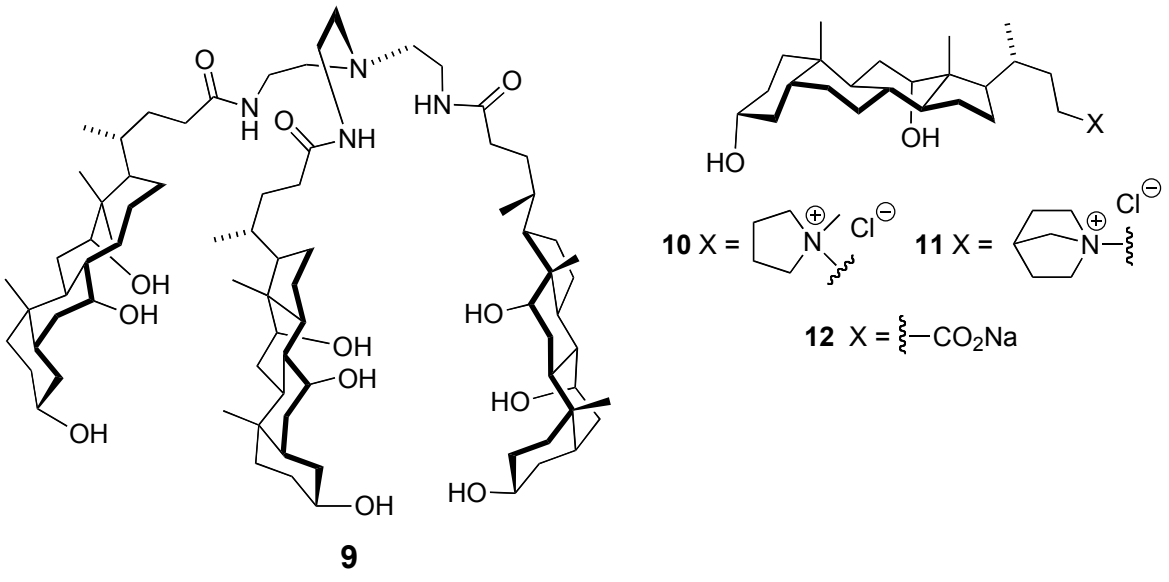

9

Figure 9: Hydrogelater 9-12 based on bile acid.[48]

The classical photodimerization of acenaphthylene **13**, forming mainly the *syn* (**14**) and *anti* (**15**) photodimers besides minor oxidation products, was assisted by the bile acid-based hydrogels (Scheme 3).

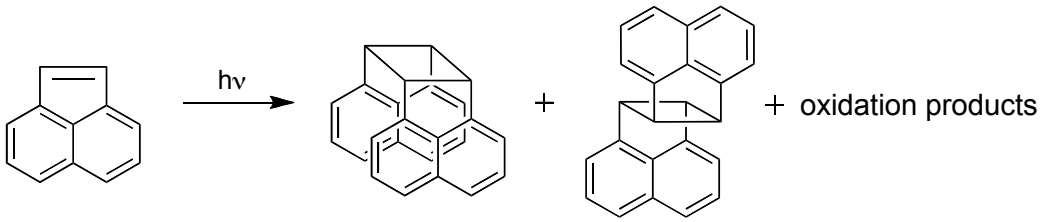

Scheme 3: Photodimerization of acenaphthylene.[48]

The properties of the gels had a major influence in the product ratios of the dimers. The *syn*/*anti* ratio of the products were three to ten times higher than those for reaction carried out in micellar solution. In general, it was observed that the more rigid or stronger the gel was, the higher the product selectivity was. The increase in rigidity was achieved by a higher amount of gelator. Then, the gelator network was more dense which led to an increase of the confinement. Therefore, the acenaphthylene molecules had less space and finally the less-hindered product was favorably formed. The product selectivity and the rigidity of the gels were **11** > **10** > **12** > **9**. Until now, the effect of the bile acid-gelator compared to classical alkyl surfactant systems is not fully explored. One aspect could be the higher rigidity and the hydrophobic environment they provide for the substrate molecules in the hydrogel.[27] In the gel state the acenaphthylene-excimer band showed a different intensity than in micellar solution which indicates a difference in molecular interaction and makes the bile acid derivatives suitable as gelators for nanoreactors.

2. Low molecular weight gels

2.1 Overview

Gels which are based on a low molecular weight gelator, LMWG, are also called supramolecular gels. They have been studied with increasing interest by scientists over the last decade. Although the numbers of publications for hydrogels is increasing at a higher rate, the ongoing interest on organogels is also visible (Figure 10).

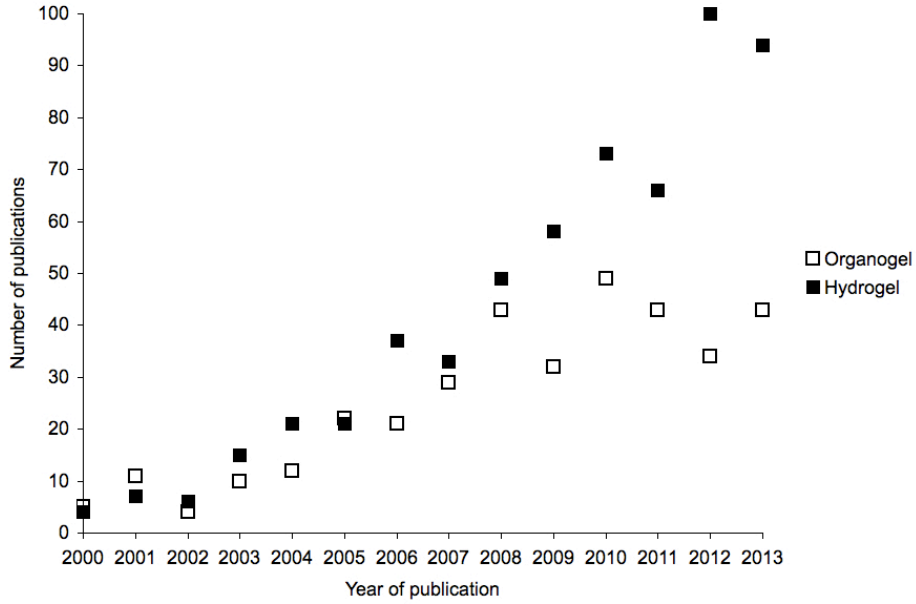

Figure 10: Comparison of the numbers of publications for hydrogels (combined answers for the key word „supramolecular hydrogel“ and „low molecular weight hydrogel“) and organogels (combined answers for the key word „supramolecular organogel“ and „low molecular weight organogel“) (from SciFinder, 10.09.2013).

Already in 19th century, E. Goldmann and E. Baumann described a low molecular weight gelator, *N*,*N*′-Dibenzoyl-*L*-cystine **16**, DBC, which forms hydrogels as well as organogels in different alcohols (Figure 11).[49] The gels from this gelator where intensively studied afterwards, characterized[50] and tested for application in biomedicine as media for drug delivery.[51] In addition to that, enhanced luminescence of Eu(III)[52] was found in DBC gels.

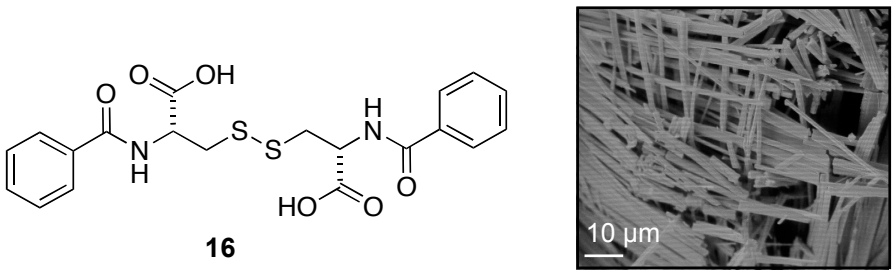

16

Figure 11: Structure of DBC **16** (left). SEM image of DBC xerogel (right).

Since then, the diversity of low molecular weight gelator structures has grown steadily. Figure 12 shows insight into the microstructure of different LMW xerogels and Figure 13 gives structures of different LMWG molecules as urea,[53] amino acid,[23] fatty acid,[54] pyrene,[55] sugar,[14] steroid and anthryl derivatives.[56]

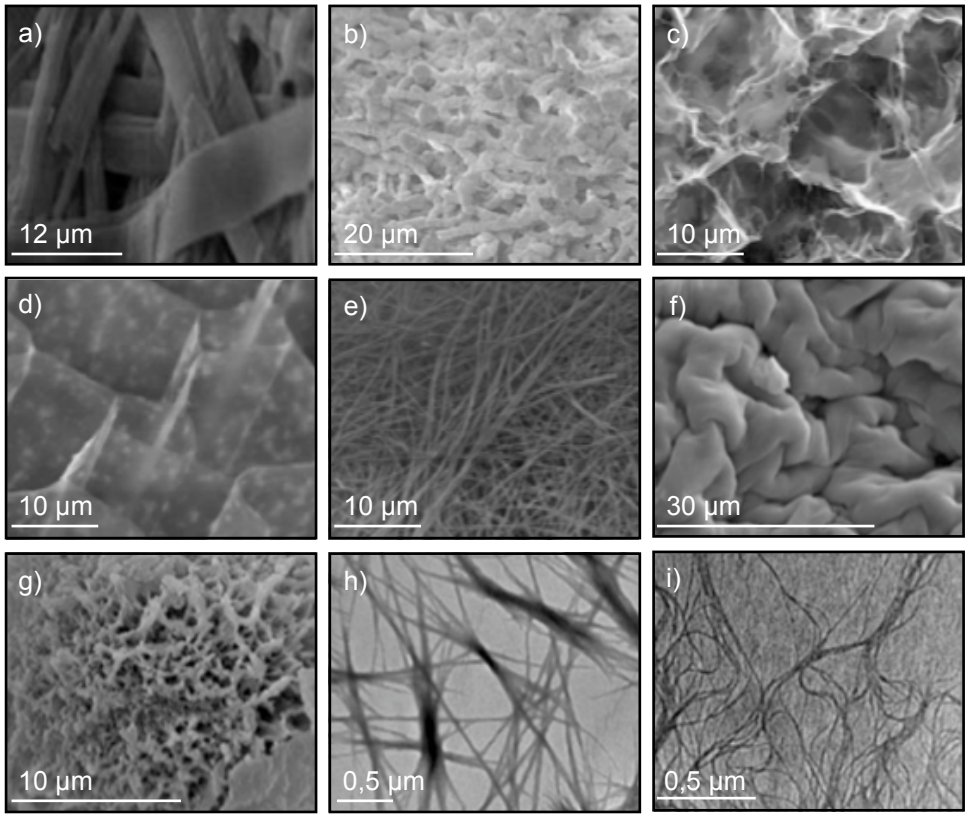

Figure 12: Images a) - g) show representative SEM pictures from Xerogels. a) toluene gel from sugar-derived gelator;[14] b) urea-based gelator from $CHCl_3$: toluene mixture 1 : 9 (v/v);[53] c)-e) hydrogels from pyrenyl-derived gelator;[55] f) and g) show toluene and isopropanol gels from amino acids;[23] TEM images h) and i) resulted from toluene gels of amino acids.[23]

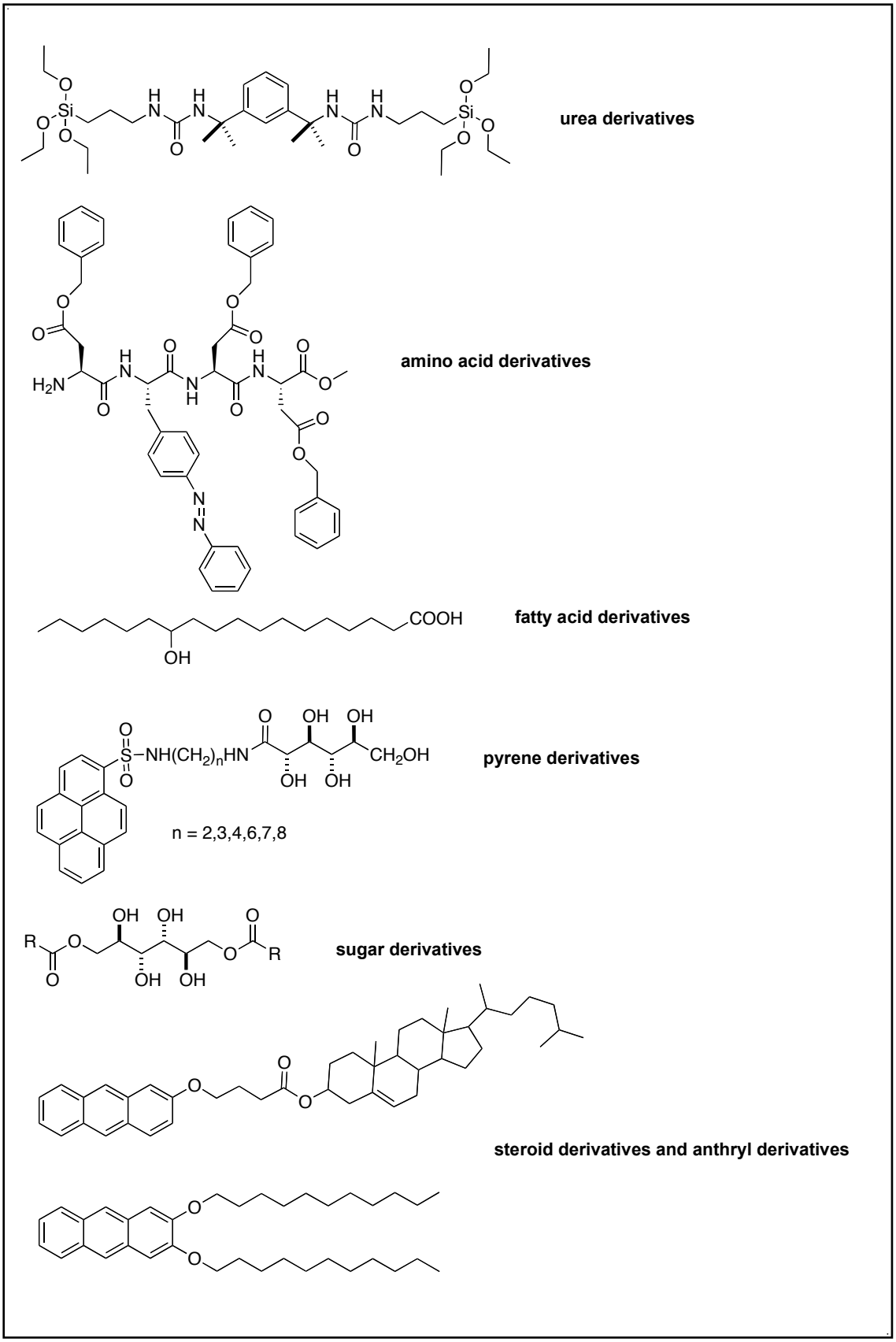

Figure 13: Excerpt on the variety of LMWG.

However, compared to most supramolecular gels derived from polymer gelator or chemical gels, their long-term stability is often limited and decisive mechanical toughness is missing which reduces their application in some areas. A significant increase in stability and strength would be necessary for their application in biomedicine.[12] Until now, a variety of different methods were developed to stabilize these gels. Addition of polymers,[57] post-polymerization of the gel fibers,[58] use of metal-ion coordination[59] and host-guest interactions[60] were reported to be suitable for the reinforcement of LMW gels. „Click"-chemistry has yielded remarkable results and showed to be a user-friendly, reliable and efficient way to enhance the properties of the gels. The Cu(I)-catalyzed cycloaddition reaction[61] between alkynes and azides, the most familiar „click"-reaction, was used by Finn and co-workers[62] for the stabilization of an already known gelator **17** from Hanabusa.[63] Finns group modified **17** with alkyne (**18**) and azide groups (**19**) at the end of their long alkyl chains (Figure 14).

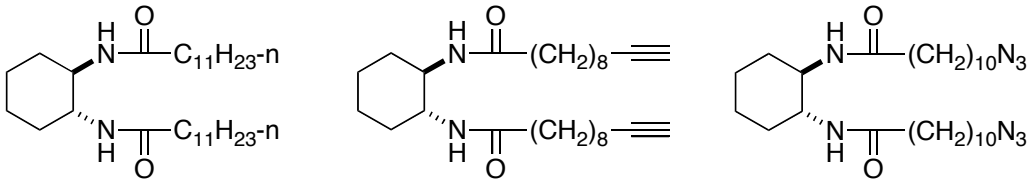

17 **18** **19**

Figure 14: Original (**17**) and modified (**18**,**19**) LMWG based on undecylamide of *trans*-1,2-diamino-cyclohexane.[62,63]

Copper iodide and linear cross-linker (**20** and **21**, Figure 15) at an optimized ratio of 10 :1 = gelator : cross-linker were used for the „click"-reaction. The reaction was carried out with Cu(I)-containing solution on top of the gel for one week, where Cu(I) can diffuse into the gel.

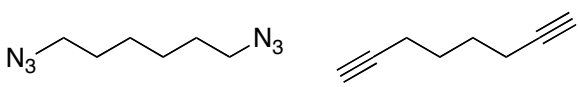

20 **21**

Figure 15: Bifunctionalized linkers for „click"-reaction.[63]

The comparison of T_{gel} measurements between unmodified and „click"-modified gels has demonstrated the success of the modification. The *gel*-to-*sol* temperature increased from initial 63 °C up to 93 °C when, in addition to the unmodified gelator, Cu(I) was incorporated

by diffusion and the modified gelator was cross-linked. As a proof of the successful „click“-reaction, ^{1}H NMR spectra showed the presence of triazole moieties.

The preservation of the thermoreversibility of the „click“-chemistry reinforced gels was the major achievement of this procedure. While other groups enhanced their gel properties by turning a LMW gel into a polymer gel, Díaz, Finn and co-workers developed a method were thermal stability was increased but the supramolecular character has been maintained (Scheme 4).[62]

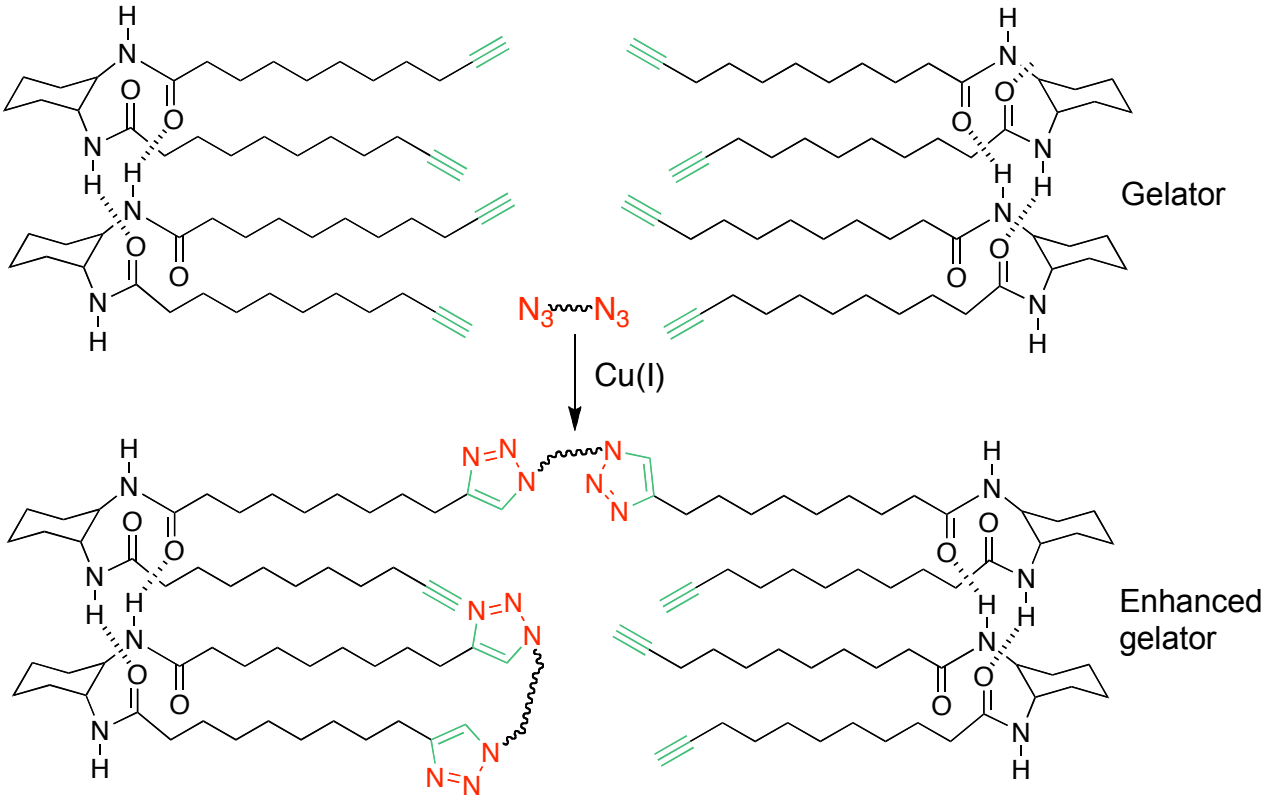

Scheme 4: „Click“-chemistry resulted in enhanced gelator properties.[62]

Inspired by this achievement, the same strategy was adopted to a much more complex photoactive organogel-system.[64] The respective multicomponent-pre-formed organogel provides a much more challenging environment for the CuAAC. The acetylene monomer for the „click“-reaction should be at least partially associated with the gel fibers, as the cycloaddition must take place in a pre-formed organogel. The coupling reaction between LMW-additives, which cannot form stable gels on their own, is carried out in the gel which acts as an effective reaction vessel.

An overview of the procedure is shown in Figure 16.[59] The preparation of CuAAC-stabilized organogels starts with the isotropic solution of the LMWG system 2 which leads

to standard organogel in system 4. System 3 shows the possibility of further strength-enhancement of the material, by addition of a suitable complementary diacetylene LMWG structure, linear diazide as cross-linker and Cu(I)-catalyst. After cross-linking, a gel with enhanced thermostability and maintained thermoreversibility is obtained (system 5). Organogels from system 4 can be charged with complementary dye-containing organogelators to obtain a multicomponent photoactive viscoelastic material (system 6). In order to create further cross-linking for a new photoactive organogel with enhanced thermal and mechanical stability (system 7), „clickable“ monomers and Cu(I)-catalyst as in system 3 could be incorporated into the system. However, a phase separation is induced when either a preformed triazole-based polymer like in system 9 (which is obtained by CuAAC of the appropriate monomers in solution), or a cross-linked material like in system 10 (made by *in situ* CuAAC of “clickable” monomers) is incorporated into the photoactive organogels.

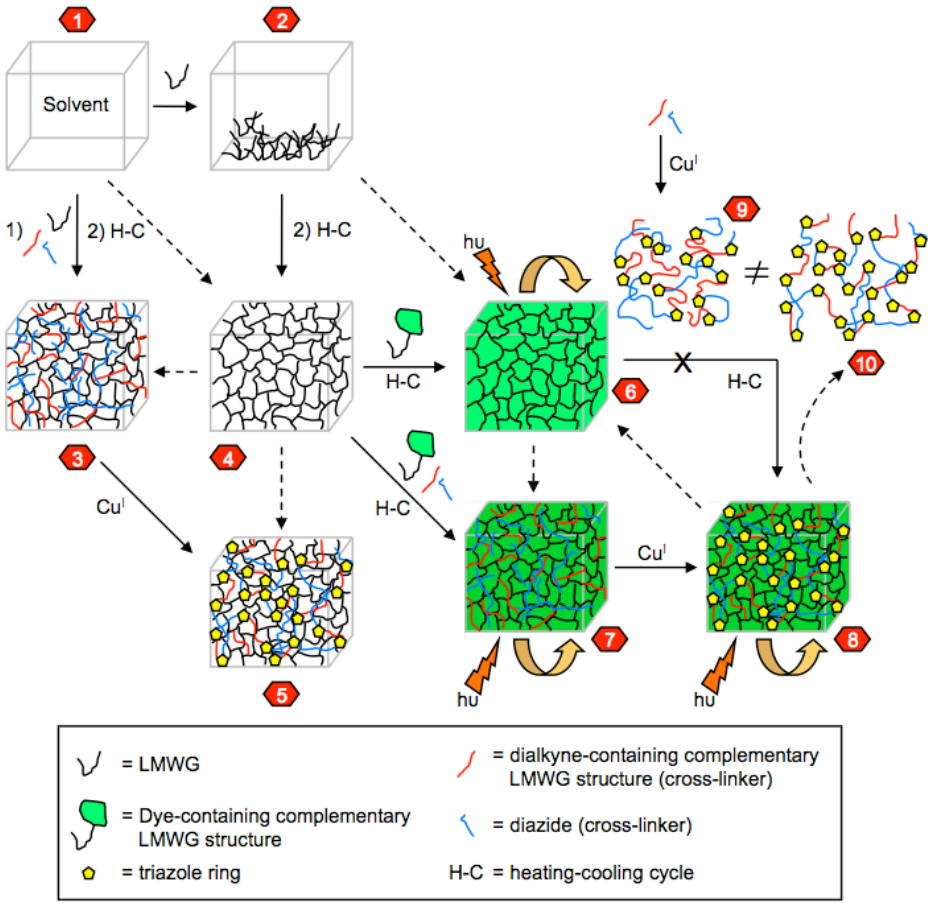

Figure 16: Strategy of CuAAC stabilization of functionalized organogels.[64]

2.2 Applications of low molecular weight organogels

The importance of low molecular weight organogels and their contribution to progress in science sometimes seems to be underrated, especially when compared to polymer hydrogels. However, these materials are not only smart, but versatile and have numerous remarkable applications.

An organogel whose morphology can be switched by ultrasound was reported in 2008 by Huang and coworkers.[13] The colesterol-based organogel can heal its morphology and surface wettability by thermal repair (Figure 17).

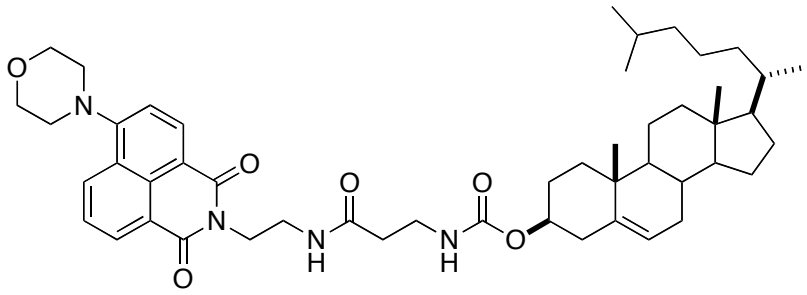

22

Figure 17: Cholesterol-based organogelator **22**.[13]

The gelation induced for example in *p*-xylene by sonication, decreased the minimum gelation concentration from 15 mg·mL^{-1} to 10 mg·mL^{-1} compared to the heating-cooling process. At the same concentration, gels prepared by sonication showed a higher T_{gel} than gels formed by heating-cooling process. A further difference is visible on SEM pictures of the xerogels. While the morphology of xylene-xerogel prepared by the heating-cooling process showed honeycomb-like 3D multi-porous vesicles with holes of 2 µm size, the xylene-xerogel prepared by sonication showed regular papillae with 5 µm size like multilayered circles (Figure 18).

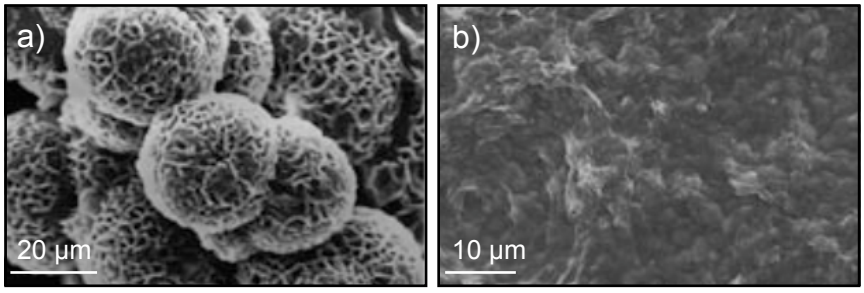

Figure 18: SEM of xylene-xerogels of **22** prepared by sonication (a)) and heating-cooling process (b)).[13]

The difference in morphology as well as the different wettability of the gel made by sonication (compared to the gel made by heating-cooling) can be reversed by a simple additional heating-cooling process.

Besides this smart behavior, LMWG based organogels are also useful materials in environmental issues. Removal of toxic dyes from wastewater is an challenging task. Of the ideal dye-adsorbing agent it requires a hydrophobic as well as a hydrophilic site. Figure 19 shows an gelator with both required domains. The xerogel of **23** efficiently adsorbed more than 97% of the crystal violet dye molecules after 24 h which was monitored by UV-Vis spectroscopy. FESEM images were taken after the adsorption experiment and clearly showed the entrapped crystal violet particles on the nanofibrillar network (Figure 19, right).[65]

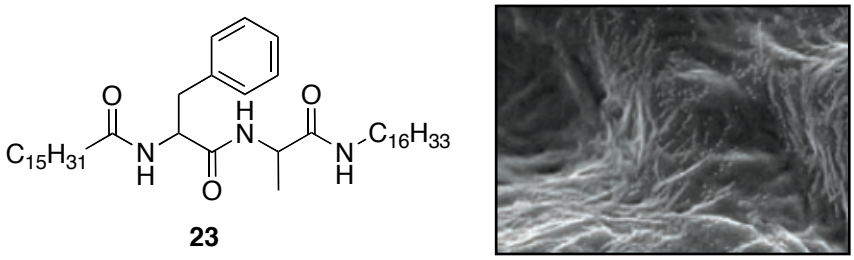

23

Figure 19: Chemical structure of dye-adsorbant organogelator **23** (left) and SEM image of respective xerogel with adsorbed crystal violet.[65]

Sugar-derived molecular organogelators **24**-**27** were developed, which turned out to be able to solidify 16 different organic solvents and oils (Figure 20).[13]

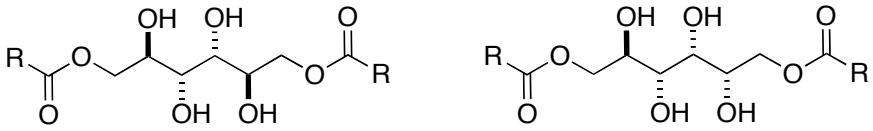

24 R = n-C_3H_7
25 R = n-C_7H_{15}

26 R = n-C_3H_7
27 R = n-C_7H_{15}

Figure 20: Sugar-derived low molecular weight organogelators.[13]

Furthermore, they selectively gelled the oil phase from oil-water mixtures at RT. Afterwards, the oil can be quantitatively recovered from the gel by vacuum distillation. As an additional benefit, the gelators are not only easily synthesized, but also environmentally benign. As a result, they can be recovered and reused several times. With these

properties, they are ideal candidates for the disposal of marine oil spills, as for starting the gelation process only an aliquot of 2.5 wt% of the gelator has to be dissolved in a hydrophilic solvent as alcohol and then added to the oil-water mixture.[13]

The capability of binding charged guest-molecules, like anions and cations, usually results in a massive change of the gel's properties. Anions can take the place of a binding site which was originally available for gelator-gelator interaction (Scheme 5).[66]

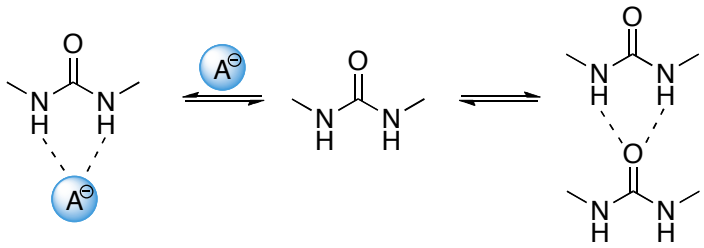

Scheme 5: Tuning of aggregation by anion binding.[66]

Due to the competitive character of water in ion-binding equilibria, there are not many examples for anion-responsive supramolecular hydrogels.[67]

Among several anion-sensitive organogels, Steed and coworkers reported a bis(urea) gelator **28** which formed gels where the crystal growth of a pharmaceutical compound **29**, carbamazepine occurred (Figure 21).[68]

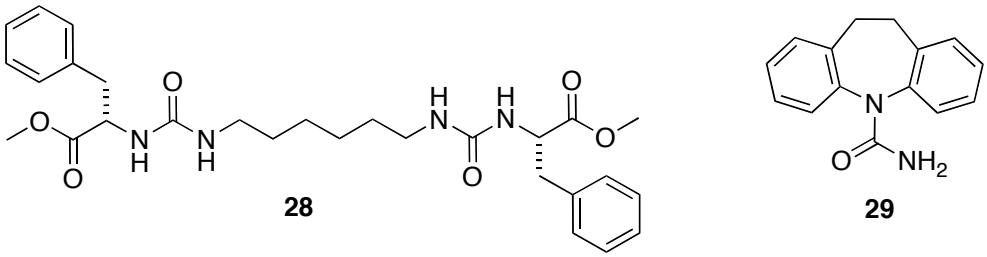

28 **29**

Figure 21: Single crystal from carbamazepine **29** is growing in organogel of gelator **28**.[68]

Figure 22 shows the application of the anion responsiveness to acetate ions. After gelation it takes 1-2 days to produce the crystal. The gel on the left contains a carbamazepine single crystal which is recovered by addition of acetate anion. The disruption of the gel makes it possible to recover the single crystal by filtration. Afterwards, the crystal can be analyzed by X-ray crystallography. In comparison to the crystallization in solution, the crystals formed in gel grew about four times slower, but the production of lager crystals was possible.[68]

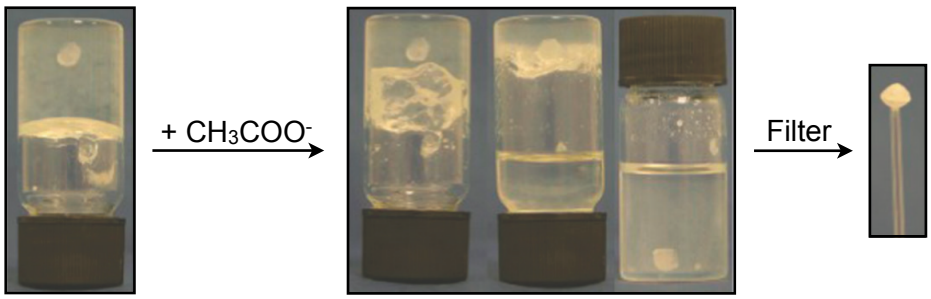

Figure 22: After addition of acetate, a crystal can be recovered from disrupted gel.[68]

The use of a supramolecular organogels was very convenient as they can serve as catalytic vessels in organocatalytic processes.[69] Compound **30** (Figure 23) showed catalytic behavior as free molecule as well as in aggregate state, but with two different results.

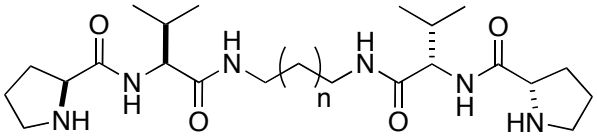

30

Figure 23: *L*-Pro-containing gelators **30**.[69]

In the aldol reaction compound **30** is a *L*-Pro-based organocatalysts with moderate activity and stereoselectivity in solution (Scheme 6, a)). Contrary to that, in gel state compound **30** is not active in the aldol reaction, but active in non-stereospecific deprotonation of the aldol reaction product leading to racemization (Scheme 6, b)).[69]

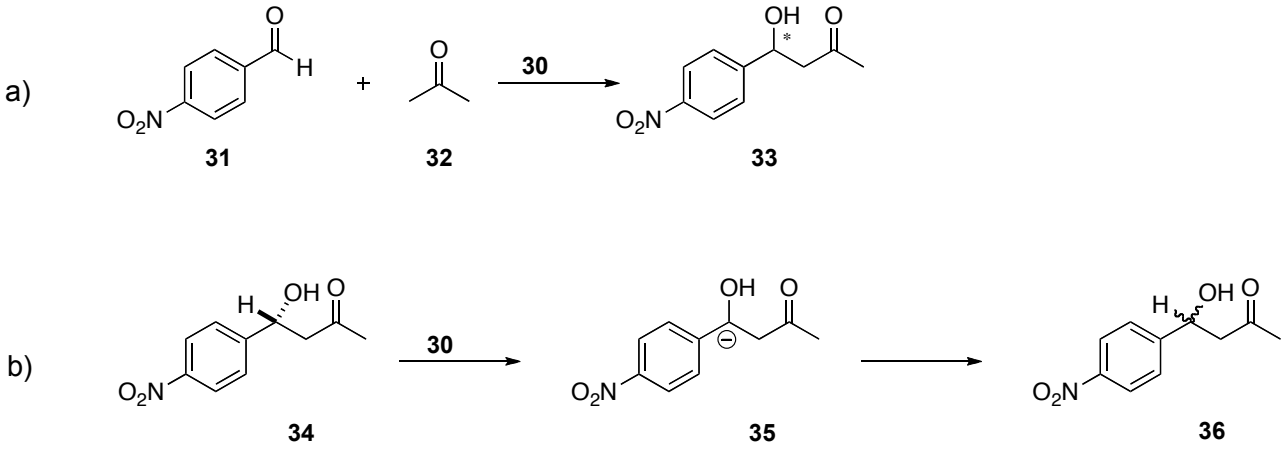

Scheme 6: Dual catalytic behavior of **30** in a) solution and b) gel state.[69]

Remarkably, supramolecular gelation can also result in a sharp change of catalytic activity. Upon aggregation, gelator molecule **37** becomes an active catalyst for the Henry reaction compared to reaction in solution (Figure 24).[70]

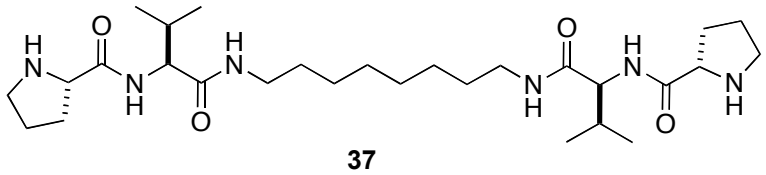

37

Figure 24: Catalyst **37** for Henry reaction in gel.[70]

As a test, the Henry reaction between 4-nitrobenzaldehyde and nitroethane was investigated (Scheme 7). Changes in the reaction temperature allowed to compare the reaction in solution at 25 °C and also in gel phase, when temperature was decreased to 5 °C at a concentration of 13 mmol·L^{-1}.

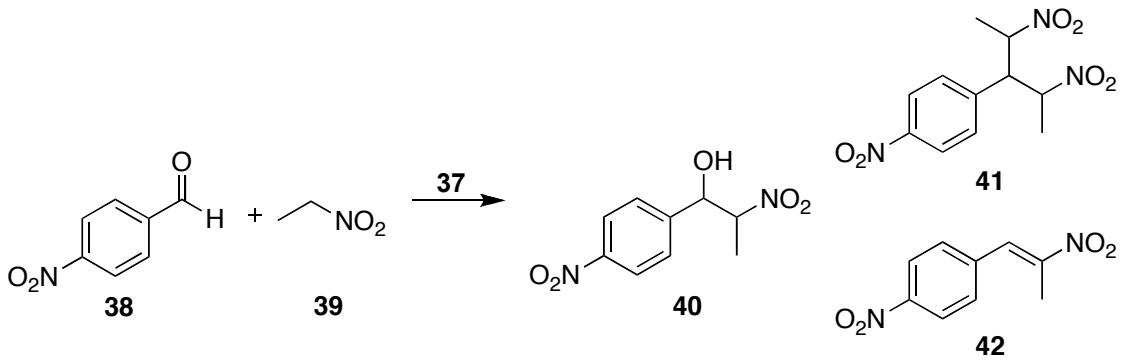

38 **39** **40** **41** **42**

Scheme 7: Henry reaction between 4-nitrobenzaldehyde and nitroethane catalyzed by **37**.[70]

Table 1 gives the obtained yield of the Henry reaction in gel and solution. For both, entry 1 and 2, the concentration of the catalyst **37** was 13 mM at a reaction time of 48 h. The results show that the *sol-gel* transition is combined with an activation of the catalyst as in gel 99% of the desired product was yielded compared to 15% in solution with additional 5% of side-product formation. It can be assumed that in solution the *L*-proline moiety of **37** undergoes a iminium intermediate while in gel state a ionic pair type mechanism is favored due to the aggregation of **37**.

Table 1: Yields of Henry reaction obtained for reaction in gel and solution.[70]

Entry	Catalyst	Temperature [°C]	Appearance	Yield [%] **40**	Yield [%] **41** + **42**
1	**37**	5	Gel	99	-
2	**37**	25	Solution	15	5

3. Characterization methods for gels

The characterization of gels is essential to obtain measurable values for comparison. The obtained values can help to draw conclusions for possible applications, too.

Minimum gelation concentration

The minimum gelation concentration, MGC, defines the lowest amount of gelator which is necessary for the gelation of a certain volume of solvent. Below MGC, a gelator is not able to build up a sufficient 3D network structure of the gelator molecules and cannot entrap the solvent molecules. That can be confirmed by the inversion of the test tube. The soft material is classified as gel if no gravitational flow occurs. Usually MGC is determined in $mol \cdot L^{-1}$ or wt.% (w/v).

Temporal stability

The temporal stability of a gel is defined as the period of time between gel formation and gel destruction. Crystallization inside the gel material or phase separation are two examples for possible destruction of gels. The temporal stability has to be monitored under constant conditions (e. g. temperature and pressure).

Thermal stability[71]

The thermal stability of a gel is described by the *gel*-to-sol phase transition temperature T_{gel}. It can be obtained by a number of different characterization methods. The following two are the most common ones:

The “Dropping ball method“

uses a small ball which is placed in the middle of the gel surface. Then the temperature is increased slowly until the gel transforms into sol and the ball touches the ground of the vial. It is important that the ball is inert (no reaction or destruction in contact with the gel) and not to heavy or to light to avoid dunking or swimming of the ball in the gel.

The "Inverse flow method"

describes the T_{gel} measurement by a sealed vial containing the gel. The vial is immersed upside-down in a thermostated oil bath and the temperature raised slowly until the gel breaks.

Fourier transform infrared spectroscopy[72]

Fourier transform infrared spectroscopy, FT-IR, can be a useful tool to analyze the precise roles of each different functional group of the gelator in the formation of bonds which then forms the 3D gelator network as for example carbonyl and amine residues, amide I band and amide II band and also aromatic groups. A change in intensity as well as a shift of the signals can be often observed between the FT-IR spectra of a gel and a solution of gelator.

Temperature-dependent ^{1}H NMR spectroscopy[23]

^{1}H NMR spectra can provide an insight into the stabilization of the gelator network by the involved protons. For this, gels have to be made from deuterated solvents and ^{1}H NMR spectra must be measured at a number of different temperatures including temperatures below and above T_{gel}. Protons which are part of the gelator network cannot be observed by ^{1}H NMR due to long correlation times. That means that any signal which is observed belongs to a gelator molecule which is dissolved in the immobilized solvent, either aggregated or disaggregated. With increasing temperature the number of dissolved gelator molecules is increasing, too. That leads to a growth in signal intensity. A temperature-induced up or downfield shift of the signals can also be observed. The point of inflection of this shift corresponds to T_{gel}.

Morphological characterization

Scanning electron microscopy, SEM, transmission electron microscopy, TEM, and atomic force microscopy, AFM, are proven tools to gain visual insight into the microscopic morphologies of gels. The microscopy techniques make it possible to observe changes in the morphology as they are caused by the change of solvent or gelator concentration. The images also make inclusion of particles (for example dyes), crystals or formation of nanoparticles visible.

For SEM samples xerogels must be prepared first. In order to preserve internal structures the gels are freeze-dried before the solvent is removed by vacuum. The

remaining xerogel has to be sputtered with metal (for example gold) prior to imaging. A copper grid is used to prepare the TEM samples by dropcasting a diluted sample of the gel on the grid. AFM samples are provided by the xerogels, too.

As a result AFM provides 3D surface topographic images, height images, of the gelator structure. The high resolution of TEM enables imaging of single fibers. SEM images show the assembly of the fibers as beams, tubes or cauliflower-like.

Rheological properties[23,44,64,73]

Oscillatory rheological measurements have to be carried out to confirm the viscoelastic state of the gel material. G*, the complex modulus, is given by the ratio of the amplitudes of stress/strain in an oscillatory experiment. It comprises two components:

1. The storage/elastic modulus, G′, which represents the ability of a material to turn back in original state after deformation.
2. The loss/viscous modulus, G″, which shows the tendency of a material to flow under stress.

G′ and G″ are calculated from measured phase angle (δ):

$$G' = G^* \cos \delta$$

$$G'' = G^* \sin \delta$$

G′ = G* (δ = 0°) for an ideal solid and G″ = G* (δ = 90°) for an ideal liquid. The rheometer directly shows the moduli in pascal. G′ > G″ is the rheological definition of a gel and shows that the elastic behavior is dominant in these materials. Three different kinds of measurements are carried out to confirm the gel nature:

1. Dynamic Strain Sweep (DSS): The capability gels to deal with mechanical stress is shown in a plot of G′ and G″ where frequency is kept constant and strain is increased until G′ < G″ marks the breaking of the gel.
2. Dynamic Time Sweep (DTS): DTS gives a plot of G′ and G″ with constant frequency and constant strain over time. This confirms the gel nature of a material over time.
3. Dynamic Frequency Sweep (DFS): The DFS plot show G′ and G″ at constant strain in dependency of increasing frequency.

Mechanical destruction of a gel into fluid state and its returning back to gel state upon resting is called thixotropy. This property can be examined by rheological measurements in three steps:

1. A DTS experiment confirms the gel state, G′ > G″ at low strain.

2. The DTS is carried out again but this time under massive increase of the strain which let the gel fracture into a solution, G′ < G″.
3. In the third step the DTS experiment is using the initial strain and for thixotropic material a recovering of the gel state, G′ > G″, can be observed.

Responsiveness to stimuli[74,75]

A further step in the characterization of gels is the investigation of their behavior when being exposed to external stimuli. The response of a gel to a stimulus results in a change of the microstructure which can lead to phase separation, or a change of shape or color. Further, it is possible that an optical, mechanical or electrical response is created. Common stimuli which are able to cause a response are temperature-changes, light, pH, chemical, mechanical and/or electro/magnetic stimuli.

This is interesting to a broad range of applications as drug delivery media or as sensors. If, for example, the gelator network collapses as a response of stimuli, incorporated pharmaceuticals can be released safely and target-oriented.

4. Objective

The main objective of this PhD work was the development of new organogels and their studies in terms of structure, functionalities, preparation techniques, gelation mechanism and potential applications.

5. References

[1] Lloyd, D. J. *Colloid Chemistry*; J. Alexander, Chemical Catalogue Company, New York, USA, 1st, edition, **1926**.

[2] Almdal, K.; Dyre, J.; Hvidt, S.; Kramer, O. *Polym. Gels Netw.* **1993**, *1*, 5-7.

[3] Flory, P. J. *Faraday Discuss. Chem. Soc.* **1974**, *57*, 7-18.

[4] Sires, U. I.; Mallory, S. B. *Postgrad. Med. J.* **1995**, *98*, 79.

[5] Chen, P; Zhang, W.; Luo, W. Fang, Y. *J. Appl. Polym. Sci.* **2004**, *93*, 1748-1755.

[6] Wichterle, O.; Lím, D. *Nature* **1960**, *185*, 117-118.

[7] Vogt, P. M.; Reimer, K.; Hauser, J.; Rossbach, O.; Steinau, H. U.; Bosse, B.; Muller, S.; Schmidt, T.; Fleischer, W. *Burns* **2006**, *32*, 698-705.

[8] Carretti, E.; Dei, L.; Macherelli, A.; Weiss, R. G. *Langmuir* **2004**, *20*, 8414-8418.

[9] Bramwell, B. L.; Williams, LaVonn, A. *Int. J. Pharm. Compd.* **2012**, *2*, 32-37.

[10] Ilmain, F.; Tanaka, T.; Kokufuta, E. *Nature* **1991**, *349*, 400-401.

[11] Osada, Y.; Khokhlov, A. R.; *Polymer gels and networks*; CRC Press, Marcel Dekker, New York, USA, 1st edition, **2002**.

[12] Sangeetha, N. M.; Maitra, U. *Chem. Soc. Rev.* **2005**, *34*, 821-836.

[13] Wu, J.; Yi, T.; Shu, T.; Yu, M.; Zhou, Z.; Xu, M.; Zhou, Y.; Zhang, H.; Han, J.; Li, F.; Huang C. *Angew. Chem. Int. Ed.* **2008**, *47*, 1063-1067.

[14] Jadhav, S. R.; Vemula, P. K.; Kumar, R.; Raghavan, S. R.; John, G. *Angew. Chem. Int. Ed.* **2010**, *49*, 7695-7698.

[15] Estroff, I. A.; Hamilton, A. D. *Chem. Rev.* **2004**, *104*, 1201-1217.

[16] Terech, P.; Weiss, R. G. *Chem. Rev.* **1997**, *97*, 3133-3159.

[17] Anac, I.; Aulasechich, A.; Junk, M. J. N.; Jakubowicz, P.; Roskamp, R. F.; Menges, B.; Jonas, U.; Knoll, W. *Macromol. Chem. Physic.* **2010**, *211*, 1018-1025.

[18] Primo, A.; Liebel, M.; Quignard, F. *Chem. Mater.* **2009**, *21*, 621-627.

[19] Sepeur, S. *Nanotechnologie;* Vincentz Network, Hannover, 1st edition, **2008**.

[20] Ghosh, A.; Ali, M. A.; *J. Mater. Sci.* **2012**, *47*, 1196-1204.

[21] Kühbeck, D.; Bijayi Dhar, B.; Schön, E.-M.; Cativiela, C.; Gotor-Fernández, V.; Díaz Díaz, D.; *Beilstein J. Org. Chem.* **2012**, *9*, 1111-1118.

[22] Yuguchi, Y.; Urakawa, H.; Kaijwara, K.; Draget, K. I.; Stokke, B. T. *J. Mol. Struc.* **2000**, 554*,* 21-34.

[23] Fatás, P.; Bachl, J.; Oehm, S.; Jiménez, A. I.; Cativiela, C.; Díaz Díaz, D. *Chem. Eur. J.* **2013**, *19*, 8861-8874.

[24] van Esch, J. H.; Feringa, B. L. *Angew. Chem. Int. Ed* **2000**, *17*, 6759-6761.

[25] Gronwald, O.; Shinkai, S. *Chem. Eur. J.* **2001**, *7*, 4328.

[26] Tanaka, T.; *Sci. Am.* **1981**, *244*, 100-123.

[27] Díaz Díaz, D.; Kühbeck, D.; Koopmans, R. J. *Chem. Soc. Rev.*, **2011**, *40*, 427-448.

[28] Zubarev, E. R.; Pralle, M. U.; Sone, E. D.; Stupp, S. *Adv. Mater.* **2002**, *14,* 198-203.

[29] Aharoni, S. M. *Synthesis, Characterization and Theory of Polymeric Networks and Gels;* S. M. Aharoni, Springer, New York, 1st edition, **1992**.

[30] D. Díaz Díaz *Nanochemistry and functional soft materials: synthesis and applications*; Talk, Regensburg, **2010**.

[31] de Loos, M.; Feringa, B. L.; van Esch, J. H. *Eur. J. Org. Chem*. **2005**, *17*, 3615-3631.

[32] Feng, C.-L.; Dou, X.; Zhang, D.; Schoenherr, H. *Macromol. Rapid Comm.* **2012**, *33*, 1535-1541.

[33] Newbloom, G. M.; Weigandth, K. M.; Pozzo, D. C. *Macromolecules* **2012**, *45*, 3452-3462.

[34] Chen, W.; Gong, W.; Ye, J.; Lin, Y.; Ning, G. *RSC Adv.* **2012**, *2*, 809-811.

[35] Ikeda, M.; Tanida, T.; Yoshii, T.; Hamachi, I. *Adv. Mater.* **2011**, *23*, 2819-2822.

[36] Mirakyan, A.; Sullivan, P. F.; Hutchins, R. D.; Lin, L.; Tustin, G. J.; Drochon B. WO2012075154, **2012**.

[37] Wang, P.; Chen, Z.; Li, J.; Wang, L.; Gong, G.; Zhao, G. Liu, H.; Theng, Z. *Ann. Microbiol.* **2013**, *63*, 957-964.

[38] Zou, J.; Zhang, F.; Chen, Y.; Raymond, J. E.; Zhang, S.; Fan, J.; Zhu, J.; Li, A.; Seetho, K.; He, X.; Pochan, D. J.; Wooley, K. L. *Soft Matter* **2013**, *9*, 5951-5958.

[39] Zhang, W.; Gonzalez, S. O.; Simanek E. E. *Macromolecules* **2002**, *35*, 9015-9021.

[40] Song, F.; Zhang, L.-M.; Li, N.-N.; Shi, J.-F. *Biomacromolecules* **2009**, *10,* 959-965.

[41] Lee, H. Y.; Nam, S. R.; Hong, J.-I. *J. Am. Chem. Soc.* **2007**, *129*, 1040-1041.

[42] Miravet, J. F.; Escuder, B. *Org. Lett.* **2005**, *7*, 4791-4794.

[43] Miravet, J. F.; Escuder, B. *Tetrahedron Lett.* **2007**, *63*, 7321-7325.

[44] Love, C. S.; Chechik, V.; Smith, D. K.; Ashworth, I.; Brennan, C. *Chem. Commun.* **2005**, 5647.-5649.

[45] Rodríguez-Llansola, F.; Escuder, B.; Miravet, J. F. *Org. Biomol. Chem.* **2009**, *7*, 3091-3094.

[46] Wang, G.; Kuroda, K.; Enoki, T.; Grosberg, A.; Masamune, S.; Oya, T.; Yakeoka, Y.; Tanaka, T. *Proc. Natl. Acad. Sci. U. S. A.* **2000**, *97*, 9861-9864.

[47] Kühbeck, D.; Saidulu, G.; Rajender Reddy, K.; Díaz Díaz, D. *Green Chem.* **2012,** *14*, 378-392.

[48] Bhat, S.; Maitra, U. *Molecules* **2007**, *12*, 2181-2189.

[49] Goldmann, E.; Baumann, E. *Physiol. Chem.* **1888**, *12*, 253-261.

[50] Menger, F. M.; Caran, K. L. *J. Am. Chem. Soc*. **2000,** *122*, 11679-11691.

[51] Diaz Diaz, D.; Morrin, E.; Schön, E.-M.; Budin, G.; Wagner, A.; Remy J.-S. *J. Mater. Chem.* **2011**, *21*, 641-644.

[52] Wang, H.; Li, X.; Fang, F.; Yang. Y. *Dalton Trans.* **2010**, *39*, 7294-7300.

[53] Piepenbrock, M.-O. M.; Clarke, N.; Foster, J. A.; Steed, J. W. *Chem. Commun.* **2011**, *47*, 2095-2097.

[54] Terech, P.; Pasquier, D.; Bordas, V.; Rossat, C. *Langmuir* **2000**, *16*, 4485-4494.

[55] Yan, N.; Xu, Z.; Diehn, K. K.; Raghavan, S. R.; Fang, Y.; Weiss, R. G. *Langmuir* **2013**, *29*, 793-805.

[56] Terech, P.; Furman, I.; Weiss, R. G.; Bouas-Laurent, H.; Desvergne, J. P.; Ramasseul, R. *Faraday Discuss.* **1995**, *101*, 345-358.

[57] Hanabusa, K.; Itoh, A.; Kimura, M.; Shirai, H. *Chem. Lett*. **1999**, *8*, 767-768.

[58] de Loos, M.; van Esch, J.; Stokroos, I.; Kellogg, R. M.; Feringa, B. L. *J. Am. Chem. Soc.* **1997**, *119*, 12675-12676

[59] Hanabusa, K.; Maesaka, Y.; Suzuki, M.; Kimura, M.; Shirai, H. *Chem. Lett*. **2000**, *10*, 1168-1169.

[60] Jeong, S. W.; Murata, K.; Shinkai, S. *Supramol. Sci.* **1996**, *3*, 83-86.

[61] Kolb, H. C.; Finn, M. G.; Sharpless, K. B.; *Angew. Chem. Int. Ed*. **2001**, *40*, 2004-2021.

[62] Díaz Díaz, D.; Rajagopal, K.; Strable, E.; Schneider, J.; Finn, M. G. *J. Am. Chem. Soc*. **2006**, *128*, 6056-6057.

[63] Hanabusa, K.; Yamada, M.; Kimura, M.; Shirai, H. *Angew. Chem. Int. Ed*. **1996**, *35*, 1949-1950.

[64] Díaz Díaz, D.; Cid, J. J.; Vázquez, P.; Torres, T. *Chem. Eur. J*. **2008**,*14*, 9261- 9273.

[65] Debnath, S.; Shome, A.; Dutta, S.; Das, P. K. *Chem. Eur. J.* **2008**, *14*, 6870-6881.

[66] Piepenbrock, M.-O. M.; Lloyd, G. O.; Clarke, N.; Steed, J. W. *Chem. Commun.* **2008**, *23*, 2644-2646.

[67] Segarr-Maset, M. D.; Nebot, V. J., Miravet, J. F., Escuder, B. *Chem. Soc. Rev.* **2013**, *42*, 7086-7098.

[68] Foster, J. A., Piepenbrock, M.-O. M.; Lloyd, G. O.; Clarke, N.; Howard, J. A. K., Steed, J. W. *Nat. Chem.* **2010**, *2*, 1037-1043.

[69] Rodríguez-Llansola, F.; Escuder, B.; Miravet, J. F. *Chem. Eur. J.* **2010**, *16*, 8480-8486.

[70] Rodríguez-Llansola, F.; Escuder, B.; Miravet, J. F. *J. Am. Chem. Soc.* **2009**, *131*, 11478-11484.

[71] Takahashi, A.; Sakai, M.; Kato, T. *Polym. J.* **1980**, *12*, 335-341.

[72] Bao, C.; Lu, R.; Jin, M.; Xue, P.; Tan, C.; Xu, T.; Liu, G.; Zhao, Y. *Chem. Eur. J* **2006**, *12*, 3287-3294.

[73] Mezger, G. *The Rheology Handbook;* Vincentz Network, Hannover, Germany, 3rd edition, **2011**.

[74] Bawa, P.; Pilay V.; Choonara, Y. E.; du Toit, L. C. *Biomed. Mater.* **2009**, *4*, 1-15.

[75] Cohen Stuart, M. A.; Huck, W. T. S.; Genzer, J.; Mueller, M.; Ober, C.; Stamm, M.; Sukhorukov, G. B.; Szleifer, I.; Tsukruk, V. V.; Urban, M. *Nat. Mater.* **2010**, *9*, 101-113.

B Ca-based metallogel and metal organic framework

1. Preface

The results of this chapter have already been published in *J. Mater. Chem.* **2012**, *22*, 14951-14963 with the title: "*Fine-tuning the balance between crystallization and gelation and enhancement of CO_2 uptake on functionalized calcium based MOFs and metallogels*". This publication was the result of a collaboration between the group of Prof. Dr. Rahul Banerjee and his students Arijit Mallic and Tamas Panda from the Physical/Materials Chemistry Division at National Chemical Laboratory in Pune, India and the group of Prof. Dr. David Díaz Díaz with his student Eva-Maria Schön from the Institut für Organische Chemie at Universität Regensburg, Germany. Further K. Sreenivas from Complex Fluids and Polymer Engineering, Polymer Science & Engineering Division at National Chemical Laboratory, India, contributed to the publication.

Eva-Maria Schön was involved in the preparation and characterization of the gel materials, including the study and optimization of the gelation properties, stability and responsiveness studies, electron microscopy imaging, comparative FT-IR, TGA and digital imaging of the materials.

2. Background

Recently, the interest in tuning the properties of LMW gels has increased. One possibility is the use of additives such as metal cations, small inorganic anions and ion pairs as in metal salts. Any LMWG based gel which incorporates metallic elements can be called metallogel.[1,2] Similar to LMW metallogels, metal-containing materials exist without the incorporation of solvent and have already been known for more than 50 years. In 1965, E. A. Tomic reported about some new porous, crystalline materials, which he called coordination polymers.[3] Three decades later they were named metal-organic frameworks, MOFs', metal-organic polymers and supramolecular structures.[4] Basically they are build up by metal ions which are linked together by multidentate LMW organic ligands (Scheme 8).

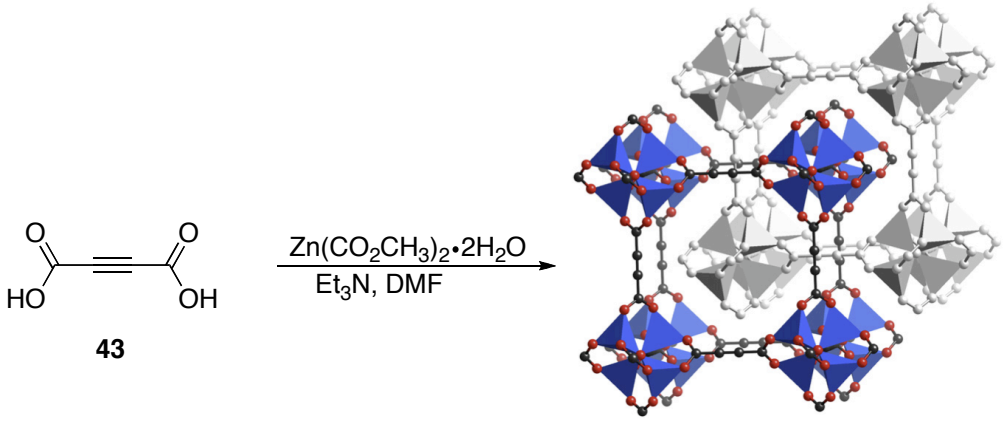

Scheme 8: Example for preparation and structure of MOF from acetylenedicarboxylic acid **43** and zinc acetate. In the MOF carbon atoms are shown as black, oxygen atoms as red and zinc atoms as blue balls.[5]

The interest for these MOFs were growing over the past years. Their uniform channels, high porosity, excellent thermal stability and chemical tailorability[6] make MOFs promising materials for application in gas adsorption,[7] in the separation and purification of gases,[8] heterogeneous catalysis,[9] drug delivery[10] and sensors,[11,12] but their brittle nature makes their use in industrial fields challenging. The combination of MOFs with further functional materials is also difficult as it often results in pore blocking and decrease of the inner surface area.[13]

A way to solve this problem is to use viscoelastic materials as metallogels, where the empty porous space of MOFs is filled with solvent molecules instead. The success of

this development was already applied in catalysis.[14] Further fields where the advantages of metallogels were adopted are for example photophysics,[15] sensing,[16] magnetic materials,[17] redox responsiveness[18] and electron emission.[19]

All of this is possible, because of the two-phase nature of the metallogels, which may enable recovering and recycling. Furthermore, the small reagents have a higher access to the highly solvated porous network compared to standard heterogeneous catalyst materials.

The focus of this chapter lies on the investigation of the equilibrium between crystallization and gelation and the possible fine-tuning based on the solvent composition. The preparation of the metal-organic functional materials, MOF and metallogel, is described as well as their characterization. Furthermore, their ability to adsorb gasses and to act as catalytic species is reported.

3. Results and discussion

3.1 Preparation of Ca-5TIA materials

For the synthesis of MOFs it needs the combination of metal cations as connectors and organic polyanions with metal coordination ability as linkers. Examples would be carboxylates, phosphonates and sulfonates. Aromatic carboxylates are useful building blocks for the synthesis of stable MOFs, because they contribute remarkably to the rigidity of the MOF. A combination of hydrogen bonding, π-π and metal-ligand interactions offer cooperative stabilization and this is a effective basic approach for the synthesis of gel-phase materials.[20] For this reason a *N*-heterocyclic, 1,2,4-triazole- and carboxyl-group-containing ligand, 5TIA, was chosen for the construction of new MOFs with template-based structural conversions.[21] The synthesis of the 5TIA ligand **46** was reported previously[22] and is formed by reaction of **44** with 5-aminoisophthalic acid **45** (Scheme 9) under release of two molecules dimethylamine **47**.

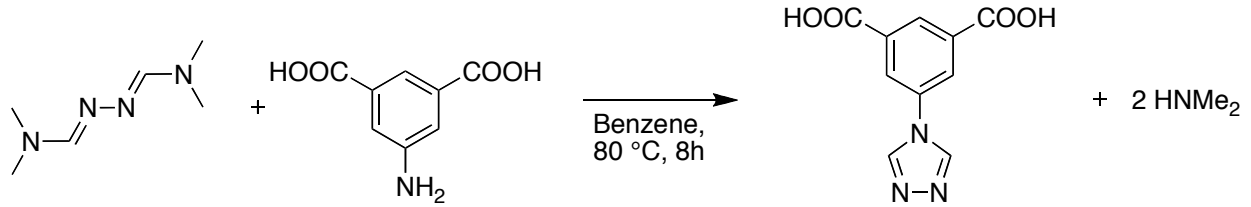

44 **45** **46** **47**

Scheme 9: Synthesis of 5TIA ligand **46**.

The 5TIA ligand provides both, nitrogen and oxygen donor atoms and therefore it is open to coordination with soft and hard metals.[23] This enabled the formation of different functional heterometallic coordination polymers.[24] The combination of the described 5TIA ligand with a hard metal like calcium offers the preparation of the respective MOF, Ca-5TIA-MOF and a novel metallogel, Ca-5TIA-Gel. This is of special interest, as up to now reports on calcium-based 3D MOFs are limited compared to other metals.[25-37] Additionally, calcium is not only non-toxic, but also highly abundant in nature (3.4% of the earth crust).[38] For example Lin and co-workers[35] reported new 3D MOFs based on Ca(II) cations and aromatic carboxylic acid ligands. These MOFs undergo remarkable destruction/construction structural transformations including a break and reformation of the Ca-O bond. Also other examples of MOFs exist where the Ca ion is connected to

anthraquinone-2,6-disulfonate[34] or 4,4′-(hexafluoroisopropylidene)bis(benzoic acid)[35] ligands.

On the one hand, Ca-5TIA-MOF as colorless crystals were obtained by stirring $Ca(CH_3CO_2)_2$ and 5TIA as ligand in a DMF/water-mixture (v/v 1 : 1) for 48 h at 85 °C (Figure 25, top). An accurate amount of water is essential for the crystal formation as DMF/ water mixtures with a water content < DMF content resulted in precipitation. On the other hand, gelation was observed when pure DMF was used instead of a mixture of solvents. At a concentration of 0.2 mol L^{-1} $Ca(CH_3CO_2)_2$, 5TIA and DMF were sonicated at RT for 30 ± 5 min. The material did not flow by inversion of the test tube[39] (Figure 25, bottom) and the gel nature was also testified by rheological measurements.

The solvent molecules entrapped inside the network structures of the gel are immobilized. Experiments confirmed that 5TIA is not capable of gelling DMF by its own, but only in combination with calcium cations a coordination polymer is developed which grows to a 3D gel network and enables gelation.

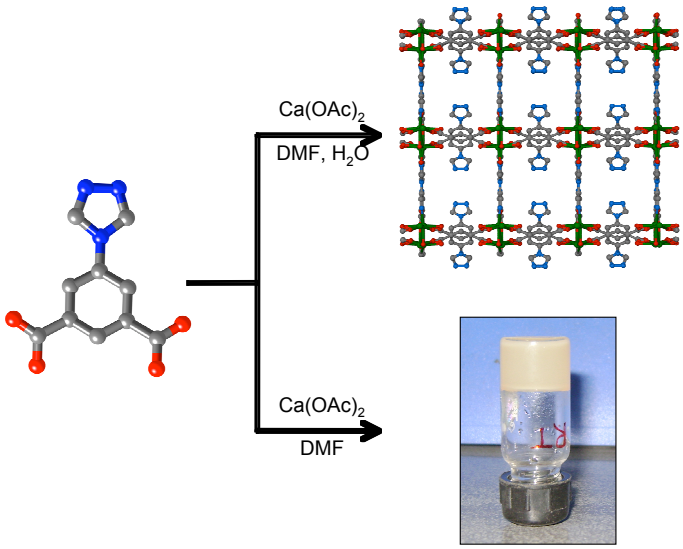

Figure 25: Preparation of Ca-5TIA-MOF (top) and Ca-5TIA-Gel (bottom).

Ca-5TIA-Gels can be obtained at different temperatures between RT and 150 °C (Figure 26b-f). All gels showed to be thermo-irreversible and both, look and microstructure were influenced by the preparation temperature. At RT bright pinkish gels were obtained (Figure 26b), at 120 °C yellowish gels were produced (Figure 26e).

Independent from the temperature, sonication of the mixture $Ca(CH_3CO_2)_2$ and 5TIA in the appropriate solvent provided more homogeneous gel samples then without

sonication. The minimum gelation concentration, MGC, for the equimolar mixture of $Ca(CH_3CO_2)_2$ and 5TIA in DMF was determined as 0.1 mol L^{-1}. That means that up to 258 solvent-molecules can be immobilized by one ligand-molecule.

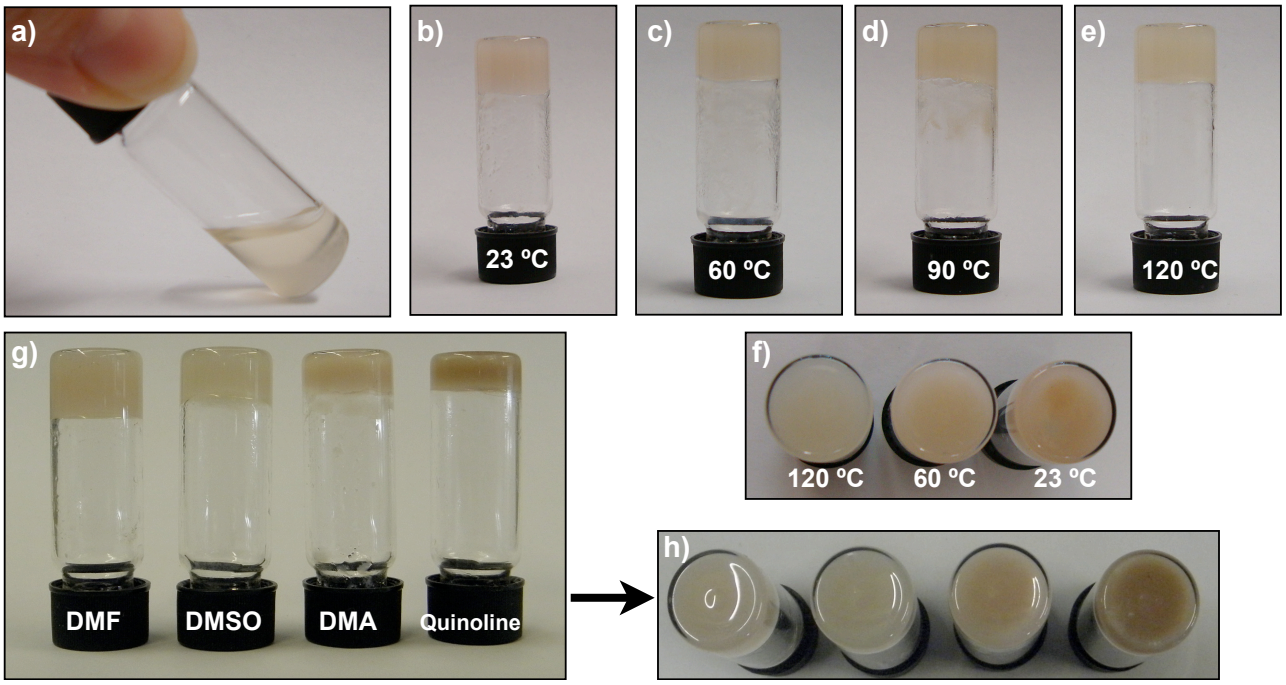

Figure 26: a) Picture of white solution obtained by mixing of 0.1 mmol $Ca(CH_3CO_2)_2$, 0.1 mmol 5TIA and 1.0 mL DMF upon sonication at RT for 15 min. b) Gels formed at RT , c) 60 °C, d) 90 °C and e) 120 °C in an oil bath for 2 h. f) Gels at RT, 60 °C and 120 °C are shown upside-down. g) and h) show gels from DMF, DMSO, DMA and quinoline at a concentration of 0.5 M.

3.2 Characterization of Ca-5TIA materials

The gelation ability of the gelator system $Ca(CH_3CO_2)_2$ and 5TIA was examined for 22 different solvents (Table 2). For this, sonication at RT for 15 min at concentrations between 0.1 and 0.5 mol L^{-1} of the gelator system were tested. In the end five solvents were gelled: DMF, DMSO, DMA, quinoline and DEF (entries 2-5,10) (Figure 26g). Both, 5TIA ligand and $Ca(CO_2CH_3)_2$ provided clear solutions in distilled water (entry 1). In all other solvents the gelator system was insoluble.

Specific solvent-gelator interactions are accounted by the Kamlet-Taft parameters (Table 14, page 173f).[40,41] They consist of three different parameters. The parameter α describes the hydrogen bond donor ability of the solvent, which is crucial in 3D networks held together by hydrogen bonding. The hydrogen bond acceptor ability is defined by the β

parameter. This parameter can also be connected with the thermal stability of a gel. The polarizability, which is related to the solvation process during the gelation phenomenon, is shown by parameter π*.

For the gelator system $Ca(CH_3CO_2)_2$ and 5TIA it can be seen on Table 2 that solvents with small α and at the same time high β and π* values are necessary for the assembly of a 3D network and therefore for the gelation. Independent from β and π* parameters, a high α parameter leads to either dissolving (Table 2, entry 1) or has at least the tendency to dissolve it (entries 7-9). Solvents with a moderate or no hydrogen donating bonds to the gelator at all and only low up to moderate hydrogen bond acceptor ability and/or polarizability resulted in insolubility of the gelator system (entries 11-22). Besides this, the ionic liquid with moderate α and low β value (entry 6) showed conspicuous aberration from the rule, because after additional heating with heat gun a partial gel was obtained.

Gelation ability under the influence of water was also tested. For this, a ratio of water : DMF of 1:20 (v/v) discovered to be the maximum. Above this limit no gelation was observed, but precipitation and crystallization. This shows how delicate the balance between crystallization and gelation is for this case.[42]

The stability of the Ca-5TIA-Gels at RT under dark conditions was at least 1.5 months. For potential application of Ca-5TIA in catalysis, the stability in contact with other solvents was tested. For this, small pieces of gels prepared in DMF by sonication at RT were placed in glass vials and covered with different solvents. Only the addition of water resulted in dissolving of the gels. Vigorous stirring resulted in fragmentation of the gel into smaller pieces. That was observed for most of organic solvents within 1 h in the following order: Methanol ~ tetrahydrofuran ~ dichloromethane ~ toluene ~ acetone > 1,4-dioxane ~ acetonitrile ~ ethyl acetate ~ DMF ~ triethylamine, whereas in chloroform the gel showed stability up to 3 h.

Table 2: Gelation ability of gelator system $Ca(CH_3CO_2)_2$ and 5TIA in various solvents.[a]

						Kamlet-Taft parameters		
Entry	Solvent	Result[b]	Conc.[c]	Time[d]	Color	α	β	π*
1	Water	S	0.2-0.5	-	-	1.17	0.47	1.09
2	DMF	G	0.2	30 ± 5 min	Pinkish	0.00	0.69	0.88
3	DMSO	G	0.4	10 ± 5[e] min	Brownish	0.00	0.76	1.00
4	DMA	G	0.67	24-48[f] h	Pinkish	0.00	0.76	0.88
5	Quinoline	G	0.5	10 ± 5[e] min	Brownish	0.00	0.64	0.92
6	[BMIM][PF_6]	G + P	0.2-0.5	-	White	0.63	0.21	1.03
7	Methanol	I[g]	0.2-0.5	-	-	0.98	0.66	0.60
8	Ethanol	I[g]	0.2-0.5	-	-	0.86	0.75	0.54
9	*i*-Propanol	I[g]	0.2-0.5	-	-	0.76	0.84	0.48
10	DEF	G	0.5	90 ± 15 min	-	-[h]	-[h]	-[h]
11	Acetone	I	0.2-0.5	-	-	0.08	0.43	0.71
12	Tetrahydrofuran	I	0.2-0.5	-	-	0.00	0.55	0.58
13	*n*-Hexane	I	0.2-0.5	-	-	0.00	0.00	-0.04
14	Diethyl ether	I	0.2-0.5	-	-	0.00	0.47	0.27
15	1,4-Dioxane	I	0.2-0.5	-	-	0.00	0.37	0.55
16	Cyclohexane	I	0.2-0.5	-	-	0.00	0.00	0.00
17	Ethyl acetate	I	0.2-0.5	-	-	0.00	0.45	0.55
18	Dichloromethane	I	0.2-0.5	-	-	0.13	0.10	0.82
19	Chloroform	I	0.2-0.5	-	-	0.20	0.10	0.58
20	Benzene	I	0.2-0.5	-	-	0.00	0.10	0.59
21	Toluene	I	0.2-0.5	-	-	0.00	0.11	0.54
22	Acetonitrile	I	0.2-0.5	-	-	0.19	0.40	0.75

[a]Upon sonication at RT for 15 min. After this time bath temperature was 27 ± 1 °C. [b]Abbreviations: S = solution, G = gel, I = insoluble (upon sonication with or without further heating with heat gun), P = precipitate. [c]Molar concentration of gelator system for gelation tests [mol·L^{-1}]. [d]Time required for gelation. [e]Gelation occurred during sonication. [f]Sonication was applied for 30 min at 50 °C. [g]A white viscous blend was obtained. [h]Unknown value.

In contrast, DMSO, toluene, cyclohexane, *n*-hexane and diethyl ether did not cause any fragmentation of the gel within 5 days and made them interesting media for use in catalytic experiments. DMSO was the solvent in which the gel showed the best stability against mechanical stirring. Only the gel covered with diethyl ether obviously changed the refraction index, as the gel became more white and opaque.

Furthermore, the exchange of $Ca(CH_3CO_2)_2$ by other calcium salts was under investigation. The gelation ability was tested with 0.1 mmol of calcium salt and 0.1 mmol of 5TIA in 1.0 mL DMF. $Ca(OH)_2$, CaO, $CaSO_4$, $CaCl_2$, $CaCO_3$ and $Ca(NO_3)_2$ were used for the experiment. Besides $Ca(CH_3CO_2)_2$ only $Ca(OH)_2$ and CaO were able to form gels. $CaCl_2$ and $Ca(NO_3)_2$ provided solutions and with $CaSO_4$ and $CaCO_3$ inhomogeneous mixtures were obtained.

UV-Vis and fluorescence spectroscopy

In contact with visible light the light pinkish, opaque Ca-5TIA-gel showed a color intensification over time (Figure 27d), which can be avoided when stored under dark conditions. The color change could be explained by intra-ligand or ligand-metal charge transfer when in contact with light.

More information about this process was collected by the measurement of UV-Vis and fluorescence spectra of Ca-5TIA-Gels at different aging times. The spectra of the ligand in DMF showed one broad absorption at 346 nm, which may belong to an intra-ligand orbital transition from *n* to π* and π to π* (Figure 27a). In contrast, Ca-5TIA-Gels had a phenyl ring absorption peak at 290 nm and a small bump at 346 nm, which could be caused by a free ligand (Figure 27b). With increasing exposure to light a clear decrease in intensity of the peak at 290 nm was observed. This is a sign for the blockade of π to π* or *n* to π* transitions between the aromatic moiety, conjugated with the lone-pair electrons of the triazole unit, or the unsaturated bonds of the carbonyl groups.

Figure 27c shows the fluorescence emission for 5TIA ligand (black) and Ca-5TIA-Gel (red). The fluorescence emission at 356 nm supposed to be a product of intra-ligand fluorescent emission. It can be seen for the free ligand and is quenched in the gel, because of the coordination of the ligands to the metal.

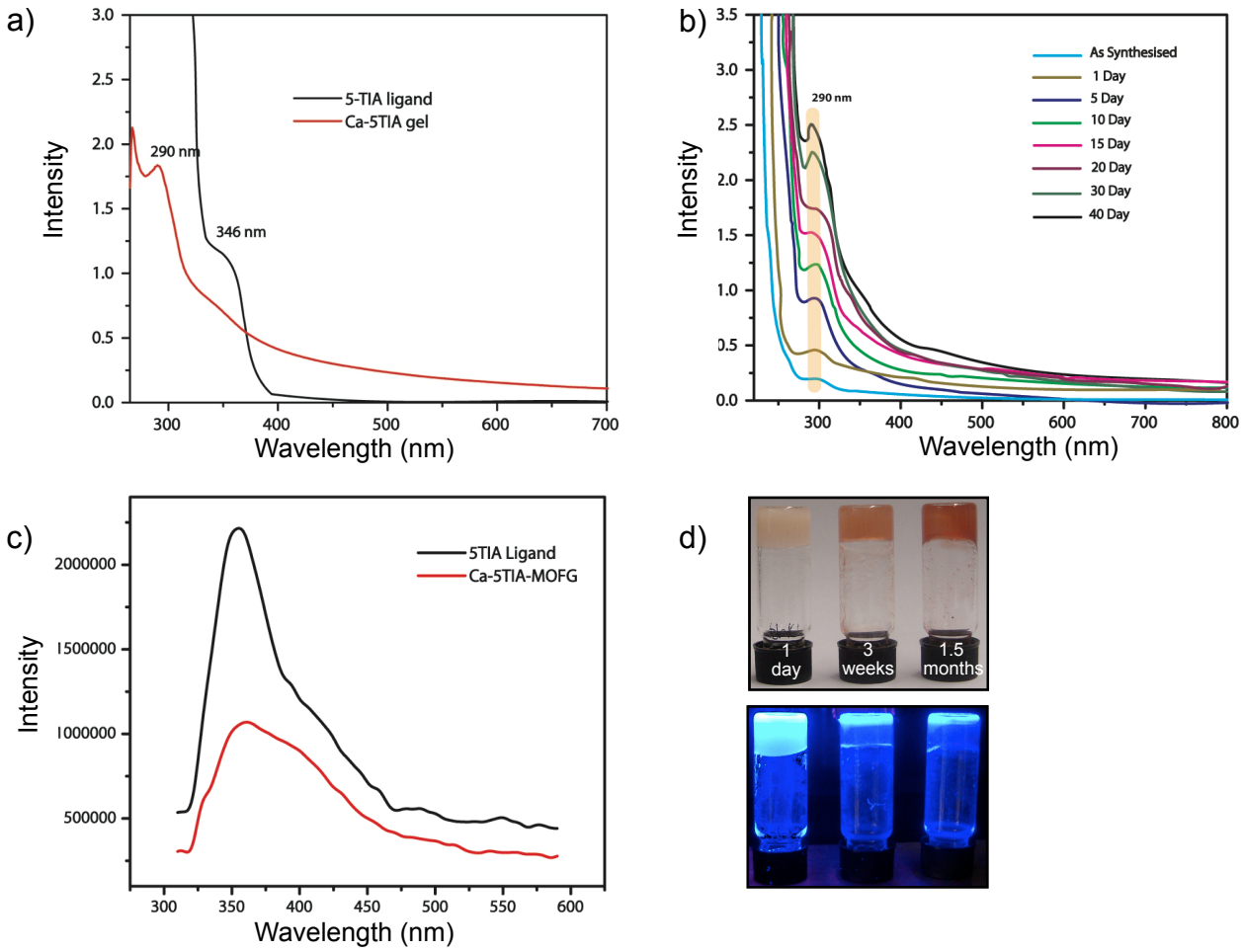

Figure 27: a) UV-Vis spectra of 5TIA ligand (black line) and Ca-5TIA-Gel (red line). b) UV-Vis spectra of Ca-5TIA-Gels at different aging times. c) Fluorescence spectra of 5TIA ligand (black line) and Ca-5TIA-Gel (red line). d) Picture of Ca-5TIA-Gels from DMF after 1 day, 3 weeks and 1.5 month (top) and pictures of the same gels under UV-light (bottom).

Thermal stability

Ca-5TIA-MOF was prepared at gram scale for detailed investigation of the 3D structure, chemical, thermal and mechanical stability. Thermal gravimetric analysis (TGA) for Ca-5TIA-MOF pointed out that these compounds have a high thermal stability (Figure 28). The TGA analysis for Ca-5TIA-MOF visualized a distinct weight-loss of 15% (90–160 ºC). That correlates with the evaporation of solvent molecules, water and DMF, on the MOF surface and the pores. The second weight-loss step of 27% (330–400 ºC) was caused by the collapse of the framework, which was also observed in the case of the Ca-5TIA-Xerogel (38% weight loss). Decomposition of the 5TIA ligand in Ca-5TIA-MOF and

Ca-5TIA-Gel resulted in the weight loss steps up to 800 °C. The the remaining residue belonged to calcium oxide. As solvent molecules were only weakly bound in the gel state, a gradual weight-loss over a broad temperature range (15%, 30-160 °C) was shown for Ca-5TIA-Gel. In contrast, the solvent molecules entrapped inside the crystalline Ca-5TIA-MOF needed a much smaller temperature range to leave the framework.

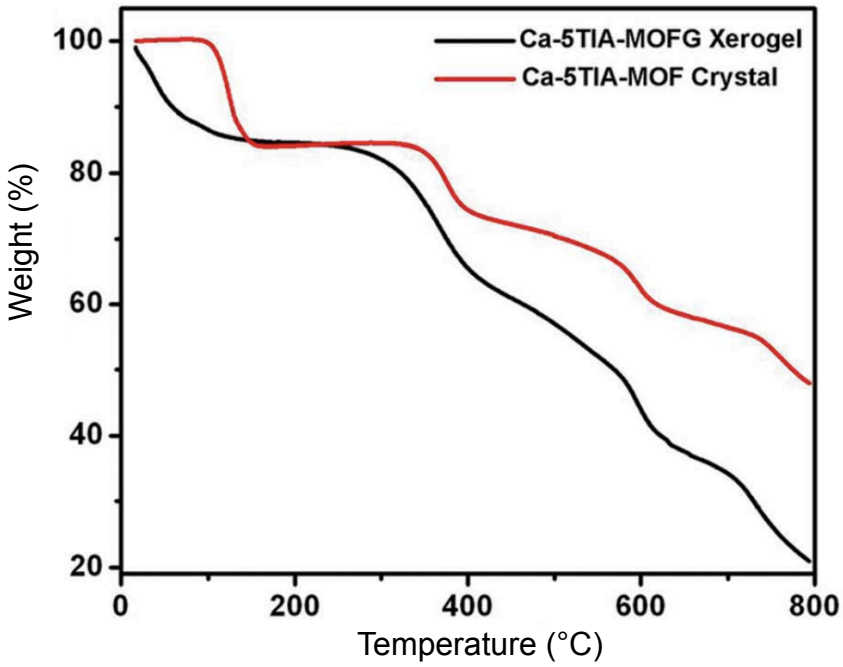

Figure 28: TGA analysis of Ca-5TIA-Xerogel (black line) and Ca-5TIA-MOF (red line).

Fourier transform infrared spectroscopy (FT-IR)

FT-IR was carried out for Ca-5TIA-Gel, Ca-5TIA-Xerogel, 5TIA and $Ca(CO_2CH_3)_2$ (Figure 29). Ca-5TIA-Gel and Ca-5TIA-Xerogel seemed to be virtually identical which points out that the internal structures are the same and that the internal structure of the gel was preserved during the preparation of the xerogel. The Carboxylate groups were shown in the coordination sphere of the metal. More than 95% of the carboxylic groups of 5TIA were deprotonated in the MOFs materials. C=O stretching frequency of free aromatic carboxylic acid of 5TIA was visible at *ca.* 1699 cm^{-1}. The coordination of carboxylic acid to metal atoms was confirmed by a shift to lower frequencies of the C=O stretching frequency (about 1550 cm^{-1}). That was shown for Ca-5TIA-Gel and Ca-5TIA-Xerogel. The overlap of the triazole and the C=O stretching frequency was supposed to be in the range of 1540-1550 cm^{-1}.

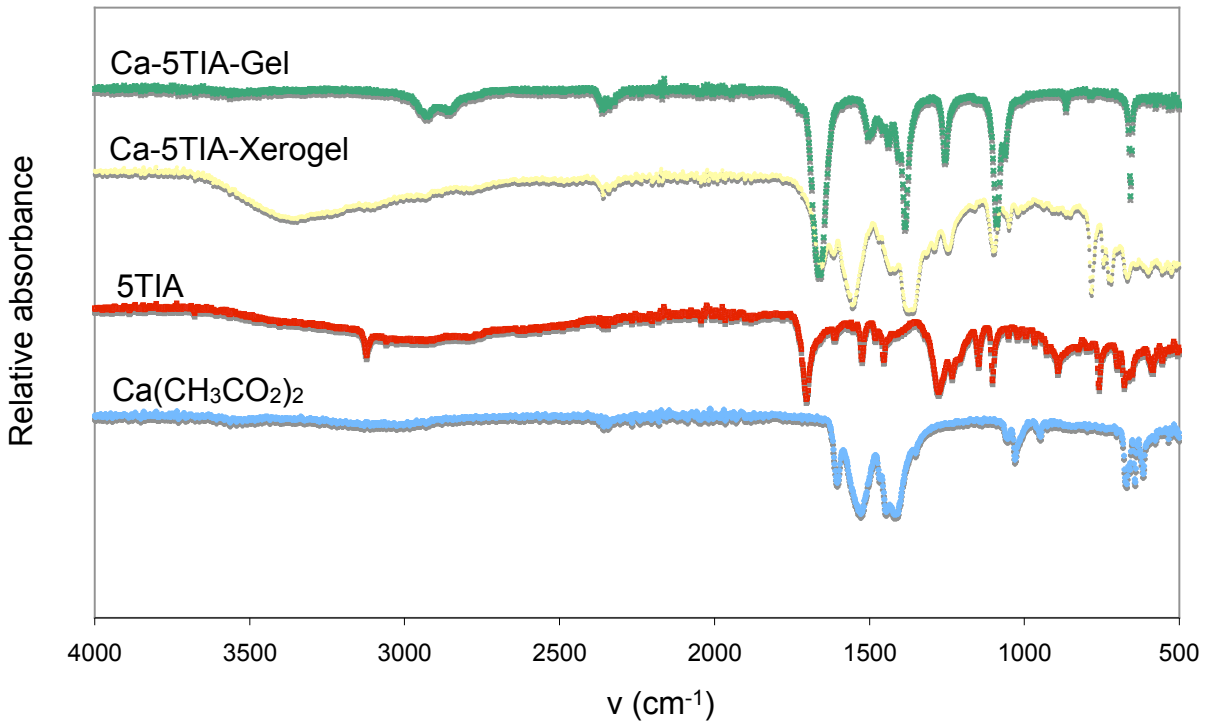

Figure 29: FT-IR spectra of Ca-5TIA-Gel (green), Ca-5TIA-Xerogel (yellow), 5TIA ligand (red) and $Ca(CH_3CO_2)_2$ (light blue).

Rheological measurements

Rheological behavior was measured to confirm the gel nature and to investigate the change in gel structure during aging. Intense pre-shearing before the rheological measurements ensured a well-defined initial state of the gel sample. The frequency dependence was very weak for storage modulus G′ right after the pre-shearing. The gel nature was confirmed as the loss modulus, G″, was lower than storage modulus, G′. G″ had a minimum at high frequencies (ω between 10 and 100 rad s^{-1}, Figure 30a). Unfortunately, the loss modulus was not significantly lower than the storage modulus and it was likely that the solid-like respond resulted from the Ca-5TIA network while the dissipation was a result of associated solvent molecules.[43]

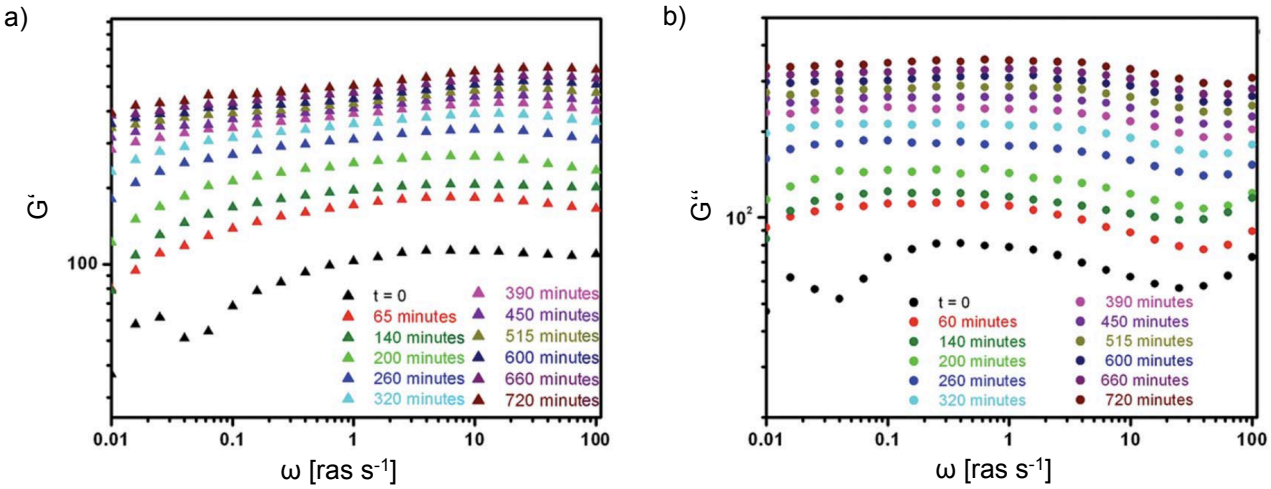

Figure 30: Rheology studies show plot of G‘ (a) and G“ (b) with aging time.

Morphological characterization

To get insight into the microstructure, SEM and TEM images of Ca-5TIA-MOF and Ca-5TIA-Gel were taken. For this, the Ca-5TIA-Gel first had to be transformed into Ca-5TIA-Xerogel by freezing the Ca-5TIA-Gel material in liquid nitrogen and subsequent drying under vacuum for removing the solvent. In most cases, a gel is build up by 1D aggregates which assembly further to create a 3D network.[44-46] One possible way to influence the microstructure is a change in the experimental protocol. Regardless of the preparation temperature, Ca-5TIA-Gels showed a high homogeneity of the fibrillar network (Figure 31a-d *vs.* e-i). In cases where only 0.75 equivalents of ligand in respect to $Ca(CO_2CH_3)_2$ were used instead of 1.0 equivalents, structures with much higher density were formed and increased with preparation temperature (Figure 31j-l). Compared to a short time at high temperature, an extended period of heating resulted in a more compact material without visible bundles, because of changes of the well-defined fibrillar clusters (Figure 31f-g *vs.* h). This evolution was also seen when samples were stored at 4 °C after initial sonication, resulting in a cobbled paving and not in a developed fibrillar network (Figure 31i).

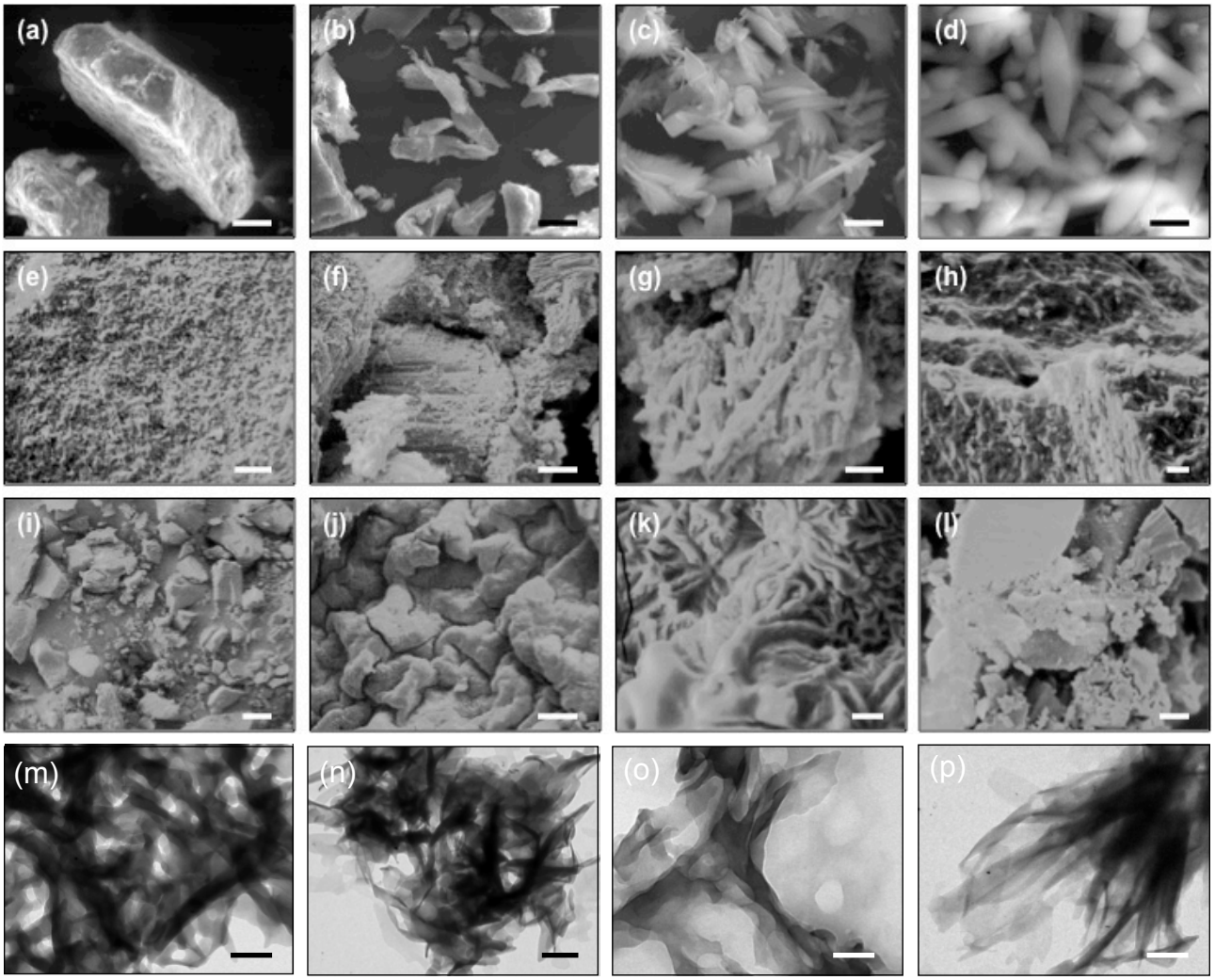

Figure 31: SEM, (a) - (l), and TEM, (m) - (p), images from Ca-5TIA-Xerogels prepared by freeze-drying of Ca-5TIA-Gels in 1 mL DMF under different conditions: (a) - (d) 0.2 mmol $Ca(CH_3CO_2)_2$ + 0.2 mmol 5TIA, US at RT fro 15 min. (a) storage at 30 °C (peach colored gel, scale bar = 50 µm). (b) storage at 60 °C (peach colored gel, scale bar = 30 µm). (c) storage at 90 °C (peach colored gel, scale bar = 5 µm). (d) storage at 120 °C (bright yellow colored gel, scale bar = 10 µm). (e) - (i) 0.1 mmol $Ca(CH_3CO_2)_2$ + 0.1 mmol 5TIA, US at RT fro 15 min. (e) storage at RT (peach colored gel, scale bar = 2 µm). (f) - (g) storage at 120 °C for 2 h (scale bars: (f) = 5 µm and (g) = 2 µm). (h) storage at 120 °C for 20 h (yellow colored gel, scale bar = 2 µm). (i) storage at 4 °C (scale bar = 100 µm). (j) - (l) 0.1 mmol $Ca(CH_3CO_2)_2$ + 0.075 mmol 5TIA, US at RT fro 15 min. (j) - (k) storage at 120 °C for 3 h (bright yellow colored gel, scale bars: (j) = 20 µm and (k) = 1 µm). (l) storage at 60 °C for 2.5 h (bright peach colored gel, scale bar = 5 µm). (m) storage at RT (scale bar = 100 nm). (n) - (o) storage at 120 °C for 2 h (scale bars: (n) = 200 nm, (o) = 100 nm). (p) storage at 120 °C for 3 h (scale bar = 200 µm).

Powder X-ray diffraction

Single crystal X-ray diffraction, PXRD, was used to characterize both, Ca-5TIA-MOF and Ca-5TIA-Gel. The measured peaks of Ca-5TIA-Xerogel and Ca-5TIA-MOF were in agreement with all major peaks of the simulated PXRD peaks for Ca-5TIA-MOF. The matching of all major peaks indicates reasonably crystalline phase purity[47] for both Ca-5TIA materials. Unreacted starting material may cause additional PXRD signals of low intensity (Figure 32).

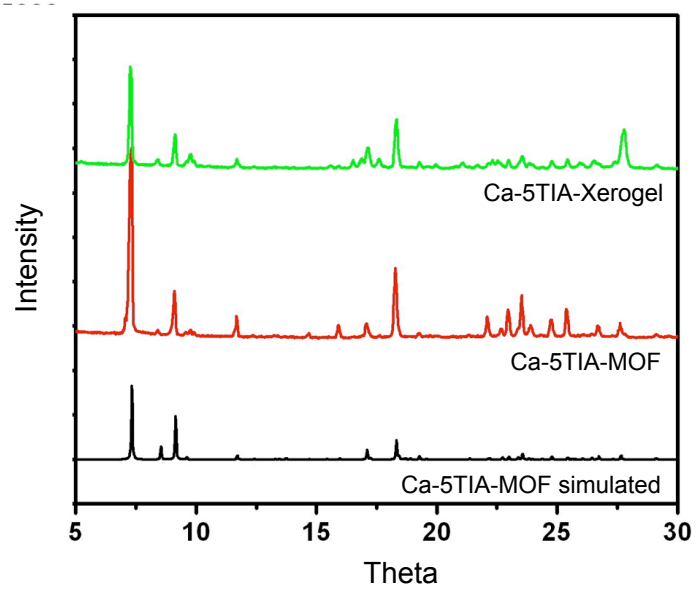

Figure 32: Comparison of PXRD patterns between Ca-5TIA-Xerogel (green), Ca-5TIA-MOF (red) and simulated pattern from the single-crystal structure (black).

Apart from that, the absence of water molecules during the gelation process as well as the influence of the counteranion in the stabilization of the gel makes it unlikely that the MOF structure was also retained in the Ca-5TIA-Gel. This assumption was proven by a failed gelation attempt where Ca-5TIA-MOF material was attempted to be converted into Ca-5TIA-Gel by sonication in DMF. Also the *in situ* coordination of the metal with the ligand and the solvation of the solvent molecules cannot be exactly reproduced by the Ca-5TIA-Xerogel. After one week only a partial gel was obtained from the xerogel. This could be caused by a structural change which is not visible by PXRD during the solvent evaporation. Another possible explanation would be the insoluble nature of the metal-complex system, which leads to a disability for the solvent to accommodate in the xerogel structure.

To get insight on the phase changes between Ca-5TIA-Gel and Ca-5TIA-Xerogel a *in situ* variable temperature PXRD was performed. The Ca-5TIA-Gel was measured at temperatures between 25 °C and 200 °C with a periodic interval of 25 °C (Figure 33). The collected pattern showed that around 100 °C the amorphous gel phase starts to convert into a crystalline xerogel. That means that an irreversible transformation of the amorphous Ca-5TIA-Gel due to removal of the solvent resulted in the crystalline Ca-5TIA-Xerogel. The small differences at temperatures > 100 °C are observed in consequence of removal of residual solvent molecules.

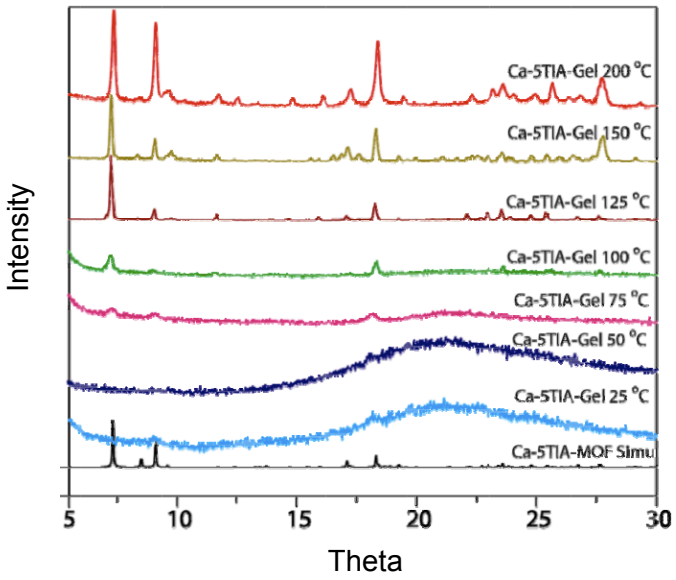

Figure 33: PXRD patterns of Ca-5TIA-Gel in a temperature range of 25-200 °C.

3.3 Application of Ca-5TIA materials in gas adsorption and catalysis

Gas adsorption

Gas uptake in both Ca-5TIA-MOF and Ca-5TIA-Gel was tested. The uptake of nitrogen, N_2, was not possible due to the aperture size of the micropores of Ca-5TIA-MOF. The pores had a similar, slightly smaller diameter, 3.6 Å, than the kinetic diameter of the N_2, 3.65 Å. In addition, the kinetic energy of N_2 was quite low at 77 K and molecules were unable to enter the pores. Remarkably, both materials were able to adsorb carbon dioxide, CO_2, and Ca-5TIA-MOF was the first reported MOF with the ability to uptake CO_2. The kinetic diameter of CO_2 (3.4 Å) allowed the uptake of the molecule in the Ca-5TIA-MOF. Figure 34 shows the comparison of adsorption properties between Ca-5TIA-MOF and

Ca-5TIA-Gel. Moreover, Ca-5TIA-Gel took up 20% more CO_2 (1.12 mmol/g for Ca-5TIA-MOF and 1.45 mmol/g for Ca-5TIA-Gel of CO_2 at 298 K and 1 atm pressure) when compared to the crystalline Ca-5TIA-MOF. This was also confirmed after several repetitions of the experiment.

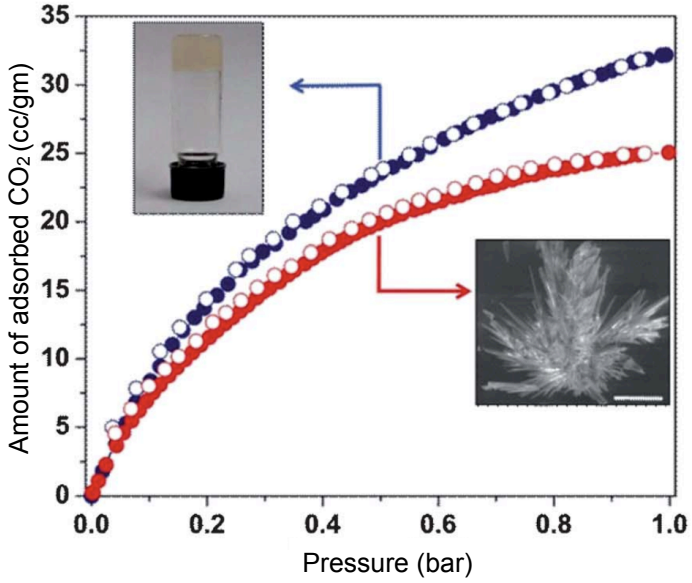

Figure 34: CO_2 adsorption isotherms (298 K) below 1.0 bar is shown in blue for Ca-5TIA-Gel and in red for Ca-5TIA-MOF. The filled circles represent the adsorption and the open circle the respective desorption.

Catalytic properties

The catalytic activity of Ca-5TIA-MOF and Ca-5TIA-Gel was also tested. They were both used as heterogeneous catalysts in the formation of benzyloxydiphenylsilane **50** by hydrosilylation reaction of benzaldehyde **48** with diphenylsilane **49** (Scheme 10).

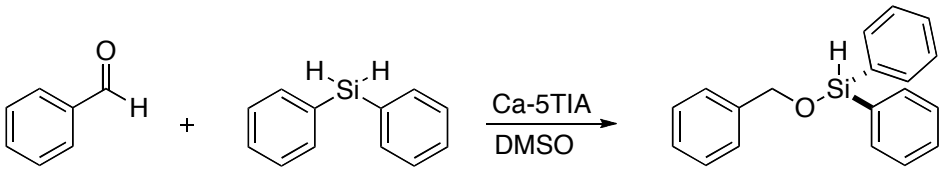

48 **49** **50**

Scheme 10: Atom-efficient hydrosilylation reaction.

As reaction medium DMSO was chosen, as it has proven before to provide the best stability for Ca-5TIA-Gel. The following three points have already been described as crucial factors for successful catalytic conversion with other Ca-based MOFs[34,36]:

1. The catalyst should provide macroporosity for low restriction in mass transport.
2. The Ca(II)-center serves as Lewis acid.
3. Coordinating solvent molecules like DMF offset the acidity of Ca(II) and enable the exchange of coordinating H_2O with other hard bases (carbonyl oxygens).

Ca-5TIA-MOF was able to catalyze the hydrosilylation, albeit with lower efficiency (about 10%) than reported before.[34,36] The reaction yielded up to 70% of the wanted silylated product within 24 h (Figure 35). Compared to the catalytic activity of the Ca-5TIA-Xerogel and Ca-5TIA-Gel, the xerogel exhibited moderately higher activity than Ca-5TIA-MOF and the gel showed a higher catalytic activity than the xerogel under comparable conditions (Figure 35):

$TOF_{1/2}$ (h^{-1}) = 0.71 (Ca-5TIA-MOF), 0.74 (Ca-5TIA-Xerogel), 1.09 (Ca-5TIA-Gel). This kind of enhanced performance in gel phase compared to solid or crystalline material has been reported for other metallogels before.[48]

Control experiments were carried out to prove that there was no leaching of the catalytic active species into solution. This was confirmed by a series of experiments where the reaction conditions (the amount of catalyst, solvent, temperature and duration) were simulated in the absence of reactants or in the presence of only one of the two reactants. For this, the catalyst (Ca-5TIA-MOF and in a second control experiment Ca-5TIA-Gel) was heated for 1 h in DMSO (65 ± 5 °C). Then the catalyst was filtered off and the liquid phase was used as reaction medium for the hydrosilylation reaction without further addition of catalyst species. For both control experiments, Ca-5TIA-MOF and Ca-5TIA-Gel, no conversion was observed. This pointed out that no leaching of the catalytic species took place, at least not above the minimum catalytic concentration. In addition, no further reaction was observed when the catalyst was removed from the reaction after 1h. Remarkably, the reaction conversion after the third run of recycling experiments was decreased less than 10% at a experimental error of ± 5%. Finally, PXRD measurement of the catalyst before and after the reaction confirmed that the catalyst did not suffer any significant damage.

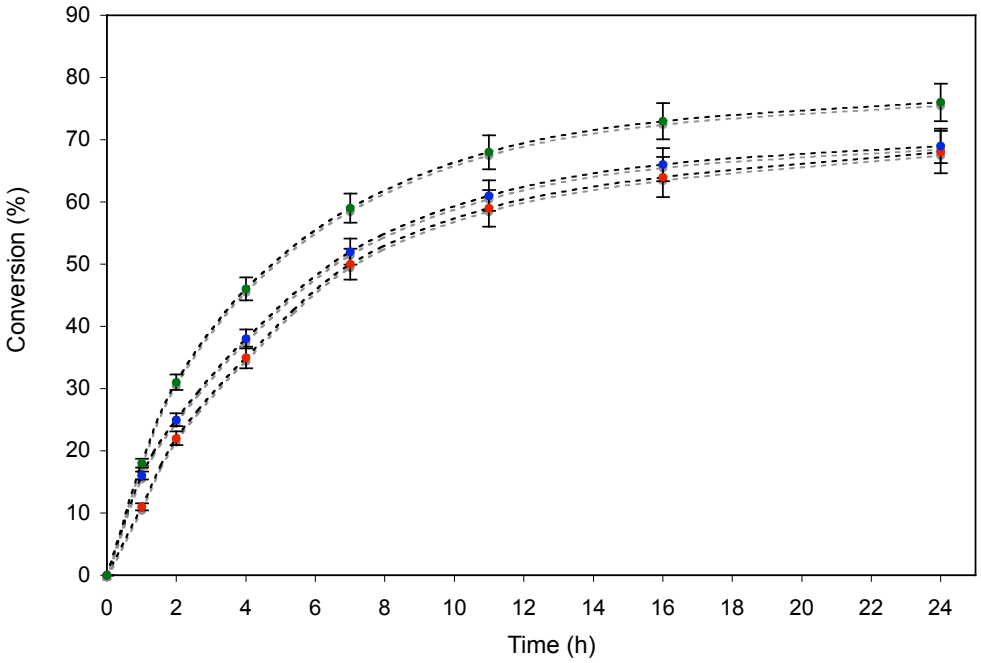

Figure 35: Kinetics for hydrosilylation reaction. Red dots are from catalysis with Ca-5TIA-MOF blue dots from Ca-5TIA-Xerogel and green dots from Ca-5TIA-Gel (catalyst loading = 10%).

4. Conclusion

In conclusion, it was demonstrated that 5TIA is a versatile ligand for the construction of new 3D MOFs and metallogels based on calcium. For the first time, a Ca-based MOF and metallogel synthesized from the same components, ligand and metal salt, were reported. Moreover, the first porous Ca-based MOF was described which was able to adsorb CO_2 at 1 atm pressure. Interestingly, Ca-5TIA-Xerogel provided 20% higher CO_2 uptake than crystalline Ca-5TIA-MOF on a molar basis. The MOF material has shown to be highly stable and to retain its crystallinity up to 400 °C as confirmed by TGA. Furthermore, Ca-5TIA-Gel also showed interesting thixotropic behavior and it is characterized by a dynamic gel microstructure, which evolves with aging time as demonstrated by rheological and X-ray scattering measurements. The match of Ca-5TIA-Xerogel and Ca-5TIA-MOF PXRD peaks with the simulated PXRD draws the conclusion that there are at least some common structural elements in the 3D network of xerogel and crystalline phases. That suggestion was also confirmed by the similarities of the FT-IR spectra. Though the absence of additional water during the gelation and the influence of the counterion in the stabilization of the gel as well as the failed gelation attempt using directly Ca-5TIA-MOF as gelator point out that gels and MOF materials possess modified internal structures. Remarkably, both synthesized materials provided modest catalytic activity in the hydrosilylation of benzaldehyde and diphenylsilane. The Ca-5TIA-Gels showed slightly enhanced catalytic performance when compared to Ca-5TIA-Xerogel and Ca-5TIA-MOF.

5. Experimental part

5.1 General remarks

Commercially available reagents and solvents for synthesis and analysis were used as received without further purification. Analytical thin layer chromatography TLC was performed on Merck TLC aluminum sheets with silica gel 60 F_{254}. For visualization UV light (254 nm) and phosphomolybdic acid as stain solution were used. For sonication a VWR™ ultrasonic cleaner (USC200TH) was used for preparation of the gels. For the recovery of the catalyst glass microfiber filters (GF/A) from Whatman® were used.

5.2 Preparation of Ca-5TIA materials

Synthesis of (1*E*,*N*'*E*)-*N*'-((dimethylamino)methylene)-*N*,*N*-dimethylformohydrazon-amide dihydrochloride (44)

Thionyl chloride (28.6 mL, 0.4 mol) was added to DMF (150 mL) at 5 °C. After addition the solution was kept at 5 °C for 24 h. Then aqueous hydrazine hydrate (5.0 mL, 0.1 mol) in 20 mL DMF was added slowly. The mixture was stirred at RT for further 48 h and the white precipitate of *N*,*N*-dimethylformamide azine dihydrochloride was then filtrated off and washed with DMF and diethyl ether resulting in the desired product (19.1 g, 89 mmol, 89%).

MP: 251 °C. **FT-IR (KBr, thin film)** ν_{max} **(cm^{-1}):** 3473(s), 3223 (w), 2951(w), 2848(w), 2031(m), 1715(s), 1609(m), 1507(s), 1398(w), 1287(s), 1228(m), 1137(s), 1054(s), 1019(m), 877(m), 672(s), 654(m), 530(m) and 496(m).

Synthesis of 5-(4*H*-1,2,4-triazol-4-yl)isophthalic acid (46)

N,*N*-dimethylformamide azine dihydrochloride (4.0 g, 18.7 mmol) and 5-aminoisophthalic acid (3.38 g, 18.6 mmol) were refluxed for 8h in 50 mL benzene. A white solid was filtered and washed with ethanol (2 × 15 mL) and diethyl ether (1 × 17 mL) (2.38 g, 10.2 mmol, 55%).

FT-IR (KBr, thin film) ν_{max} **(cm^{-1}):** 3119(s), 2906 (w), 1699 (s), 1519 (m), 1448 (m), 1286 (s), 1224 (s), 1143 (m), 1095 (m), 889 (m), 843 (m), 755 (m) and 665 (m).

Preparation of 5TIA-MOF

In a 5 mL vial 5TIA (44.6 mg, 0.2 mmol), $Ca(CO_2CH_3)_2$ (31.6 mg, 0.2 mmol) and 3.0 ml DMF:H_2O (v/v 1:1) were sonicated for 30 min at RT. Afterwards, the vial was stored for 48 h at 85 °C. Colorless plate like crystals were formed, filtered off with Whatmann® filter paper and washed thoroughly with 99.9% ethanol. The obtained Ca-5TIA-MOF, $[Ca_2(5TIA)_2(H_2O)_2 \cdot DMF]$, was dried at RT under air atmosphere for 1h (22.7 mg, 0.035 mmol, 35%).

FT-IR (KBr, thin film) ν_{max} **(cm^{-1}):** 3216 (m, br), 1670 (m), 1616 (m), 1550 (s), 1450 (m), 1381 (s), 1297 (w), 1244 (m), 1170 (w), 1085 (m), 1043 (w), 900 (w), 773 (m), 740 (m), 683 (m).

Elemental analysis: calculated for ($C_{10}H_4N_3O_5Ca$) in %: C, 40.24; H, 1.96; N, 21.82; found: C, 39.20; H, 1.99; N, 22.24.

Preparation of Ca-5TIA-Gel

$Ca(CH_3CO_2)_2$ (31.6 mg, 0.2 mmol) and 5-triazole isophthalic acid (0.2 mmol, 44.6 g) were weighed into a 5 mL vial. 2.0 mL of DMF were added and the mixture sonicated for ca. 15 min until formation of a homogeneous white solution. The solution was kept at different temperatures, 30 °C, 60 °C, 90 °C and 120 °C for 2 days. Gels were formed for each case.

FT-IR: (KBr, thin film) ν_{max} **(cm^{-1}):** 3349 (m, br), 1617 (m), 1550 (s), 1436 (m), 1386 (s), 1297 (w), 1248 (m), 1168 (w), 1096 (m), 1051 (w), 900 (w), 773 (m), 731 (m) and 669 (w).

Preparation of Ca-5TIA-Xerogel

Ca-5TIA-Xerogel has been prepared by freeze-drying method. For this a Ca-5TIA-Gel was first frozen in liquid nitrogen and then kept under high vacuum for 24 h. A light yellowish powder was obtained.

5.3 Characterization of Ca-5TIA materials

Thermogravimetric analyses (TGA)

TGA analysis was performed on a TG50 Mettler-Toledo analyzer or a SDT Q600 TG-DTA analyzer under N_2 atmosphere at a heating rate of 10 ºC min^{-1} within a temperature range of 20-800 °C.

Gas chromatography (GC)

GC analysis of the reactions were recorded using a HP 5790-A GC. It was equipped with a FID detector and a capillary column OV-1. As carrier gas helium was used, as internal standard served *n*-dodecane at a oven temperature of 250 °C.

Scanning electron microscopy (SEM)

A Zeiss DSM 950 scanning electron microscope and FEI, QUANTA 200 3D Scanning Electron Microscope with tungsten filament as electron source (10 kV) was used to take SEM pictures. A nano-sized Au film was sputtered prior to imaging on the samples on carbon tape. A SCD 040 Balzers Union was used for the imaging.

Transmission electron microscopy (TEM)

A FEI Tecnai G2 F20 X-TWIN TEM (200 kV) was used for the record of TEM pictures. The preparation of the TEM samples included a drop-casting of the sample at a concentration of 10^{-3} M from isopropanol on copper grids TEM Window (TED PELLA, INC. 200 mesh).

Fourier transform infrared spectroscopy (FT-IR)

FT-IR spectra were recorded on a Bruker Optics ALPHA-E spectrometer with a universal Zn-Se ATR (attenuated total reflection) accessory or using a Diamond ATR (Golden Gate) in a range of 600−4000 cm^{-1}.

UV-Vis spectroscopy

UV-Vis spectra were taken with a Perkin Elmer Lambda-35 UV-Vis spectrometer. 5TIA was measured in solution in DMF at 0.01 M. Ca-5TIA-Gel was measured as dispersed material in DMF as well as a coating on a quartz plate, which gave the same results. For preparation of the dispersed sample 12 mg of Ca-5TIA-Gel was mixed with 5 mL DMF and diluted twice. The UV-Vis measurements over time were performed with the quartz plate which were coated with the gel.

Fluorescence spectroscopy

Steady state fluorescence emission was determined using a Fluorolog HORIBA JOBIN VY on fluorescence spectrophotometer. 5TIA was measured in solution in DMF at 0.01 M. Ca-5TIA-Gel was measured as dispersed in DMF as well as a coating on a quartz plate,

which gave the same results. For preparation of the dispersed sample 12 mg of Ca-5TIA-Gel was mixed with 5.0 mL DMF and diluted twice. The UV-Vis measurements over time were performed with the quartz plate which was coated with the gel.

Powder X-ray diffraction (PXRD)

A Philips PANalytical diffractometer for Cu K_α radiation (λ= 1.5406 Å) was used for recording of PXRD patterns with a scan speed of 2° min^{-1} and step size of 0.02° in 2*θ*.

Rheological measurements

Rheological measurements were carried out with a A-ARES rheometer which was equipped with a force rebalance transducer. A Couette geometry with cup and bob diameter of 27 and 25 nm at a height of 30 nm was used. After gel preparation it was transferred to the cup of the rheometer geometry and coated with a very small amount of low viscosity fluorinated oil on top of the sample to avoid solvent evaporation during the experiment. First of all the smallest strain at which reasonable torque values were given (ten times of the transducer resolution limit) was discovered by strain sweep measurements. Then frequency sweep measurements were done in a dynamic mode as function of the aging time of the gel (frequency: 10^{-2} - 10^{2} rad^{-1}; strain: 1%). After a pre-shear step, which ruptured the structure, a well-defined initial state for the gel was obtained. After the pre-shearing-step the time was set as zero and the aging effect was investigated from this time on. To confirm reproducibility of the measurements they were carried out at least two times.

5.4 Application of Ca-5TIA materials in gas adsorption and catalysis

Gas adsorption

Gas adsorption experiments at low pressure, ranging from 0 to 760 Torr, were performed on a Quantachrome Quadrasorb automatic volumetric instrument at 77 K, for N_2. CO_2 adsorption was also measured in the range between 0 and 760 Torr at 298 K. Calcium aluminosilicate adsorbents removed water traces and other impurities from H_2 to provide ultra high-purity H_2 for the volumetric system. Ca-5TIA-MOF crystals were soaked in dry CH_2Cl_2 : MeOH (v/v 1:1) for 12 h. New CH_2Cl_2 : MeOH (v/v 1:1) was added for additional 48 h for the removing of solvent molecules from the framework. The Ca-5TIA-MOF was

dried at RT overnight under vacuum (< 10^{-3} Torr). The samples were heated up to 60 °C for 12 h under vacuum and additionally heated up to 100 °C for 12 h to remove all coordinated solvent molecules.

Catalytic activity

Catalytic activity of the Ca-5TIA materials was tested with the hydrosilylation of benzaldehyde with diphenylsilane as model reaction. The Ca-5TIA materials were supposed to act as Lewis-acid catalyst for the hydrosilylation. For the catalysis experiment benzaldehyde (10.6 mg, 0.1 mmol), diphenylsilane (36.9 mg, 0.2 mmol) and dry and degassed DMSO (1.0 mL) were stirred carefully at 65 ± 5 °C under argon atmosphere in the presence of Ca-5TIA-MOF catalyst (10 mol% with respect to benzaldehyde). The reaction progress was controlled by TLC and GC. For this, 10 µL of the reaction solution were quenched with water and extracted with Et_2O before injected into GC. For the recycling experiments Ca-5TIA-materials were packed and locked up in a borosilicate glass fiber filter paper. After every recycling step DMSO was used to wash the catalyst. Then the catalyst was centrifuged and dried under high vacuum at 50 °C. $TOF_{1/2}$ indicates the average turn-over frequency and here is defined as molar ratio of converted substrate to catalyst per h. This is calculated from the reaction time after 50% of the starting material was converted.

6. References

[1] Fages, F. *Angew. Chem. Int. Ed.* **2006**, *45*, 1680-1682.

[2] Lloyd, G. O; Steed, J. W. *Nature Chem.* **2009**, 437-442.

[3] Tomic, E. A. *J. Appl. Polym. Sci.* **1965**, *9*, 3745-3752.

[4] Czaja, A. U.; Trukhan, N.; Müller U. *Chem. Soc. Rev.* **2009**, *38*, 1284-1293.

[5] Tranchemontagne, D. J.; Hunt, J. R.; Yaghi, O. M. *Tetrahedron* **2008**, *64*, 8553-8557.

[6] Park, K. S.; Ni, Z.; Côté, A. P.; Choi, J. Y.; Huang, R. D.; Uribe-Romo, F. J.; Chae, H. K.; O'Keeffe, M.; Yaghi, O. M. *Proc. Natl. Acad. Sci. USA* **2006**, *103*, 10186-10191.

[7] Férey, G. *Chem. Soc. Rev.* **2008**, *37*, 191-214.

[8] Chen, B.; Xiang, S.; Quian G. *Acc. Chem. Res.* **2010**, *8*, 1115-1124.

[9] Ma, L.; Abney, C.; Lin, W. *Chem. Soc. Rev.* **2009**, *38*, 1248-12.

[10] Vallet-Regí, M.; Balas, F.; Arcos, D. *Angew. Chem. Int. Ed.* **2007**, *46*, 7548-7558.

[11] Xie, Z.; Ma, L.; deKrafft, K. E.; Jin, A.; Lin, W. *J. Am. Chem. Soc.* **2010**, *132*, 922-923.

[12] Chen, B. L.; Wang, L. B.; Xiao, Y. Q.; Fronczek, F. R.; Xue, M.; Cui, Y. J.; Qian, G. D. *Angew. Chem. Int. Ed.* **2009**, *48*, 500-503.

[13] Han. S.; Wei, Y.; Valente, C.; Forgan, R. S.; Gassensmith, J. J.; Smaldone, R. A.; Nakanishi, H.; Coskun, A.; Stoddart, J. F.; Grzybowski, B. A. *Angew. Chem. Int. Ed.* **2011**, *50*, 276-279.

[14] Tu, T.; Assenmacher, W.; Peterlik, H.; Weisbarth, R.; Nieger, M.; Dotz K. H. *Angew. Chem. Int. Ed.* **2007**, *46*, 6368-6371.

[15] Shirakawa, M.; Fujita, N.; Tani, T.; Kanekob, K.; Shinkai, S. *Chem. Commun.* **2005**, *33*, 4149-4151.

[16] Bu, H. Z.; English, A. M.; Mikkelsen, S. R. *Anal. Chem.* **1996**, *68*, 3951-3957.

[17] Roubeau, O.; Colin, A.; Schmitt, V.; Clérac, R. *Angew. Chem. Int. Ed.* **2004**, *43*, 3283-3286.

[18] Tsuchiya, K.; Orihara, Y.; Kondo, Y.; Yoshino, N.; Ohkubo, T.; Sakai, H.; Abe, M. *J. Am. Chem. Soc.* **2004**, *126*, 12282-12283.

[19] Shirakawa, M.; Fujita, N.; Tani, T.; Kaneko, K.; Ojima, M.; Fujii, A.; Ozaki, M.; Shinkai, S. *Chem. Eur. J.* **2007**, *13*, 4155-4162.

[20] Pires, M. M.; Chmielewski, J. *J. Am. Chem.* **2009**, *131*, 2706-2712.

[21] Panda, T.; Pachfule, P.; Banerjee, R. *Chem. Commun.* **2011**, *47*, 7674-7676.

[22] Lässig, D.; Lincke, J.; Krautscheid, H. *Tetrahedron Lett.* **2010**, *51*, 653-656.

[23] Neofotistou, E.; Malliakas, C. D.; Trikalitis, P. N. *CrystEngComm* **2010**, *12*, 1034-1037.

[24] Eubank, J. F.; Wojtas, L.; Hight, M. R.; Bousquet, T.; Kravtsov, V. C., Eddaoudi, M. **2011**, *133*, 17532-17535.

[25] Platers, M. J.; Howie, R. A.; Roberts, A. J. **1997**, *9*, 893-894.

[26] Fei, Z.; Geldbach, T. J.; Scopelliti, R.; Dyson, P. J. *Inorg. Chem.* **2006**, *45*, 6331-6337.

[27] Volkringer, C.; Loiseau, T.; Ferey, G.; Warren, J. E. Wragg, D. S.; Morris, R. E. *Solid State Sci.* **2007**, *9*, 455-458.

[28] Shuai, Q.; Chen, S.; Gao, S. *Inorg. Chim. Acta* **2007**, *360*, 1381-1387.

[29] Aliouane, K.; Rahahlia, N.; Guehria-Laidoudi, A.; Lecomte, C. *Acta Crystallogr. Sect. E: Struct. Rep. Online* **2007**, *63*, 1834-1836.

[30] Volkringer, C.; Marrot, J.; Ferey, G.; Loiseau, T. *Cryst. Growth Des.* **2008**, *8*, 685-689.

[31] Dietzel, P. C.; Blom, R.; Fjellvag, H. *Anorg. Allg. Chem.* **2009**, *635*, 1953-1958.

[32] Platero Prats, A. E.; de la Pensa-O'Shea, V. A.; Iglesias, M.; Snejko, N.; Monge, A., Gutierrez-Puebla, E. *ChemCatChem* **2010**, *2*, 147-149.

[33] Platero-Prats, A. E.; de la Pena-O'shea, V. A., Snejko, N.; Monge, A.; Gutierrez-Puebla, E. *Chem. Eur. J.* **2010**, *16*, 11632-11640.

[34] Platero-Prats, A. E. Iglesias, M.; Snejko, N.; Monge, A.; Gutierrez-Puebla, E. *Cryst. Growth Des.* **2011**, *11*, 1750-1758.

[35] Liang, P.-C.; Liu, H.-K.; Yeh, C.-T.; Lin, C.-H.; Zima, V. *Cryst. Growth Des.* **2011**, *11*, 699-708.

[36] Yeh, C. T.; Lin, W. C.; Lo, S. H.; Kao, C. C.; Lin, C. H.; Yang, C. C. *CrystEngComm* **2012**, *14*, 1219-1222.

[37] Neogi, S.; Navarro, J. A. R.; Bharadwaj, P. K. *Cryst. Growth Des.* **2008**, *8*, 1554-1558.

[38] Binder, H. H. *Lexikon der chemischen Elemente;* S. Hirzel Verlag, Stuttgart, **1999**.

[39] Takeuchi, M.; Kageyama, S. *Colloid Polym. Sci.* **2003**, *281*, 1178-1183.

[40] Kamlet, M. J.; Abboud, J. L. M.; Abraham, M. H., Taft, R. W. *J. Org. Chem.* **1983**, *48*, 2877-2887.

[41] Edwards, W.; Lagadec, C. A.; Smith, D. K. *Soft Matter* **2011**, *7*, 110-117.

[42] Adams, D. J.; Morris, K.; Chen, L.; Serpell, L. C.; Bacsa J.; Day, G. M. *Soft Matter* **2010**, *6*, 4144-4156.

[43] Trappe, V.; Weitz, D. A. *Phys. Rev. Lett.* **2000**, *85*, 449-452.

[44] Dastidar, P. *Chem. Soc. Rev.* **2008**, *37*, 2699-2715.

[45] Pal, A.; Basit, H.; Sen, S.; Aswasl, V. K.; Bhattacharya, S. *J. Mater. Chem.* **2009**, *19*, 4325-4334.

[46] Jones, C. D.; Tan, J. C.; Lloyd, G. O. *Chem. Commun.* **2012**, *48*, 2110-2112.

[47] Carr, C. S.; Shantz, D. F. *Chem. Mater.* **2005**, *17*, 6192-6197.

[48] Zhang, J.; Wang, X.; He, L.; Chen, L.; Su, C.-Y.; James, S. L. *New J. Chem.* **2009**, *33*, 1070-1075.

C Multicomponent liquid organogelator systems

1. Preface

The results of this chapter, referring to multicomponent liquid organogelator system I, MGS I, have already been published in *Soft Matter* **2012**, *8*, 3446-3456 with the title: „*Competition between gelation and crystallisation of a peculiar multicomponent liquid system based on ammonium salts*“.

This publication is the result of a collaboration between the group of Prof. Dr. David Díaz Díaz with his students Eva-Maria Schön, Iti Kapoor, Jürgen Bachl and Dennis Kühbeck from the Institut für Organische Chemie at Universität Regensburg, Germany and the group of Prof. Dr. Rahul Banerjee and his student Subhadeep Saha from the Physical/ Materials Chemistry Division at National Chemical Laboratory in Pune, India. Furthermore, Carlos Cativiela from the Instituto de Síntesis Química y Catálisis Homogénea in Zaragoza, Spain, Stefano Roelens from the Istituto di Metodologie Chimiche, Consiglio Nazionale delle Ricerche, Dipartimento die Chimica at Università di Firenze in Firenze, Italy, and José Juan Marrero-Tellado from the Instituto Universitario de Bio-Orgánica at Universidad de La Laguna in La Laguna, Tenerife, Spain, contributed to the publication with preliminary experiments, measurements and critical discussions.

Eva-Maria Schön was involved in the preparation and characterization of the multicomponent liquid organogelator system and the gel materials, including the study and optimization of the gelation properties, stability and responsiveness studies, DSC, comparative FT-IR and digital imaging of the materials.

After the results of MGS I were published in 2012 an attempt to improve the properties of the multicomponent liquid organogelator system and gels was carried out. The resulting multicomponent liquid organogelator system II, MGS II, was discovered by Eva-Maria Schön. Prof. Dr. David Díaz Díaz was collecting SEM pictures and Jürgen Bachl provided compound **76**.

2. Background

Multicomponent gelator systems are based on the concept that for formation of a gel more than one species is added to the solvent for gelation. That offers the possibility to tailor the gels' properties by a change of the component concentration, ratio, or addition of a further additive.[1] The simplest imaginable multicomponent gelator system includes two different components which are added to the solvent. These systems have been widely investigated.[2-25]

One example for a two-component gelator system is the bis(2-ethylhexyl) sodium sulfosuccinate **51** that forms inverse micelles when it is dissolved alone in nonpolar solvent. In a combination with *p*-chlorophenol **52** organogels from nonpolar solvents can be obtained (Figure 36).[23]

The gelation ability of a two-component gelator system consisting of a dendritic *L*-lysine-based peptide **53** and a simple aliphatic diamine **54** (n = 6-12) was investigated in 2004 (Figure 36).[24] Interestingly, with increasing chain length of the aliphatic diamine from 6 to 12 carbon atoms also the *sol*-to-*gel* temperature increased from 4 °C to 105 °C.

Hanabusa and co-workers reported that the combination of *N*-dodecyl-*L*-lysine esters and *N*-dodecyl-*L*-amino acids produced an organic salt through acid-base interactions. One example is given in Figure 36 with **55** as amine and **56** as acid component. These compounds were able to build up a 3D network through hydrogen bonding and van der Waals interaction which provided organogels.[25]

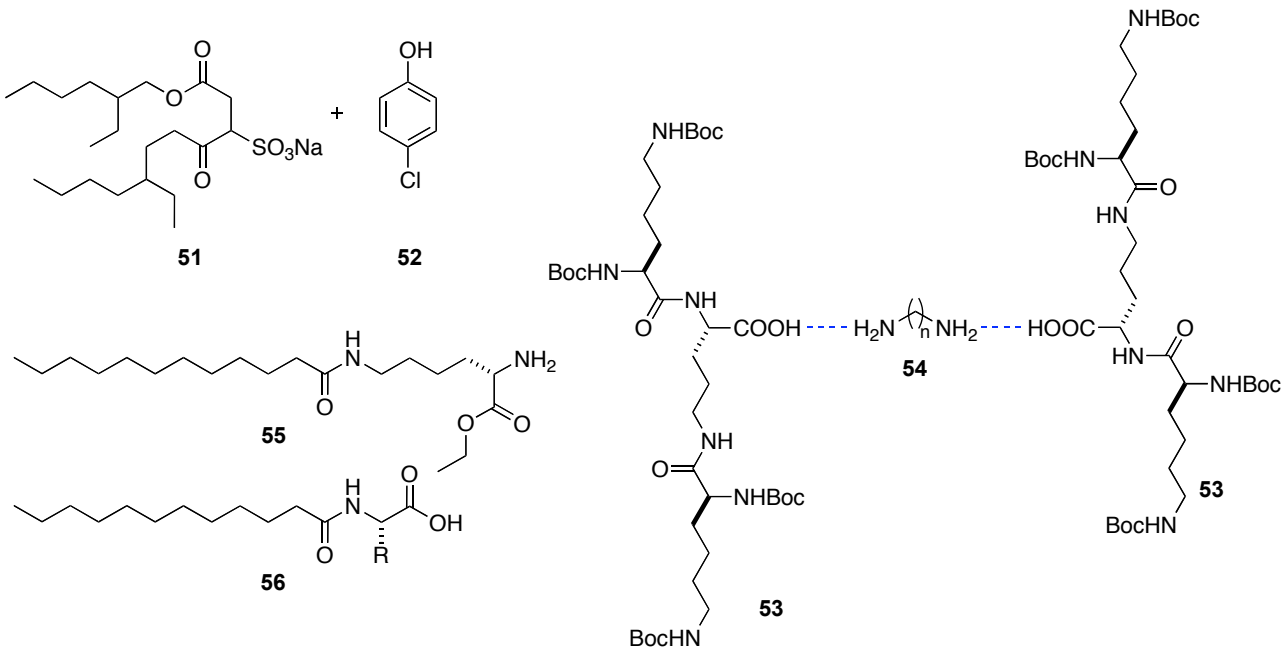

Figure 36: Selection of two-component gelator systems.[23-25]

So far, three different classes of multicomponent gels are known and have been studied. In the first class, all used components are necessary to obtain gel material. That means that none of the components is able to form a gel on its own. The second class consists of at least two gelators, which co-assemble or self-sort into certain structures. The third class requires at least one gelator and one non-gelling additive. The additive can have influence on the assembly process of the gelator molecules and control the gels' properties.[26]

In this chapter, multicomponent gels of the first class are under investigation. Two liquid gelator systems are compared regarding their gelation ability and their applicability will be measured by the characteristics of their respective gels. Remarkably, both multicomponent liquid gelator systems consist of five different compounds at a certain stoichiometry and concentration which is crucial for the formation of gels. Moreover, the gels of both systems show an outstanding and fascinating "arm wrestling" competition between gelation and crystallization phenomena.

3. Results and discussion

3.1 Preparation of MGS

The multicomponent liquid organogelator system I, MGS I, was first discovered by serendipity during the realization of a standard protocol of tartaric acid-mediated racemic resolution experiment for (±)-*trans*-1,2-diaminocyclohexane.[27] During the cleaning up of the glassware after the experiment, it was observed that the mixture of (1*R*,2*R*)-1,2-diaminocyclohexane *L*-tartrate,[28,29] methanol and aqueous HCl was able to form jelly-like material upon contact with acetone (Figure 37).

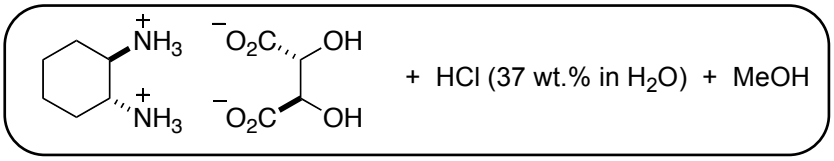

Figure 37: Composition of the multicomponent liquid organogelator system.

There was no data about the solubility of (1*R*,2*R*)-1,2-diaminocyclohexane *L*-tartrate **57** (Figure 38) in literature. The only information was the publication from Gilheany and co-workers, where they used a suspension of the salt in methanol at a concentration of 1.04 mol·L^{-1}.[30] The salt was found to be insoluble, neither at RT nor after sonication or heating with a heat gun in a series of tested solvents: methanol, ethanol, isopropanol, *n*-butanol, *n*-hexanol, glycerol, acetone, acetonitrile, dioxane, tetrahydrofuran, diethyl ether, methylene chloride, chloroform, xylol and *n*-hexane in a concentration range of 0.04-0.08 mol·L^{-1}. As the first observation in the resolution experiment pointed out, methanol as well as aqueous HCl were both necessary to dissolve the salt.

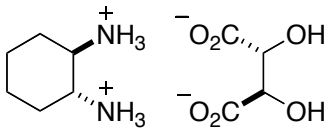

57

Figure 38: (1*R*,2*R*)-1,2-diaminocyclohexane *L*-tartrate salt **57**.

For determination of the optimal molar composition of the multicomponent gelator solution a detailed two-variables screening was performed. The first variable was defined by the

tartrate salt concentration in methanol and the second variable by the number of equivalents of HCl with respect to the salt. This resulted in a 2D matrix with 132 elements (Table 3), prepared from a 0.3075 mol·L^{-1} methanol-HCl stock solution to minimize the experimental error. Table 3 shows that at least 2.0 equivalents of HCl are necessary to dissolve the salt and provide a clear solution. Samples with less than 2.4 equivalents of HCl needed to be sonicated to dissolve the salt. It was found that there were no significant differences in the results when the salt **57** was either purchased from commercial suppliers or synthesized following the general protocol.[27]

Table 3: 2D Matrix showing the concentration of salt **57** in methanol [M] and the amount of HCl (equivalents respects to the salt) necessary to prepare a transparent and stable MGS I solution.[a]

[M]↓ HCl→	1.0	1.3	1.5	1.7	1.8	1.9	2.0	2.1	2.2	2.3	2.4
0.06	I (30)	I (30)	I (30)	I (30)	I (10)	I (10)	S (2)	S (2)	S (1)	S (1)	S (0)
0.07	I (30)	I (30)	I (30)	I (30)	I (10)	I (10)	S (2)	S (2)	S (1)	S (1)	S (0)
0.08	I (30)	I (30)	I (30)	I (30)	I (10)	I (10)	S (2)	S (2)	S (1)	S (1)	S (0)
0.09	I (30)	I (30)	I (30)	I (30)	I (10)	I (10)	S (2)	S (2)	S (1)	S (1)	S (0)
0.10	I (30)	I (30)	I (30)	I (30)	I (10)	I (10)	S (2)	S (2)	S (1)	S (1)	S (0)
0.128	I (30)	I (30)	I (30)	I (30)	I (10)	I (10)	S (2)	S (2)	S (1)	S (1)	S (0)
0.20	I (30)	I (30)	I (30)	I (30)	I (10)	I (10)	S (2)	S (2)	S (1)	S (1)	S (0)
0.25	I (30)	I (30)	I (30)	I (30)	I (10)	I (10)	S (2)	S (2)	S (1)	S (1)	S (0)
0.30	I (30)	I (30)	I (30)	I (30)	I (10)	I (10)	C	C	C	C	C
0.40	I (30)	I (30)	I (30)	I (30)	I (10)	I (10)	C	C	C	C	C
0.50	I (30)	I (30)	I (30)	I (30)	I (10)	I (10)	C	C	C	C	C
1.00	I (30)	I (30)	I (30)	I (30)	I (10)	I (10)	C	C	C	C	C

[a]Abbreviations: I (t) = after t min of sonication still insoluble material is observed; S (t) = after t min of sonication a clear solution was formed; C = crystal growth over time. For higher concentrations crystals are growing within hours.

When concentrations higher than 0.3 mol·L^{-1} of HCl were used to dissolve the salt, spontaneous growth of large monocrystals at RT were observed (Figure 39, right). NMR measurements and single crystal XRD studies confirmed that the crystals corresponded to (1*R*,2*R*)-1,2-diaminocyclohexane dihydrochloride **58** (Figure 39, left). For this reasons the

concentration of HCl in the multicomponent liquid organogelator system was defined to be 2.4 equivalents.

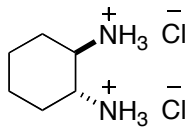

58

Figure 39: MGS I solution with crystals (left) from (1*R*,2*R*)-1,2-diaminocyclohexane dihydrochloride **58** (right).

The received solutions from Table 3 were evaluated in terms of gelation ability for a few solvents: dioxane, acetone, acetonitrile and tetrahydrofuran. For the given 2.4 equivalents of HCl, the gel-like materials with the highest temporal stability were obtained at a salt concentration between 0.1-0.15 mol·L^{-1}. For the following experiments multicomponent liquid organogelator system I was prepared with 0.128 mol·L^{-1} of salt **57** and 2.4 equivalents of HCl. It has to be mentioned, that also combinations with higher HCl content were able to deliver gel-like material, but they all showed much lower temporal stability. Also combinations with lower salt **57** concentration were able to act as gelator system. However, the scope of solvents which can be gelled was smaller.

The stability of the multicomponent liquid organogelator solution did not suffer within 7 days when stored sealed and in the dark. This was tested by using multicomponent liquid organogelator solutions of different age for gel preparation and comparison of the temporal stability of the gels. When the MGS was stored for longer than 7 days some decline was observed in the temporal stability of the produced gels.

Besides this, the most important factors for the reproducibility of the organogels is that the gelator solution has the right salt and HCl concentration and is clear and free of any solid particles which would act as nucleating agent. All these factors would enhance the crystallization of (1*R*,2*R*)-1,2-diaminocyclohexane dihydrochloride **58** and therefore enhance the destruction of the gel. In summary, the comprehensive study led to a 0.128 mol·L^{-1} methanolic solution of (1*R*,2*R*)-1,2-diaminocyclohexane *L*-tartrate **57** and 2.4 equivalents of concentrated HCl (37 wt.% in aqueous solution) as optimal MGS, which corresponds to a molar ratio of (1*R*,2*R*)-1,2-diaminocyclohexane *L*-tartrate : MeOH : HCl :

H_2O = 1 : 193 : 2.4 : 8.3. As will be clarified later, the presence and stoichiometry of each component were found to play a key role in the gelation process.

Experiments trying to replace methanol by other polar, but nonprotic solvents were carried out in order to avoid competing H-bonding, which will be discussed later. The replacement of the solvents could increase the temporal stability of the aggregates. Therefore, the solubility of (1*R*,2*R*)-1,2-diaminocyclohexane *L*-tartrate was determined in other solvents. As a result four further solvents were found to be appropriate to dissolve the salt in combination with aqueous HCl in the above described stoichiometry: dimethyl sulfoxide (DMSO), dimethylformamide (DMF), *N*-methyl-2-pyrrolidone (NMP) and dimethylacetamide (DMA). However, the solutions from DMF, DMA and NMP were not stable, as they showed color change and crystallization after one day (Figure 40). Nevertheless, the solution in DMSO remained stable and was still clear and homogenous after 2 months.

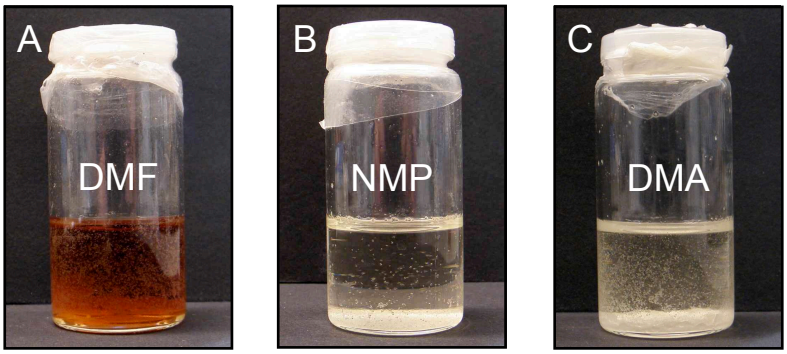

Figure 40: Crystallization and color change occurred for solutions from DMF (A), NMP (B) and DMA (C) within one day after preparation.

A two-variables screening for the determination of the optimal molar composition of the gelator solution, as first carried out for the methanol-based multicomponent liquid organogelator solution, MGS I, was now repeated for the DMSO-based multicomponent liquid organogelator solution, MGS II, to examine the range in which salt **57** can be dissolved (Table 4). The results of the screening matrix for MGS II were comparable with the results for MGS I, as both needed at least 2.0 equivalents of HCl to dissolve the salt **57** (Table 4). Contrary to MGS I, MGS II still provided a clear solution for a concentration of 0.30 mol·L^{-1} of **57** and this solution remained stable for more than one week without crystallization.

For a better comparison with gelation tests of MGS I, MGS II was also prepared for the following experiments with 2.4 equivalents of aqueous HCl at a 0.128 mol·L^{-1} concentration of **57**.

Table 4: 2D Matrix showing the concentration of salt **57** in DMSO [M] and the amount of HCl (equivalents respects to the salt) necessary to prepare a transparent and stable MGS I solution.[a]

[M]↓ HCl→	1.9	2.0	2.1	2.2	2.3	2.4	2.5
0.08	I (30)	I (60)	S (5)	S (2)	S (10 s)	S (0)	S (0)
0.10	I (30)	I (60)	S (5)	S (2)	S (10 s)	S (0)	S (0)
0.128	I (30)	S (60)	S (5)	S (2)	S (10 s)	S (0)	S (0)
0.20	I (60)	S (30)	S (5)	S (2)	S (10 s)	S (0)	S (0)
0.30	I (60)	S (5)	S (5)	S (2)	S (10 s)	S (0)	S (0)

[a]Abbreviations: I (t) = after t min of sonication still insoluble material is observed; S (t) = after t min of sonication a clear solution was formed.

3.2 Preparation of organogels

The formation of gel material from MGS I at RT by addition of a small amount of MGS I to a solvent was extremely fast.[31,32] An appropriate homogenization of MGS I and solvent before gelation was prevented by such fast kinetics. As a result, a significant amount of the solvent remained liquid. Fluid-filled cavities in the non-homogeneous gel material were formed and the material easily disrupted upon mechanical stress, as shaking of the vial.

However, homogeneous organogels from MGS I were obtained when the solvents were cooled down close to their freezing points before MGS I was added. This procedure probably slowed the gelation kinetics dramatically down and enabled the formation of homogeneous gels from isotropic solutions containing the solvent and MGS I. A small amount of non-gelled liquid remained on the gel regardless of the MGS I concentration. Thus, the degree of gel formation was quantified 30 min after removing of the cooling bath by turning the vial upside-down and collecting of the non-gelled liquid (Table 5).

A series of factors were observed to have significant influence on the gel formation during the experimental procedure: 1. Control of the solvent temperature, 2. extensive stirring and 3. design of the glass wall.

The solvent temperature had to be close to its freezing point. Good stirring of MGS I and solvent at low temperature provided an isotropic solution. Both factors could be used to regulate the nucleation processes[33] and afford the formation of most stable and homogeneous gels. The wall thickness and diameter of the glass vial had an influence on the gelation concentration, the gelation kinetics and the gel stability, as they affected the stirring efficiency as well as the promotion of heat transfer through the vial. That influenced directly the amount of energy transferred to the solvent mixtures.

Considering these factors, 40 solvents were evaluated with respect to their gelation ability for MGS I (Table 5). The state of the materials was examined by the “stable-to-inversion“ of the test tube method (Figure 41). The insertion of a thermocouple (2 mm in diameter) into the solution after removing of the cooling bath exhibited that most of the time the gelation process started already below 0 °C.

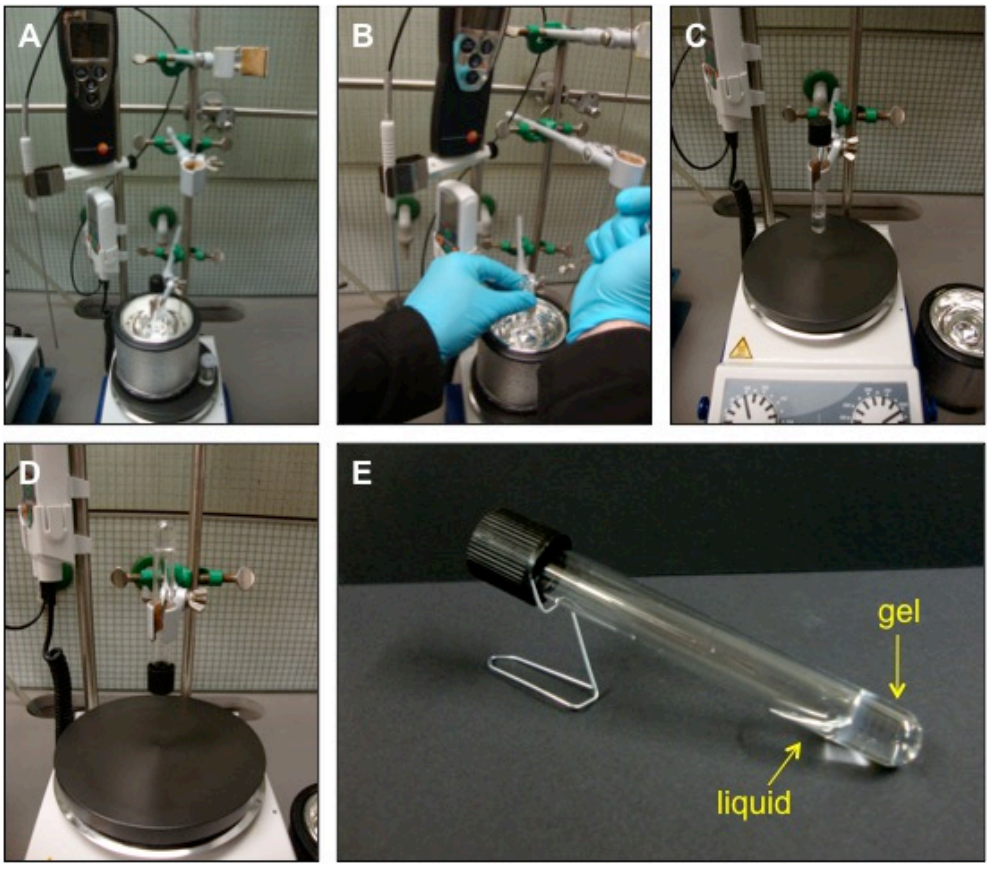

Figure 41: Organogel preparation from MGS I: Picture A shows the cooling of the solvent in a test tube. Picture B illustrates the careful hand-shaking of the test tube after addition of MGS I. After the removing of the cooling bath (picture C) the isotropic solution warms up to RT and gelation starts. Inversion of the test tube confirmed the gel state in picture D. Picture E exemplifies the difference between 1,4-dioxane gel and non-gelled liquid 30 min after removing of the cooling bath.

For the preparation of gels from MGS II, the analogous procedure was carried out as for preparation of gels from MGS I. However, an addition of MGS II to the solvent in the cooling bath was not possible as the MGS II was frozen in the syringe. This can be explained, as MGS II consists mostly of DMSO which has a high freezing point of 19 °C. When MGS II in the syringe came near the cooled glass vial with the solvent it already started to freeze.

After a series of experiments it was found that the fast addition of the solvent to a specific volume of MGS II in a glass vial was the only possible way to provide complete gelation of the solvents. Addition of MGS II to the solvent resulted in solution or partial gelation.

3.3 Characterization of MGS organogels

Table 5 displays that MGS I was able to gel different oxygenated and nitrogenated solvents at very low concentrations (Table 5, entries 1-12). For halogenated, aromatic, or hydrocarbon solvents (Table 5, entries 13-15) no gel formation was observed in contrast. The solvents in Group I (Table 5, entry 13) contain methylene chloride, 1,2-dichloroethane, carbon tetrachloride, DMF, DMA, DMSO, ethanol, *n*-hexane, benzene, toluene, ethylene glycol, dibutyl ether, NMP and water. Group II (Table 5, entry 14) consists of chloroform, 1,2-dichlorobenzene, nitrobenzene *n*-octane, glycerol, cyclohexane, tetrachloroethylene, and carbon disulfide. Group III (Table 5, entry 15) includes the ionic liquid [BMIM][PF_6], pyridine and methyl *tert*-butyl ether.

After mixing of MGS I with solvents of group I solutions were obtained, whereas group II solvents and MGS I were immiscible. MGS I and solvents of group III provided initially solutions, but for all of these solvents precipitation occurred afterwards. Only in the case of methyl *tert*-butyl ether, a turbid gel-like material was formed, but this broke into smaller pieces after inversion of the test tube.

The volume of the MGS I that produced organogels was determined by varying the added volume of MGS I in a range of 100-300 µL per mL of tested solvent. The reported values of MGS I were chosen based on both the highest temporal stability and the minimum amount of non gelled solvent. These volume values were in a range of 80-250 µL, which corresponds to a concentration of 0.3-0.7 wt.% referred to the salt **57**.

Table 5: Gelation ability of MGS I in different solvents.[a]

Entry	Solvent	gv[b] [µL]	T_{mix}[c] [°C]	Non-gelled liquid[d] [µL]	T_d[e] [°C]	Aspect phase[f]	Temporal stability[g]
1	NM	100	-20	40 ± 20	95[h]	TG	2-4 h
2	ACN	100	-40	40 ± 20	62	OG	1-3 d
3	BN	150	-10	240 ± 50	152	TG	1-2 h
4	ACT	250	-90	110 ± 20	43	OG	2-5 h
5	CHN	150	-10	115 ± 20	84[h]	TG	2-3 h
6	MBN	100	-80	70 ± 10	68	OG	3-4 d
7	DME	100	-50	40 ± 20	65	OG	1-4 h
8	MEE	100	-60	60 ± 10	128	OG	3-4 d
9	ETAC	250	-78	80 ± 15	44	OG	9-24 h
10	THF	150	-78	40 ± 20	54	TG	4-5 d
11	DEE	180	-100	90 ± 30	52	OG	3-4 d
12	DOX	80	13	50 ± 30	89	TG	2-3 d
13	Group I	-	-	-	-	M	-
14	Group II	-	-	-	-	I	-
15	Group III	-	-	-	-	P	-

[a]1.0 mL of solvent was used in every experiment. Abbreviations: ETAC = ethyl acetate; THF = tetrahydrofuran; DME = 1,2-dimethoxyethane; MEE = 2-methoxyethyl ether; DEE = diethyl ether; CHN = cyclohexanone, MBN = 3-methylbutan-2-one; ACN = acetonitrile; BN = benzonitrile; DOX = 1,4-dioxane; ACT = acetone; NM = nitromethane. [b]Necessary volume of MGS I; [c]Cooling bath temperature; [d]Non-gelled liquid, 30 min after gel formation, average values resulting from at least 6 independent experiments; [e]Gel destruction temperature measured by DSC, experimental error = ± 2 °C; [f]Abbreviations: TG = transparent/translucent gel, OG = opaque gel; M = miscible; I = immiscible, P = precipitate; [g]Stability of the gels over time, stored undisturbed in a vertical position at 23 ± 2 °C; [h]T_d was determined for this case by a Kugelrohr-based method with an apparent error of ± 5 °C for CHN and ± 10 °C for NM; Stability was judged by the destruction of the colored gel.

Furthermore, the gelation ability of MGS II was investigated. Table 6 shows the oxygenated and nitrogenated solvents which were gelled by MGS II (Table 6, entries 1-10, 12). Except for DCM (Table 6, entry 11) halogenated, aromatic, or hydrocarbon solvents (Table 6, entries 13-15) were not gelled. Solvents described in Group I (Table 6, entry 13) are containing water, DMF, DMA, benzene, toluene, ethanol, NMP, glycerol, 2-propanol

and methanol. Group II (Table 6, entry 14) consists of cyclohexane, methyl *tert*-butyl ether, *n*-hexane and DEE. Group III (Table 6, entry 15) includes the ionic liquid [BMIM][PF_6], pyridine and methyl *tert*-butyl ether. As described above for MGS I, after mixing of MGS II with solvents of group I solutions were obtained, whereas group II solvents and MGS II were immiscible. MGS II and solvents of group III provided initially solutions, but for all solvents precipitation occurred afterwards.

Contrarily to gels from MGS I it was found that the removal of the liquid on top did not enhance the temporal stability, but resulted in further leakage of fluid from the gel until it was covered with a liquid film again. For that reason the liquid was not further quantified but in general the volume of liquid was below 100 µL.

The volume of the MGS II which was necessary to afford organogels was determined in a range between 20-100 µL, which corresponds to a concentration of 0.1-0.3 wt.% referred to the salt **57**. Interestingly, every tested solvent had a very small range of MGS II volume which provided gels. For this reason the volume of gelator solution cannot be increased without suffering of gel stability or even gelation at all. For example, ACN gels from MGS I need a gelation volume of 100 µL to be obtained. Contrary the ACN gel from MGS II is provided from 30 µL of gelator solution. If 100 µL of MGS II were used instead, only a solution was obtained. For this reason, it is not possible to compare MGS I and MGS II gels at the same volume of gelator solution, but the gels are compared at their highest temporal stability, although that means a difference in gelator concentration.

Some MGS II gels showed a remarkable enhancement in temporal stability for gels from DME, BN, NM and MEE. Compared to the gelation volume for MGS I organogels, MGS II organogels need up to 12 times (for ETAC) less, but also for all other solvents the decrease of volume is at least 2 times.

Table 6: Gelation ability of MGS II in different solvents.[a]

Entry	Solvent	gv[b] [µL]	T_{mix}[c] [°C]	T_d[d] [°C]	Aspect phase[e]	Temporal stability[f]
1	NM	40	RT	96	OG	7-9 d
2	ACN	30	RT	71	TG	1-2 d
3	BN	50	RT	149	TG	1-2 d
4	ACT	40	RT	42	TG	4-16 h
5	CHN	40	RT	123	TG	1-2 h
6	MBN	20	RT	75	TG	6-9 d
7	DME	30	RT	72	TG	4 d
8	MEE	30	RT	129	OG	5-9 d
9	ETAC	20	RT	56	TG	1-3 d
10	THF	20	RT	56	TG	1-3 d
11	DCM	100	RT	45	OG	1-3 h
12	DOX	20	RT	-	TG	5-24 h
13	Group I	-	-	-	M	-
14	Group II	-	-	-	I	-
15	Group III	-	-	-	P	-

[a]1.0 mL of solvent was used in every experiment. Abbreviations: ETAC = ethyl acetate; THF = tetrahydrofuran; DME = 1,2-dimethoxyethane; MEE = 2-methoxyethyl ether; DCM = methylene chloride; CHN = cyclohexanone, MBN = 3-methylbutan-2-one; ACN = acetonitrile; BN = benzonitrile; DOX = 1,4-dioxane; ACT = acetone; NM = nitromethane. [b]Necessary volume of MGS I; [c]Cooling bath temperature; [d]Gel destruction temperature measured by DSC, error = ± 2 °C; [e]Abbreviations: TG = transparent/translucent gel, OG = opaque gel; M = miscible; I = immiscible, P = precipitate; [f]Stability of the gels over time, stored undisturbed in a vertical position at 23 ± 2 °C.

Appearance of the gels

Interestingly, MGS I and MGS II gels from the same solvent did not always show the same appearance (Figure 42). In summary MGS I provided only 5 transparent gels (Table 5, entries 1, 3, 5, 10 and 12), whereas 9 transparent gels were obtained from MGS II (Table 6, entries 2-7, 9, 10 and 12). The off-white opaque organogels showed different degrees of translucence which indicates the presence of aggregates smaller than λ = 400-700 nm.

Figure 42 shows a selection of organogels from MGS I (top) and a selection of organogels from MGS II (bottom) with different degrees of translucence.

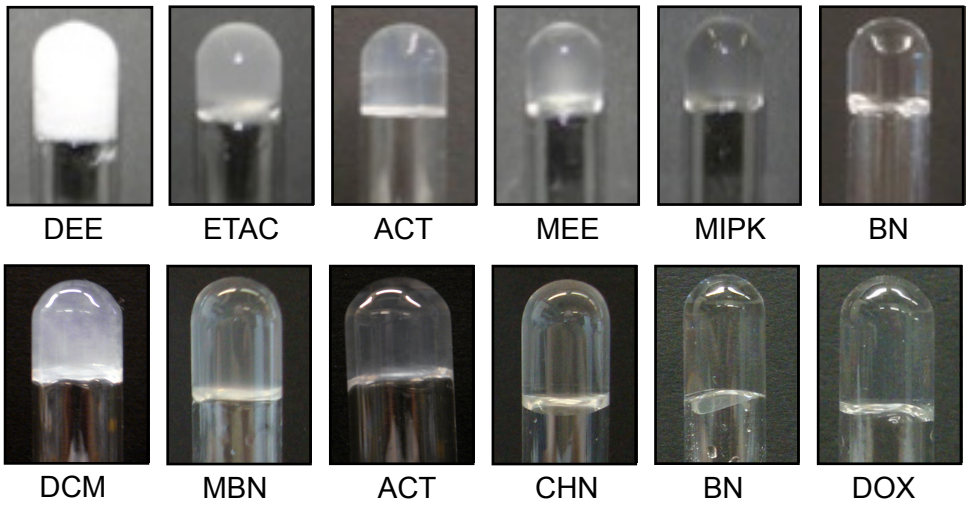

Figure 42: Digital photographs from MGS I (top) and MGS II (bottom) organogels.

Aging of the gels

During the evaluation of the temporal stability of the gels from MGS I and MGS II the competition between gelation and crystallization phenomena was observed (Figure 43).

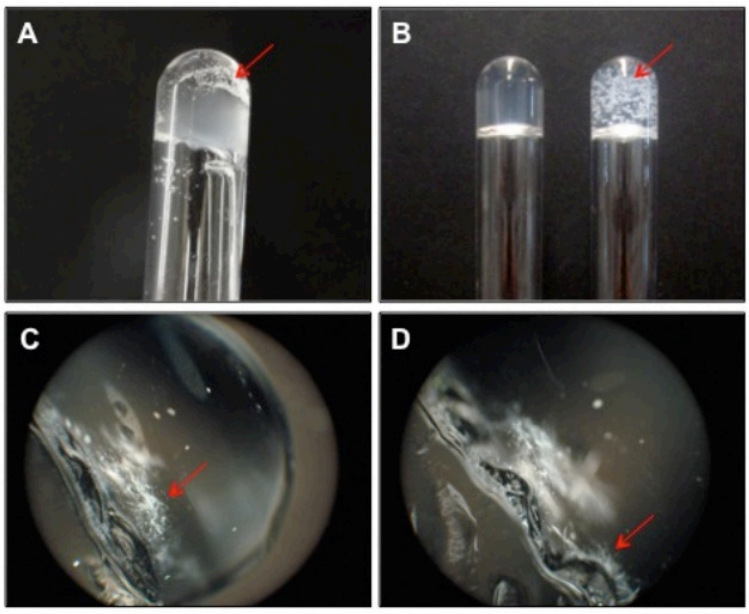

Figure 43: Crystal formation inside of MGS I gels; Digital photograph A shows the destruction of the MGS I ACN gel after crystallization, whereas picture B compares between the initial translucent ACN gel and the crystal-containing gel prepared with 200 µL of MGS I; The optical microscope images C and D exhibit small crystals formed close to the gel-air interface in a ETAC gel from MGS I.

The growth of (1*R*,2*R*)-1,2-diaminocyclohexane dihydrochloride crystals inside both gel materials was associated with the weakening of the gels over time. Lack of stability was defined when the gels were not able to resist the inversion of the tube any longer or were fragmented or partially liquefied. Dynamic gel-crystal transitions have been previously related to the Ostwald rule of stages.[34]

The aging over time for a MGS I gel from ETAC (top) and for a MGS II gel from DCM (bottom) is shown in Figure 44. The MGS II gel showed first crystallization in the whole gel and then gradual destruction of gel whereas the MGS I gel already has formed not only crystals, but also a solvent cavity at the bottom of the vial which leads to destruction by inversion of the glass vial. This solvent cavities at the bottom can be observed during the aging for all MGS I gels, but are exceptional for gels from MGS II. The different preparation methods could cause this behavior.

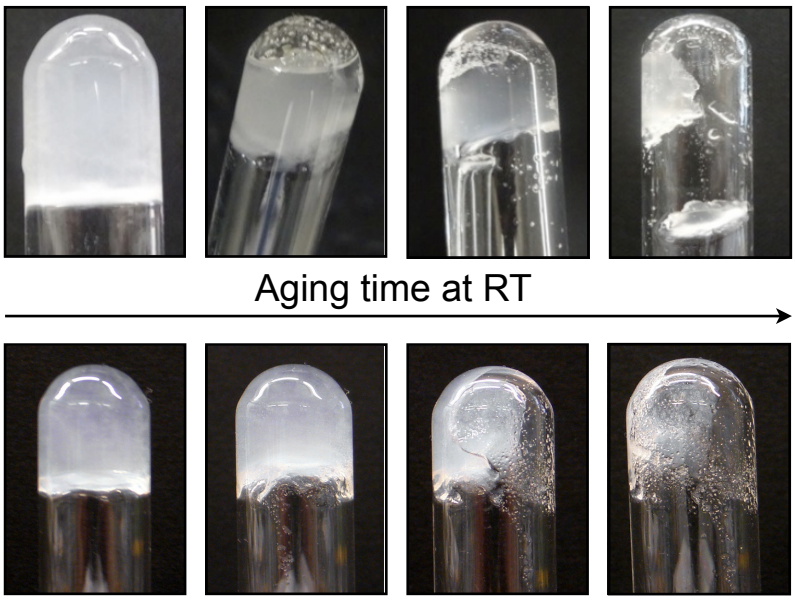

Figure 44: Digital photographs of a MGS I gel from ETAC (top) and of a MGS II gel from DCM (bottom) over the time.

Solvent parameters

Kamlet-Taft solvent parameters[35] (Table 14, page 173f) account for specific interactions between the molecules of the solvent and the gelator molecules.[36] The MGS systems here describe remarkable samples of *sol*-to-*gel*-to-*crystal* phase evolution.[37] The transient gels right on the border between dissolution and crystallization could contribute to explain that it is significant to find a correlation between solvent parameters like Kamlet-

Taft parameters and gel properties, like thermal and temporal stability. In Figure 45 the clear determination of the ability of the solvent to be gelled by MGS was described as a function of Kamlet-Taft parameters fitted by a Gaussian function. Solvents with a higher tendency for formation of relatively stable gels were those presenting no hydrogen-bond donor ability (e.g. $\alpha \approx 0.0$), intermediate hydrogen-bond acceptor ability (e.g. $\beta \approx 0.4$) and moderate polarizability (e.g. $\pi^* \approx 0.6$) at the same time. Contrary solvents with either lower or higher β and π^* values caused precipitation or complete solubilization of the mixture, regardless of the α value.

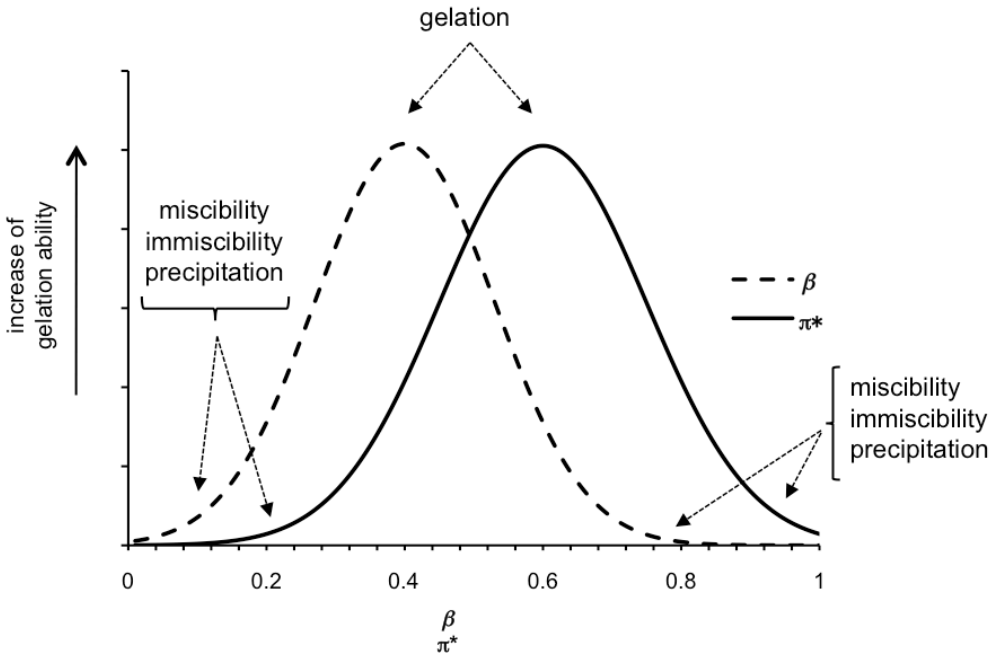

Figure 45: Correlation between β and π^* solvent parameters and gelation ability of MGS. The model is based on 29 different solvents.

Influence of the components on the gelation ability of MGS

As both MGS are based on chiral building blocks of salt **57** the effect on the enantiomeric purity of the salt and its effect on gel formation was investigated as chirality plays a central role in the functional properties of gel-based materials.[38,39] When MGS I solutions with enantiomeric purity of 0 - 80% were used the obtained material in THF was not able to resist the inversion of tube test without flowing of material (Figure 46, top). Only a MGS I with 100% enantiomeric purity provided gels which were stable to the inversion of tube test. The same results were achieved by preparation of THF organogels with MGS II. Just

with a enantiomeric purity, ee, of 100% a gel was formed which was stable to inversion of the tube (Figure 46, bottom).

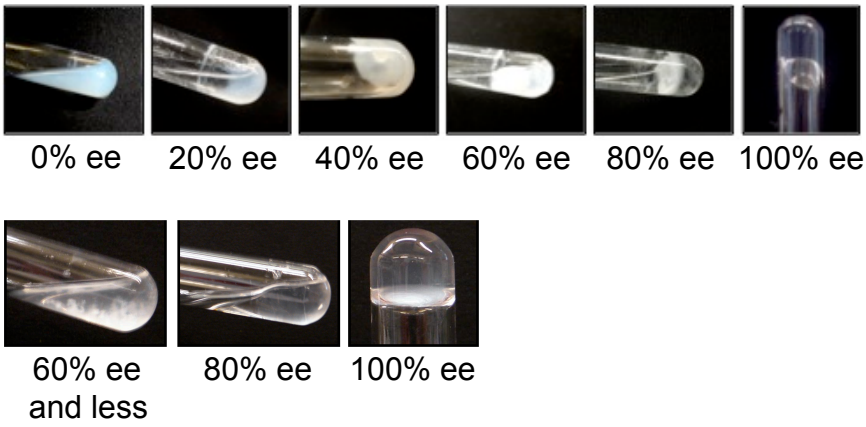

Figure 46: Investigation of enantiomeric purity, ee ranging from 0 - 100% for MGS I (top) and MGS II (bottom).

Interestingly, diasteriomeric (1*R*,2*R*)-1,2-diaminocyclohexane *D*-tartrate obtained gels, but they had a much lower temporal stability compared to original MGS, due to a enhanced crystal formation.

In further experiments the influence of the salt structure on the gel stability was examined. For this the *L*-tartaric acid was exchanged by a row of different dicarboxylic acid derivatives. As result transient gels in different organic solvents were produced with MGS I and II based on diethyl *L*-tartrate **59**, succinic acid **60**, adipic acid **61**, dibenzoyl *L*-tartrate **62**, phthalic acid **63** and *L*-malic acid **64** (Figure 47). In the case of phthalic acid **63** MGS I provided only a partial gel-like material.

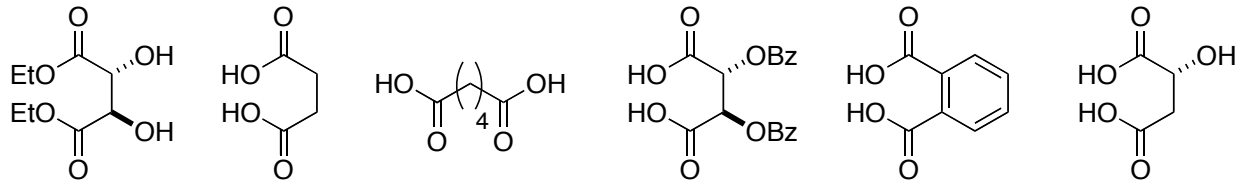

Figure 47: Structures of different dicarboxylic acids and ester for exchange with *D*-tartaric acid.

The temporal stability of these gels were under the half of the gels from original MGS I (Table 7). Remarkably, the exchange of the acid did not show the same influence on the

gel stability in case of MGS II (Table 7). The importance of carboxylic acid groups and a chiral moiety for the formation of relatively self-standing gel networks were only indicated by the MGS I gels made with dibenzoyl *L*-tartrate **62** and *L*-malic acid **64** as they provided gels with some higher temporal stability than for the other acids.

Table 7: Effect of dicarboxylic acid on the gelation ability.[a]

Acid	**59**	**60**	**61**	**62**	**63**	**64**
MGS I			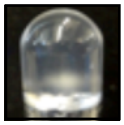		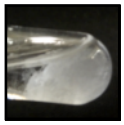	
	2-3 h	3-4 h	2-3 h	10-15 h	PG	8-12 h
MGS II	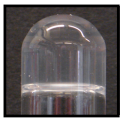	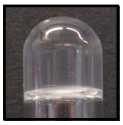	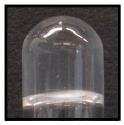		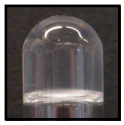	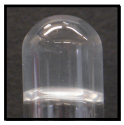
	3 d	3 d	3 d	3-4 d	3 d	3 d

[a] For comparison, in each experiment 1.0 mL THF was used and beside the exchanged acid prepared at the standard conditions as MGS I or MGS II THF gels. Abbreviation: PG = partial loose gel. Temporal stability is provided for each gel.

Moreover, the replacement of (1*R*,2*R*)-1,2-diaminocyclohexane by other diamines was studied. Ethylenediamine **65**, *N*,*N*,*N*′,*N*′-tetramethylbutane-1,2-diamine **66**, *N*,*N*,*N*′,*N*′-tetramethylethane-1,2-diamine **67**, 1,6-diaminohexane **68**, (1*R*,2*S*)-1,2-diaminocyclohexane **69** and (1*R*,2*R*)-*N*,*N*′-dimethyl-1,2-cyclohexanediamine **70** were chosen to serve as replacements (Figure 48).

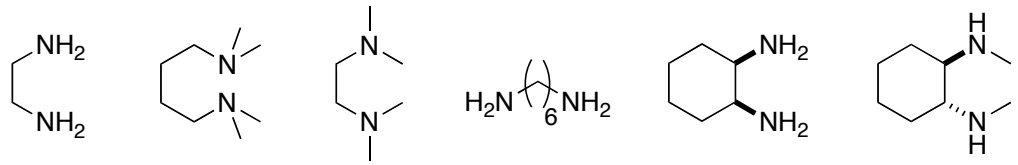

65 **66** **67** **68** **69** **70**

Figure 48: Structures of different diamines for exchange with (1*R*,2*R*)-1,2-diaminocyclohexane.

Non-stable MGS I gels were obtained with the potential gelator solutions prepared with diamines **68**, **69** and **70** (Table 8). However, the prepared MGS II gels with **69** were stable for 1-2 days. MGS II gels from **65**, **68** and **70** were unstable and resulted in precipitation.

The multicomponent mixtures in MeOH using diamines **65**-**67** (ca. 0.13 M) were always turbid even in the presence of higher amounts of HCl (> 2.4 equivalents). Therefore, no further optimization studies were made with these diamines (Table 8).

Table 8: Effect of diamine on the gelation ability.[a]

Diamine	**65**	**66**	**67**	**68**	**69**	**70**
MGS I	I	I	I	P	P	P
MGS II	P	I	I	P	 1-2 d	P

[a]For comparison, in each experiment 1.0 mL THF was used and beside the exchanged diamine prepared at the standard conditions as MGS I or MGS II THF gels. Abbreviations: P = precipitate, I = insoluble in stock solution. Temporal stability is provided for the gel.

The necessity of each single component presented in the optimal MGS I was investigated by a series of experiments. First a solution without *L*-tartaric acid was prepared from (1*R*, 2*R*)-1,2-diaminocyclohexane, methanol and aqueous HCl. The MGS I gels from this solution turned out to be very weak as it took less than 1 h for the gels to convert into partial gel-like materials or precipitates. Opposed to MGS I, the temporal stability of MGS II gels without *L*-tartaric acid decreased only to the half. As discussed before the replacement of methanol or DMSO by other solvents did not allow the tartrate salt to be dissolved or showed a stable, clear solution. The exchange of aqueous HCl (37%) by aqueous HBr (48%) gave solutions with the ability to form gels, although with approximately 80% lower temporal stability compared to optimal MGS. That was caused by a faster formation of crystals. The addition of 1 extra equivalent of water resulted in the crystallization of (1*R*,2*R*)-1,2-diaminocyclohexane *L*-tartrate within 1 h. The anhydrous MGS I gelator solution was prepared from commercial 1.25 M MeOH/HCl solution. A temporal stability of less than 1 h was observed for the water-free MGS I.

Mechanistic considerations

Although MGS I and II based gels provide a stable extended non-covalent network, it is not the thermodynamic minimum. A detailed crystallographic study of this salt

demonstrated that it exhibits a highly interconnected bidirectional hydrogen-bonding polymeric network. The constitutional element of the supramolecular aggregate is a tweezer-shaped pattern which involves hydrogen-bonding interactions between ammonium nitrogen as donor and hydroxyl group oxygen as acceptor (Figure 49). The ammonium groups act as donor for the carboxylate groups in one direction and the hydroxyl group in the other. This interaction pattern needed for the development of an extended network is determined by the defined chiral centers in the tartrate salt. Canal-like cavities delimited by the carboxylate, ammonium and hydroxyl groups are easily envisaged from the top view of the assembly.[40]

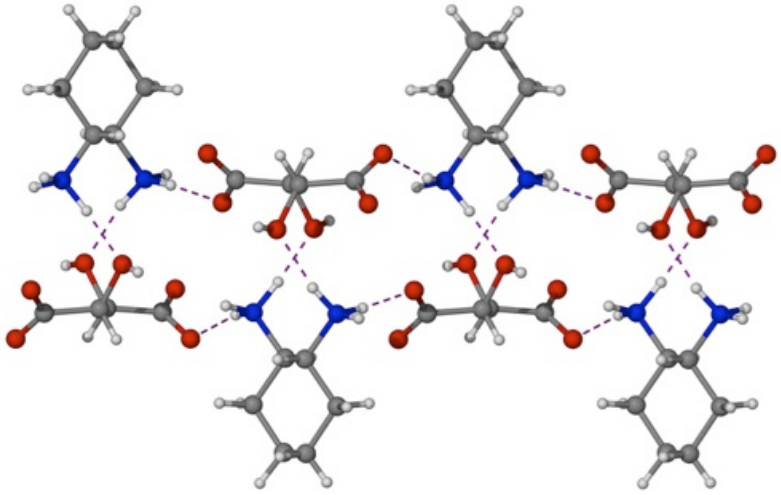

Figure 49: Crystallographic data of (1*R*,2*R*)-1,2-diaminocyclohexane *L*-tartrate, *top* view on the tweezer-shaped hydrogen-bonds between amino and hydroxy groups.

A plausible mechanism to explain the formation of the short-lived gel is indeed based on the compact nature of the tartrate salt **57**. When **57** is suspended in methanol, hydrogen-bonds of the polymeric system are too strong to interact efficiently with the solvent, as they are inaccessible. In the presence of aqueous HCl, the ion-paired carboxylate-ammonium groups are initially surrounded by chloride ions, water molecules and solvent molecules of the polar solvation shell.[41] Therefore a complex hydrogen-bonded network is created which makes it possible to solubilize all these species in methanol. Slowly the complex solution tends to evolve from the metastable phase to the thermodynamic equilibrium position. The energetic minimum for the system is defined by the crystallization of the poorly soluble (1*R*,2*R*)-1,2-diaminocyclohexane dihydrochloride **58** upon completion of the

ionic dissociation-exchange process and the consequent release of the soluble *L*-tartaric acid (Figure 50).

When a small amount of the complex solution is mixed with a second organic solvent which provides moderate hydrogen-bond acceptor properties, nonprotic and less polar than methanol, the solubility of the multicomponent aggregates decreases but still held within the dense hydrogen-bonded network.

The elusive balance of interactions between methanol, water and organic nonprotic solvent molecules should take place, as this allows the interfacial stabilization of the tartrate complex for enough time to permit its isotropic supramolecular assembly of limited solubility before the ionic exchange is completed and leads to the collapse of the gel and formation of **58**.

As shown before the crystallization rate of **58** can be fine-tuned amongst others by the concentration of salt **57** and the number of HCl equivalents in the solution. The irreversible transition to the thermodynamically stable equilibrium position and therefore the destruction of the strong hydrogen-bonding network of the metastable gels can be accelerated by additional energetic contribution as mechanical stress or heat.

All products were characterized by NMR and elemental analysis, as well as by XRD in case of crystalline **58** obtained from MGS. The exceptional ability of salt **57** to assemble supramolecular hydrogen-bond-based structures was reported previously.[42]

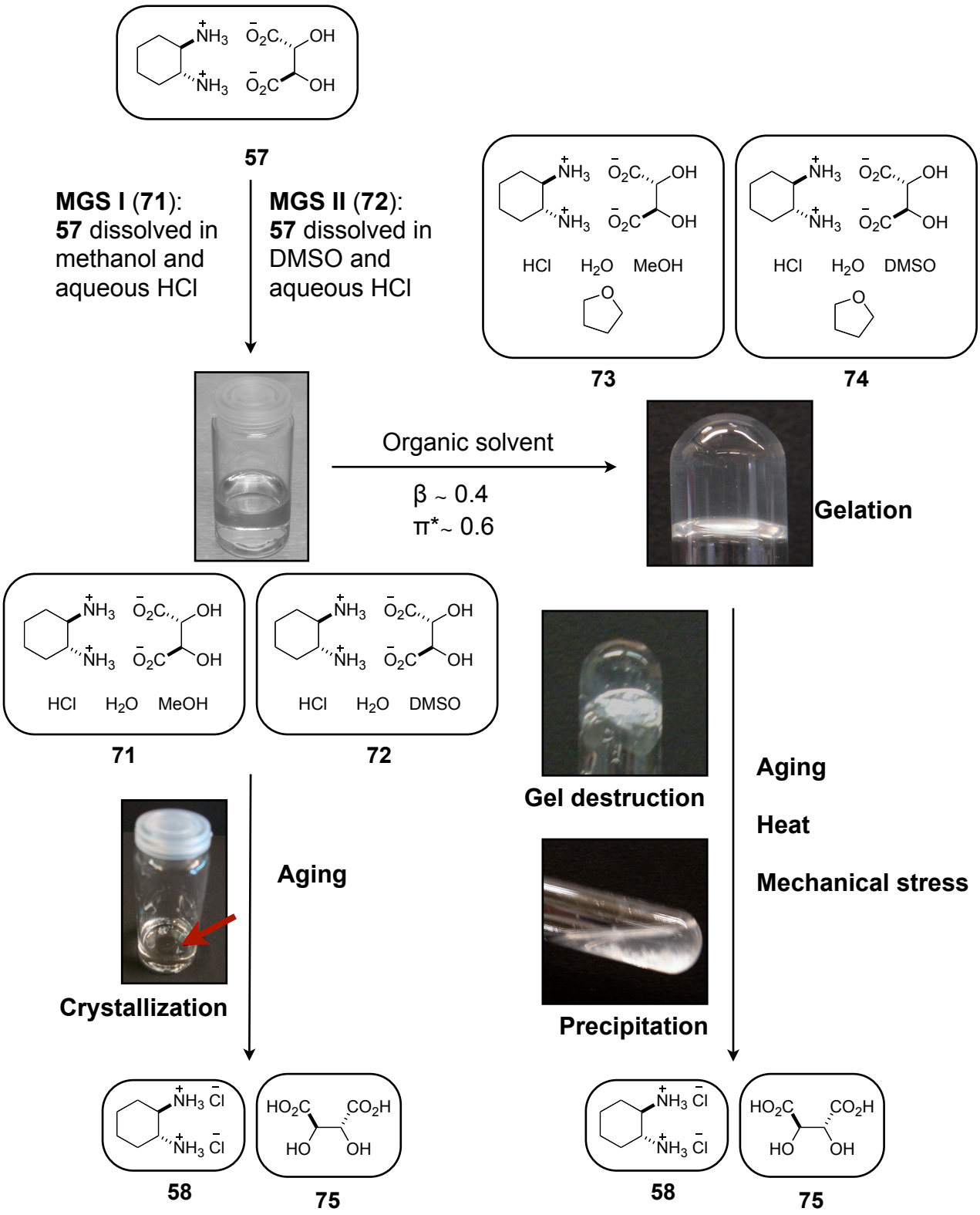

Figure 50: Overview on gelation and crystallization process in MGS I and MGS II and the respective gels.

The proposed mechanism for gelation based on the HCl-induced ionic dissociation-exchange of the salt **57** and the formation of a transient chloride-containing assembly **58** in

solution, resembling that in the crystalline state,[43,44] are supported by a series of experiments from this chapter:

1. The formation of jelly aggregates with much lower stability when
   a. MGS was prepared using (1*R*,2*R*)-1,2-diaminocyclohexane and *L*-tartaric acid instead of pre-organized hydrogen-bonded polymeric salt **57**, resulting in a much faster formation of **58**
   b. the tartaric acid counterpart was eliminated from MGS
   c. aged MGS was used
   d. the tartaric acid and the diamine were exchanged by alternatives, which cannot replicate the strongly hydrogen-bonded, ion-paired gels of **57**
   e. non-enantiomerically pure MGS solutions were used.
2. The thermodynamic formation of **58** as crystals from MGS or after destruction of MGS gel.
3. The delicate balance between the concentration of each component to maximize the half-life of the gel material.
4. The evidence of transient gelation even when highly concentrated MGS were used.

Thermal stability

Although MGS I and MGS II provide supramolecular organogels, the gels were not thermoreversible. Mechanical stress as well as heating of the gel samples led to their destruction by the acceleration of crystal growth. The precipitated (1*R*,2*R*)-1,2-diamino-cyclohexane dihydrochloride was insoluble and unable to get back into the solution at RT or upon heating. The low mechanical resistibility and the lack of a clear transition to a liquid phase made the “dropping ball method“ inappropriate for the thermal characterization of these materials. Figure 51 presents an alternative method to the dropping-ball method, based on a Kugelrohr distillation apparatus. The sample vial is held inside the chamber with a thermometer close to the gel. After the chamber is in a vertical position the heating was started. Unfortunately, this method still depends on human judgement to determine the moment in which the change takes place from gel-material to destroyed gel. However, also DSC measurements provided reproducible data about the first endothermic transition, which was associated with the temperature at which the destruction of the gel network took place, T_d.

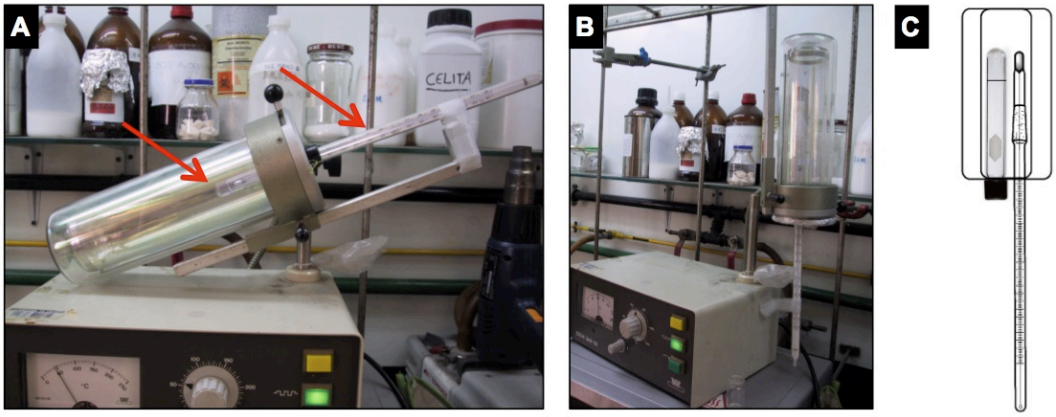

Figure 51: Kugelrohr distillation apparatus as alternative procedure to the dropping-ball method.

The agreement of the obtained T_d values with the values from DSC was extraordinary (Figure 52).

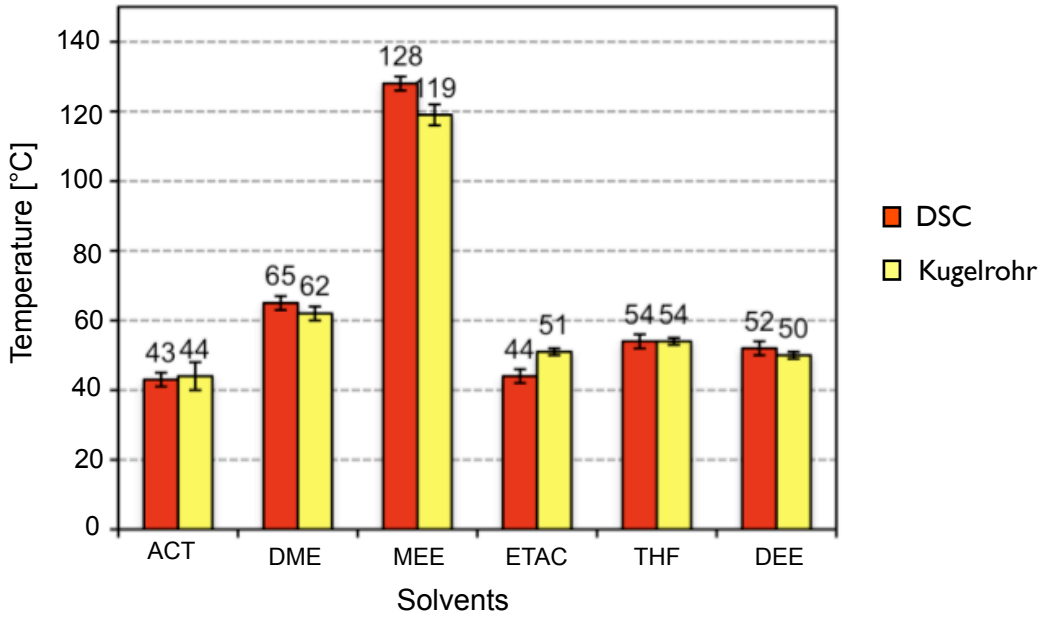

Figure 52: Comparison between T_d for MGS I gels measured by DSC and Kugelrohr apparatus. The results represent the average of multiple randomized experiments.

The results validated both methods to provide a reliable fingerprint for the thermal destruction of the gel network. Nevertheless, in order to obtain reliable thermodynamic data as enthalpic contributions, DSC measurements should be optimized for each material. The use of sample holders with higher sample volume and the *in situ* preparation of the gels prior measurement could be more appropriate for investigation of the gels.

Figure 53 presents an overview of a row of DSC thermograms from MGS I (top) and MGS II gels (bottom).

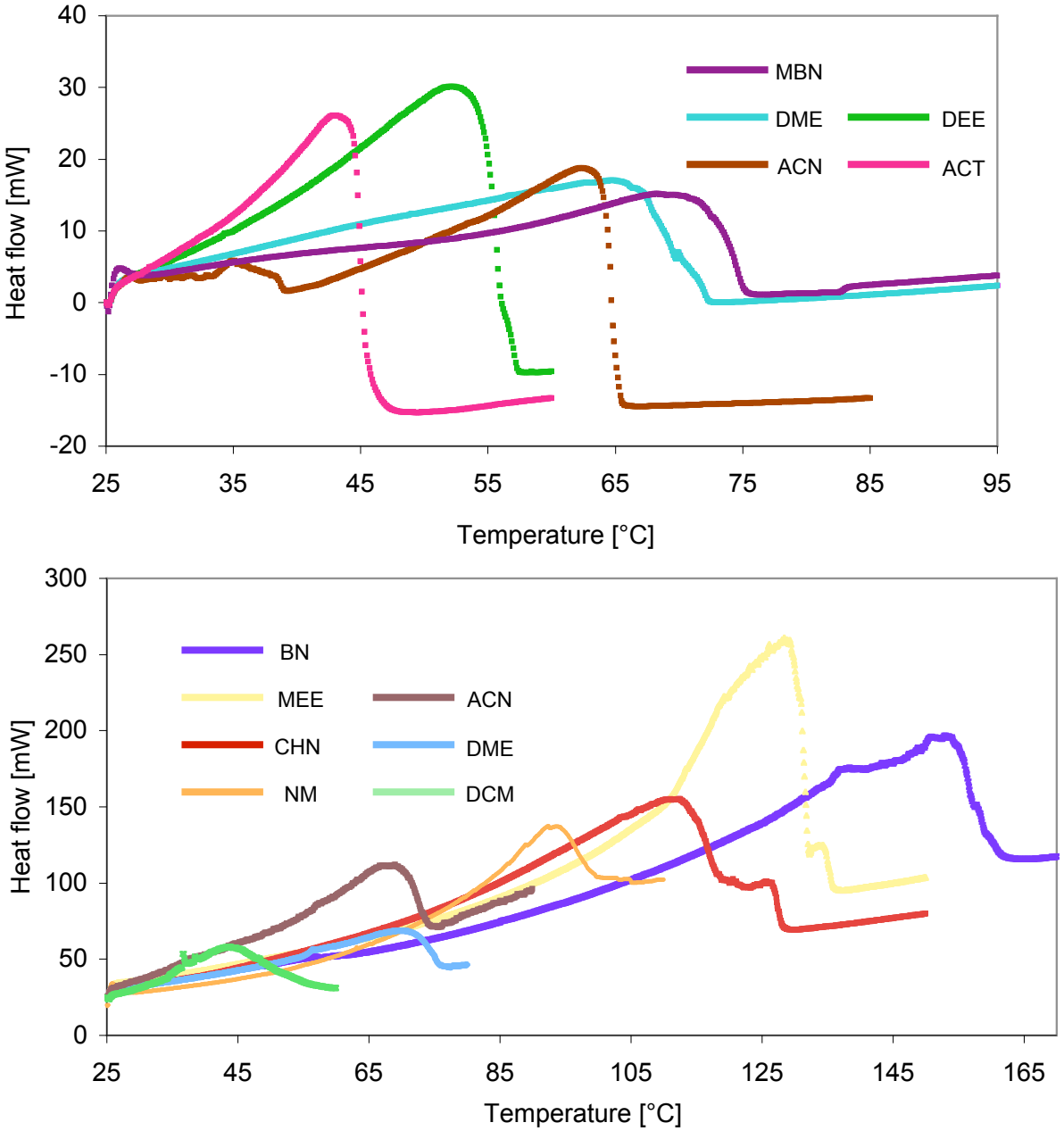

Figure 53: DSC thermograms of MGS I gels (top) and MGS II gels (bottom) from different solvents. Each plot represents the average of two random measurements.

As indicated in Table 5 and Table 6 some MGS II gels provide a higher thermal stability than the corresponding gels from MGS I. For ACN an increase of 9 °C for T_d is achieved, remarkably 40 °C for CHN, 7 °C for MBN, again 7 °C DME and 12 °C for ETAC. In Figure

54 the comparison of DSC thermograms between MGS I and MGS II gels from DME (top) and ACN (bottom) is shown.

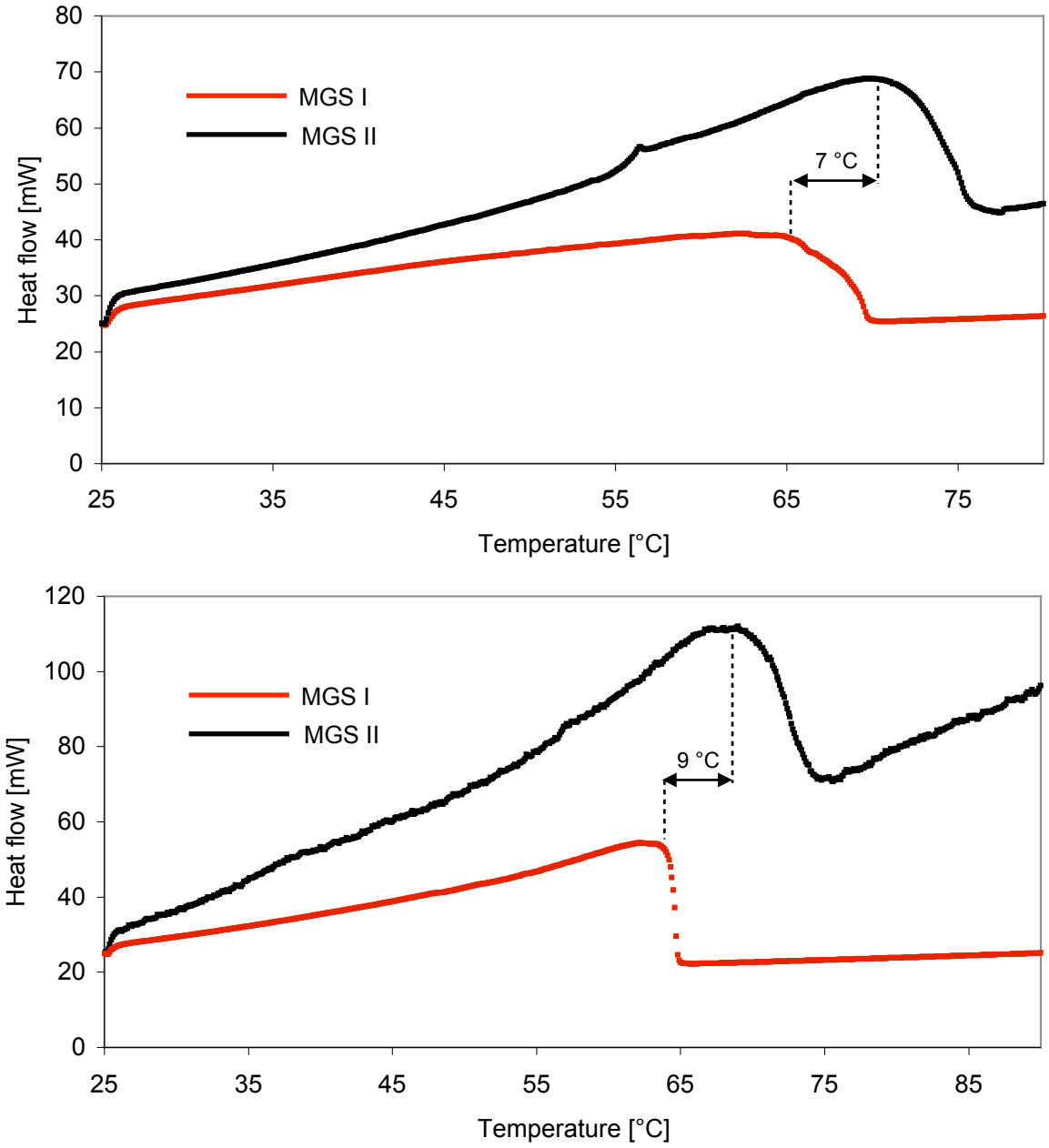

Figure 54: DSC thermograms showing the comparison of T_d between MGS I and MGS II gels from DME (top) and ACN (bottom).

Despite most supramolecular gels, which are showing a clear increasing *gel*-to-*sol* transition temperature with increasing of the gelator concentration, T_d for MGS derived gels enhanced only slightly with increasing amount of MGS. Interestingly, the MGS I gel from 1,4-dioxane showed the first endothermic transition at ~ 81, 84 and 88 °C when 40,

50 and 75 µL of MGS I were used (Figure 55). However, the use of higher amounts i.e. 100 µL destabilized the gel phase with decreasing T_d to 83 °C. The gel with higher MGS I volume also showed a lower temporal stability.

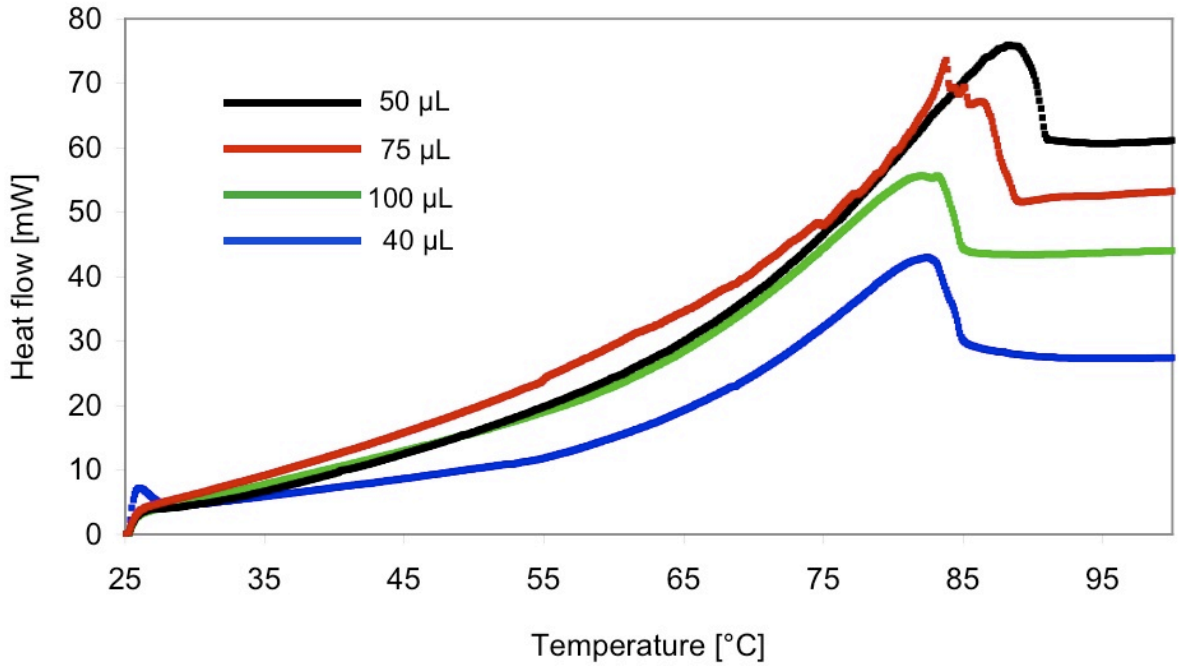

Figure 55: DSC thermograms from MGS I DOX gels prepared with different volume of MGS I.

FT-IR

As expected the FT-IR spectra of both MGS and gel-based materials displayed the stretching vibration band of both carboxylic (1710-1749 cm^{-1}) and ammonium (3250-2350 cm^{-1}) groups. Hydrogen-bond association bands in the range of 3600-3200 cm^{-1} were also found for the gel material. However, for accurate interpretations of the spectra it should be considered that alkane, water and methanol O-H stretching bands are also overlapped in the above regions. Thus, no further conclusive information could be obtained from these spectra.

Dynamic rheological measurements of model gels

Dynamic rheological measurements for MGS I and MGS II gels were carried out to confirm the gel state of the materials. Rheological characterization was performed for two model systems, THF and DOX. A similar flow behavior can be also expected for other solvents. Dynamic time sweep, DTS, experiments at 0.1% strain and frequency of 1 Hz showed that

the loss modulus, G″ was about one order of magnitude lower than the storage modulus, G′ (Figure 56). That indicates the poor flexibility of the gels.

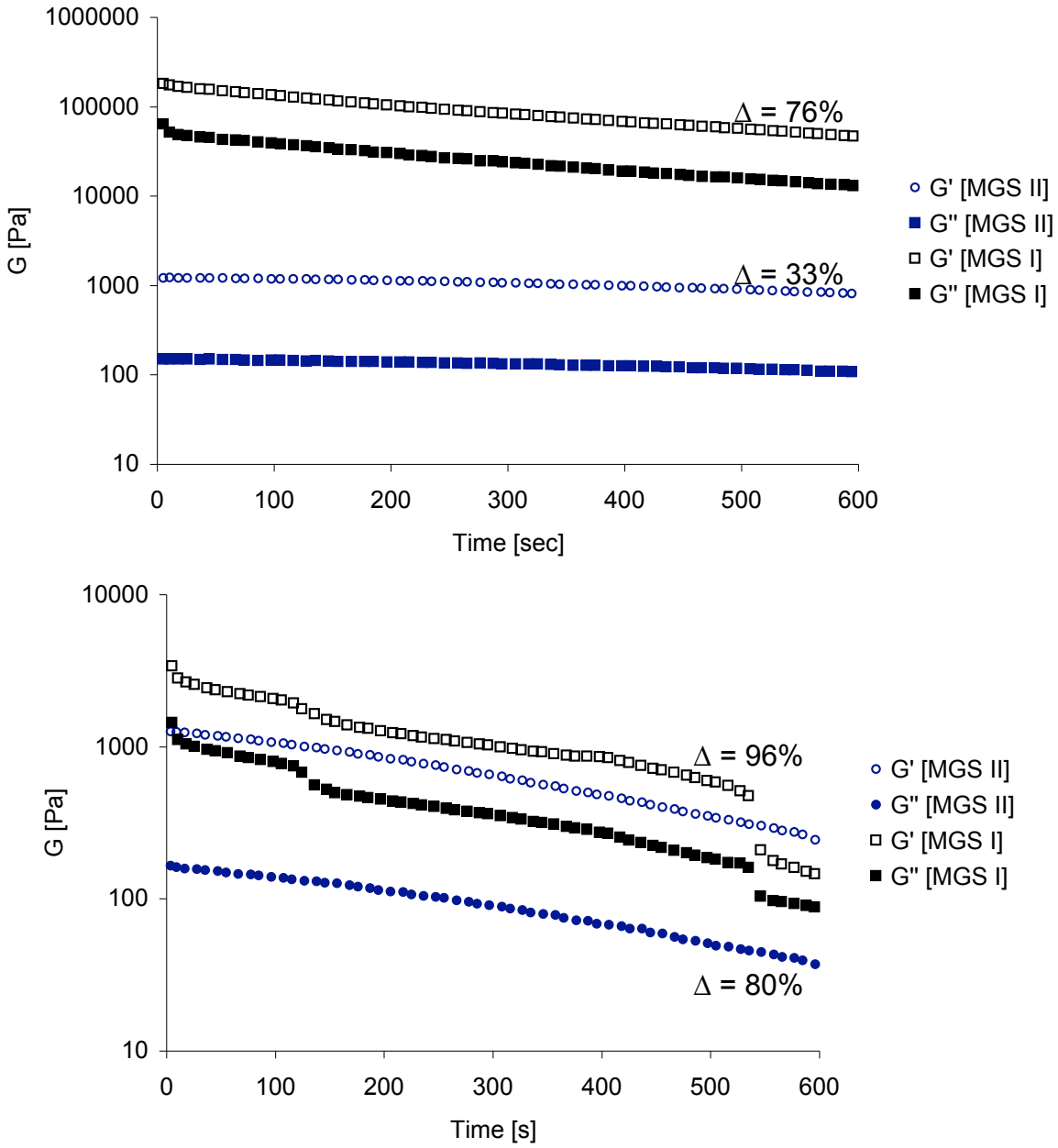

Figure 56: DTS experiments of THF gels (top) and DOX (bottom) made from MGS I and MGS II showing a remarkable decrease of G‘ and G‘‘ values.

Furthermore, DTS for both, MGS I and MGS II gels showed a decrease of G′ and G″ over the time. Interestingly, MGS II gels showed significant lower G′ and G″ values compared to MGS I gels. However, compared to the decrease of MGS I gels the decrease for MGS II gels is remarkably lower. After 10 min of aging time G′ for MGS I DOX gel was reduced about 76% of the starting value, but only 33% for MGS II DOX gel (Figure 56, top). For

THF MGS I gels showed a decrease of 96% compared to 80% of DOX gels from MGS II (Figure 56, bottom). That clearly shows the low tolerance of the gels to external shear force, which was in agreement with the disruption and liquid leakage of the transient gels when manipulated with a spatula. The constant tan δ values (tan δ = G″/G′) displayed that the mechanical damping properties of the gels did not suffer major changes during the 10 min of the experiment. However, a rise in the tan δ value was obtained when the experiment was proceeded.

Microscopy studies

The imaging of the xerogels from MGS I and MGS II was used to gain insight into the microstructure of the aggregates in different solvents (Figure 57). SEM images visualized a highly entangled fibrillar-like morphology in the freeze-dried MGS I gel derived from the gel in 1,4-dioxane (Figure 57, D). Most of the samples were characterized by the presence of aligned basalt-like (Figure 57, F-H) or cobbled pave-like dense packed structures (Figure 57, A,B and J), depending on the solvent used to prepare the gels. The former structures showed uniform diameters of 2-3 μm, whereas the latter structures presented large cluster aggregates of 20-40 μm in diameter.

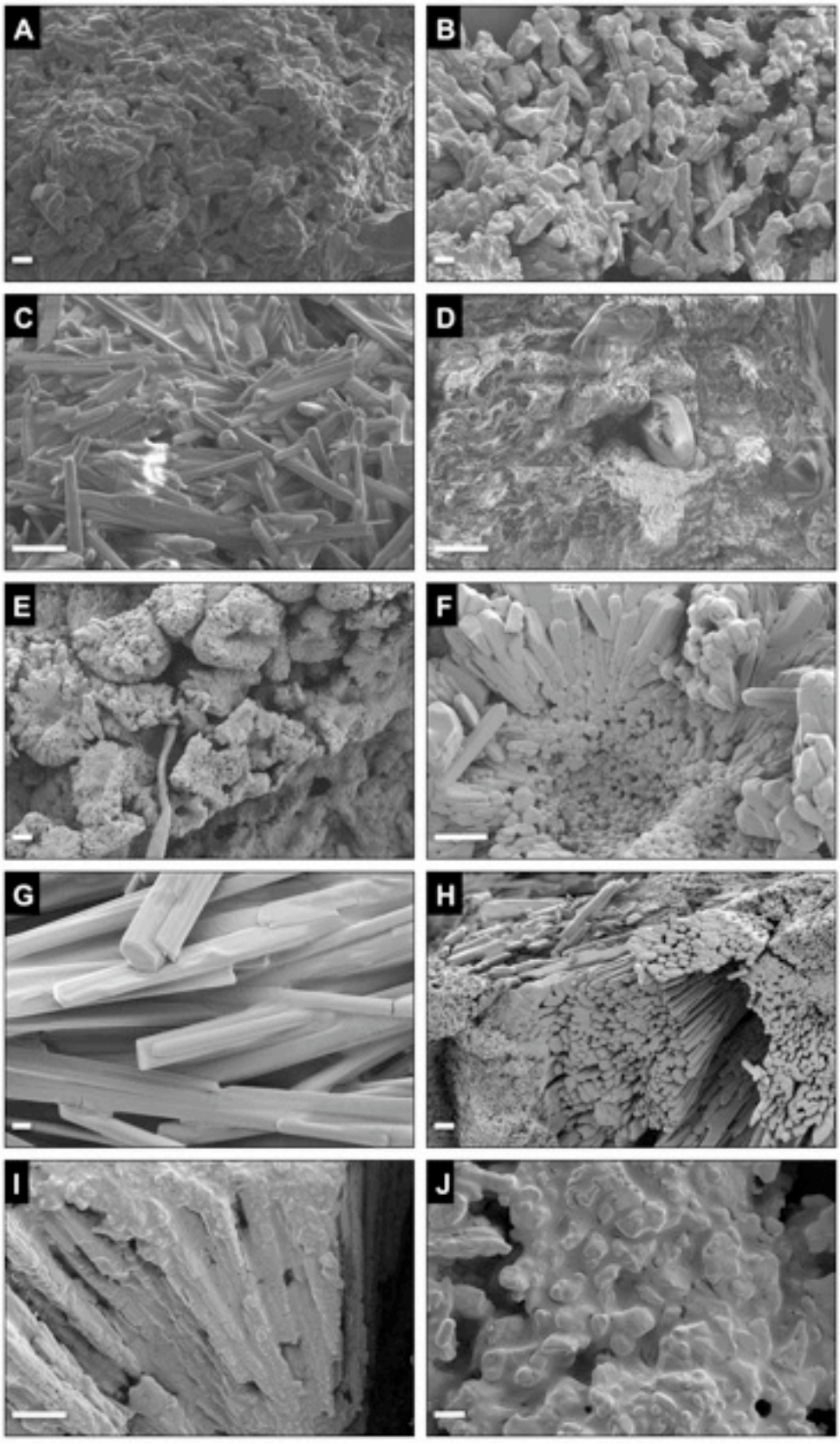

Figure 57: SEM images of different MGS I xerogels. A = ETAC gel (scale bar = 20 µm); B = DME (20 µm); C = THF (10 µm); D = DOX (10 µm); E = BN (20 µm); F = BN (10 µm); G = ACN (1 µm); H = (20 µm); I = MBN (10 µm); J = DEE (30 µm).

Nevertheless, as MGS II gels were prepared at an extremely low concentration and DMSO was hard to remove by vacuum it was almost impossible to obtain enough xerogel material for SEM studies. Finally enough xerogel for the gel with the highest MGS II concentration, DCM, was provided. The corresponding SEM images (Figure 58) provide a very dense and crumbly structure.

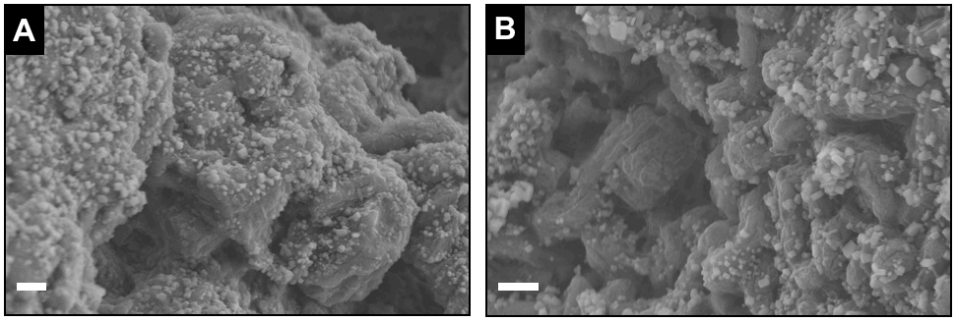

Figure 58: SEM images of MGS II xerogel from DCM (scale bar A = 20 µm, scale bar B = 20 µm).

3D Images from of the surface topography were obtained by atomic force microscopy (Figure 59). In general, the images showed aligned mountain-range-shaped surfaces with average heights in a range of 25-100 nm and apparent diameters of about 100-200 nm for the largest individual feature. The lower limit was not considered significant as it is dictated by the size of the AFM tip.

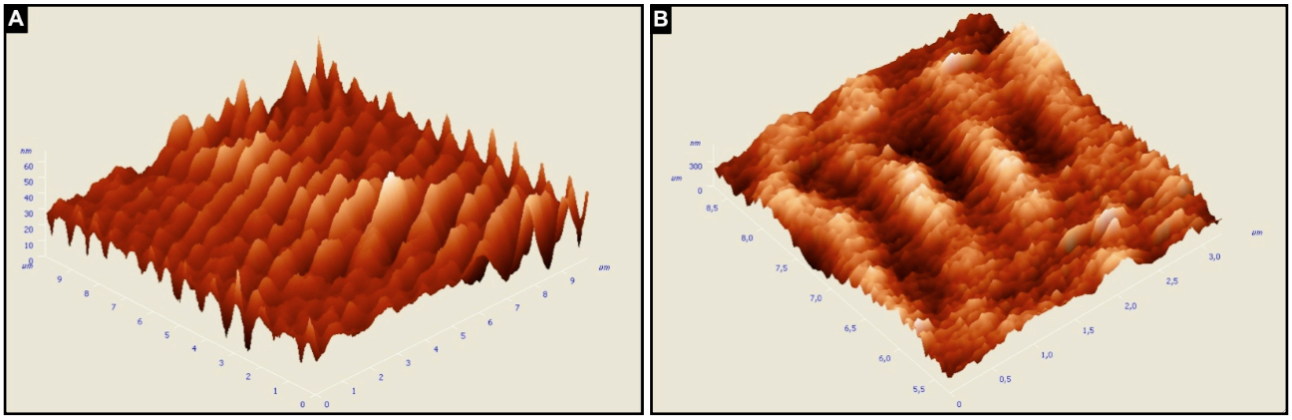

Figure 59: 3D-Surface topographic AFM images. AFM image of the xerogel prepared from the gel in BN (A); AFM image of the xerogel prepared from the gel in ETAC.

XRD structures

The crystal structure of (1*R*,2*R*)-1,2-diaminocyclohexane *L*-tartrate **57** and its diastereomer (1*R*,2*R*)-1,2-diaminocyclohexane *D*-tartrate were reported previously.[43] (Figure 60). Salt **57** presented a highly interconnected bidirectional hydrogen-bonding network defined by a tweezer-shaped constitutional unit, consisting of 10-membered hydrogen-bonded rings involving ammonium nitrogen donors and oxygen acceptors in one direction with hydroxyl groups and in another with carboxylate groups. The side views showed a hollow-brick structure of the bilayered core. In contrast, the diastereomer (1*R*,2*R*)-1,2-diamino-cyclohexane *D*-tartrate showed opened gaps in the crystal lattice as a result of the imperfect matching of partners. These gaps were found to be filled with the two water molecules hydrogen-bonded to one hydroxyl group and one carboxylate oxygen. Despite the disruption of the hydrogen-bonding interactions, the layered structure of the core, the stacking of the cyclohexane residues and the canal-like framework were still retained, albeit with a lower level of organization. The optimal molecular recognition that occurs between the matched pairs of partners in the case of **57** compared to its diastereoisomer was also observed during the formation of the transient gels. For example the use of **57** provided stable MGS I gels in THF for about 4-5 days, whereas the use of its diastereoisomer provided transient gels that were destroyed after 8 h. Thus, (1*R*,2*R*)-1,2-diaminocyclohexane *D*-tartrate also afforded the formation of gel-like materials but with lower temporal stability than its diastereoisomer **57**. Crystal structures of tartrate salts have proven to be useful as they allowed to discuss reasonable supramolecular synthons of gelator and non-gelator salts.[45] Both, experimental evidences and literature precedents supported the proposed mechanism for the formation of transient gels made from MGS.

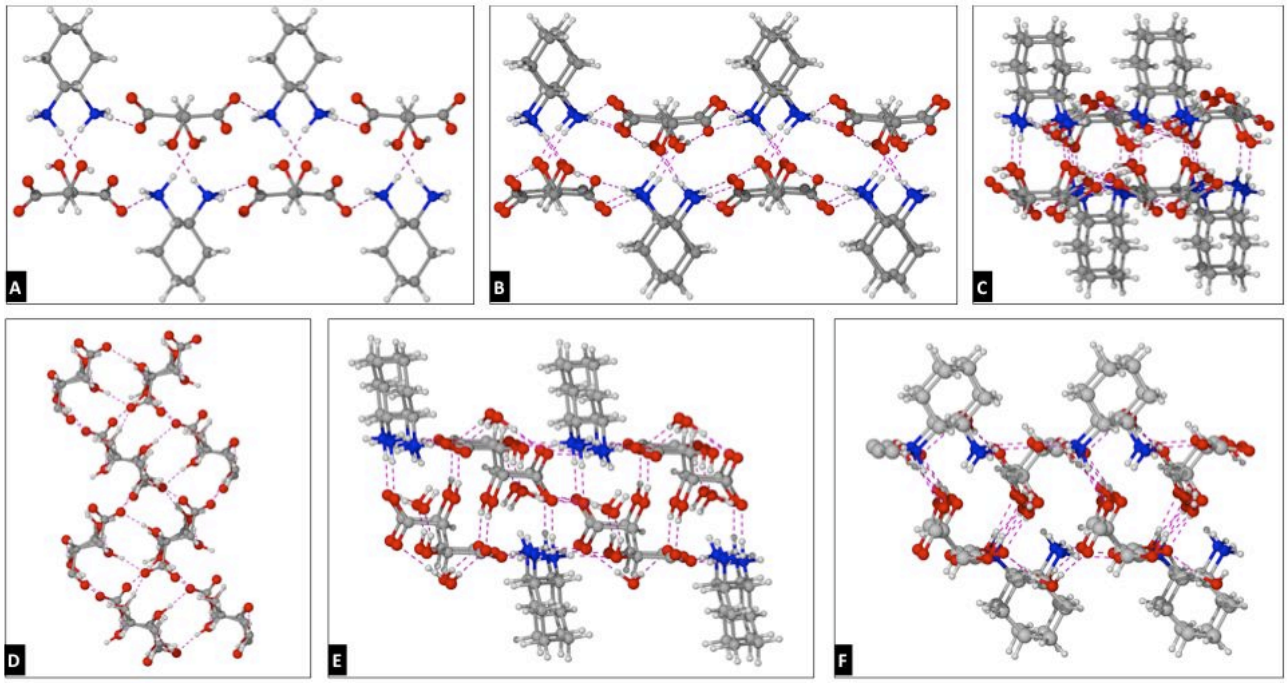

Figure 60: Top view of **57** down the *a* axis and showing a tweezer-shaped hydrogen-bonding between amino and hydroxy groups (A); Two of the previous networks overlapped (B); Side view of **57** down the *b* axis showing the bilayered cored (C); Side view of **57** down the *c* axis showing the hydrogen-bonded network (D); Top view of diastereomer (1*R*,2*R*)-1,2-diaminocyclohexane *D*-tartrate down the *b* axis showing two molecules of water bound to tartrate hydroxy and carboxylate groups (E); Side view of diastereomer (1*R*,2*R*)-1,2-diaminocyclohexane *D*-tartrate down the *a* axis showing the hydrogen-bonded network.

Compound **58** isolated after gel destruction consisted on intergrown crystals that made it not suitable for PXRD measurement. However, the product was unequivocally characterized by NMR and elemental analysis. The structure of **58** spontaneously crystallized from MGS I was confirmed by XRD (Figure 61).

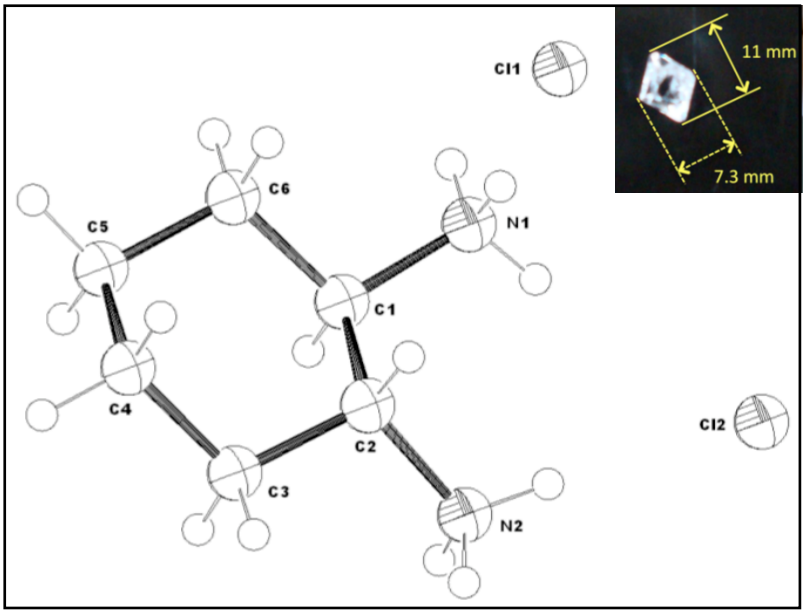

Figure 61: Ortep diagram of the crystal structure of **58**; inset shows a photograph with isolated crystal from **58**.[45]

3.4 Phase selective gelation

The ability of a gelator to gel selectively one of two phases is desired, as it could find application in oil-spill recovery.[40] However, both MGS showed now ability to gel an organic solvent in presence of water, as the gelator solution dissolved in the water phase.

When the potential formation of multicomponent organogel particles was tested with MGS II on the interphase between pentane - nitromethane - 1,2-dichlorobenzene it resulted in complete gelation of the NM phase. If the two solvents (Figure 62) were not layered, but mixed it was not possible to selectively gel one solvent, as only a partial gel was obtained. Moreover, it was found that DOX, NM, BN, ACN and ACT were selectively gelled by MGS II at minimum gelation volume when it was layered with pentane (Table 9).

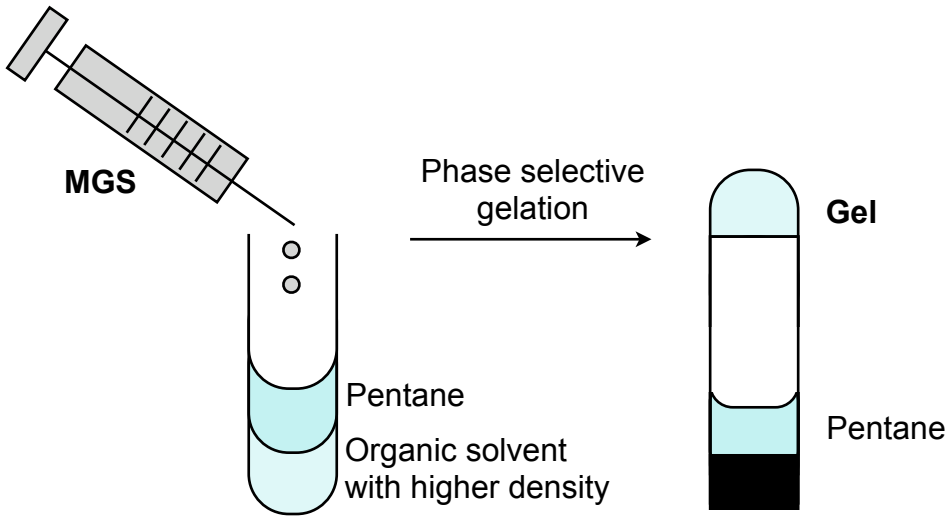

Figure 62: Illustration of phase selective gelation.

For DME, MEE, DCM, MBN, CHN, ETAC and THF no gelation was obtained, even by increasing the MGS II volume. In contrast, adding MGS I to pentane-layered solvent provided no selective, but partial gelation. As standard MGS I gels are prepared by cooling of the solvent the phase selective gelation experiments were repeated under the respective temperatures. Interestingly, after cooling of the solvent the phase selective gelation by MGS I succeeded for NM, ACN, ACT, DME and MEE. Unfortunately the temporal stability of the gels was reduced extremely. For all solvents the growing of crystals started after 2 h whereas the gels obtained from MGS II showed the same temporal stability as for standard preparation.

Table 9: Phase selective gelation with MGS I and MGS II at RT.[a]

Entry	Solvent	gv [µL] MGS I	Results MGS I	gv [µL] MGS II	Results MGS II
1	NM	100	PG	40	G
2	ACN	100	G+G	30	G
3	BN	150	PG	50	G
4	ACT	250	G+P	40	G
5	CHN	150	S	40	S
6	MBN	100	PG	20	S
7	DME	100	PG	30	S
8	MEE	100	PG	30	S
9	ETAC	250	G+P	20	S
10	THF	150	PG	20	S
11	DEE	180	PG	--	--
12	DOX	80	G+P	20	G
13	DCM	--	--	100	G+P

[a]The experiments were carried out with 1.0 mL pentane, 1.0 mL respective solvent and gv as described in Table 5 and 6. Abbreviations: gv = volume of MGS I or MGS II, G = gel, PG = partial gel, S = solution, G+P = gelation of solvent and pentane.

The results from rheological measurements of the NM gel obtained by phase selective gelation were in good agreement with the values from NM gel, prepared by standard procedure.

3.5 Semi-interpenetrating supramolecular network

To enhance the temporal and mechanical stability of the MGS gels the idea of assembling a second supportive network arose. Interpenetrating polymer networks, IPN, were already reported as polymers consist of two or more networks which are not covalently bonded to each other but at least partially interlaced on a molecular base. These networks cannot be separated without breaking of chemical bonds.[46] A Semi-interpenetrating network, semi-IPN, comprises a polymer network and interlaced LMWG fibers (Figure 64).[47] As consequence of the supramolecular nature of the second network the two networks can be

separated without breaking. As both MGS are providing LMWG based networks a second LMWG network would create a new example of interpenetrating networks, Semi-Interpenetrating Supramolecular networks, SISN.

Gelator **76** (Figure 63) was reported in 1998 from Hanabusa. It was chosen, because of its structural analogy to **57**.[48]

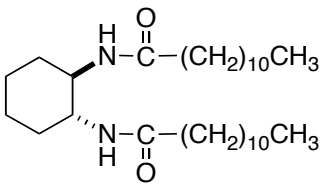

76

Figure 63: Gelator **76** for preparation of SISN.

As model solvent ACT was selected as both gelators were able to gel this solvent. The MGC of **76** in 1.0 mL ACT was defined as 1.0 mg. To ensure that **76** only supported the gelator network of **57** a concentration below the MGC of **76** was used.

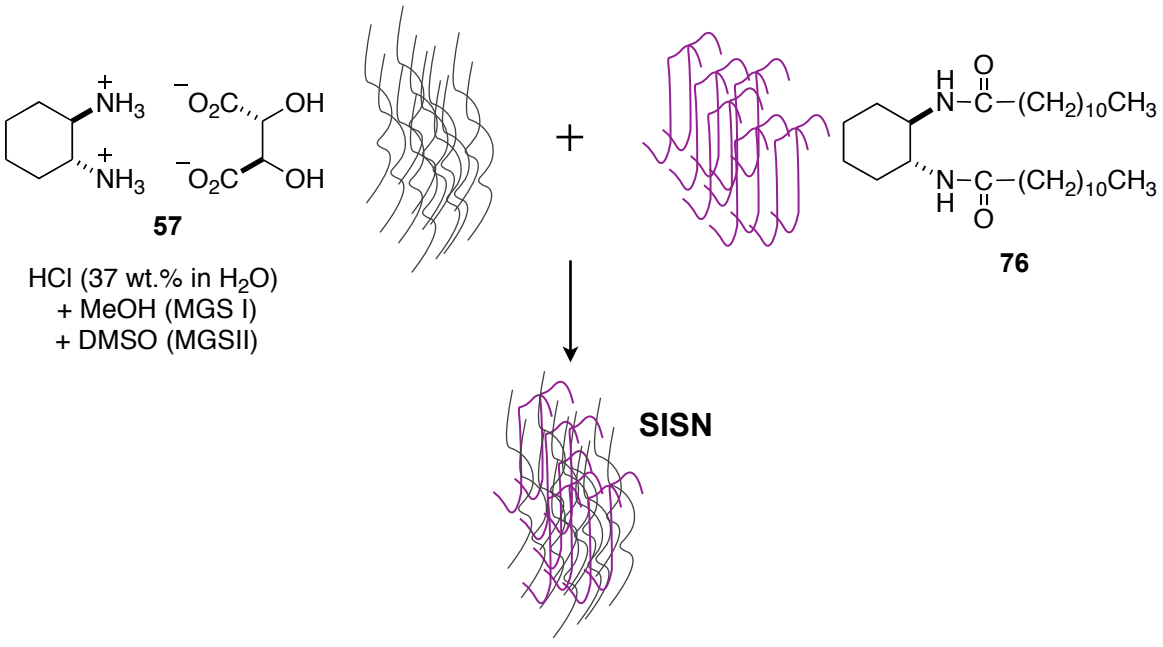

Figure 64: Schematic illustration of the formation of SISN from MGS and **76**.

The interpenetrating networks can be differentiated by the formation process. A sequential IPN is formed when a second network interlaces a first network which already existed.[49]

Contrary to that, a simultaneous IPN is prepared by a process where the networks are formed concurrently at the same time.[50] As MGS gels are sensitive to any kind of modification it was preferred to test the simultaneous formation first.

For preparation of gels from **76** the gelator must be dissolved by heat in the solvent prior gelation. A hot ACT solution with 0.08 wt.% of **76** was added to 24 µL MGS (0.08 wt % respective to **57**). For both, MGSI and MGS II 24 µL were below MGC. Only for MGS II a stable gel was provided while MGS I delivered solution.

Figure 65 provides SEM pictures from single and combined networks. Picture A and B shows the flexuous fibers of the 1.0 wt.% ACT gel from **76**. In picture C the crumbly structure of MGS II xerogel in DCM can be seen (100 µL·mL^{-1}). Picture D derived from a ACT xerogel with 0.08 wt.% of **76** and 24 µL of MGS II, proofs the formation of SISN. The crumbly texture of the MGS II pervades the fibers from **76** like a cobweb.

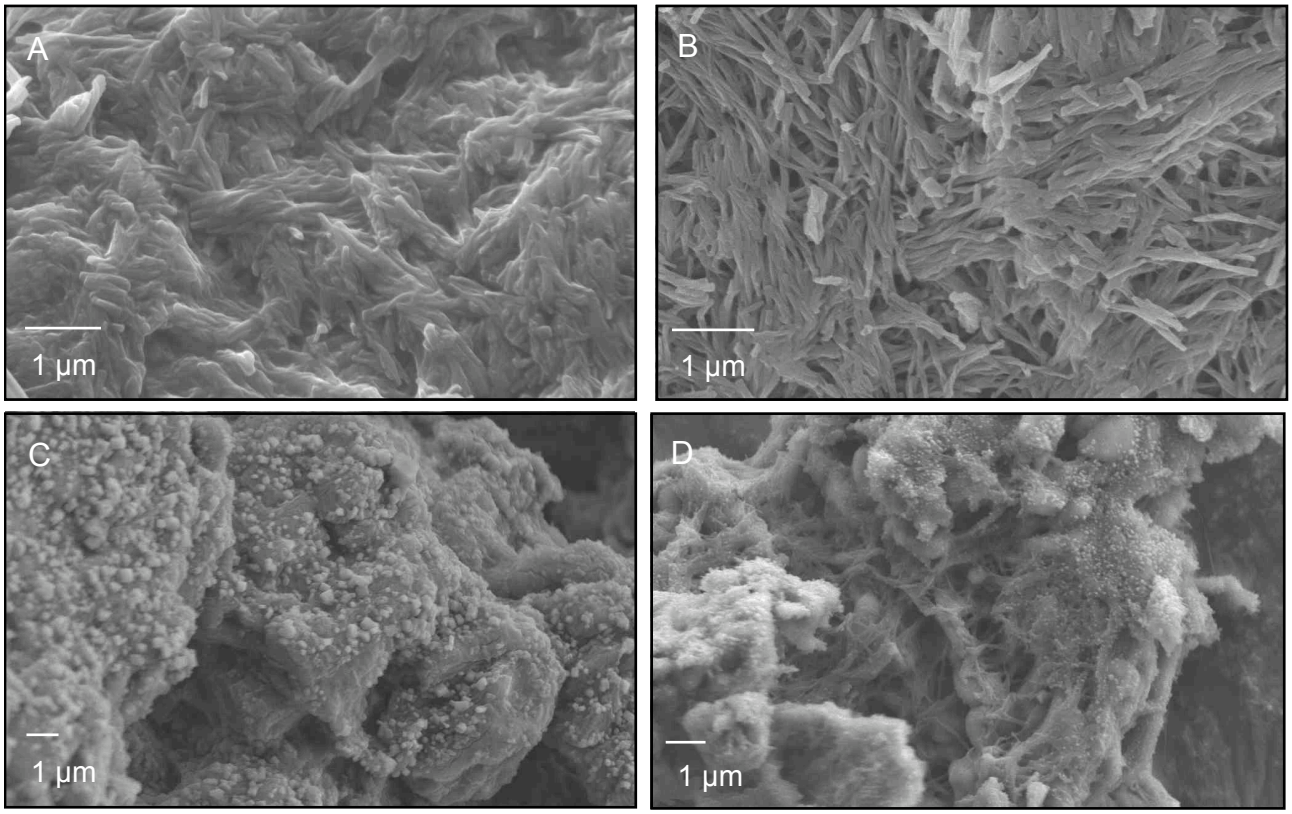

Figure 65: SEM images of **76** xerogel in ACT (A, B), MGS II xerogel from DCM (C) and SISN xerogel from ACT (D).

Unfortunately the temporal stability of the gel was not enhanced. Although the gel was still stable to the inversion of the test tube, the crystals of **58** were formed all over the gel which was a further proof of the coexistence of the two networks.

4. Conclusion

The two multicomponent gelator solutions, MGS I ((1*R*,2*R*)-1,2-diaminocyclohexane *L*-tartrate, methanol, aqueous HCl) and MGS II ((1*R*,2*R*)-1,2-diaminocyclohexane *L*-tartrate, DMSO, aqueous HCl), showed the formation of transient gel aggregates at either low (MGS I) or room temperature (MGS II). The gelation mechanism based on the self-assembly of the tartrate salt which performed a unpredictable competition between crystallization and gelation which always ended in crystallization of (1*R*,2*R*)-1,2-diaminocyclohexane dihydrochloride and therefore destruction of the gels. Both MGS were able to gel a number of oxygenated and nitrogenated solvents with moderate polarity. Remarkably, MGS II gels were formed at gelator concentrations at least 2 but up to 12 times smaller than MGS I gels. Also in terms of temporal and thermal stability MGS II gels showed appreciable improvement. Further, the experiments pointed out that for both MGS (1*R*,2*R*)-1,2-diaminocyclohexane played the key role of the structural direction, whereas the complementary tartaric acid partner acted as stabilizer of the supramolecular network, although MGS II gels showed a higher tolerance to the replacements than MGS I gels. The hydrochloric acid was essential for the solubilization of the salt, but higher concentrations always enhanced the crystal growing. As consequence, the irreversible destruction of the gels occurred, which indicated the metastable nature of the gel phase that cannot be accessed from the thermodynamically equilibrated state. The addition of a second gelator below its MGC only succeeded with MGS II ACT gel. Unfortunately the obtained semi-interpenetrating supramolecular network showed no improvement in temporal stability. Phase selective gelation between organic solvents with different density was successfully performed with MGS II without the weakening of the obtained gels‘ properties.

5. Experimental part

5.1 General remarks

Commercially available reagents and solvents for synthesis and analysis were used as received without further purification. Volumetric flasks were used for preparation of precise stock solutions. During solubility tests a VWR^{TM} ultrasonic cleaner, USC200TH, was used. After 30 min the temperature of the ultrasonic water bath increased up to 33 ± 2 °C. Compound **76** was prepared according to literature synthesis.[48]

5.2 Preparation of MGS and organogels

Synthesis of (1*R*,2*R*)-1,2-diaminocyclohexane *L*-tartrate

1.0 mmol of (±)-1,2-diaminocyclohexane was added dropwise to a 0.03 M solution of 1.0 mmol *L*-tartaric acid in water at 90 °C. In order to keep the mixture solubilized the temperature can be increased gradually until 100 °C. The solution was cooled down to RT and kept overnight at 4 °C. The formed crystals were filtered out, washed with ice-water, methanol and dried under vacuum to afford the product as a white crystalline solid. The recrystallization process was repeated twice.

Elemental analysis for $C_{10}H_{20}N_2O_6$ (%): calculated: C: 45.45, H: 7.63, N: 10.60; found: C: 45.49, H: 7.65, N: 10.58.

Solubility test of (1*R*,2*R*)-1,2-diaminocyclohexane *L*-tartrate

The solubility tests were carried out at a salt concentration of 0.04-0.08 M with 1 min of heat treatment and 15 min of sonication.

Preparation of MGS I

For the preparation of MGS I first of all a stock solution from methanol and hydrochloric acid was prepared. In a 50 mL volumetric flask 0.27 mL 37 wt.% hydrochloric acid in aqueous solution were mixed with dry methanol. 7.5 mL of this stock solution was mixed afterwards with 253.8 mg of (1*R*,2*R*)-1,2-Diaminocyclohexane *L*-tartrate. Thorough manual shaking of the mixture resulted in a transparent solution at a concentration of 0.128 mol·L^{-1}.

Preparation of MGS II

The preparation of MGS II was carried out analogously to the preparation of MGS I. The only exception was the use of DMSO (99.5%) instead of dry methanol.

Preparation of MGS I based organogels

Screw-capped, round-bottom glass vials with 10 cm length, 1 cm in diameter and a wall thickness of 1 mm were used for the preparation of organogels. Usually 1.0 mL of a respective dry solvent was cooled down in the vial close to the freezing temperature. For that the vial was kept in a cooling bath for at least 5 min to ensure that the addition took place at the desired low temperature. Then the appropriate amount of MGS I was added at once under gentle hand stirring of the glass vial. It was necessary to add MGS I in a way that the drops are able to slip down at the wall of the vial to reduce the effect of the container diameter. To avoid partial cloudy areas inside the transparent gels the mixing had to be effective and could also performed by a magnetic stirring bar (ca. 1000-2500 rpm). The vial was aloud to rest for one further min in the cooling bath. Afterwards, the clear and homogeneous solution was warmed up to RT by removing of the cooling bath. Gelation of the material inside the vial was inspected after 30 min at RT. Therefore the vial was turned upside-down. If the test tube was kept upside down for hours the gravitational forces caused the gel to fall down or fragment into small pieces. It was important to use glass vials of the same dimensions to enable the most reliable comparison between the samples

Preparation of MGS II based organogels

The same glass vials as for preparation of MGS I organogels were also used for MGS II organogels. Contrary to MGS I organgogels, MGS II organogels were produced at RT. The appropriate amount of MGS II was placed at the bottom of the glass vial and 1.0 ml of the respective solvent was added fast but without the formation of bubbles. The clear and homogeneous solution turned into gel, which was proven by turning the vial upside-down after 10 min.

5.3 Characterization of MGS organogels

Nuclear magnetic resonance spectroscopy (NMR)

NMR spectra were recorded on a Bruker Avance-300 spectrometer at ambient temperature.

Fourier transform infrared spectroscopy (FT-IR)

FT-IR spectroscopy was carried out on a Biorad Excalibur spectrometer, equipped with a Specac Golden Gate Diamond Single Reflection ATR-System.

Differential scanning calorimetry (DSC)

DSC thermograms were obtained with a Perkin-Elmer DSC7. The measurements were performed under a dynamic nitrogen atmosphere with a gas flow rate of 20 mL min^{-1} and a heating rate of 3 °C min^{-1}. The samples were placed into open aluminum pans from Perkin-Elmer and they were also used empty as reference. The measurements were carried out in a temperature range starting from 25 °C up to 60-160 °C, depending of the organogel. The reported values are the resulting averages from at least two independent measurements. Furthermore, the thermograms from MGS I were compared with the measurements of the destruction temperature, T_d, with a Büchi GKR-50 Kugelrohr apparatus.

Field emission scanning electron microscopy (FESEM)

A Zeiss Merlin field emission scanning electron microscope with an accelerating voltage of 10 kV was used to take SEM pictures of the xerogels. For this a nano-sized Pt film was sputtered prior to imaging on the samples on carbon tape (40 mA, 60 seconds). A SCD500 Leica EM device was used for the imaging.

Atomic force microscopy (AFM)

AFM images of the samples were carried out with Tapping Mode (Integra Probe Nano Laboratory, NT-MDT) at 1 Hz scanning rate with a TiN tip (NT-MDT Nanoprobe tip NSG01 series) at a drive frequency of 115-190 kHz and a force constant of 2.5-10 N m^{-1}.

Rheological measurements

Rheological measurements were performed with advanced rheometer AR 2000 from TA Instruments which was equipped with a cooling system (Julabo C). A 20 mm plain plate geometry (stainless steel) was used. First strain sweep measurements were carried out to estimate the strain in % at which reasonable torque values were given (about 10 times of the transducer resolution limit). Afterwards, frequency sweep measurements and time sweep measurements were performed. The gels were transferred from the vial to the plate of the rheometer and coated with a very small amount of low viscosity oil on top of the sample to avoid solvent evaporation during the experiment.

Optical microscopy

Pictures from crystals under a Wild Makroskop M420 optical microscope were taken with a Canon Power shot A640 digital camera to follow the formation of crystals in gel over the time with a magnification of 15.6.

X-ray diffraction (XRD)

Analysis was performed with a SuperNova diffractometer from Agilent Technologies Inc. A microfocus copper source was used together with an Atlas CCD camera. The determination of the cell parameters was carried out in six different goniometer orientations by omega scans.

Turbidity measurements

The measurement of turbidity was performed at RT with a Camlab CW8100 Portable Turbidimeter, calibrated with T-CAL standards. The device was equipped with a infrared LED (λ = 860 nm) as light source and a photodiode scattered light detector at an angle of 90°. To ensure the homogeneity of the samples and to avoid bubbles the vials were vigorously shaken for 1 min before measurement. The vials were rotated in the sample chamber about 45° after each measurement for each sample until the reading matches within ±0.001 nephelometric turbidity units (NTU).

5.4 Phase selective gelation

Screw-capped, round-bottom glass vials with 10 cm length, 1 cm in diameter and a wall thickness of 1 mm were used for phase selective gelation experiments. 1.0 mL of pentane

was layered upon 1.0 mL of a respective dry solvent. The respective volume of MGS was added over the solvents via syringe. A quick shaking with hand allowed the MGS to mix with the whole volume of the solvent. The gel formation was confirmed after 5 min by turning the vial upside down and removing the liquid pentane.

5.5 Semi-interpenetrating supramolecular network

SISN was prepared in a screw-capped, round-bottom glass vials with 10 cm length, 1 cm in diameter and a wall thickness of 1 mm. The respective amount of MGS was filled in the vial and slightly warmed via heat gun. 0.8 mg of **76** were dissolved in 1.0 mL acetone by careful heating. The mixing of the gelator solution in acetone with MGS was performed with a syringe. The formation of bubbles was avoided by a fast and consistent addition. After the obtained solution was cooled down the gelation was confirmed by inversion of the test tube.

6. References

[1] Hirst, A. R.; Smith, D. K. *Chem. Eur. J.* **2005**, *11*, 5496-5508.

[2] Hanabusa, K.; Miki, T.; Taguchi, Y.; Koyama, T.; Shirai, H. *J. Chem. Soc. Chem. Commun.* **1993**, *18*, 1382-1384.

[3] Inoue, K.; Ono, Y.; Kanekiyo, Y.; Ishi-I, T.; Yoshihara, K.; Shinkai, S. *J. Org. Chem.* **1999**, *64*, 2933-2937.

[4] Jeong, S. W.; Shinai, S. *Nanotechnology* **1997**, *8*, 179-185.

[5] Yagai, S.; Higashi, M.; Karatsu, T.; Kitamura, A. *Chem. Mater.* **2004**, *16*, 3582-3585.

[6] Numata, M.; Shinkai, S. *Chem. Lett.* **2003**, *32*, 308-309.

[7] Sugiyasu, K.; Numata, M.; Fujita, N.; Park, S. M.; Yun, Y. J.; Kim, B. H.; Shinkai, S. *Chem. Commun.* **2004**, *17*, 1996-1997.

[8] Partridge, K. S., Smith, D. K.; Dykes, G. M.; McGrail, P. T. *Chem. Commun.* **2001**, *4*, 319-320.

[9] Ayabe, M.; Kishida, T.; Fujita, N.; Sada, K.; Shinkai, S. *Org. Biomol. Chem.* **2003**, *1*, 2744-2747.

[10] Ballabh, A.; Trivedi, D. R.; Dastidar, P. *Chem. Mater.* **2003**, *15*, 2136-2140.

[11] Trivedi, D. R.; Ballabh, A.; Datisdar, P. *Chem. Mater.* **2003**, *15*, 3971-3973.

[12] Jung, J. H.; Ono, Y.; Shinkai, S. *Tetrahedron Lett.* **1999**, *40*, 8395-8399.

[13] Kawano, S. Fujita, N.; Shinkai, S. *Chem. Commun.* **2003**, *12*, 1352-1353.

[14] Dykes, G. M.; Smith, D. K. *Tetrahedron* **2003**, *59*, 3999-4009.

[15] Willemen, H. M.; Vermonden, T.; Marcelis, A. T. M.; Sudhölter, E. J. R. *Langmuir* **2002**, *18*, 7102-7106.

[16] Gerkensmeier, T.; Decker B.; Schwertfeger, M.; Buchheim, W.; Mattay, J. *Eur. J. Org. Chem.* **2002**, *13*, 2120-2125.

[17] de Loos, M.; van Esch, J.; Kellog, R. M.; Feringa, B. L. *Angew. Chem. Int. Ed.* **2001**, *40*, 613-616.

[18] Maitra, U.; Kumar, P. V.; Chandra, N.; D'Souza, L. J.; Prasanna, M. D.; Raju, A. R. *Chem. Commun.* **1999**, 595-596.

[19] Babu, P.; Sangeetha, N. M., Vijaykumar, P.; Maitra, U.; Rissanen, K.; Raju, A. R. *Chem. Eur. J.* **2003**, *9*, 1922-1932.

[20] Friggeri, A.; Gronwald, O.; van Bommel, K. J. C.; Shinkai, S.; Reinhoudt, D. N. *J. Am. Chem. Soc.* **2002**, *124*, 10754-10758.

[21] Ishi-i, T.; Iguchi, R.; Snip., E.; Ikeda, M.; Shinkai, S. *Langmuir* **2001**, *17*, 5825-5833.

[22] Jung, J. H.; Lee, S. J.; Rim, J. A.; Lee, H.; Bae, T.-S.; Lee, S. S.; Shinkai, S. *Chem. Mater.* **2005**, *17*, 459-462.

[23] Tan, G.; John, V. T.; McPherson, G. L. *Langmuir* **2006**, *22*, 7416-7420.

[24] Hirst, A. R.; Smith, D. K.; Feiters, M. C.; Geurts H. P. M. *Langmuir* **2004**, *20*, 7070-7077.

[25] Suzuki, M.; Saito, H.; Hanabusa, K. *Langmuir* **2009**, *25*, 8579-8585.

[26] Buerkle, L. E.; Rowan, S. J *Chem. Soc. Rev.* **2012**, *41*, 6089-6102.

[27] Guo, C.; Qiu, J.; Zhang, X.; Verdugo, D.; Larter, M. L.; Christie, R.; Kenney P.; Walsh, P. J. *Tetrahedron* **1997**, *53*, 4145-4158.

[28] Asperger, R. G.; Liu, C. F. *Inorg. Chem.* **1965**, *4*, 1492-1494.

[29] Larrow, J. F.; Jacobsen, E. N.; Gao, Y.; Hong, Y.; Niw, X.; Zepp, C. M. *J. Org. Chem.* **1994**, *59*, 1939-1942.

[30] Schanz, H.-J.; Linseis, M. A., Gilheany, D. G. *Tetrahedron Asymmetry* **2003**, *14*, 2763-2769.

[31] Sada, K.; Tani, T.; Shinkai, S. *Synlett* **2006**, *18*, 2364-2374.

[32] Ayabe, M.; Kishida, T.; Fujita, N.; Sada, K.; Shinkai, S. *Org. Biomol. Chem.* **2003**, *1*, 2744-2747.

[33] Wang, R.-Y.; Liu, X.-Y., Narayanan, J.; Xiong, J.-Y.; Li, J.-L. *J. Phys. Chem. B* **2006**, *110*, 25797-25802.

[34] Desiraju, G. R.; Curtin, D. Y.; Paul, I.C. *J. Am. Chem. Soc.* **1977**, *99*, 6148.

[35] Kamlet, M. J.; Abboud, J. L. M.; Abraham, M. H.; Taft, R. W. *J. Org. Chem.* **1983**, *48*, 2877-2887.

[36] Edwards, W.; Lagadec, C. A.; Smith, D. K. *Soft Matter* **2011**, *7*, 110-117.

[37] Takahashi, A.; Sakai, M.; Kato, T. *Polym. J.* **1980**, *12*, 335-341.

[38] Dzolic, Z.; Wolsperger, K.; Zinic, M. *New J. Chem.* **2006**, *30*, 1411-1419.

[39] Brizard, A.; Oda, R.; Huc, I. *Top. Curr. Chem.* **2005**, *256*, 167-218.

[40] Hanessian, S.; Simard, M.; Roelens, S. *J. Am. Chem. Soc.* **1995**, *117*, 7630-7645.

[41] Gregory, J.; Semmens, M. J. *J. Chem. Soc. Faraday Trans. 1* **1972**, 68, 1045-1052.

[42] Dapporto, P.; Paoli, P.; Roelens, S. *J. Org. Chem.* **2001**, *66*, 4930-4933.

[43] Hanessian, S.; Simard, M; Roelens, S. *J. Am. Chem. Soc.* **1995**, *78*, 7630-7645.

[44] Sahoo, P.; Adarsh, N. N.; Chacko, G. E.; Raghavan, S. R.; Puranik V. G.; Dastidar, P. *Langmuir* **2009**, *25*, 8742-8750.

[45] Abu-Surrah, A. S.; Al-Allaf, T. A. K.; Klinga, M.; Ahlgren, M. *Polyhedron* **2003**, *22*, 1529-1534.

[46] Shivashankar, M.; Mandal, B. K. *Int. J. Pharm. Pharm. Sci.* **2012**, *4*, 1-7.

[47] Li, P.; Dou, X.-Q.; Tang, Y.-T.; Zhu, S.; Gu, J.; Feng, C.-L.; Zhang, D. *J. Colloid Interface Sci.* **2012**, *387*, 115-122.

[48] Hanabusa, K., Yamada, M.; Kimura, M.; Shirai, H *Angew. Chem. Int. Ed.* **1996**, *35*, 1949-1951.

[49] Manoj, N. R.; Raut, R. D.; Sivaraman, P.; Ratna, D.; Chakraborty, B. C. *J. Appl. Polym. Sci.* **2005**, *96*, 1487-1491.

[50] Sperling, H.; Mishra, V. *Polym. Adv. Tech.* **1996**, *7*, 197-208.

D Ag-based metallogels

1. Preface

The results of this chapter were obtained from a collaboration between the group of Prof. Dr. David Díaz Díaz and his student Eva-Maria Schön from the Institut für Organische Chemie at Universität Regensburg, Germany and Stefano Roelens from the Dipartimento Di Chimica at Università di Firenze, Italy.

Stefano Roelens supported the project with a preliminary experiment and critical discussions. Prof. Dr. David Díaz Díaz was collecting the SEM pictures.

2. Background

The high affinity of silver(I) ions towards nitrogen atoms can build up metallogels by direct self-assembly to form 1D linear supramolecular structures in suitable solvents.[1] Moreover, silver-based metallogels, from water[2-4] and organic solvents,[5-10] are known to be suitable materials in the production of silver nanoparticles.

Interestingly, the gelation can also be induced, or enhanced by the silver ions. In 2003, Shinkai and coworkers found that pyridine containing cholesterol compounds **77**-**79** have exhibited huge differences in their gelation ability, although they are are structurally almost identical (Figure 66).[11] Compound **77** acted as „supergelator“ as it brought 16 of 19 solvents into gel state while compound **79** gelled 12 solvents, but 10 of them only partially, and compound **78** was only able to gel just two of them. These differences could be explained by the helical arrangement of the pyridine moieties. The pyridine-groups of **77** are arranged in a radial fashion around the central cholesterol column in the aggregates of **77** and give them stability whereas pyridyl nitrogen of compound **78** has a perpendicular orientation to the column, and two neighboring nitrogen atoms are facing each other.

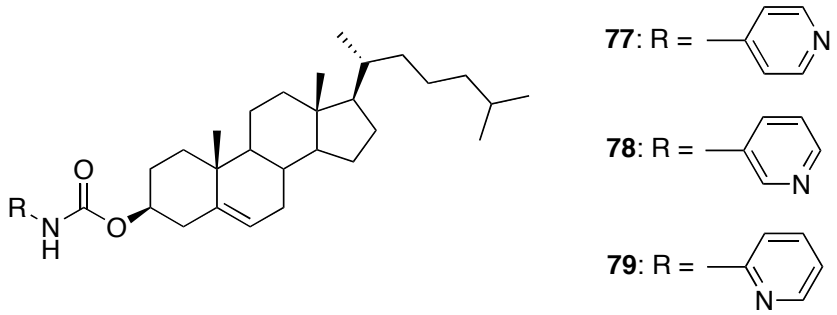

Figure 66: Pyridine containing cholesterol based gelators **77**-**79**.[11]

Addition of silver trifluoromethanesulfonate, $AgSO_3CF_3$, resulted in an interaction with the pyridyl nitrogen of compound **78** which lead to gelation in diphenyl ether. An increase in T_{gel} of diphenyl ether gels of **78** was observed at a $[AgSO_3CF_3]$ $[Gelator]^{-1}$ rate of 0.06-0.08, compared to decrease for T_{gel} of compound **77** (Figure 67). Interestingly, T_{gel} of compound **79** remained almost unaffected.

Furthermore, a morphological change from rod-like clusters before, to fibrillar aggregate after addition of $AgSO_3CF_3$ confirmed the interaction of Ag(I) ions with pyridyl nitrogen of compound **78**.

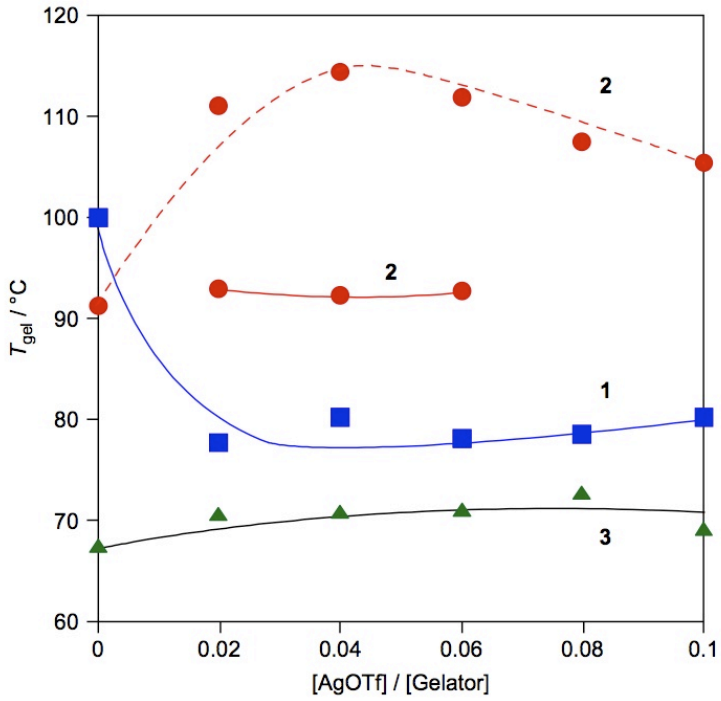

Figure 67: Plots of T_{gel} versus [$AgSO_3CF_3$] [Gelator]$^{-1}$ at a concentration of 10 mg·mL^{-1} (solid line) and 15 g·mL^{-1} (dashed line).[11]

Although silver based homo- and heterochiral coordination polymers of diamino-cyclohexane as bridging ligand were already published in 2006,[12] in this chapter the gelation ability for the system silver trifluoromethanesulfonate and (1*R*,2*R*)-1,2-diaminocyclohexane were reported for the first time. The scope of solvents, the preparation method, as well as alternatives for silver salt and amine were explored. Furthermore, the production of silver nanoparticles was under investigation.

3. Results and discussion

3.1 Preparation of metallogels

Solubility and crystallization studies of (1*R*,2*R*)-1,2-diaminocyclohexane **80** and silver trifluoromethanesulfonate revealed a clear tendency to gel toluene (Figure 68). As no data were found in the literature that this system is able to form gels, it was decided to explore this simple system further.

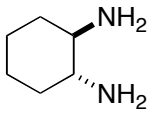

80

Figure 68: Structure of (1*R*,2*R*)-1,2-diaminocyclohexane **80**.

Three different experimental paths were investigated for their suitability of gelation of the $AgSO_3CF_3$ + ligand **80** system:

1. First the heating-cooling method was carried out. $AgSO_3CF_3$ was dissolved in hot toluene, but ligand **80** did not dissolve, instead it changed its color into a dark brownish at higher temperatures.
2. Sonication of equimolar $AgSO_3CF_3$ and **80** in toluene for 10 min at 0.3 mmol·mL^{-1} provided gels after 3 days.
3. The mixing of equimolar solutions of $AgSO_3CF_3$ and **80** provided gels at RT, too. Remarkably, the gelation occurred within 10 min after addition of $AgSO_3CF_3$ solution to **80** in solution at a concentration of 0.05 mmol·mL^{-1}.

3.2 Characterization of metallogels

The gelation ability of the gelator system $AgSO_3CF_3$ + **80** was examined for 28 different solvents (Table 10). Opaque organogels from seven aromatic solvents were obtained in a concentration range of 0.05-0.2 mmol·mL^{-1} (entries 1-7). In chlorinated aromatic solvents partial gels were provided at a concentration of 0.3 mmol·mL^{-1} (entries 8-10). Due to the low solubility of $AgSO_3CF_3$ in these solvents the use of higher concentration was not possible. Metal salt $AgSO_3CF_3$ and ligand **80** were insoluble in group I solvents: *n*-hexane,

cyclohexane, carbon tetrachloride and [BMIM][PF_6] (entry 11), whereas solutions were provided in group II solvents: DMSO, DMF, ACN, CHN, ACT and NMP (entry 12). Group III included water, methanol, THF, DOC, DEE, ETAC DCM and chloroform (entry 13). Sonication of $AgSO_3CF_3$ and **80** at an equimolar ratio in these solvents resulted in dispersions.

Table 10: Gelation ability of equimolar $AgSO_3CF_3$ + **80** in different solvents.[a]

Entry	Solvent	Result	MGC[b]	Aspect phase	Kamlet-Taft parameters		
					α	β	π*
1	Toluene	G	0.05	OG	0.00	0.11	0.54
2	Benzene	G	0.05	OG	0.00	0.10	0.54
3	Benzonitrile	G	0.1	OG	0.00	0.37	0.90
4	Nitrobenzene	G	0.1	OG	0.00	0.30	1.01
5	Mesitylene	G	0.2	OG	0.00	-[c]	0.41
6	O-xylene	G	0.2	OG	-[c]	-[c]	-[c]
7	M-xylene	G	0.2	OG	0.00	-[c]	0.47
8	Chlorobenzene	PG	0.3	OG	0.00	0.07	0.71
9	1,2-Dichlorobenzene	PG	0.3	OG	0.00	0.30	0.77
10	1,3-Dichlorobenzene	PG	0.3	OG	0.00	0.30	0.67
11	Group I	I	1.0				
12	Group II	S	0.02				
13	Group III	D					

[a]1.0 mL of solvent was used in every experiment. Abbreviations: Gel = gel, PG = partial gel, I = insoluble, S = solution, D = dispersion. [b]Equimolar concentration in mmol·mL^{-1}. [c]Unknown value.

Solvent parameters

The aromatic solvents used in the gelation process showed no hydrogen bond donor ability with an α parameter of 0.00. A low β parameter revealed a small hydrogen bond acceptor ability and at the same time a medium to high polarizability (π* parameter) referring to the Kamlet-Taft parameters (Table 14, page 173f).

Aging

All provided gels were opaque with different degrees of yellowish color which derived of the slight yellowish touch of compound **80**. The initial pale yellow gels underwent a color intensification over time as shown in Figure 69.

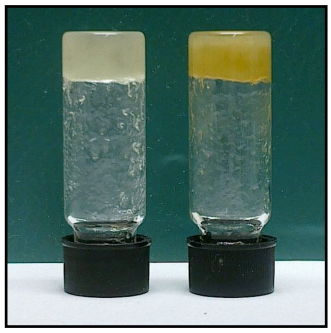

Figure 69: Toluene gel at MGC two days (left) and two weeks (right) after preparation.

Initially the appearance of silver nanoparticles was assumed, based on previous reports in the literature.[10] However, UV-Vis spectroscopy of the toluene gel at different ages did not show the presence or growth of the referring band.

The color intensification was not depending on visible light, as it also occurred with gels which were stored in the dark. It was implicated that compound **80** caused the color change, as it became brownish when in contact with air and also changed its color to brownish upon heating.

Influence of the components on the gelation ability

Control experiments showed the necessity of presence of both $AgSO_3CF_3$ and ligand **80**. At MGC, $AgSO_3CF_3$ provides solution and precipitation occurred for higher concentration. Experiments pointed out that already a small aberration of the 1.0 : 1.0 stoichiometry of $AgSO_3CF_3$: compound **80** led only to formation of partial gels for 1.0 : 1.3 and 1.3 : 1.0. In addition, 2.0 : 1.0 and 3.0 : 1.0 of $AgSO_3CF_3$: compound **80** caused no gelation.

Furthermore, the influence of the counterion was examined. Silver hexafluoro-antimonate, silver nitrate, silver sulfate, silver acetate, silver carbonate, silver fluoride and silver benzoate were insoluble in toluene by either sonication at RT or heating. Also silver tetrafluoroborate and silver perchlorate showed poor solubility in toluene, but provided partial gel in combination with insoluble material. As both $AgSO_3CF_3$ and compound **80**

were water soluble, they were tested at an equimolar ratio for hydrogelation. Unfortunately, only solutions were obtained.

The exchange of the diamine with *cis*-1,2-diaminocyclohexane, *trans*-1,2-diamino-cyclohexane and 1,2-diaminocyclohexane (*cis* + *trans*) at a concentration four times higher than MGC in toluene, resulted only in partial gelation and showed that the compounds were not appropriate. Moreover, the use of 1,5-diaminopentane as replacement led to precipitation and 1,3-diaminopropane turned into a solution. The only amine which was able to replace compound **80** for the preparation of stable, opaque gels was DABCO (Figure 70). Gel with compound **81** as ligand was prepared by mixing of equimolar $AgSO_3CF_3$ solution with solution of **81** in toluene at a MGC of 0.15 mmol·mL^{-1}.

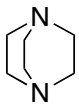

81

Figure 70: Silver metallogel from $AgSO_3CF_3$ and DABCO as ligand.

Environmental responsiveness

Furthermore, the behavior of the toluene gel from $AgSO_3CF_3$ and ligand **80** was investigated when being exposed to external stimuli. The gel remained stable despite the mechanical treatment of the gel with a spatula. However, the gel was not sliceable as it was not hard enough, but rather sticky. Additionally, the gel was exposed to thermal stress. The inversion of tube method was applied on the toluene gel at MGC, but even at 120 °C the gel remained stable. The inversion of tube method in oil bath is not appropriate for higher temperatures, as the sealed screw-caps of test vials start to leak and oil enters the vial. Besides that, the response to chemical stimuli was examined. After addition of 1.0 mol·L^{-1} aqueous HCl, the gel was destroyed immediately by the formation of white precipitate, silver chloride (Figure 71). A black precipitate resulted from the addition of 1.0 mol·L^{-1} aqueous NaOH to the gel. Slow destruction of the gel was observed in contact with pure water, because the pH turned from neutral into basic, as compound **80** dissolved into the solution. After addition of methanol, ACN, ACT, DOX, DMF, BN and DMSO the gel dissolved, too.

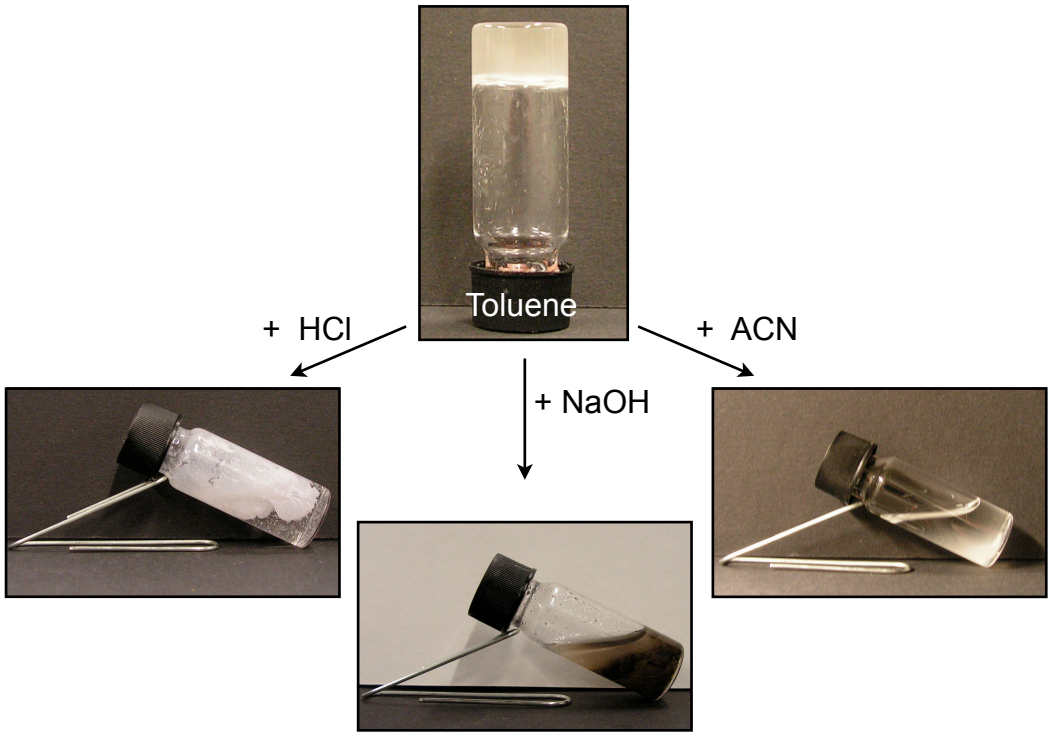

Figure 71: Responsiveness of toluene gel in contact with HCl and NaOH solutions, as well as organic solvents like ACN.

Dynamic rheological measurements

Rheological behavior was measured to confirm the gel nature (Figure 72). The comparison of DTS at constant frequency (1.0 Hz) and strain (0.1 %) was carried out for toluene gel with **80** or **81** as ligand for $AgSO_3CF_3$ at 0.1 mmol·mL^{-1}. Although the G′ and G″ values for gels with **80** as ligand are almost 40 times higher, the tanδ value for the **81** gel (tanδ = 0.109 ± 0.009) was more constant and promised a higher mechanical damping than gel with **80** (tanδ = 0.211 ± 0.024).

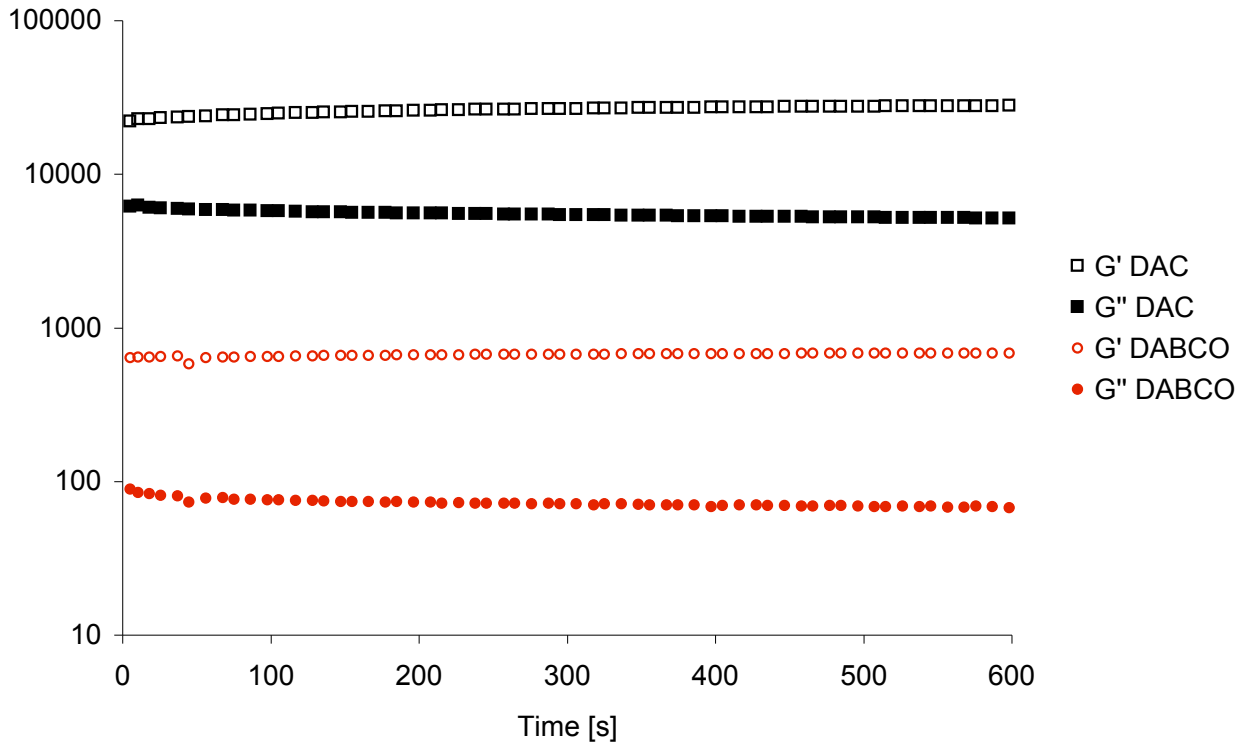

Figure 72: Comparative DTS between toluene gel from **80** (black squares) and **81** (red dots) as ligand for $AgSO_3CF_3$ at 0.1 mmol·mL^{-1}.

Microscopy studies

For an insight into the microstructure, SEM images were taken (Figure 73). They revealed an irregular, fibrillar-like morphology in the xerogels of gelator system $AgSO_3CF_3$ and **80** from mesitylene (A), m-xylene (B), toluene (C), toluene (D) and benzene (F). Interestingly, the replacement of ligand **80** by **81** caused a change in the gelator network from several micrometer long fibers to tiles smaller than 1 µm (E).

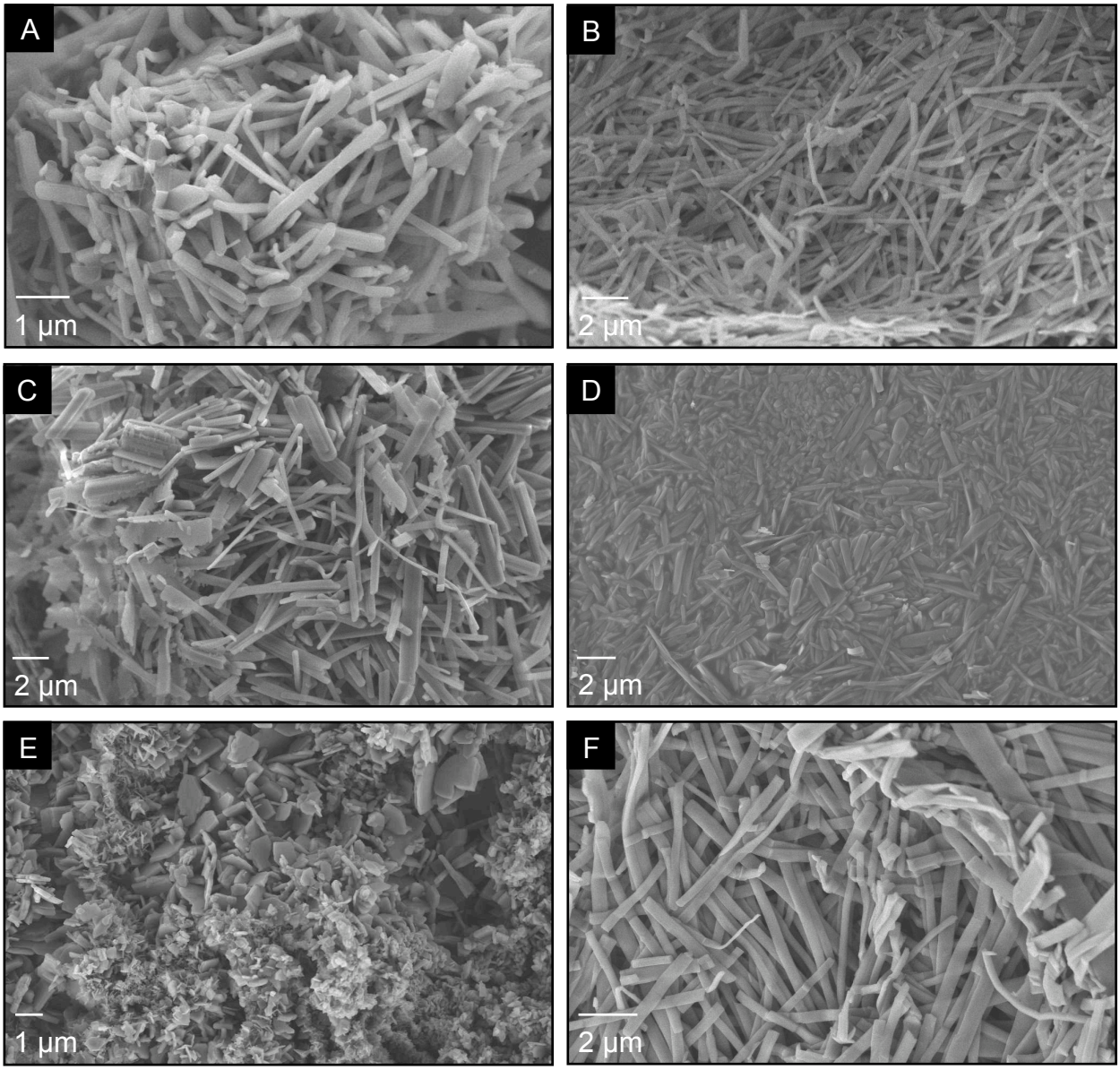

Figure 73: SEM images from freeze-dried organogels based on $AgSO_3CF_3$ and **80** in different aromatic solvents at MGC: mesitylene (A), m-xylene (B), toluene (C), toluene (D) and benzene (F). SEM image from freeze-dried toluene gel based on $AgSO_3CF_3$ and **81**(E).

4. Conclusion

In conclusion, stable silver-based metallogels can be generated by using $AgSO_3CF_3$ and **80** as ligand at an equimolar ratio. The $AgSO_3CF_3$ + **80** system is able to gel a number of aromatic solvents at a concentration range of 0.05-0.20 mmol·L^{-1}. The mixing of $AgSO_3CF_3$ solution and solution made of **80** as preparation method has to be preferred in opposition to the preparation by sonication at RT, because the sonicated gels need a longer formation time, although the MGC is six times higher. The restriction in solubility makes a replacement of $AgSO_3CF_3$ by other silver salts difficult. Besides **80**, **81** is also an appropriate ligand in combination with $AgSO_3CF_3$. However, **81** gels need higher MGC with lower temporal stability at the same time. SEM images reveal the structural difference between the $AgSO_3CF_3$ + **80** and $AgSO_3CF_3$ + **81** systems. A fibrillar network is provided with **80** as ligand, whereas with **81** a tiles structure is building up.

5. Experimental part

5.1 General remarks

Commercially available reagents and solvents for gel preparation were used as received without further purification. During solubility tests and for gel preparation, a VWR™ ultrasonic cleaner, USC200TH, was used.

5.2 Preparation of metallogels

Preparation by sonication

Silver trifluoromethanesulfonate (77.1 mg, 0.3 mmol) and (1*R*,2*R*)-1,2-diaminocyclohexane (34.2 mg, 0.3 mmol) were sonicated in 1.0 mL dry toluene for 10 min at RT. The gel was formed after three days.

Preparation by mixing of solutions

Silver trifluoromethanesulfonate (12.8 mg, 0.05 mmol) was dissolved in 0.5 mL dry toluene by slight warming. A solution of (1*R*,2*R*)-1,2-diaminocyclohexane in dry toluene was prepared by sonication of the amine (5.7 mg, 0.05 mmol) in 0.5 mL solvent. The addition of the silver salt solution to the amine solution via syringe has to be carried out fast and without the formation of bubbles. After the addition it was necessary to shake the vial briefly and vigorously for proper mixing. The gel was obtained within 10 min at RT.

5.3 Characterization of metallogels

Rheological measurements

Rheological measurements were performed with advanced rheometer AR 2000 from TA Instruments which was equipped with a cooling system (Julabo C). A 20 mm plain plate geometry (stainless steel) was used. First strain sweep measurements were carried out (1.0 Hz) to estimate the strain in % at which reasonable torque values were given (about 10 times of the transducer resolution limit). Afterwards, frequency sweep measurements and time sweep measurements were performed (0.1 % strain, 1.0 Hz).

Field emission scanning electron microscopy (FESEM)

A Zeiss Merlin field emission scanning electron microscope with an accelerating voltage of 10 kV was used to take SEM pictures of the xerogels. For this, prior to imaging a nano-sized Pt film was sputtered on the samples on carbon tape (40 mA, 60 seconds). A SCD500 Leica EM device was used for the imaging.

UV-Vis spectroscopy

Absorption spectra were recorded on a Varian Cary BIO 50 UV-Vis scanning spectrophotometer by use of a 1 cm quartz cuvettes.

6. References

[1] Tam, A. Y.-Y.; Yam, V. W.-W *Chem. Soc. Rev.* **2013**, *42*, 1540-1567.

[2] Lee, J. H.; Kang, S.; Lee, J. Y.; Jung, J. H. *Soft Matter* **2012**, *8*, 6557-6563.

[3] Xiang, Y.; Chen, D. *Eur. Polym. J.* **2008**, *43*, 4178-4187.

[4] Boonkaew, B.; Suwanpreuksa, P.; Cuttle, L.; Barber, P. M.; Supahol, P. *J. Appl. Polym. Sci.* **2014,** DOI: 10.1002/app.40215.

[5] Piepenbrock, M.-O. M.; Clarke, N.; Steed, J. W. *Soft Matter* **2011**, *7*, 2412-2418.

[6] Kim, J.; Park, C.-H.; Kim, S.-H.; Yoon, S.; Piao, L. *Bull. Korean Chem. Soc.* **2011**, *9*, 3267-3273.

[7] Chen, Y.-C., Wang, H.; Li, D.-M.; Zheng, Y.-S. *Eur. J. Org. Chem.* **2013**, *4*, 1521-1529.

[8] Mantion, A.; Guex, A. G.; Foelske, A.; Mirolo, L.; Fromm, K. M.; Painsi, M.; Taubert, A. *Soft Matter* **2008**, *4*, 606-617.

[9] Li, Y.; Liu, M. *Chem. Commun.* **2008**, *43*, 5571-5573.

[10] Ray, S.; Das, A. K.; Banerjee, A. *Chem. Commun*. **2006**, *26*, 2816-2818.

[11] Shin-ichiro Kawano, Norifumi Fujita, Kjeld J. C. van Bommel, Seiji Shinkai, *Chem. Lett.*, **2003**, 32, 12-13.

[12] Kalf, I.; Braun, M.; Wang, Y.; Englert, U. *CrystEngComm.* **2006**, *8*, 916-922.

E Organogels from multifunctional LMW urea gelator

1. Preface

The results of this chapter were obtained from a collaboration between the group of Prof. Dr. David Díaz Díaz and his student Eva-Maria Schön from Institut für Organische Chemie at Universität Regensburg, Germany and the group of Dr. Raquel Herrera and Dr. Eugenia Marqués-López from CSIC in Zaragoza, Spain.

Compounds **87**, **88**, **91**, **92** and **93** were synthesized by Dr. Raquel Herrera and Dr. Eugenia Marqués-López. Prof. Dr. David Díaz Díaz was collecting the SEM pictures.

2. Background

The development of various artificial urea-based gelators has been widely reported in the literature.[1-11] Specifically, the urea group (Figure 74, left) is an effective functional group for the creation of continuous aggregates through intermolecular hydrogen bonding.[12] Oxygen atoms of the carbonyl groups and hydrogen atoms of the amine groups are connected by hydrogen bonds (Figure 74, right) which leads to directional assembly and results in the formation of supramolecular architectures.

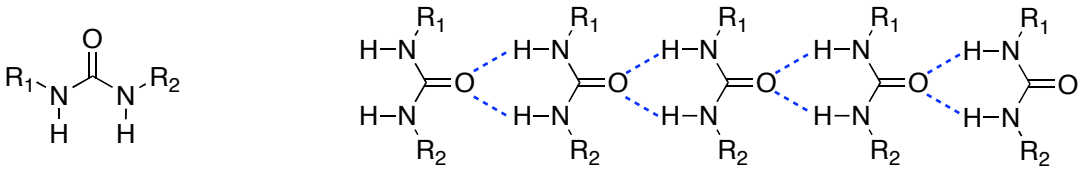

Figure 74: Urea moiety (left) and an example of a continuous intramolecular hydrogen bonding pattern of urea groups (right).

Among all the ureas described as gelators, mono-, bis- and tris-urea compounds have been observed to build up supramolecular gels from organic solvents (Figure 75).[12] For example, a mono-urea LMWG **82** with incorporated electroactive tetrathialfulvalene group was observed to gel organic solvents as cyclohexane and 1,2-dichloroethane.[13] The addition of tetracyanoquinodimethane led to the destruction of the 1,2-dichloroethane gel, because of the formation of a charge-transfer complex which resulted in oxidation of the tetrathialfulvalene group. Schalley and co-workers reported bis-urea gelator **83** which was substituted with two benzo-21-crown-7-residues. The *gel-sol* transition of gel in ACN was controlled by three different ways: 1. Binding of potassium ions with the crown ether residues, 2. binding of chloride ions with the urea group and 3. the formation of pseudo-rotaxane with ammonium ions.[14] An example for a tris-urea compound is given by LMWG **84** which provided reversible *gel-sol* phase transition as response of chemical stimuli. The acetone gel of **84** showed sensitivity to fluoride, chloride and tetrafluoroborate anions. Re-gelation was induced by sonication of the solutions with metal salts as $ZnBr_2$. [15]

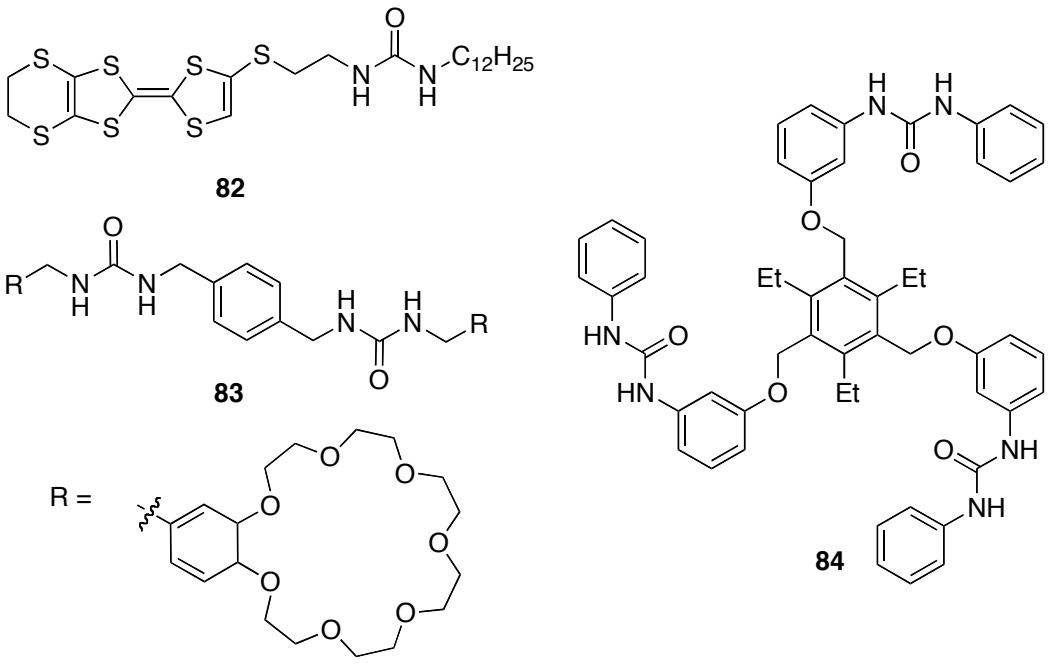

Figure 75: Selection of urea-based organogelators.

The following chapter presents the investigation of a mono-urea LMWG for a variety of organic solvents. The study showed the unique gelation ability of the gelator and that all its functional groups and chiral information was necessary for gelation. The gels were characterized and their application in phase selective gelation and in sensing of silver ions was demonstrated.

3. Results and discussion

3.1 Preparation of organogels

The synthesis of compound **87** was reported previously (Scheme 11).[16] It was easily accessible from the reaction of amine **85** with isocyante **86**. During the purification of compound **87**, its ability to gel solvents was discovered. As no data about the gelation ability of **87** were found in the literature, it was decided to explore the system further.

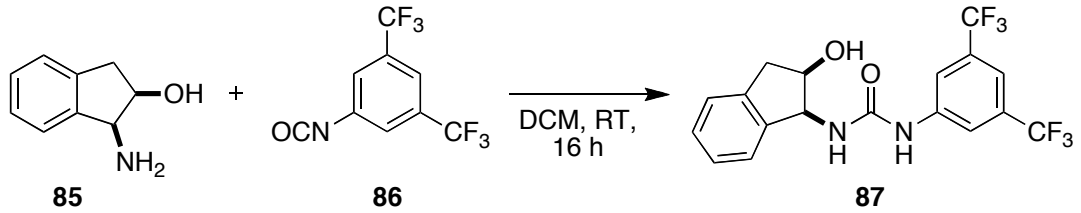

85 **86** **87**

Scheme 11: Synthesis of gelator **87**.

The gels were prepared by adding the gelator **87** to a screw-capped glass vial (4.5 cm length x 1.2 cm diameter). 1.0 mL of solvent were added and the vial was closed. The vial was gently heated until an isotropic solution was obtained. After cooling down slowly to RT, the gel material was formed. The resulting material was preliminarily classified as gel, as it was able to resist the inversion of the vial without collapsing. In order to prove the gel nature of the material, it was further characterized by rheological measurements.

It was also attempted to obtain gels by sonication. For this, the glass vial with gelator **87** and corresponding solvent was sonicated at RT for 1h. Afterwards, no gelation was observed, but undissolved material was still present. A further test with pre-dissolved gelator **87** was carried out in three model solvents, toluene, glycerol (90 wt.%) and DCM. The referring amount of gelator **87** at MGC was pre-dissolved in 20 µL DMSO, followed by the addition of the solvent. After resting for 10 min at RT the three solutions remained liquid. The three test vials were sonicated for 30 min, but no gelation was induced.

3.2 Characterization of organogels

The gelation ability of **87** was examined for 33 different solvents. The heating-cooling process was carried out at concentrations between 1.0 - 50.0 mg·mL^{-1}. The results

indicated gelation of 14 solvents with MGC in the range of 3.0 - 25.0 mg·mL^{-1} (Table 11, entries 1-14). Gelation attempts in both water and heptane resulted in insolubility of **87** even at 2 h of sonication, or heating (Table 11, entry 15). Solvents of group II (Table 11, entry 16) provided solutions of **87** at concentration of 50 mg·mL^{-1}: rapeseed oil, ACT, ETAC, ethanol, methanol, DMSO, ACN, DOX, DMF, BN, DME, THF, methyl *tert*-butyl ether, MBN, CHN, DMA, and DEE.

Table 11: Extent of gelation ability for compound **87** in 1.0 mL of solvent investigated per heating-cooling process.

Entry	Solvent	Result[a]	MGC [mg·mL^{-1}]	Time[b]	T_{gel}[c]	Aspect phase
1	Toluene	G	3.0	30 ± 5 min	55	TG
2	Benzene	G	3.0	30 ± 5 min	41	TG
3	Chlorobenzene	G	3.6	5 - 10 min	54	TG
4	1,2-Dichlorobenzene	G	3.6	5 - 10 min	62	TG
5	1,3-Dichlorobenzene	G	3.6	5 - 10 min	64	TG
6	Mesitylene	G	3.5	5 ± 1 h	--[d]	TG
7	O-xylene	G	3.5	8 ± 2 h	--[d]	TG
8	M-xylene	G	3.5	5 ± 1 h	--[d]	TG
9	Nitrobenzene	G	50	30 ± 5 min	41	OG
10	Glycerol (90 wt.%)	G + I	3.0	40 ± 10 min	74	TG
11	Dichloromethane	G	4.0	20 ± 5 min	46	TG
12	Chloroform	G	7.0	45 ± 10 min	--[d]	TG
13	Carbon tetrachloride	G + I	5.0	10 ± 5 min	84	TG
14	Nitromethane	G	25	24 h	--[d]	TG
15	Group I	I	1	-	-	-
16	Group II	S	50	-	-	-

[a]Abbreviations: G = gel, I = insoluble, S = solution, MGC = minimum gelation concentration, TG = transparent gel, OP = opaque gel. [b]Time required for gelation. [c]*Gel-sol* temperature upon heating with inverse-tube method (heating rate: 2 °C min^{-1}).[d]Upon inversion of the test tube for longer than 5 min at RT the gel was broken.

For gels made from glycerol (90 wt.%) and carbon tetrachloride (Table 11, entries 10 and 13) a small amount of **87** remained insoluble. Also at lower concentrations no gelation

occured. Instead, only solutions were provided, although a small amount of undissolved **87** was still visible. Figure 76 shows a selection of transparent (toluene, benzene, chlorobenzene, 1,2-dichlorobenzene, chloroform, glycerol (90 wt.%) and nitromethane) and opaque organogels (nitrobenzene) derived from compound **87**.

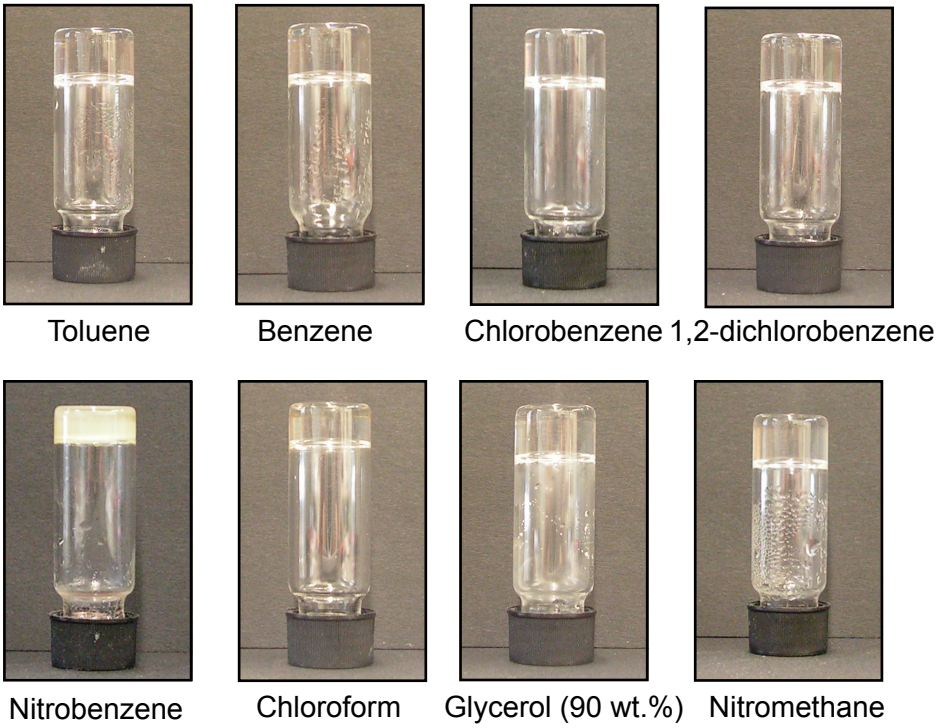

Figure 76: Digital photographs of upside-down vials containing gels from gelator **87** in different solvents.

Solvent parameters

Table 11 revealed that compound **87** enabled gelation of aromatic, as well as chlorinated solvents and therefore had the tendency to form gels with solvents with a low hydrogen bond donor ability (α parameter) of the Kamlet-Taft parameters (Table 14, page 173f). Furthermore, the low β parameter of these solvents pointed out that the hydrogen bond acceptor ability was low, too. At the same time, the solvents provided middle to high polarizability (π* parameter). Interestingly, glycerol (90 wt.%) was an exception to this observation, as it was gelled by **87**, although it showed a very high value for the α parameter. This aberration could explain, why **87** is not completely dissolved in glycerol (90 wt.%), but always a small rest of undissolved material was visible. Also nitromethane owns a moderate α parameter which resulted in the high MGC of 25 $mg \cdot mL^{-1}$.

Aging of the gels

Gels from **87** at MGC were stable for at least one month at RT. However, during the evaluation of the temporal stability of gels in toluene, slow destruction by crystal growth was observed after 4-5 weeks. For this reason, the maximum gelation concentration for gels in toluene was defined as concentration where no crystallization occurred within 2 weeks (8 mg·mL^{-1}). Also gels with growing crystals inside the gel material showed no further destruction and the gels were still able to resist the inversion of the tube test. The images in Figure 77 show the bunch of fine needle crystals which were slowly growing in toluene gel at MGC (left) and the fast growing irregular crystals from toluene gel at a concentration of 15 mg·mL^{-1} within 1 h (right).

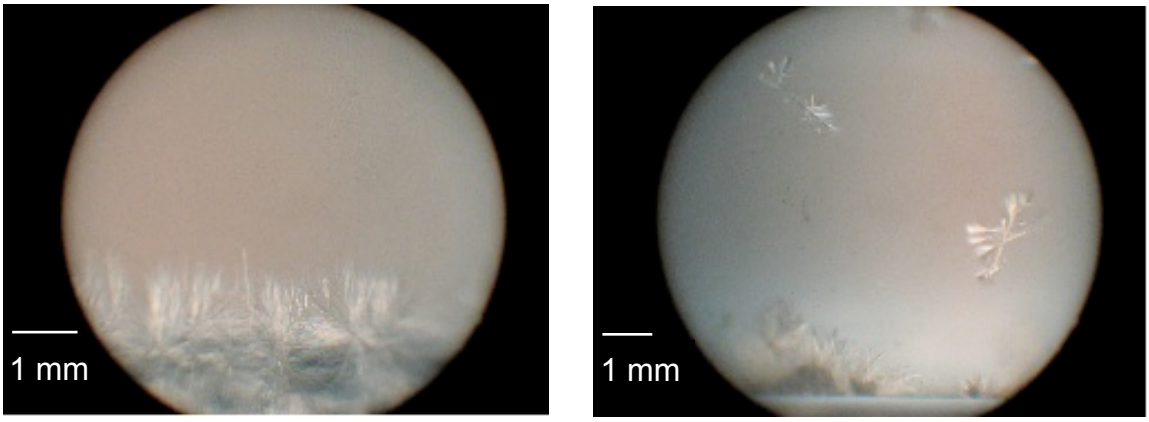

Figure 77: Crystals in toluene gels at MGC (left) and tolluene gel at concentration of 15 mg·mL^{-1} (right).

Gelation ability of related compounds

The investigation of the gelation ability of **87** led to further experiments where the influence of the functional groups of the compound on gelation was explored by gelation tests with structural related compounds (Figure 78). Toluene, DCM and glycerol (90 wt.%) were chosen as model solvents where gelator **87** showed gelation ability at 3.0, 4.0 and 3.0 mg·mL^{-1} respectively. The replacement of the carbonyl group by a thiocarbonyl (compound **88**) resulted in formation of solutions in toluene and DCM (both 50 mg·mL^{-1}). For glycerol (90 wt.%), already low concentration (3.0 mg·mL^{-1}) resulted in precipitation (Table 12). The symmetrical compound **89** resulted from a second 1,3-bis(trifluoro-methyl)benzene moiety attached at the urea group. Crystallization (in DCM at 1.0 mg·mL^{-1} and in toluene at 4.0 mg·mL^{-1}) and insolubility (in glycerol (90 wt.%) at 1.0 mg·mL^{-1}) was

found for this compound in the three model solvents. Compound **90**, diphenylurea, is also a symmetric molecule which gave crystals in DCM (1.0 mg·mL^{-1}) and precipitated in glycerol (90 wt.%;3.0 mg·mL^{-1}), but was insoluble in toluene (1.0 mg·mL^{-1}). Also the diastereomer of **87**, compound **91** was investigated. No 3D structure for building-up a gelator network was possible here, as the experiments all resulted in precipitation at concentrations of 1.0 mg·mL^{-1} in DCM or glycerol (90 wt.%) and 2.0 mg·mL^{-1} in toluene. Compound **92** was missing the hydroxy group of compound **87**. This group seems to also play a key role, as it was not possible to obtain a gel material without it. All three model solvents showed precipitation at 8.0 mg·mL^{-1} for DCM and toluene and 1.0 mg·mL^{-1} for glycerol (90 wt.%).

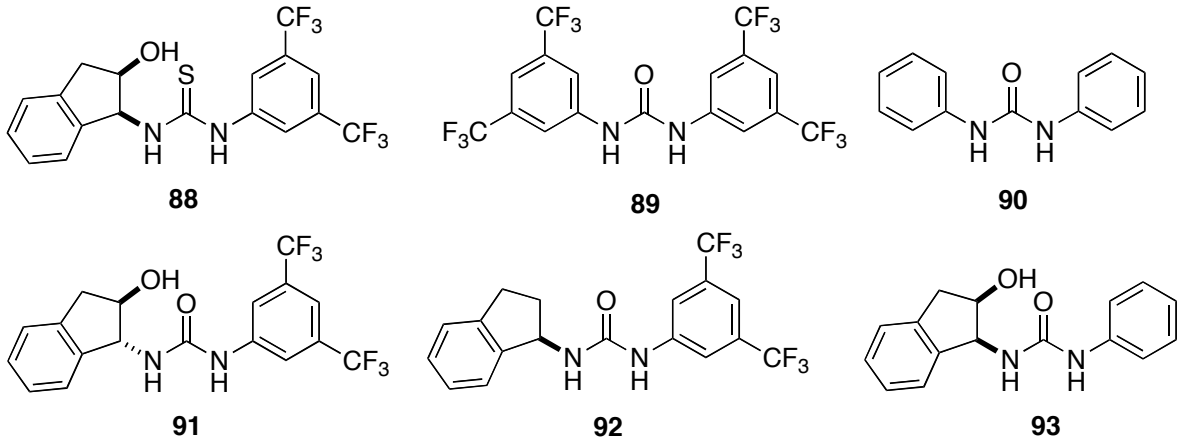

Figure 78: Compounds with structure related to **87**.

Table 12: Comparison of gelation ability of urea-based gelators.[a]

	87	**88**	**89**	**90**	**91**	**92**	**93**
DCM	G: 4 .0	S: 50	C: 1.0	C: 1.0	P: 1.0	S: 1.0 P: 8.0	C: 1.0
Toluene	G: 3.0	S: 50	S: 2.0 C: 4.0	I: 1.0	S: 1.0 P: 2.0	S: 1.0 P: 8.0	G(C): 3.0
Glycerol (90 wt.%)	G: 3.0	S: 1.0 P: 3.0	I: 1.0	P: 3.0	P: 1.0	P: 1.0	G: 5.0

[a]Abbreviations: G = gel, G(C) = gel with crystals inside, I = insoluble upon heating, or sonication for 20 min, S = solution, P = precipitation from solution, C = crystallization from solution. All concentrations are given in mg·mL^{-1}.

It was investigated that the lack of both trifluoromethane groups obviously had the lowest influence on gelation ability by comparison of compound **93** with compound **87**. Despite the crystallization in DCM at low concentration, **93** was providing a weak gel from toluene at 3 mg·mL^{-1} (Figure 79, left). However, crystals were already growing 10 min after preparation. At concentrations below 3 mg·mL^{-1} only partial gelation was obtained, but also here crystals started to grow within 30 min. Interestingly, compound **93** was able to form stable gels in glycerol (90 wt.%) (Figure 79, right), although a higher MGC was needed than for compound **87**. The formation of the glycerol (90 wt.%) gel with compound **93** took 3 h which was almost five times longer than compound **87** needed to gel the glycerol (90 wt.%) at MGC.

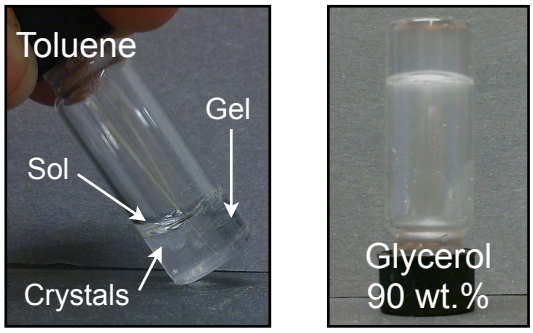

Figure 79: Toluene gel from compound **93** at 3 mg·mL^{-1} (left) and glycerol gel at 5 mg·mL^{-1} (right).

Influence of the enantiomeric purity on gelation

Furthermore, the effect of enantiomeric purity of **87** was under investigation. It was observed that ee below 80% resulted in formation of precipitate (Figure 80, left). The sample with 80% ee resulted in a mixture of gel material and precipitate. After two days this material broke down and only the sample with 100% ee provided a homogeneous, transparent and stable gel (Figure 80, right).

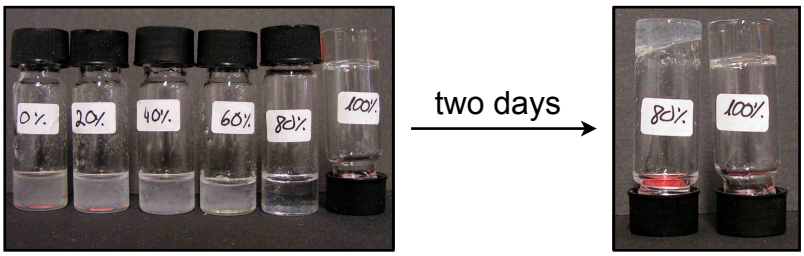

Figure 80: Influence of enantiomeric pureness on gelation ability.

Thermal stability

As these LMWG gels are formed by self-assembly of the single gelator molecules by non-covalent forces, they were able to undergo the *gel*-to-*sol* process by heating and subsequent cooling down to RT to reform a gel again. The experiment was repeated five times for the toluene gel to confirm the thermoreversibility of the gelation process. The *gel*-to-*sol* transition temperature, T_{gel}, was 41 °C for the toluene gel right after preparation and 40 °C after five heating-cooling cycles. T_{gel} was determined for the organogels at MGC by the "inverse flow method" as average of at least two random measurements. The vials were put upside-down into an oil bath and the temperature increased at a heating rate of 2 °C min^{-1} with an estimated error of ± 2 °C. T_{gel} was defined as the temperature were the gel began to flow. Unfortunately, some gels were too fragile and were destroyed within 5 min after turning the test vials upside down at RT (NM, mesitylene, o-xylene, m-xylene and chloroform). For the other solvents, T_{gel} measurements were carried out at least two times (Table 11).

With increasing gelator concentration, T_{gel} was also increasing for gels in toluene from 41 °C at 3 mg·mL^{-1} and 79 °C at 7 mg·mL^{-1}. Further increment in the concentration did not raise T_{gel} (Figure 81).

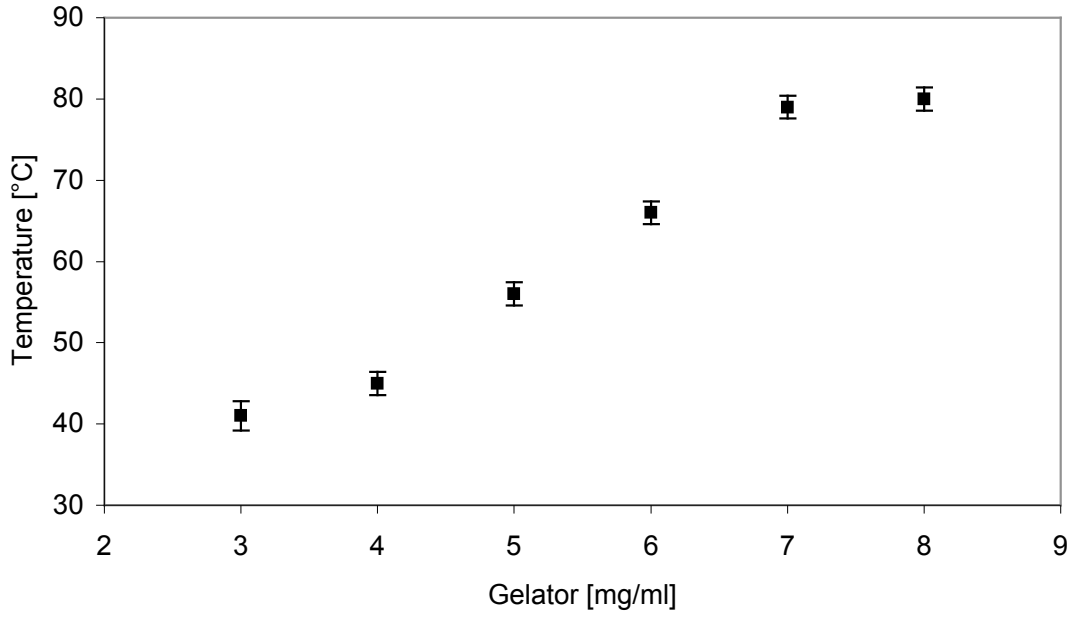

Figure 81: Development of T_{gel} with increasing concentration of gelator **87**.

A rise was also visible when T_{gel} were measured for gels at different water-glycerol mixtures (Figure 82). With increasing glycerol content, T_{gel} was also increasing. Gels at 60 wt.% and glycerol were to fragile to stand the inversion of the test tube. Furthermore, T_{gel} rose from 64 °C at 70 wt.% up to 74 °C at 90 wt.%. Interestingly, **87** was not soluble in commercially available 99 wt.% glycerol, which indicated that a certain amount of water was necessary for the dissolution process of **87** and therefore for gel formation.

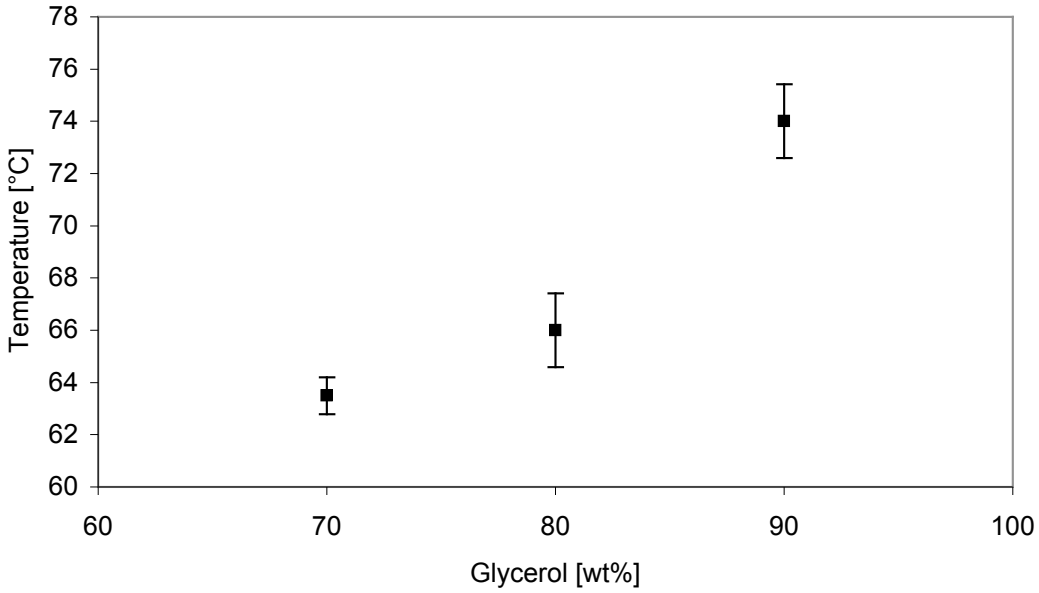

Figure 82: Developement of T_{gel} with decreasing water content of water-glycerol mixture.

Themperature-dependent ^{1}H NMR spectroscopy

^{1}H NMR turned out to be a powerful tool for the study of the hydrogen-bonding in self-assembled aggregates[17-22] and also one of the major driving forces for the supramolecular gelation of **87**. ^{1}H NMR spectra from a model [D_8]toluene gel at a concentration of 8 mg·mL^{-1} were recorded to gain an insight into the protons which were involved in building up the self-assembled network. The destruction of the intermolecular hydrogen bonding was observed by recording of spectra every 5 °C in a temperature range between 27-70 °C (Figure 83).

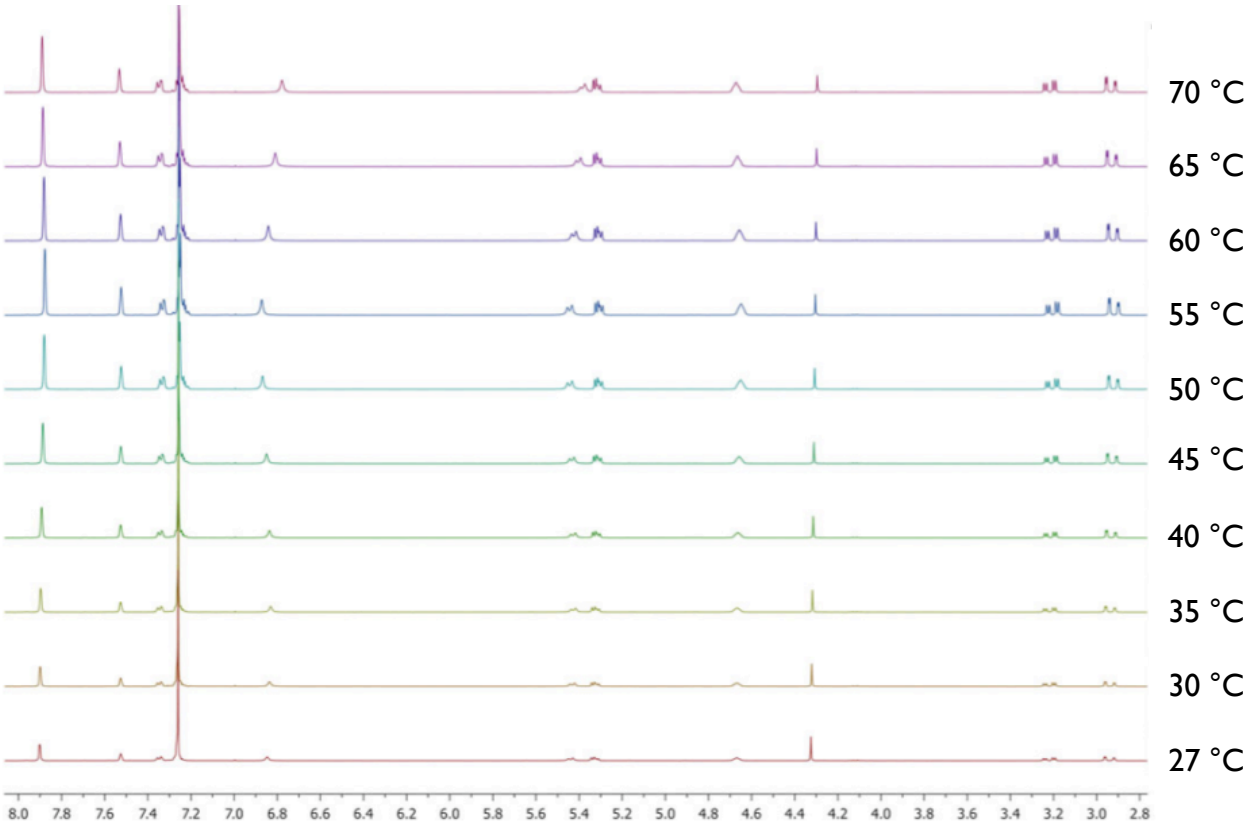

Figure 83: Combined ^{1}H NMR spectra from **87** in [D_8]toluene with increasing temperature.

Previous studies revealed that protons from molecules which are part of the gel network cannot contribute to the signals in ^{1}H NMR spectra due to long correlation times.[23] Therefore, the recorded signals were derived from either aggregated or non-aggregated molecules of **87** dissolved in the immobilized solvent. With increasing temperature the mobility of the molecules also increased which led to a raise of the proton signals. Figure 84 provides an amplification of the combined ^{1}H NMR spectra and shows a gradual increase of the signal upon heating.

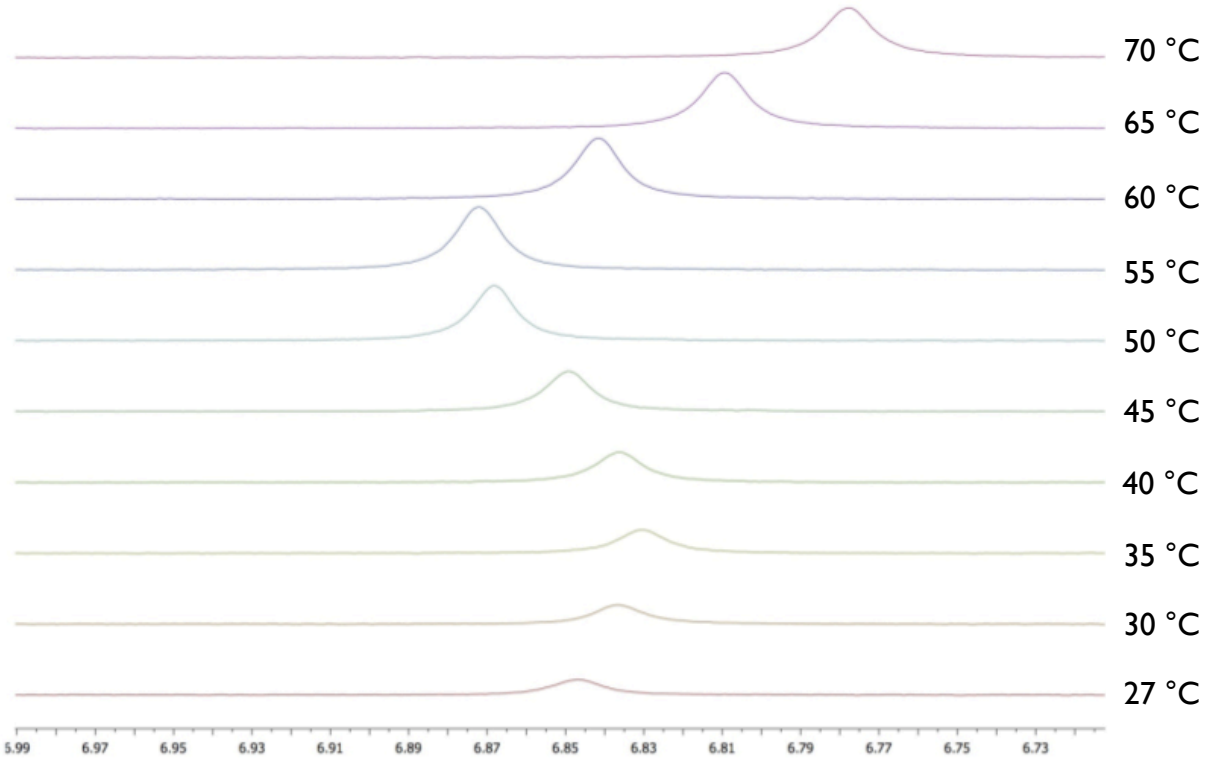

Figure 84: Representative thermal induced chemical shift of N-H proton.

Furthermore, a gradual chemical shift of the amide proton induced by increasing temperature was observed (Figure 84). This chemical shift was recorded for all proton signals to a varyied extent. The amide N-H proton signal first shifted downfield upon heating from 27-55 °C ($d\delta / dT = 8.9 \times 10^{-4}$ ppm K^{-1}) and afterwards an upfield shift from 55-70 °C ($d\delta / dT = 6.3 \times 10^{-3}$ ppm K^{-1}) was observed (Figure 85).

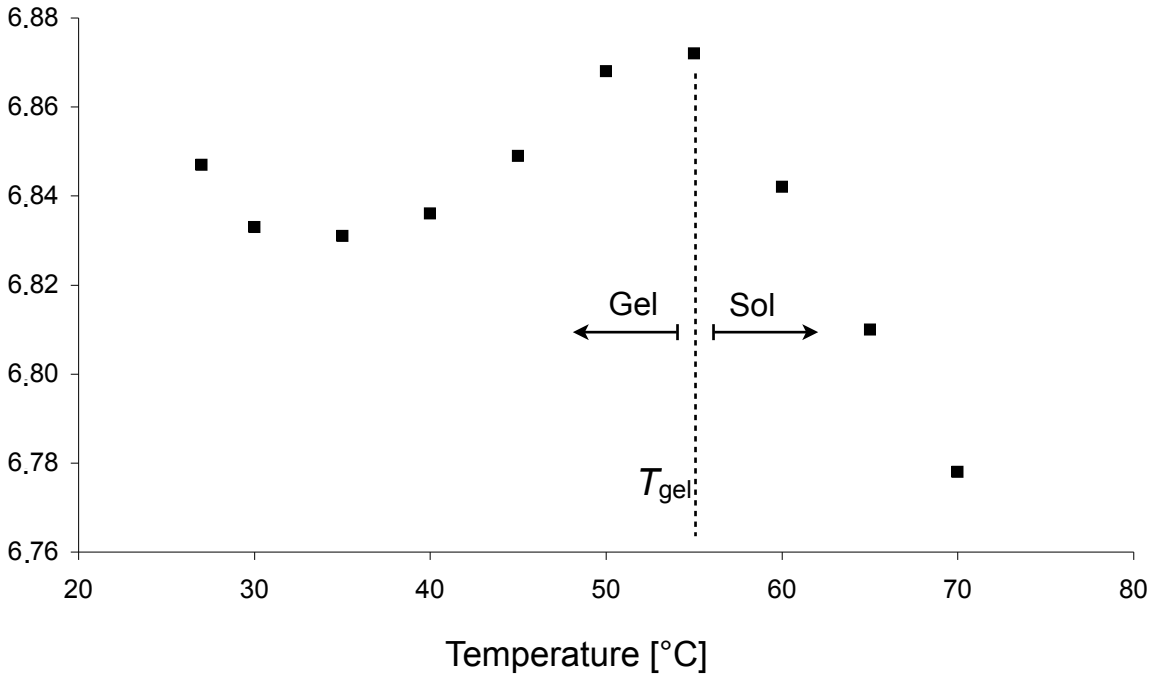

Figure 85: Graphical illustration of the chemical shift with inflection point.

The point of inflection (55 °C) corresponded to T_{gel} as reported before.[24,25] The difference in T_{gel} observed with the inversion of tube method and the T_{gel} of the gel in the NMR tube can be explained by the extremely different dimensions of the test vials.

Rheology

Oscillatory rheological measurements revealed the viscoelastic state of the gel material. As a model, gel **87** in glycerol (90 wt.%) was chosen at a concentration of 5 mg·mL^{-1}. A DSS measurement (Figure 86, top) with increasing strain from 0.1 up to 100% at a frequency of 1.0 Hz marked the breaking of the gel (G″ > G′) at 5.1%. A relatively constant tanδ (G″/G′) value was obtained during the DFS measurement of the glycerol gel at 0.1 % strain which was according to a good tolerance against external forces (Figure 86, bottom).

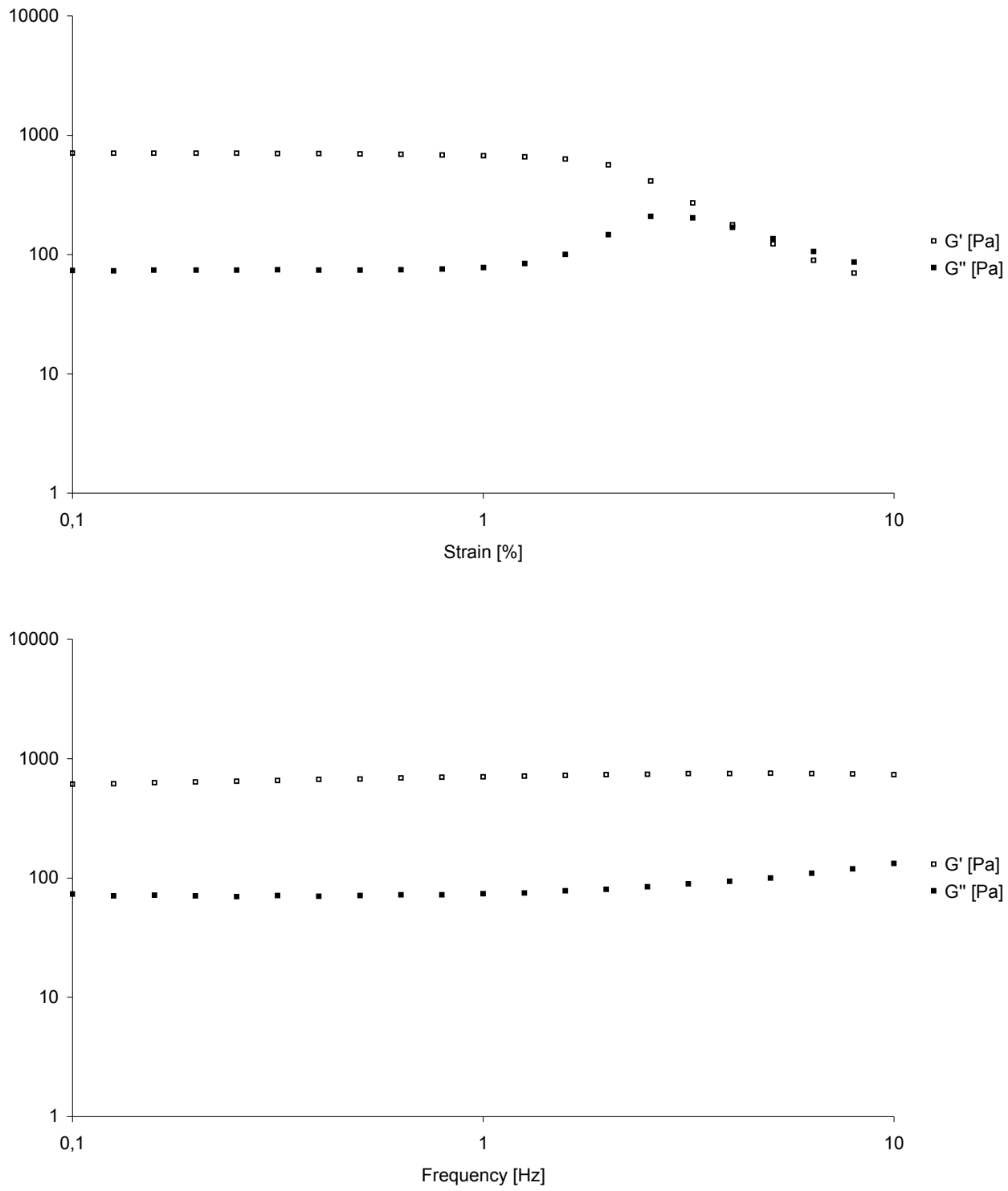

Figure 86: DSS (top) and DFS (bottom) measurement of glycerol gel at 5 mg·mL^{-1}.

A plot of G′ and G″ at constant frequency (1.0 Hz) and strain (0.1%) was obtained by a DTS measurement (Figure 87). It confirmed the stability of the material over the time (tanδ (G″/G′) = 0.105 ± 0.001).

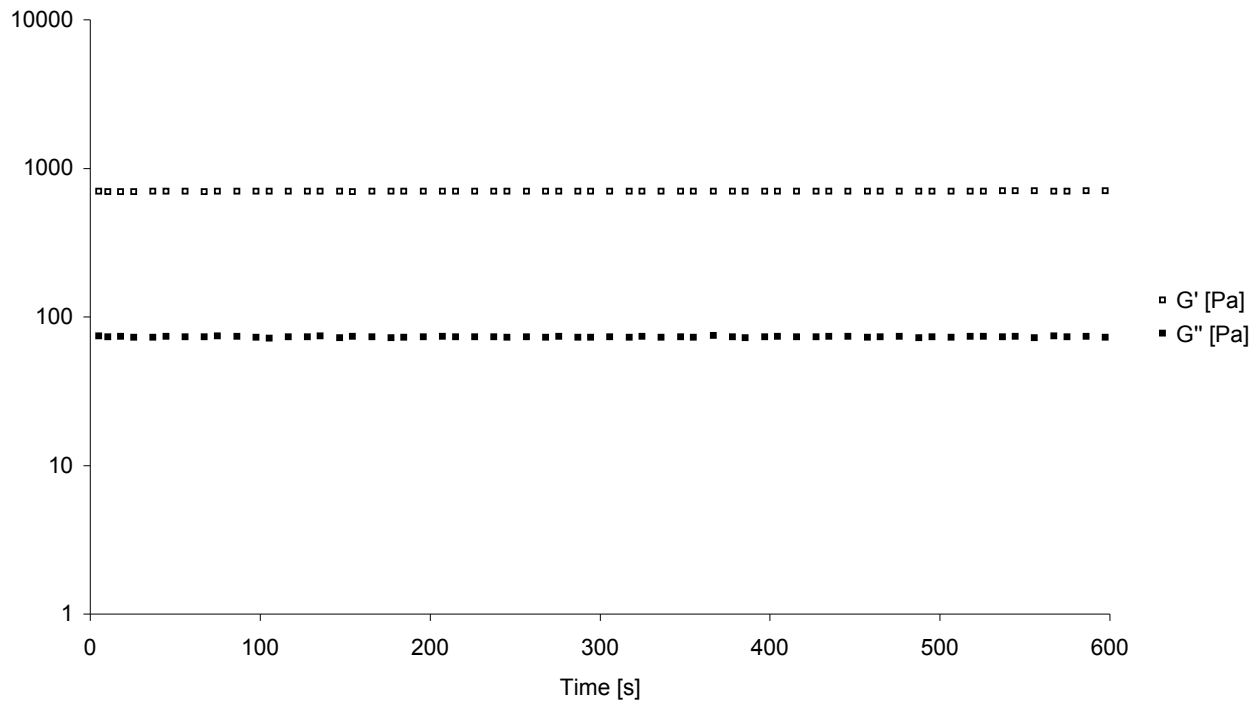

Figure 87: DTS measurement of glycerol gel as function of the aging time.

Interestingly, the gel showed a smart thixotropic response to large external strain. This remarkable property is important for the application of the gels in real-life.[23] The thixotropic nature was confirmed by a rheological experiment, divided into three steps (Figure 88):

1. First a shear strain as for DTS experiment above was applied for 20 min (DTS 1, 1.0 Hz, 0.1% strain, tanδ = 0.107 ± 0.002), confirming the gel state of the material (G′ > G″).
2. In the second step an increased shear strain was applied for 30 min (DTS 2, 1.0 Hz, 10000% strain) resulting in destruction of the gel (G″ > G′).
3. The third step allowed the material to recover at initial shear strain (DTS 3, 1.0 Hz, 0.1% strain). After 3 h a recovery of 100% was proven as the average tanδ went back to the start value (0.108 ± 0.002).

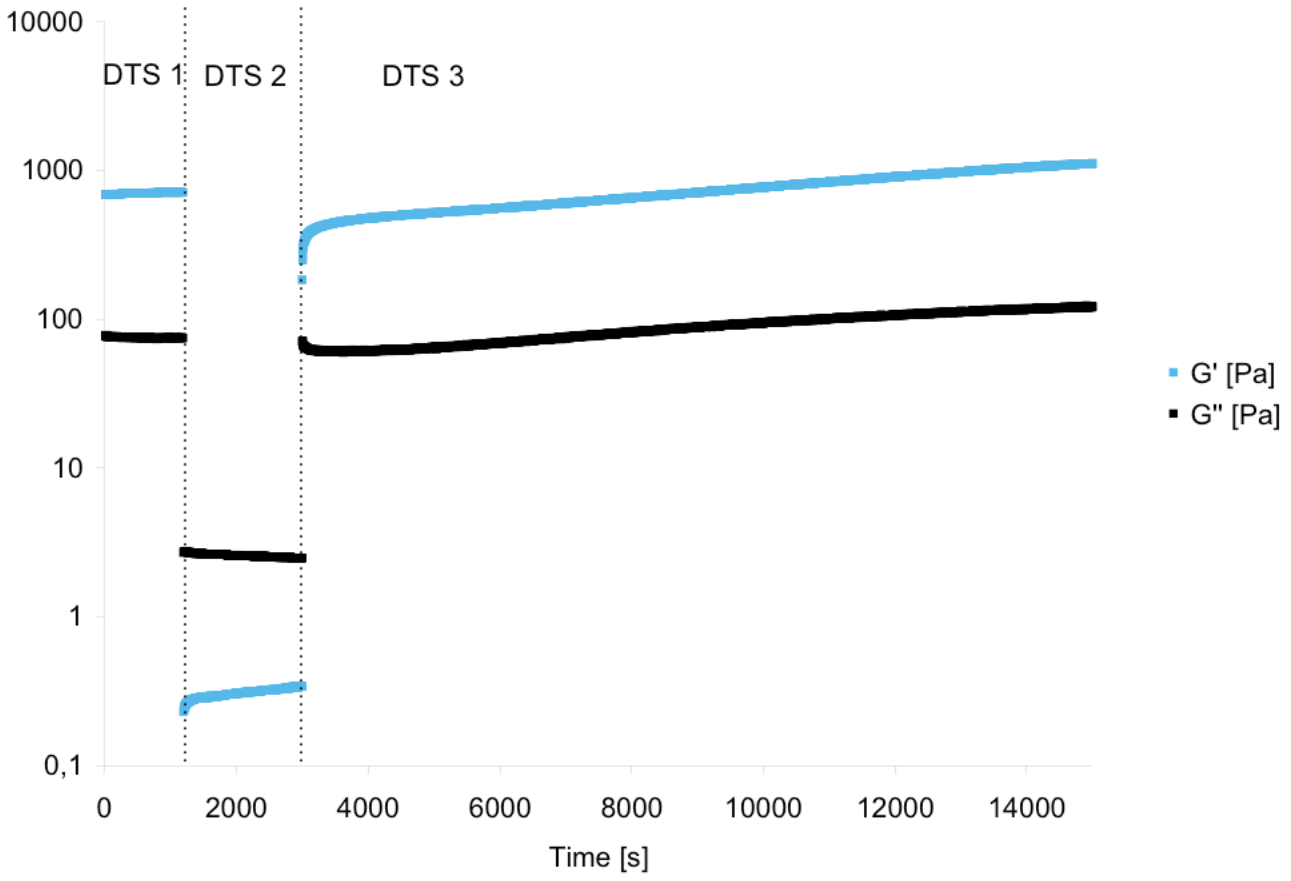

Figure 88: Self-healing ability of gel in glycerol.

Microscopy

Structural anisotropies of toluene and DCM organogels were observed by an optical microscope equipped with a polarization filter (Figure 89). The birefringence under polarized light was switched on in the gel material and was switched off in the isotropic solution that was received after heating of the gel. In this respect, the control of the birefringence is important for potential use as optical device.[26]

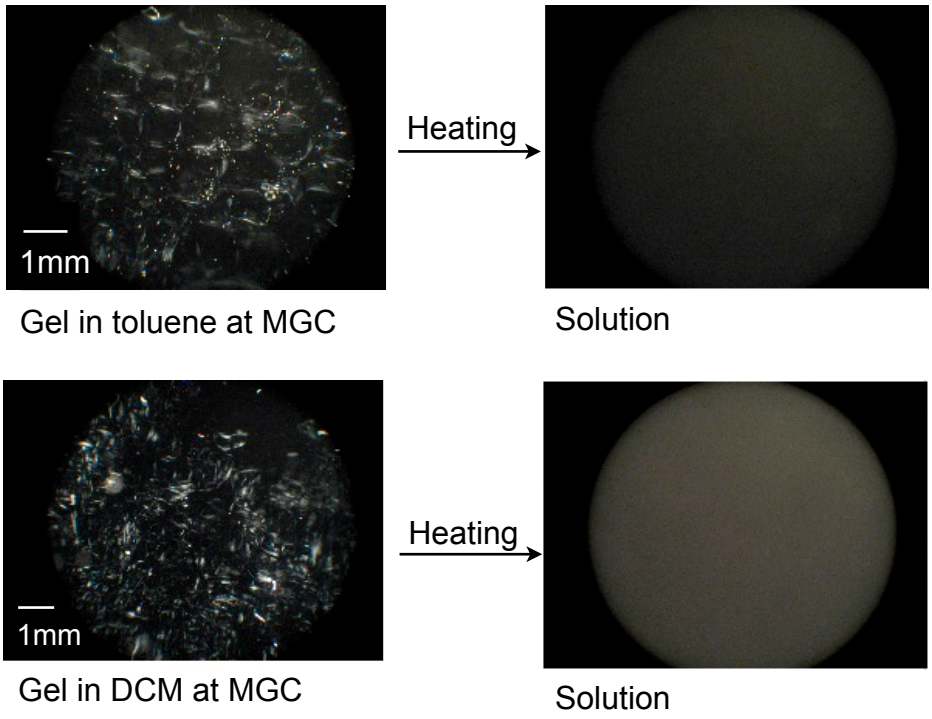

Figure 89: Optical photographs of birefringence in toluene (top) and DCM (bottom) gels.

Furthermore, SEM pictures of the corresponding xerogels provided a 3D appearance of the surface structure of **87** in different solvents (Figure 90). The Images revealed the remarkable influence of the solvent nature on the morphology of the supramolecular aggregates. The variety starts with a lamellar layer structure from NM xerogel in Figure 90, A. Accurate laths (D) with 100-400 nm width made of mesitylene and interlaced fibers with high crosslink density (C, G and H) were also obtained, as well as high density structures (B,F) from nitrobenzene.

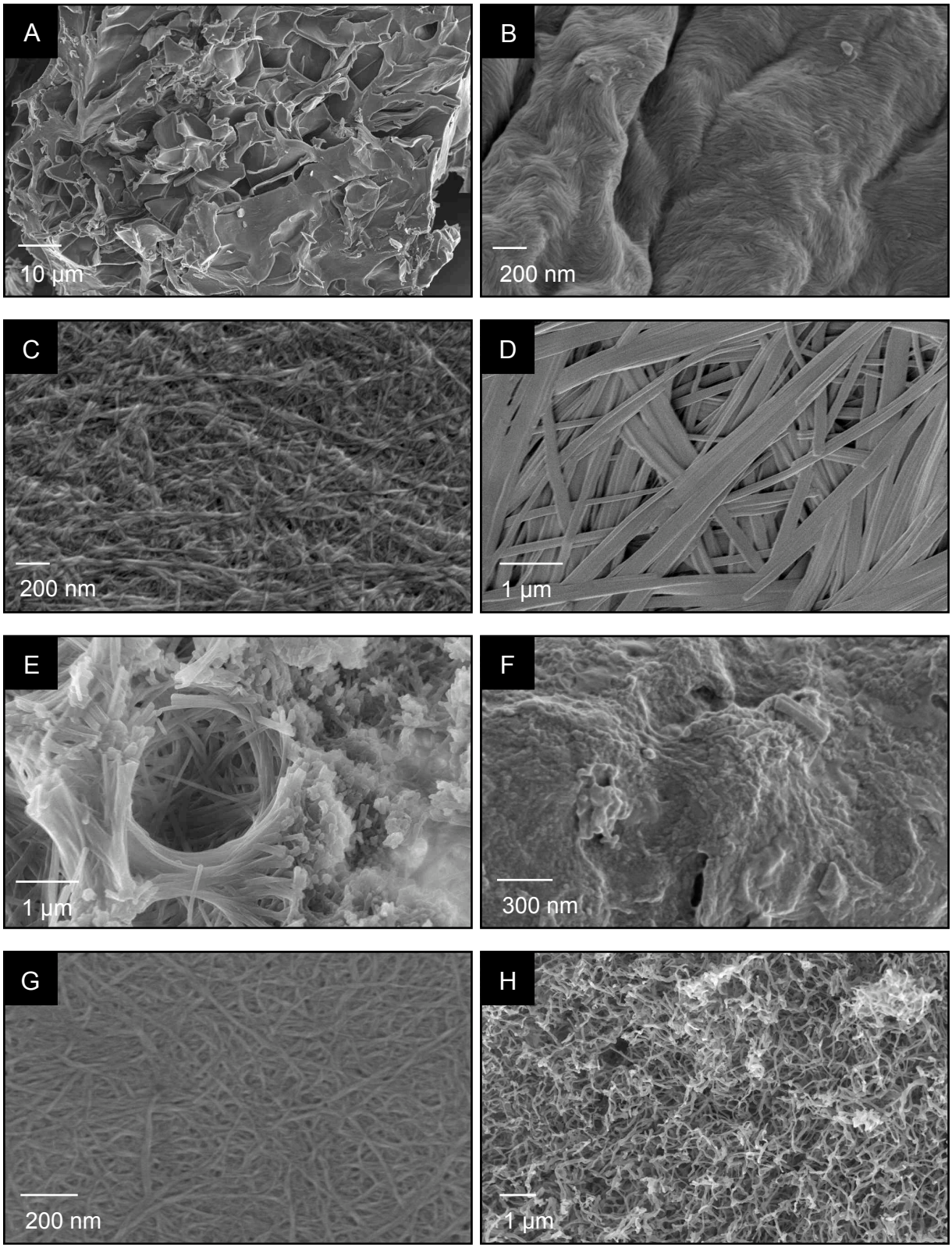

Figure 90: SEM images from freeze-dried gels at MGC based on **87** in organic solvents: NM (A), toluene (B), benzene (C), mesitylene (D), DCM (E), nitrobenzene (F), m-xylene (G) and carbon tetrachloride (H).

Additionally, TEM images of toluene (left) and DCM (right) showed single fibers of the network (In Figure 91).

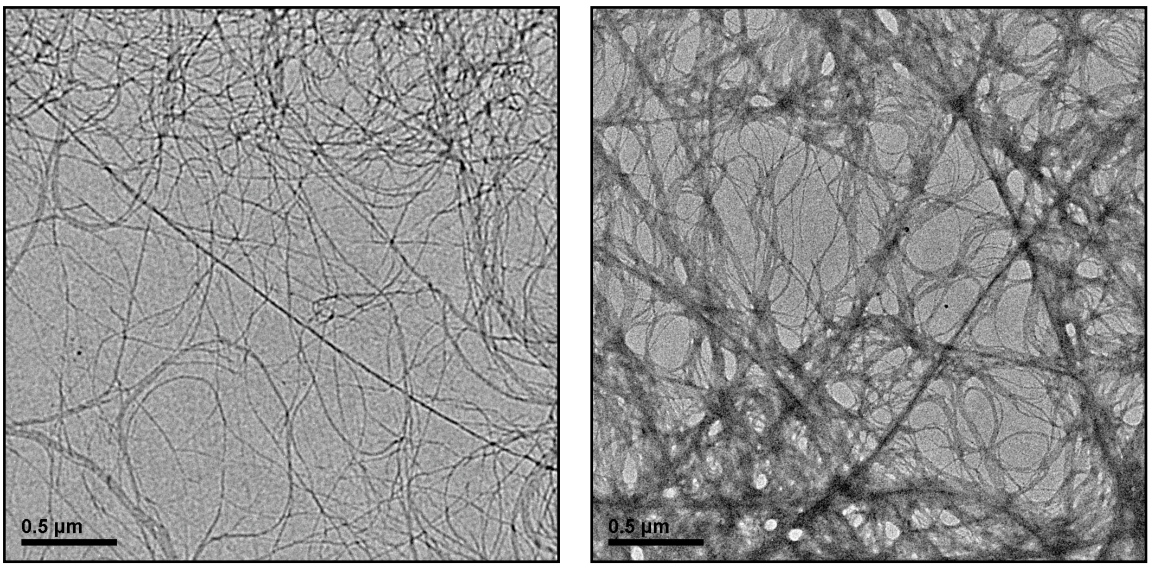

Figure 91: Representative TEM images of xerogel of **87** in toluene (left) and DCM (right) prepaired at their MGC as decribed in Table 11.

3.3 Application in silver sensing and phase selective gelation

Silver sensing

Besides their sensitiveness to temperature, supramolecular organogels often show response to other external factors as chemical additives.[23,27-30] The responsiveness towards chemical stimuli of the three model gels of **87** at MGC was tested (Table 13). The gels showed stability against water, aqueous NaOH, HCl, $CuSO_4$ and NaI solution at 0.1 mol·L^{-1}. Addition of concentrated HCl (37 wt.%) or THF to the gel material resulted in degradation and dissolving.

Table 13: Chemical responsiveness test of toluene, glycerol (90 wt.%) and DCM gel at MGC.[a]

Stimulus	Toluene gel	Glycerol gel	DCM gel
Water	Stable[b]	Stable	Stable
NaOH (0.1 mol·L^{-1})	Stable[b]	Stable	Stable
HCl (0.1 mol·L^{-1})	Stable[b]	Stable	Stable
HCl (37 wt.%)	Sol	Sol	Sol
THF	Sol	Sol	Sol
$CuSO_4$ (0.1 mol·L^{-1})	Stable[b]	Stable	Stable
NaI (0.1 mol L^{-1})	Stable[b]	Stable	Stable
$AgNO_3$ (0.1 mol·L^{-1})	Stable[b]	Stable[c]	Stable
KOAc (0.1 mol·L^{-1})	Stable[b]	Stable	Stable

[a]0.2 mL of test solution were placed on 1.0 mL gel material. [b]The gels were stable when kept at 7°C. [c]A color-change of the gel from colorless to orange occurred while the gel material remained stable and the solution colorless.

Observations pointed out that glycerol gels from **87** also had the ability to selectively detect silver ions as in a first experiment 0.1 mol·L^{-1} $AgNO_3$ solution, placed over the gel, changed the color of the gel material from colorless to orange-brownish. The color-change for glycerol gel at MGC was visible within 30 min after the silver solution was placed above the gel. The surface of the gel material which was in contact with the silver solution first turned into a brownish-orange tone, before the whole gel changed its color. When the silver solution was added to glycerol (90 wt.%) without **87** no change occurred. The glycerol gel of **87** also showed responsiveness other aqueous silver salt solutions as silver trifluoromethanesulfonate and silver acetate at 0.1 mol·L^{-1}.

As a first task, the minimum concentration of silver ions in solution, which were necessary to activate a visible color-change was under investigation. For this, the 0.1 mol·L^{-1} $AgNO_3$ stock solution was diluted. It turned out that after 24 h a color change was still visible with the bare eye for a silver ion concentration of 0.01 mmol·L^{-1} (Figure 92).

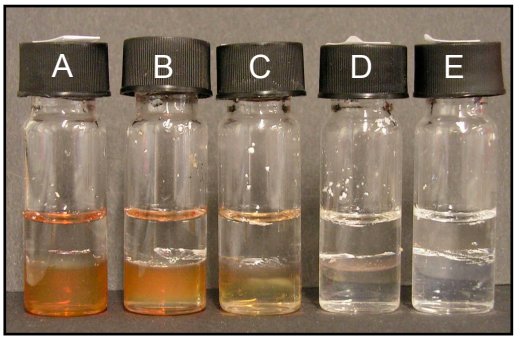

Figure 92: Experiments with $AgNO_3$ solutions at different concentrations indicated the minimum responsiveness of the glycerol gel (A = 100 mmol·L^{-1}, B = 10 mmol·L^{-1}, C = 1 mmol·L^{-1}, D = 0.1 mmol·L^{-1}, E = 0.01 mmol·L^{-1}).

Furthermore, it was tested if additional cations from a second salt could prevent the color change caused by the silver sensing. Figure 93 provides the result from an experiment where glycerol gels at MGC were supplied with three different salt solutions. The vial on the left side contained, additionally to the gel, a $AgNO_3$ solution at 0.1 mol L^{-1}, the vial in the middle contained the gel material and a solution with $AgNO_3$ and KNO_3 at 0.1 mol L^{-1} and the vial on the right side contained KNO_3 at 0.1 mol L^{-1}. The image in Figure 93 was taken after 24 h and revealed that the color-change with additional cations was still visible. However, the intensity of the gel color compared to the gel supplied with the silver solution without further additives decreased apparently. Therefore, only the silver cations and not the nitrate anions caused the color, because otherwise vial C would be colored, too.

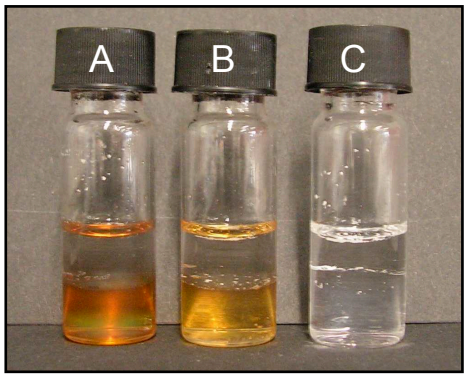

Figure 93: Glycerol gel 24 h after being equipped with additional $AgNO_3$ solution (A), $AgNO_3$ and KNO_3 solution (B) and KNO_3 solution (C).

To test if the silver responsiveness depends only on gelator **87** or the gelator-glycerol combination is necessary to obtain color-change, eight different solvents were used to provide solutions from **87** at 1.0 mg·mL^{-1} (Figure 94).

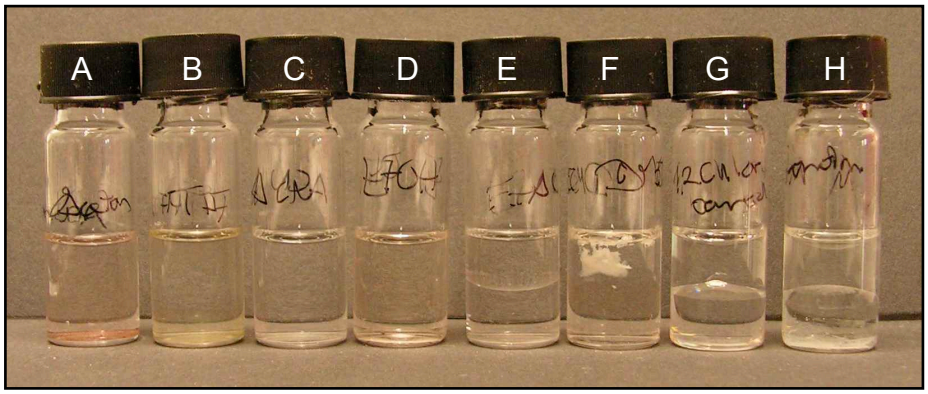

Figure 94: Test of silver-responsiveness in 1.0 mg·mL^{-1} of **87** solutions (A = ACT, B = THF, C = ACN, D = ethanol, E = ETAC, F = DMSO, G = 1,2-dichlorobenzene, H = NM).

1.0 mL of a 0.1 mol·L^{-1} $AgNO_3$ solution were added to the prepared solutions of **87** and allowed to react for 24 h. At this concentration the color-change was clearly visible for the solution of **87** in glycerol (90 wt.%), although that pointed out that the gel material was not necessary for detection of the silver ions. For 1.0 mg·mL^{-1} of **87** in ACT and THF a light, but visible change in color was observed. In contact with silver ions the solution of **87** in ACT turned into pinkish color, whereas THF turned into a yellowish shade. That observation pointed out that **87** was able to identify silver ions in other solvents beside glycerol (90 wt.%), but the color intensity which was achieved by this unique combination could not be repeated. The major advantage which was provided by the silver responsive glycerol gel was its simple and convenient application. A piece of gel material was just placed in a vial and the solution to be tested on presence or absence of silver ions was added (Figure 95, left). The gel changed its color as the solution contained 0.1 mol·L^{-1} $AgNO_3$. The separation of solution and gel was promptly carried out by decantation of the solution (Figure 95, middle). Afterwards, the gel material was still stable enough to be transferred out of the vial (Figure 95, right).

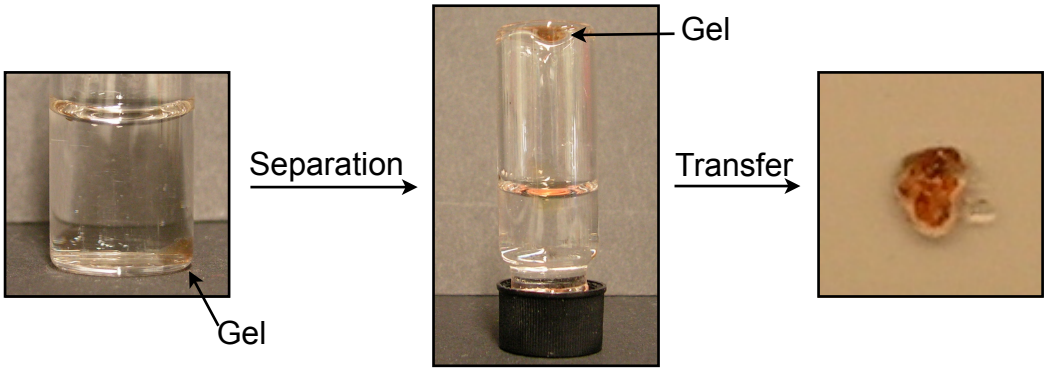

Figure 95: Silver detection of a solution by a piece of glycerol gel (left) and its removal from the solution (middle, right).

Phase selective gelation

The phase selective gelation from a solvent mixture is an eminent task in environmental issues if one of the solvents is water (p. 19f). Interestingly, the organic solvents gelled by **87** were found to be suitable in phase selective gelation. As glycerol is water-soluble, it was the only exception. In a standard procedure 1.0 mL of solvent and 1.0 mL of water were mixed in a glass vial with the corresponding amount of gelator **87**. The gelator was dissolved by heating and vigorously shaking ensured a homogenous dispersion. After cooling of the mixture down to RT the organic phase was gelled whereas the water phase remained in liquid state.

Figure 96 provides eleven examples from phase selective gelation of **87** at MGC. Depending on the density of the organic solvent compared to water, the gel material was formed at the bottom of the vial (solvent density > 1.0 kg m^{-3}) or above the water phase (solvent density < 1.0 kg m^{-3}).

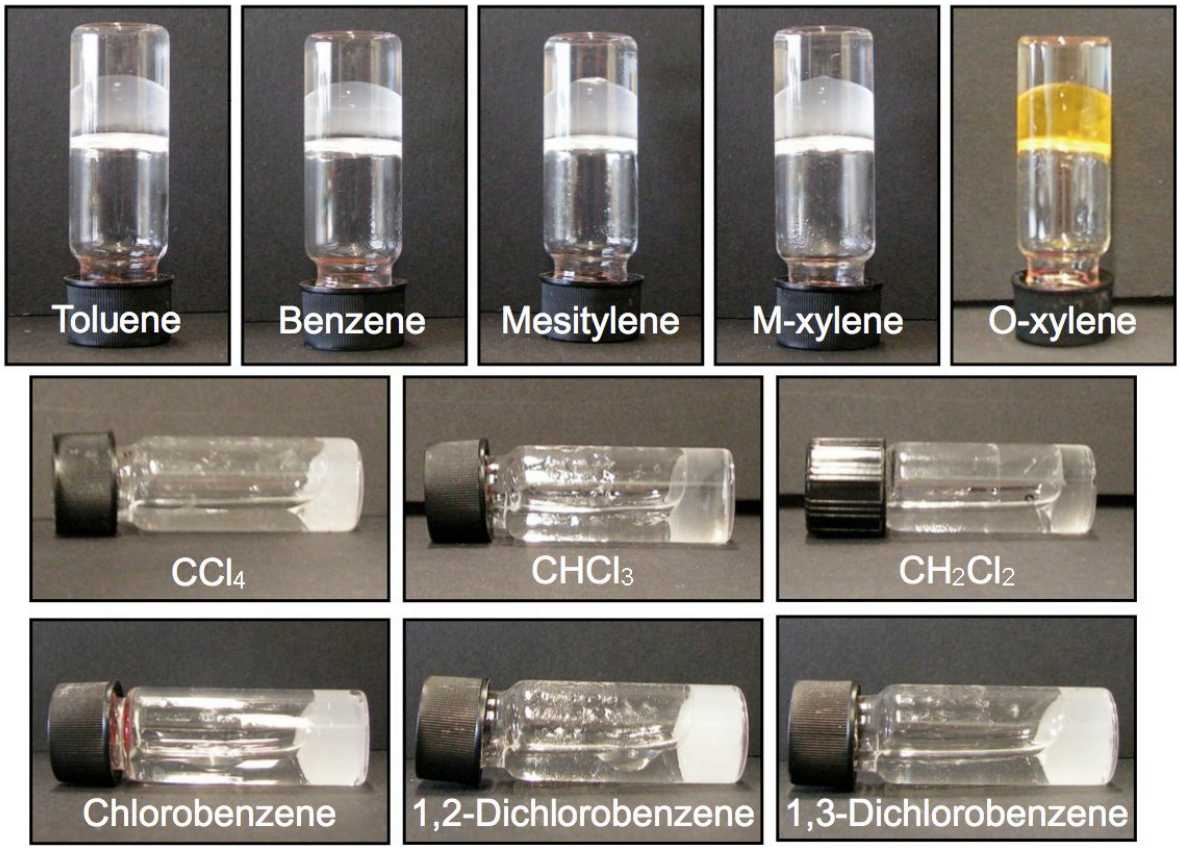

Figure 96: Examples from phase selective gelation of organic solvent/water systems.

Although the gels were not longer transparent but opaque, their stability remained unchanged. This was controlled by the comparison of T_{gel} from standard prepared toluene gel (41 ± 2 °C) and T_{gel} from toluene gel from phase selective gelation (46 ± 2 °C). Additionally, the ability of **87** to gel phase selectively was evaluated for a higher volume. Instead of 1 mL for each phase, 50 mL were now used for the experiment (Figure 97).

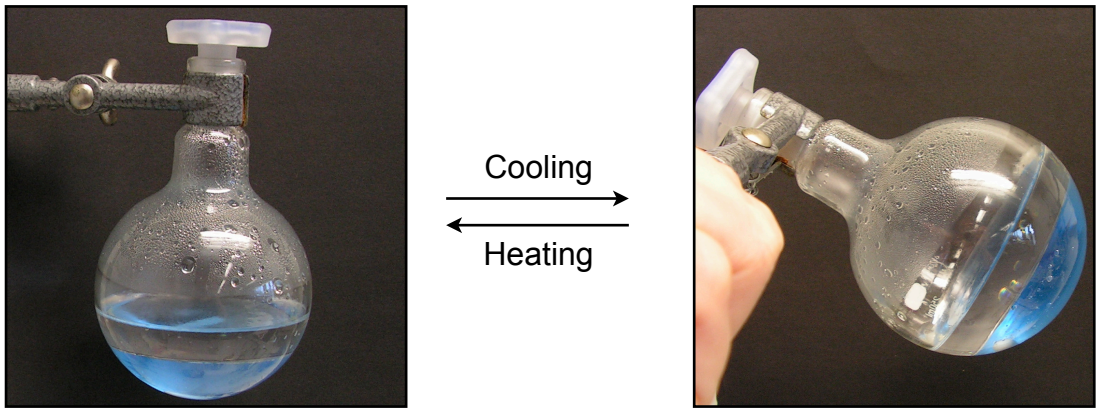

Figure 97: Phase selective gelation through **87** from two-phase toluene/water system.

Evans blue served as dye and enabled a more obvious differentiation between water and toluene phase. Vigorous stirring while heating the flask ensured a homogeneous dispersion of the toluene in water. After the complete dissolving of **87** in the hot solvent, the stirring was turned off and phases separated again (Figure 97, left). Gelation of the toluene phase upon cooling has proven the excellent phase selective gelation ability of **87** (Figure 97, right). The liquid state of the lower water phase was verified by the moving of the remanent magnetic stir bar.

4. Conclusion

In conclusion, literature known compound **87** was proven to operate as gelator in supramolecular self-assembly for fourteen aromatic and halogenated solvents as well as nitromethane and glycerol-water mixtures. The gels were easily prepared by heating-cooling process and provided thermoreversibility. The thermal stability was investigated by the “inverse flow method“. Experiments pointed out the necessity of every functional group as well as the enantiomeric pureness of compound **87** for gelation. The rheological investigation characterized the material as gel and revealed interesting thixotropic behavior. SEM images illustrated the versatile organization of the gelator molecules in 3D structures in various solvents. It was also demonstrated that **87** selectively solidified the organic phase from organic solvent-water mixtures at MGC of the organogels upon heating of the gelator-solvent mixtures. Remarkably, silver responsive nature was shown by **87** in combination with glycerol. Moreover, the glycerol gels of **87** turned out to be a useful and convenient tool for silver sensing, as it was easily separated from the test solution.

5. Experimental part

5.1 General remarks

Commercially available reagents and solvents for synthesis and analysis were used as received without further purification. Analytical thin layer chromatography was performed on Merck TLC alumina sheets silica gel 60 F 254. Visualization was accomplished with UV light (254 nm) and phosphomolybdic acid as stain. Purification of reaction products was carried out by flash chromatography using silica-gel (0.063-0.200 mm) or medium pressure liquid chromatography using pre-packed silica columns.

^{1}H NMR and ^{13}C NMR

^{1}H NMR spectra were recorded on a Bruker AVANCE–II at 400 MHz and ^{13}C NMR spectra were recorded at 100 MHz, using DMSO-d_6 and D_3CCOCD_3 as the deuterated solvents. Chemical shifts were reported in the δ scale relative to residual DMSO (2.50 ppm for ^{1}H NMR and 39.43 ppm for ^{13}C NMR) and acetone (2.05 ppm for ^{1}H NMR).

Optical rotation

The optical rotation was determined in a Jasco DIP-370 polarimeter.

Melting points

The melting points were measured with a Gallenkamp Variable Heater.

Mass spectrometry

ESI ionization method and mass analyzer type Bruker Daltonics Esquire3000 plus were used for the MS measurements.

Fourier transform infrared spectroscopy (FT-IR)

FT-IR spectroscopy was carried out on a Nicolet Avatar 360.

HPLC

High performance liquid chromatography was carried out using a Waters 2695 Alliance detector.

5.2 Synthesis of compounds

General procedure for the preparation of compounds 87, 88, 91, 92, 93

To a stirred solution of isothiocyanate (1.1 mmol), or isocyanate (1.1 mmol) in CH_2Cl_2 (5.0 mL), the corresponding commercially available amine (1.0 mmol) was added in one portion. After stirring the resulting solution at room temperature overnight, the solvent was evaporated under reduced pressure and the product was purified by flash chromatography or medium pressure liquid chromatography (SiO_2 hexane/EtOAc 7:3). ^1H and ^{13}C NMR spectra for compound **87**[16] and **88**[31] were consistent with values reported in the literature.

1-(3,5-Bis(trifluoromethyl)phenyl)-3-((1*R*,2*R*)-2-hydroxy-2,3-dihydro-1H-inden-1-yl)urea (91)

Following the general procedure, compound **91** was obtained as white solid in 92% yield. M.p. 232-234 °C. $[\alpha]^{20}_D$ 88.1 (*c* 0.74, DMSO). ^1H NMR (400 MHz, DMSO-d_6) δ 9.21 (br s, 1H), 8.14 (s, 2H), 7.57 (s, 1H), 7.22- 7.19 (m, 4H), 6.89 (d, *J* = 8.3 Hz, 1H), 5.33 (d, *J* = 5.5 Hz, 1H), 4.95 (dd, *J* = 6.7, 8.1 Hz, 1H), 4.29-4.22 (m, 1H), 3.14 (dd, *J* = 7.1, 15.6 Hz, 1H), 2.72 (dd, *J* = 7.27, 15.6 Hz, 1H). ^{13}C NMR (100 MHz, DMSO-d_6) δ 154.9, 142.4 141.8, 139.6, 130.5 (q, *J* = 32.5 Hz, *C*C F_3), 127.6, 126.6, 124.6, 123.8, 123.3 (q, *J* = 272.8 Hz, *C*F_3), 117.5-117.2 (m, 1C), 113.6-113.4 (m, 1C), 77.9, 61.6, 38.5. IR (KBr film) (cm^{-1}) v 3395, 3326, 2923, 2853, 1634, 1278, 1129, 1073, 749. MS (ESI) calculated for $C_{18}H_{14}F_6N_2NaO$ 427.1; found 427.1 [M+Na].

(*R*)-1-(3,5-Bis(trifluoromethyl)phenyl)-3-(2,3-dihydro-1H-inden-1-yl)urea (92)

Following the general procedure, compound **92** was obtained as white solid in 75% yield. M.p. 215-217 ºC. $[\alpha]^{20}_D$ -48.7 (*c* 0.77, DMSO). ^1H NMR (400 MHz, CD_3COCD_3) δ 8.58 (br s, 1H), 8.20 (s, 2H), 7.55 (s, 1H), 7.36-7.34 (m, 1H), 7.26-7.17 (m, 3H), 6.34 (br d, *J* = 7.3 Hz, 1H), 5.35 (q, *J* = 7.7 Hz, 1H), 2.96 (ddd, *J* = 3.6, 8.7, 15.9 Hz, 1H), 2.89-2.81 (m, 1H), 2.59-2.51 (m, 1H), 1.91-1.82 (m, 1H). ^{13}C NMR (100 MHz, DMSO-d_6) δ 154.6, 143.9, 142.7, 142.4, 130.5 (q, *J* = 32.5 Hz, *C*CF_3), 127.4, 126.3, 124.5, 123.7, 123.3 (q, *J* = 272.8 Hz, *C*F_3), 117.4-117.3 (m, 1C), 113.6-113.4 (m, 1C), 54.5, 33.3, 29.5. IR (KBr film) (cm^{-1}) v 2923, 2853, 1639, 1457, 1276, 1130. MS (ESI) calculated for $C_{18}H_{14}F_6N_2NaO$ 441.1; found 441.1 [M+Na].

1-((1*S*,2*R*)-2-Hydroxy-2,3-dihydro-1H-inden-1-yl)-3-phenylurea (93)

Following the general procedure, compound **93** was obtained as white solid in 94% yield. M.p. 224-226 ºC. $[\alpha]^{20}_{D}$ +53.9 (*c* 0.64, DMSO). ^{1}H NMR (400 MHz, DMSO-d_6) δ 8.85 (s, 1H), 7.45 (d, *J* = 8.5 Hz, 1H), 7.26-7.18 (m, 6H), 6.91 (t, *J* = 7.3 Hz, 1H), 6.44 (d, *J* = 8.7 Hz, 1H), 5.24 (d, *J* = 4.2 Hz, 1H), 5.10 (dd, *J* = 5.0, 8.5 Hz, 1H), 4.45 (dd, *J* = 4.1, 8.9 Hz, 1H), 3.07 (dd, *J* = 4.8, 16.2 Hz, 1H), 2.80 (d, *J* = 16.2 Hz, 1H). ^{13}C NMR (100 MHz, DMSO-d_6) δ 155.2, 143.1, 140.5, 140.3, 128.6, 127.0, 126.2, 124.8, 123.8, 120.9, 117.4, 72.0, 57.1, 39.6. IR (KBr film) (cm^{-1}) v 3469, 3365, 3292, 2923, 2854, 1623, 1568, 1458, 1246,1050, 766, 748, 735. MS (ESI) calculated for $C_{16}H_{16}F_6N_2NaO$ 291.1; found 291.1 [M +Na].

5.3 Preparation of organogels

The gels were prepared by weighing of the gelator **87** in a screw-capped glass vial (4.5 cm length x 1.2 cm diameter). 1.0 mL of solvent were added and the vial was closed. The vial was gently heated with a heat gun until a isotropic solution was obtained. The gel material was formed after the solution was allowed to cool down slowly to RT. The resulting material was preliminarily classified as gel if it was able to resist the turning of the vial upside down. The cooling rate of the gels was not controlled.

5.4 Characterization of organogels

Temperature-dependent ^{1}H NMR

Temperature-dependent ^{1}H NMR studies were carried out on a 400 MHz Bruker Avance instrument equipped with a BVT 2000 heating system (Bruker BioSpin GmbH).

Optical microscopy

A Wild Makroskop M420 optical microscope was used to investigate crystals in gels. The microscope was equipped with a Canon Power shot A640 digital camera for digital imaging. An additional polarization filter was used to observe the gel material under polarized light.

Rheological measurements

Rheological measurements were performed with advanced rheometer AR 2000 from TA Instruments which was equipped with a cooling system (Julabo C). A 20 mm plain plate geometry (stainless steel) was used. First strain sweep measurements were carried out to estimate the strain in % at which reasonable torque values were given (about 10 times of the transducer resolution limit). Afterwards, frequency sweep measurements and time sweep measurements were performed. Additionally, the thixotropic behavior of the gel material was investigated in an experiment with three steps. First a DTS experiment confirmed the gel state, G′ > G″ at low strain. Then DTS was carried out again but this time under massive increase of the strain which let the gel fracture into a solution, G′ < G″. In the third step the DTS experiment was using the initial strain and for the thixotropic material a recovering of the gel state, G′ > G″, was observed.

Field emission scanning electron microscopy (FESEM)

A Zeiss Merlin field emission scanning electron microscope with an accelerating voltage of 10 kV was used to take SEM pictures of the xerogels. For this, a nano-sized Pt film was sputtered prior to imaging on the samples on carbon tape (40 mA, 60 seconds). A SCD500 Leica EM device was used for the imaging.

UV-Vis spectroscopy

Absorption spectra were recorded on a Varian Cary BIO 50 UV-Vis scanning spectrophotometer by use of a 1 cm quartz cuvettes.

5.5 Application in silver sensing and phase selective gelation

Silver sensing

For responsiveness tests, the gel material was prepared as described at 5.3. The gel was allowed to rest for at least 1 h before used in further experiments.

Phase selective gelation

In a screw-capped glass vial (4.5 cm length x 1.2 cm diameter) MGC of **87** was filled in. 1.0 mL of respective solvent and 1.0 mL of distilled water were added. The vial was closed and heated carefully with a heat gun under shaking of the vial until the gelator was

dissolved. After cooling down to RT, the inversion of the tube confirmed the formation of gel.

6. References

[1] Terech, P.; Weiss, R. G. *Chem. Rev.* **1997**, *97*, 3133-3159.

[2] Van Esch, J. H.; Feringa, B. L. *Angew. Chem. Int. Ed.* **2000**, *39*, 2263-2266.

[3] Abdallah, D. J.; Weiss, R. G. *Adv. Mater.* **2000**, *12*, 1237-1247.

[4] Gronwald, O.; Shinkai, S. *Chem. Eur. J.* **2001**, *7*, 4328-4334.

[5] Estroff, L. A.; Hamilton, A. D. *Chem. Rev.* **2004**, *104*, 1201-1218.

[6] Sangeetha, N. M; Maitra, U. *Chem. Soc. Rev.* **2005**, *34*, 821-836.

[7] De Loos, M.; Feringa, B. L.; van Esch, J. H. *J. Org. Chem.* **2005**, *17*, 3615-3631.

[8] George, M.; Weiss, R. G *Acc. Chem. Res.* **2006**, *39*, 489-497.

[9] Piepenbrock, M. O. M.; Lloyd, G. O.; Clarke, N.; Steed, J. W. *Chem. Rev.* **2010**, *110*, 1960-2004.

[10] Steed, J. W. *Chem. Commun.* **2011**, *47*, 1379-1383.

[11] John, G.; Jadhav, S. R.; Menon, V. M.; John, V. T. *Angew. Chem. Int Ed.* **2012**, *51*, 1760-1762.

[12] Yamanaka, M. *J. Incl. Phenom. Macrocycl. Chem.* **2013**, *77*, 33-48.

[13] Wang, C.; Zhang, D.; Zhu, D. *J. Am. Chem. Soc.* **2005**, *127*, 16372-16373.

[14] Qi, Z.; de Molina, P. M.; Jiang, W.; Wang, Q.; Nowosinski, K.; Schulz, A.; Gradzielski, M.; Schalley, C. A. *Chem. Science* **2012**, *3*, 2073-2082.

[15] Yamanaka, M.; Nakagawa, T.; Aoyama, R.; Nakamura, T. *Tetrahedron* **2008**, *64*, 11558-11567.

[16] Herrera, R. P.; Monge, D.; Martín-Zamora, E.; Fernández, R.; Lassaletta, J. M. *Org. Lett.* **2007**, *17*, 3303-3306.

[17] Suzuki, M.; Nanbu, M.; Yumoto, M.; Shiraib, H.; Hanabusa, K. *New J. Chem.* **2005**, *29*, 1439-1444.

[18] Suzuki, M.; Nigawara, T.; Yumoto, M.; Kimura, M.; Shirai, H.; Hanabusa, K. *Org. Biomol. Chem.* **2003**, *1*, 4124-4131.

[19] Yang, H.; Yi, T.; Zhou, Z.; Zhou, Y.; Wu, J.; Yu, M.; Li, F.; Huang, C. *Langmuir* **2007**, *23*, 8224-8230.

[20] John, G.; Jung, J. H.; Masuda, M.; Shimizu, T. *Langmuir* **2004**, *20*, 2060-2065.

[21] Wang, C.; Zhang, D.; Zhu, D. *Langmuir* **2007**, *23*, 1478-1482.

[22] Bieser, A. M.; Tiller, J. C. *J. Phys. Chem. B* **2007**, *111*, 13180-13187.

[23] Fatás, P.; Bachl, J.; Oehm, S.; Jiménez, A. I.; Cativiela, C.; Díaz, D. D. *Chem. Eur. J.* **2013**, *19*, 8861-8874.

[24] Makarevic, J.; Jokic, M.; Raza, Z.; Stefanic, Z.; Kojic-Prodic, B.; Zinic, M. *Chem. Eur. J.* **2003**, *9*, 5567-5580.

[25] Allix, F.; Curcio, P.; Pham, Q. N.; Pickaert, G.; Jamart-Grégoire, B. *Langmuir* **2010**, *26*, 16818-16827.

[26] Fischer, R. E.; Tadic-Galeb, B.; Yoder, P. R. *Optical System Design;* McGraw Hill 2nd edition, **2008**.

[27] Edwards, W.; Smith, K. *Chem. Commun.* **2012**, *48*, 2767-2769.

[28] Chen, Q.; Zhang, D.; Zhang, G.; Zhu, D. *Langmuir* **2009**, *25*, 11436-11441.

[29] Xue, P.; Sun, J.; Xu, Q.; Lu, R.; Takafuji, M.; Ihara, H. *Org. Biomol. Chem.* **2013**, *11*, 1840-1847.

[30] Zhou, C.; Gao, W.; Yang, K.; Xu, L.; Ding, J.; Chen, J.; Liu, M.; Huang, X.; Wang, S.; Wu, H. *Langmuir* **2013**, *44*, 13568-13575.

[31] Herrera, P.; Sgarzani, V.; Bernardi, L.; Ricci, A. *Angew. Chem. Int. Ed.* **2005**, *44*, 6576-6579.

F Summary

1. Summary

In this thesis, four low molecular weight gelator based organogel systems were under investigation. Besides the exploration of two novel metallogels, a multicomponent liquid organogelator system and its organogels were discovered. Additionally, the gelation ability of a urea-based compound was analyzed.

B Ca-based metallogel and metal organic framework

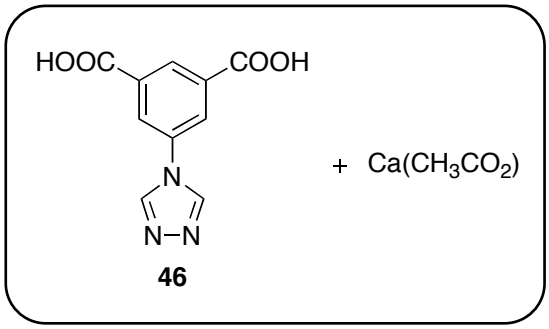

46

In this chapter, the application of the versatile 5TIA ligand **46** for the construction of new Ca-based metal organic frameworks and metallogels with calcium acetate, 5TIA-MOF and 5TIA-Gel was described. A fine balance between crystallization of MOF, or formation of a metallogel was regulated by the amount of water in the system. The first reported Ca-based metallogels can be obtained from five different organic solvents with small α and at the same time high β and π* values referring to the Kamlet-Taft parameters. The absence of additional water during the gelation, the influence of the counterion in the stabilization of the gel and the failed gelation attempt using Ca-5TIA-MOF as gelator pointed out that Ca-5TIA-MOF and Ca-5TIA-Gel possess modified internal structures. The gel material was further characterized by its thermal and rheological behavior and FT-IR and PXRD pattern. Both materials, MOF and metallogel showed the ability to uptake the gas CO_2. Compared to the crystalline Ca-5TIA-MOF, Ca-5TIA-Gel was able to adsorb 20% more CO_2 gas. Furthermore, both materials showed moderate catalytic activity towards the hydrosilylation of benzaldehyde and diphenylsilane, where slightly enhanced catalytic performance was provided by Ca-5TIA-Gels.

C Multicomponent liquid organogelator system I and II:

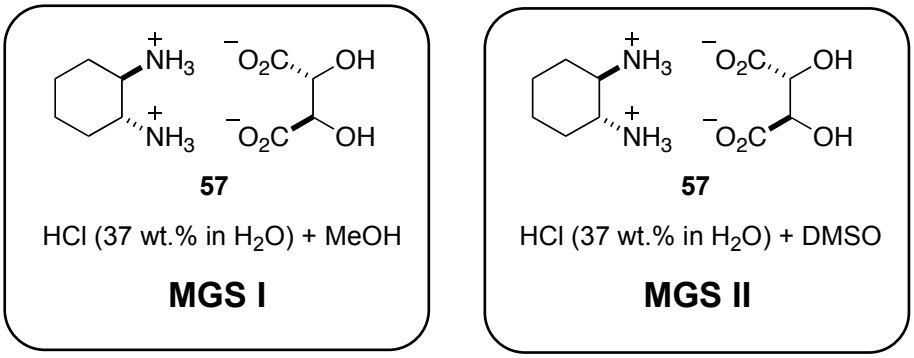

The investigation of two multicomponent organogelator solutions based on (1*R*,2*R*)-1,2-diaminocyclohexane *L*-tartrate **57** dissolved with the help of aqueous HCl in methanol (MGS I) and DMSO (MGS II) was carried out. The gelator solutions were able to form a row of transient gels in organic solvents either at RT (MGS II) or at low temperatures, close to the freezing-point of the referring solvents (MGS I). Remarkably, gels from MGS II needed a 2-12 times lower amount of gelator solution, compared to MGS I gels. For both, gelator solution and gel the crystallization of (1*R*,2*R*)-1,2-diaminocyclohexane dihydrochloride was observed. Crystal growth always destroyed the gels which led to a short lifetime in the range of a few hours up to several days, depending on the respective solvent. Experiments have proven that (1*R*,2*R*)-1,2-diaminocyclohexane played the key role in terms of structural direction, whereas the tartaric acid acted as stabilizer of the supramolecular network, although MGS II gels showed a higher tolerance to its replacement than MGS I gels. Furthermore, it was shown that the salt, methanol, hydrochloric acid and water had to be used in a specific stoichiometry, whereas aberrations led to shorter lifetime of the gels or no gelation at all:(1*R*,2*R*)-1,2-diaminocyclohexane *L*-tartrate : MeOH : HCl : H_2O = 1 : 193 : 2.4 : 8.3. Phase selective gelation from two non-mixed organic solvents was provided by MGS II at RT and MGS I at low temperatures, although the gels from MGS I had a lower temporal stability. Furthermore, experiments towards the fabrication of semi-interpenetrating network were carried out for enhancing of gel properties.

D Ag-based metallogels

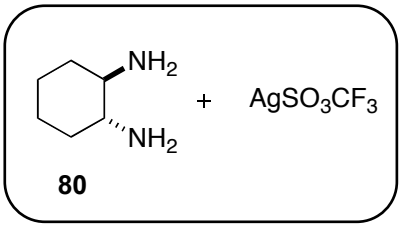

In chapter D the preparation of silver-based metallogel from (1*R*,2*R*)-1,2-diamino-cyclohexane **80** and silver trifluoromethanesulfonate at an equimolar ratio was demonstrated. The system $AgSO_3CF_3$ + **80** was able to gel a number of aromatic solvents at a concentration range of 0.05-0.20 mmol·L^{-1}. Due to the low solubility of $AgSO_3CF_3$ in chlorinated aromatic solvents it was not possible to raise the concentration and only partial gels were obtained. The mixing of $AgSO_3CF_3$ solution and solution made of **80** as gel preparation method was shown to be preferable in opposite to the preparation by sonication at RT, because the gelation time for sonication was longer and the MGC was six times higher. The exchangeability of $AgSO_3CF_3$ by different silver salts was tested in order to investigate the specificity of the counterion. Besides **80**, **81** also showed to be an appropriate ligand in combination with $AgSO_3CF_3$. The results showed that the morphology of the gelator network could be tuned based on the used ligand.

E Organogels from new LMW urea gelator

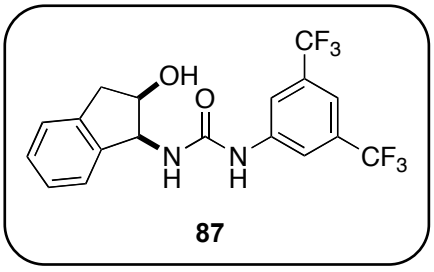

Urea-based compound **87** was proven to operate as gelator in supramolecular self-assembly for 14 aromatic and halogenated solvents as well as nitromethane and glycerol-water mixtures. The gels were easily prepared by heating-cooling process and provided thermoreversibility. The thermal stability was investigated by the “inverse flow method“. Experiments pointed out the necessity of every functional group as well as the

enantiomeric purity of compound **87** for gelation. The rheological investigation characterized the material as gel and revealed interesting thixotropic behavior. SEM images illustrated the versatile organization of the gelator molecules in 3D structures in various solvents. It was also demonstrated that **87** selectively solidified the organic phase from organic solvent-water mixtures at MGC of the organogels upon heating of the gelator-solvent mixtures. Remarkably, silver-responsive nature was shown by **87** in combination with glycerol. Moreover, the glycerol gels of **87** turned out to be useful and convenient tools for silver sensing, as they were easily separated from the test solution.

2. Zusammenfassung

In dieser Arbeit wurden vier verschiedene Organogele, welche auf niedermolekularen Gelatoren basieren, untersucht. Neben der Entdeckung von zwei neuartigen Metallogelen wurde ein flüssiges Multikomponenten-Organogelatoren-System und die dazugehörigen Organogele untersucht. Zusätzlich wurde die Eignung eines Harnstoff-basierten Moleküls als Gelator analysiert.

B Ca-basierende Metallogele und metall-organische Gerüste

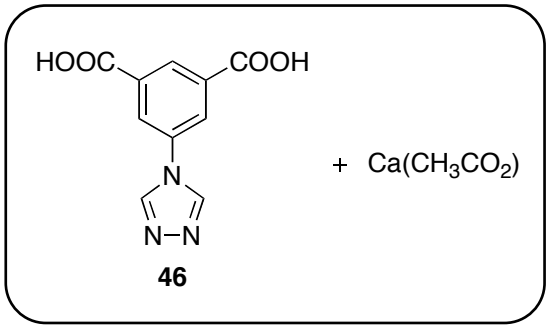

46

In diesem Kapitel wurde der vielseitige 5TIA Ligand **46** für die Herstellung neuer Ca-basierender Metall-organische Gerüste und Metallogele, Ca-5TIA-MOF und Ca-5TIA-Gel, mit Calciumacetat verwendet. Der feine Balanceakt zwischen Kristallisation und Gelieren wurde durch den Wassergehalt im System reguliert. Das erste Metallogel in der Literatur, welches auf Kalzium basiert, konnte in fünf verschiedenen organischen Lösungsmitteln hergestellt werden. Dabei musste, bezogen auf die Kamlet-Taft Parameter, der α Parameter klein sein, bei gleichzeitig hohem β und π* Parameter. Dass ein Metallogel nur ohne zusätzliches Wasser erhalten und kein Gel direkt von Ca-5TIA-MOF gebildet werden konnte, deutete darauf hin, dass Ca-5TIA-MOF und Ca-5TIA-Gel Unterschiede in ihren Gerüst-Strukturen aufwiesen. Zudem wurde das Ca-5TIA-Gel anhand seiner thermalen und rheologischen Eigenschaften charakterisiert und sowohl FT-IR, als auch PXRD Spektren aufgenommen. Beide Materialien, Ca-5TIA-MOF und Ca-5TIA-Gel zeigten die Fähigkeit CO_2 Gas aufzunehmen. Verglichen mit dem kristallinen Ca-5TIA-MOF war das Ca-5TIA-Gel zu einer 20% höheren CO_2 Aufnahme in der Lage. Darüber hinaus zeigten sowohl Ca-5TIA-MOF, als auch Ca-5TIA-Gel die Fähigkeit als Katalysator in der

Hydrosilylierungs-Reaktion zwischen Benzaldehyd und Diphenylsilan zu wirken, wobei sich das Ca-5TIA-Gel als der bessere Katalysator erwies.

C Flüssiges Multikomponenten-Organogelator-System I und II

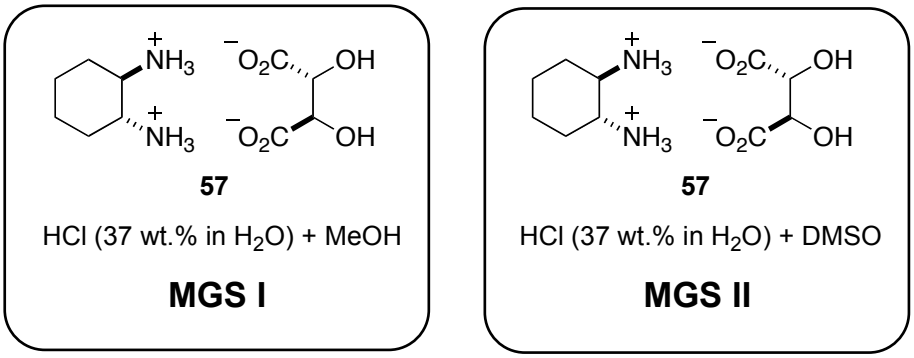

In Kapitel C wurde die Untersuchung zweier Multikomponenten-Organogelator-Lösungen basierend auf (1*R*,2*R*)-1,2-Diaminocyclohexan *L*-Tartrat, gelöst mit Hilfe von wässriger HCl in Methanol (MGS I) oder DMSO (MGS II) gezeigt. Mit den Gelator-Lösungen gelang es Gele in verschiedenen organischen Lösungsmitteln bei Raumtemperatur (MGS II), oder niedrigen Temperaturen (MGS I), nahe dem Gefrierpunkt des Lösungsmittels, herzustellen. Bemerkenswerterweise benötigte man für die Darstellung von auf MGS II basierenden Gelen 2-12 Mal weniger Gelator-Lösung im Vergleich zu Gelen die auf MGS I basieren. Für die Gelator-Lösungen, als auch für die Gele wurde die Kristallisation von (1*R*,2*R*)-1,2-Diaminocyclohexan Dihydrochlorid beobachtet. Das Auftreten der Kristalle resultierte stets in der Zerstörung der Gele, was, abhängig vom Lösungsmittel, zu einer kurzen Lebensdauer der Gele von wenigen Stunden bis einigen Tagen führte. Experimente zeigten, dass (1*R*,2*R*)-1,2-Diaminocyclohexan die strukturgebene Schlüsselrolle spielte, wohingegen das Tartrat nur als Stabilisator des supramolekularen Netzwerks agierte, da es durch andere Carbonsäuren ausgetauscht werden konnte, was allerdings eine Verkürzung der Stabilität der Gele zur Folge hatte. Dabei zeigten MGS II Gele eine größere Toleranz gegenüber den ersetzenden Carbonsäuren. Darüber hinaus wurde gezeigt, dass jede Komponente der Gelator Lösung in einer bestimmten Stöchiometrie eingesetzt werden muss, da ansonsten Gele mit verkürzter Lebensdauer gebildet werden, oder gar keine Gelierung stattfindet: (1*R*,2*R*)-1,2-Diaminocyclohexan *L*-Tartrat : MeOH : HCl : H_2O = 1 : 193 : 2.4 : 8.3. Phasen-selektives Gelieren in zwei nicht vermischten organischen Lösungsmitteln konnte bei Raumtemperatur (MGS II) und bei

niedrigen Temperaturen gezeigt werden, wobei die Gele von MGS I eine verkürzte Lebensdauer hatten. Außerdem wurde versucht, durch die Herstellung von Semi-Interpenetrierenden-Netzwerken die Eigenschaften der Gele weiterzuentwickeln.

D Ag-basierende Metallogele

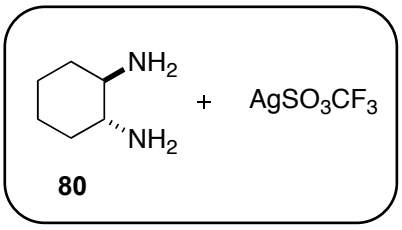

80

In Kapitel D wurde die Herstellung eines auf Silber basierenden Metallogels aus (1*R*, 2*R*)-1,2-Diaminocyclohexan **80** und Silbertrifluormethansulfonat im äquimolaren Verhältnis beschrieben. Das System $AgSO_3CF_3$ + **80** war fähig in einer Konzentration von 0.05-0.20 mmol·L^{-1} eine Reihe aromatischer Lösungsmittel zu gelieren. Aufgrund der geringen Löslichkeit von $AgSO_3CF_3$ in chlorhaltigen, aromatischen Lösungsmitteln war es nicht möglich die Konzentration zu erhöhen und so konnten nur partielle Gele erhalten werden. Es stellte sich heraus, dass als Herstellungsmethode das Mischen der Lösungen von $AgSO_3CF_3$ und **80** gegenüber der Herstellung mit Hilfe des Ultraschallbads bevorzugt werden muss, da die MGC beim Mischen sechs mal geringer und die Dauer bis zur Gelbildung kürzer war. Der Austausch von $AgSO_3CF_3$ mit verschiedenen Silbersalzen wurde durchgeführt, um auf die Bedeutung des Gegenions hinzuweisen. Neben **80** wurde auch DABCO als geeigneter Ligand in Kombination mit $AgSO_3CF_3$ erforscht. Die Ergebnisse wiesen darauf hin, dass die Morphologie des Gelator-Netzwerks durch die Verwendung verschiedener Liganden beeinflusst werden konnte.

E Organogele basierend auf einem neuen LMW Urea-Gelator

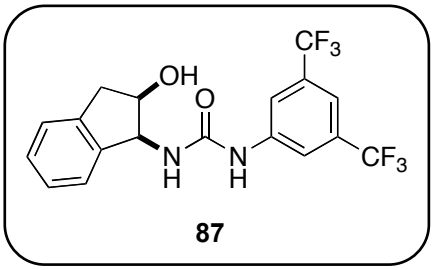

87

Der literaturbekannte Organokatalysator **87** war fähig, supramolekulare Gele in 14 verschiedenen aromatischen und halogenierten Lösungsmitteln, so wie in Nitromethan und Glycerol-Wasser Mischungen zu bilden. Die Gele konnten durch den einfachen Heating-Cooling-Prozess hergestellt werden und waren zudem thermoreversibel. Durch die “inverse flow method“ wurde die thermale Stabilität der Gele untersucht. Experimente deuteten auf die Notwendigkeit aller funktionellen Gruppen hin, damit Verbindung **87** als Gelator wirken kann. Außerdem konnten Gele nur mit der enantiomerenreinen Verbindung **87** erhalten werden. Durch rheologische Untersuchungen wurde das Material als Gel bestätigt und desweiteren thixotropes Verhalten beobachtet. SEM-Bilder zeigten die vielfältige Organisation der Gelatormoleküle in 3D Strukturen in den verschiedenen Lösungsmitteln. Es wurde gezeigt, dass Gelator **87** fähig war, selektiv die organische von einer wässrigen Phase zu gelieren, wenn das Lösungsmittel-Wassergemisch bis zur Auflösung des Gelators bei MGC erhitzt wurde. Bemerkenswert war die Resonanz des Glycerol-Gels von **87** auf Silberionen. Es konnte gezeigt werden, dass dieses Gel ein nützliches und praktisches Mittel zur Aufspürung von Silberionen in Lösungen ist, da es sich leicht von den Testlösungen separieren ließ.

G Appendices

1. NMR spectra

^{1}H NMR (400 MHz):	upper image
^{13}C NMR (100 MHz):	lower image
Solvent compound **91**, **93**:	DMSO-d_6
Solvent compound **92**:	CD_3COCD_3

1-(3,5-Bis(trifluoromethyl)phenyl)-3-((1*R*,2*R*)-2-hydroxy-2,3-dihydro-1H-inden-1-yl)urea (91)

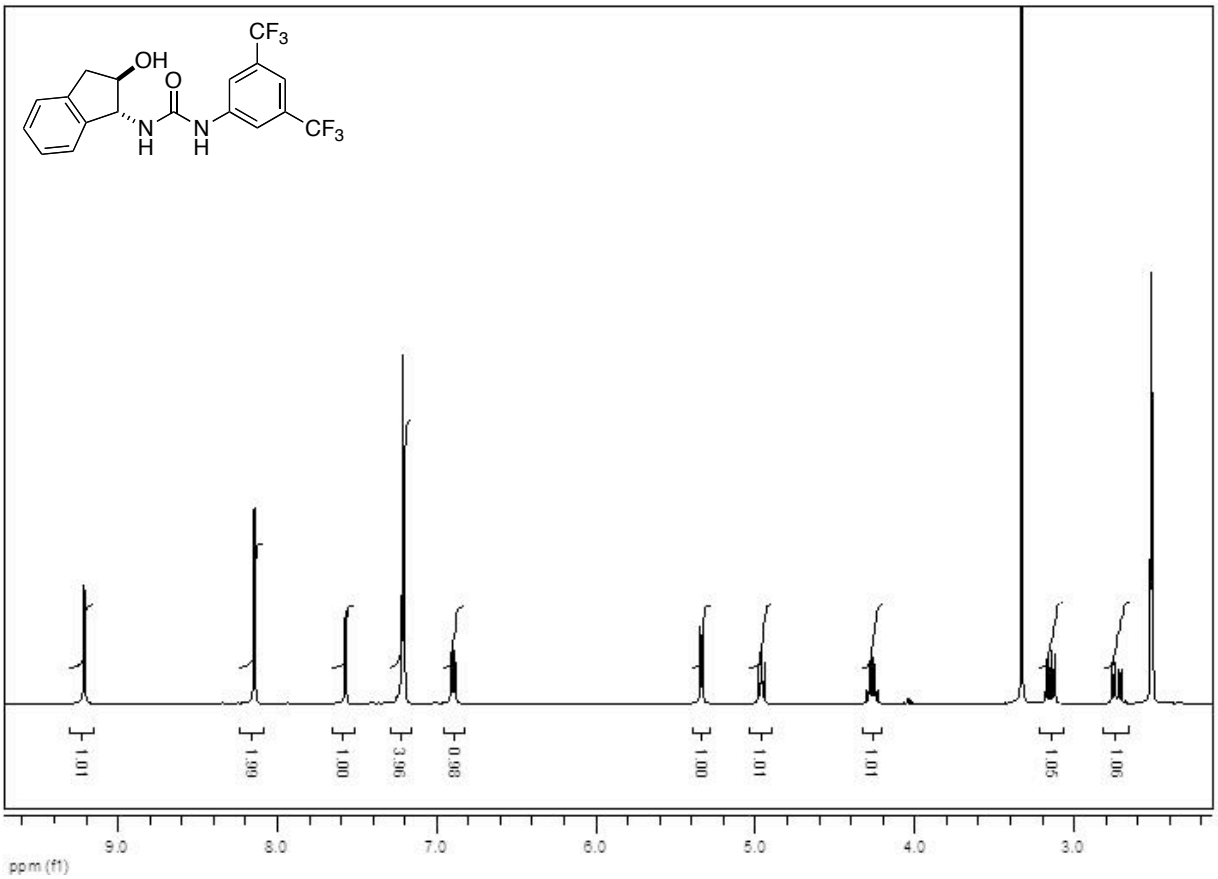

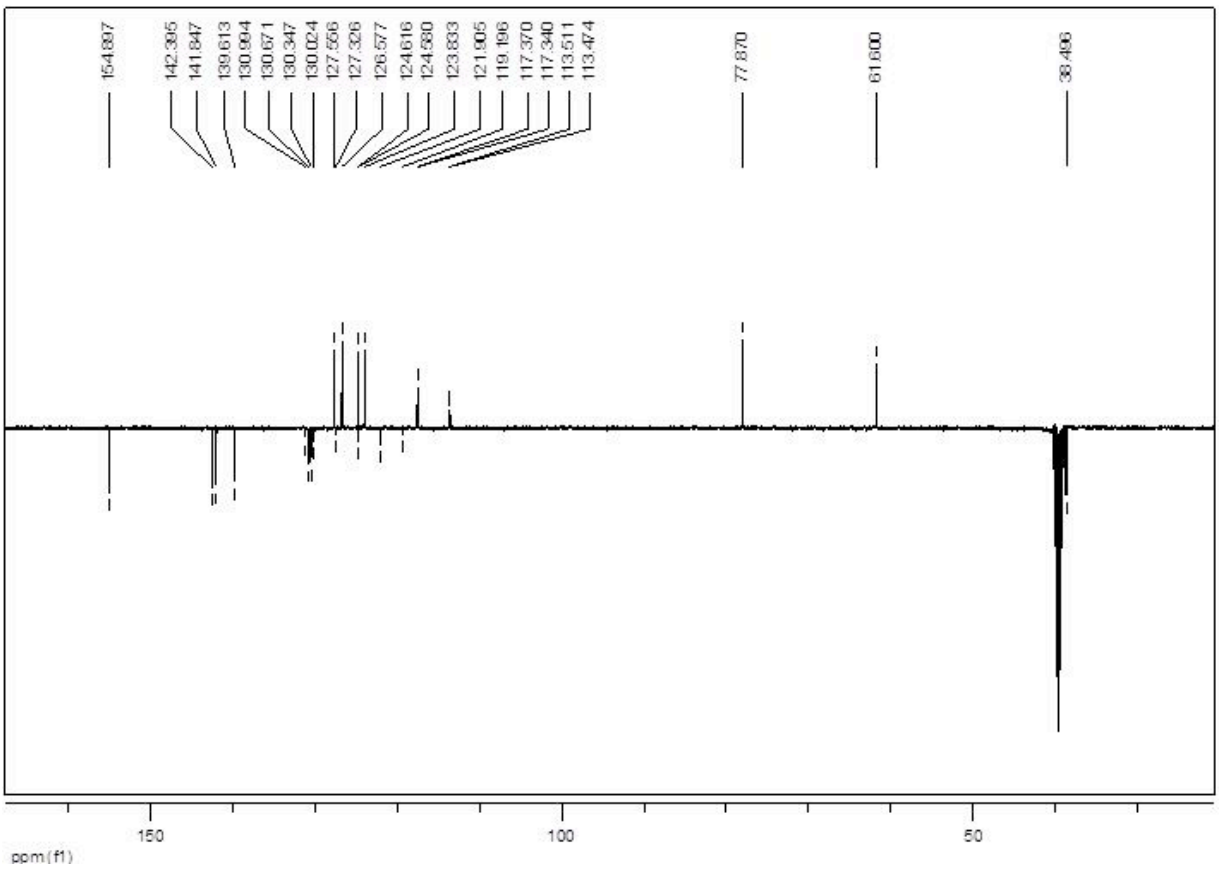

(*R*)-1-(3,5-Bis(trifluoromethyl)phenyl)-3-(2,3-dihydro-1H-inden-1-yl)urea (92)

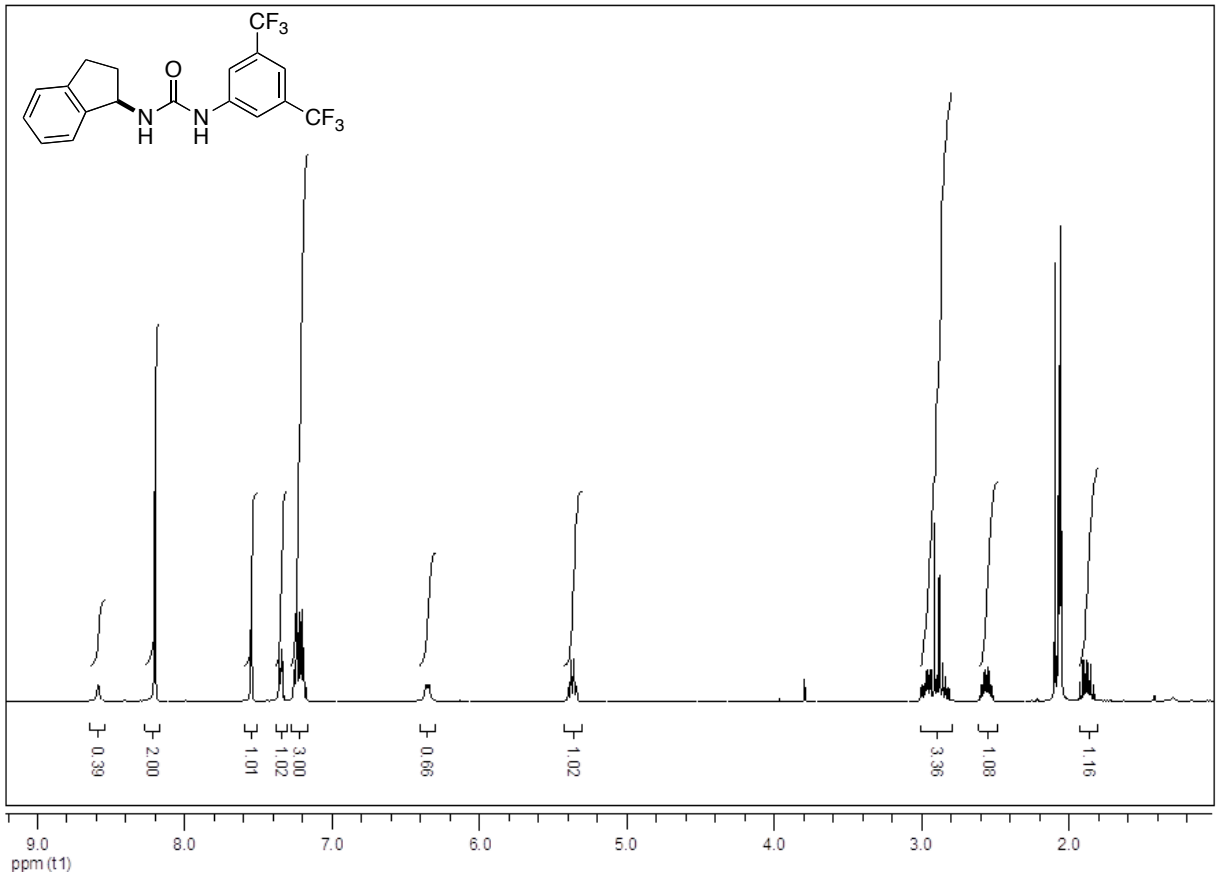

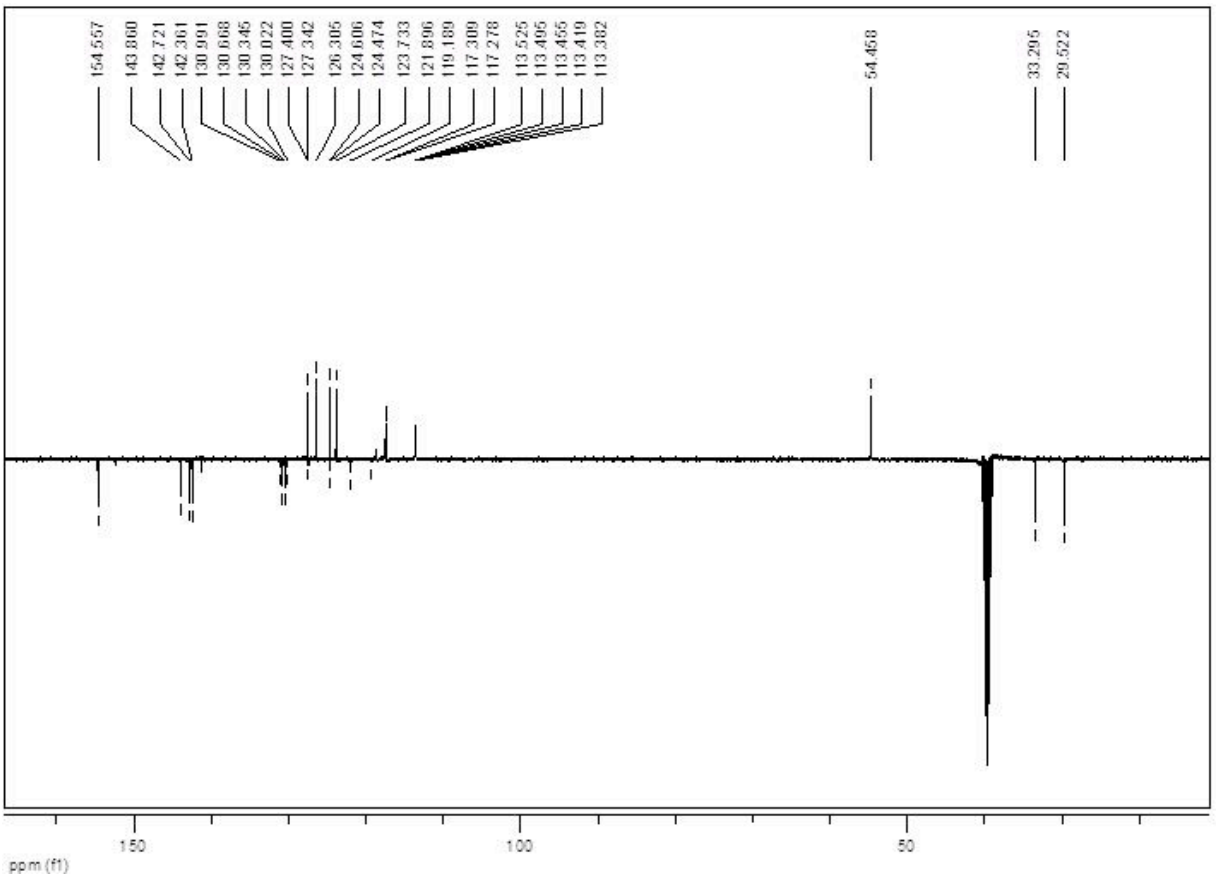

1-((1*S*,2*R*)-2-Hydroxy-2,3-dihydro-1H-inden-1-yl)-3-phenylurea (93)

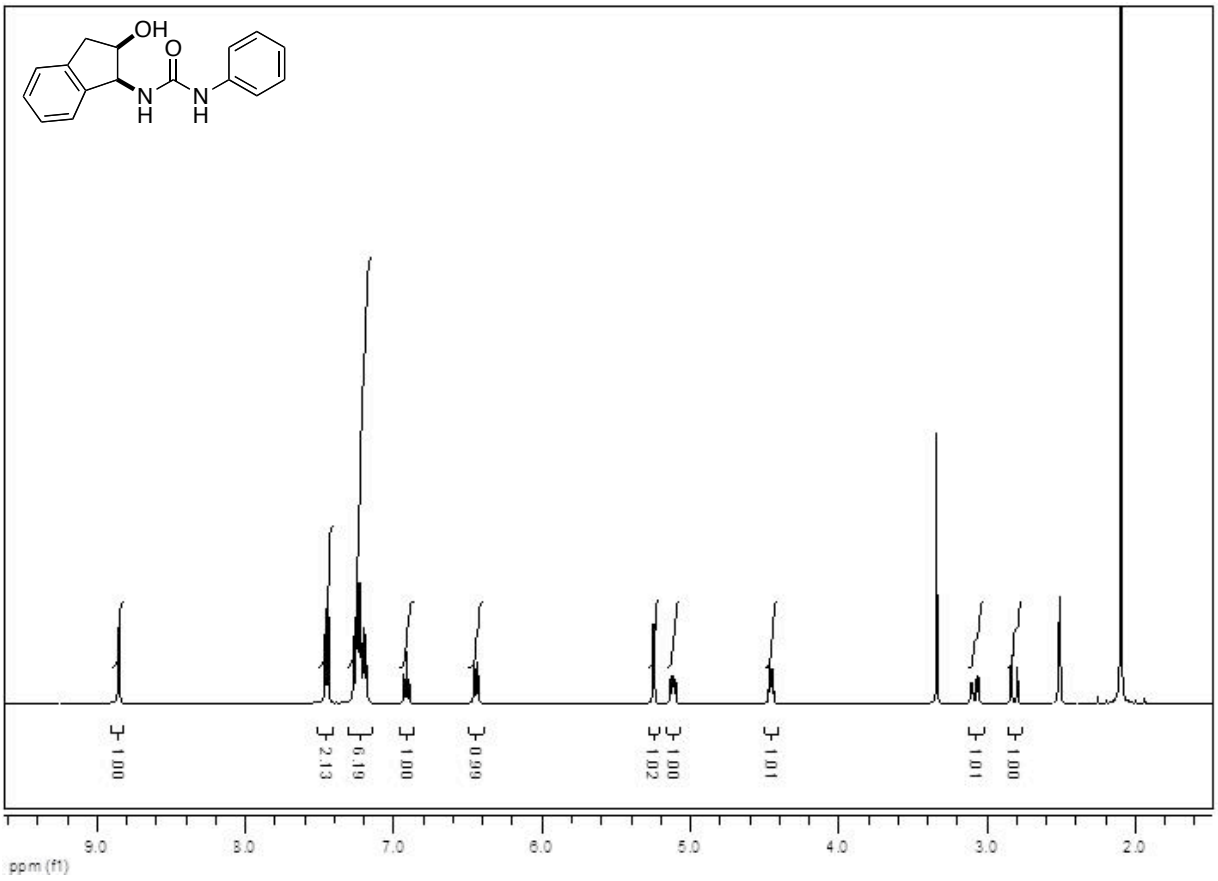

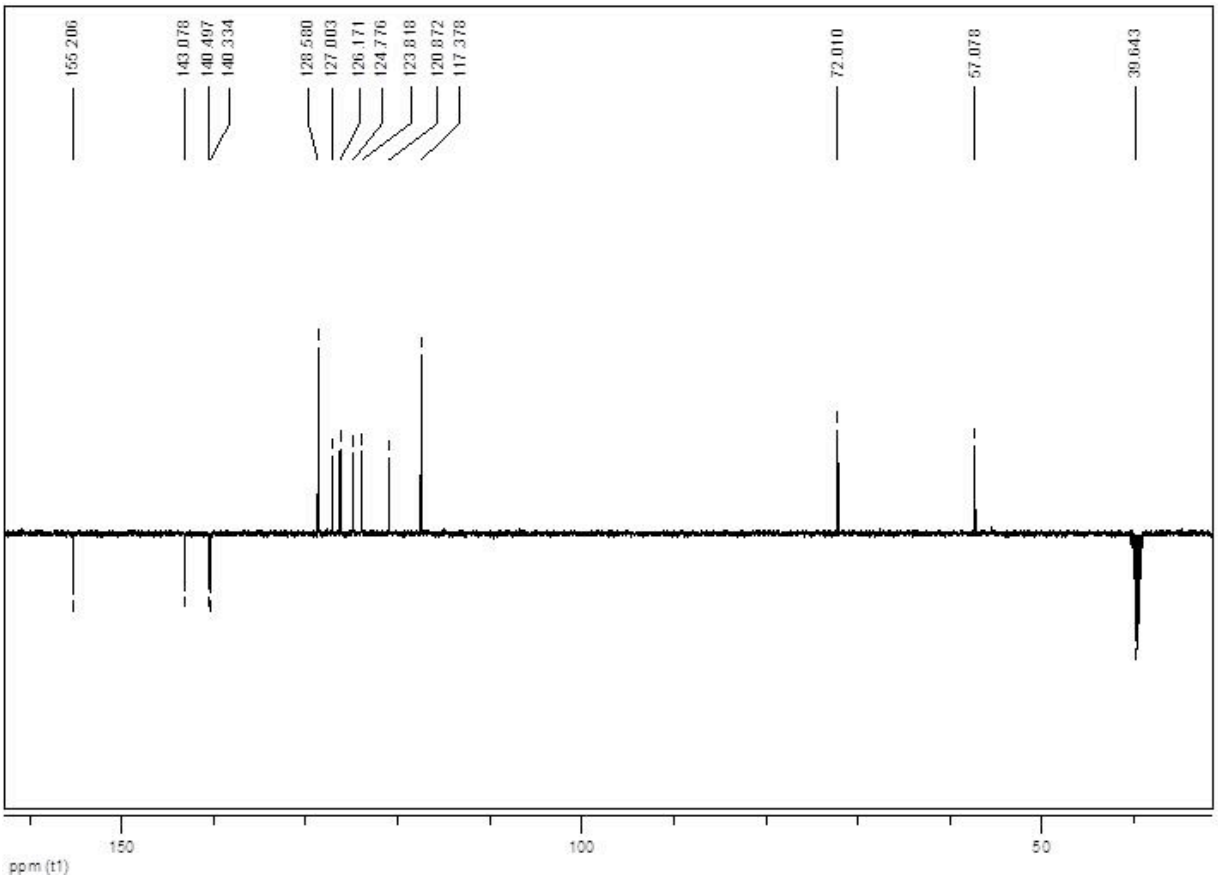

Temperature-dependent ^{1}H NMR (400 MHz) of 8 $mg \cdot mL^{-1}$ compound **87** in $CDCl_3$

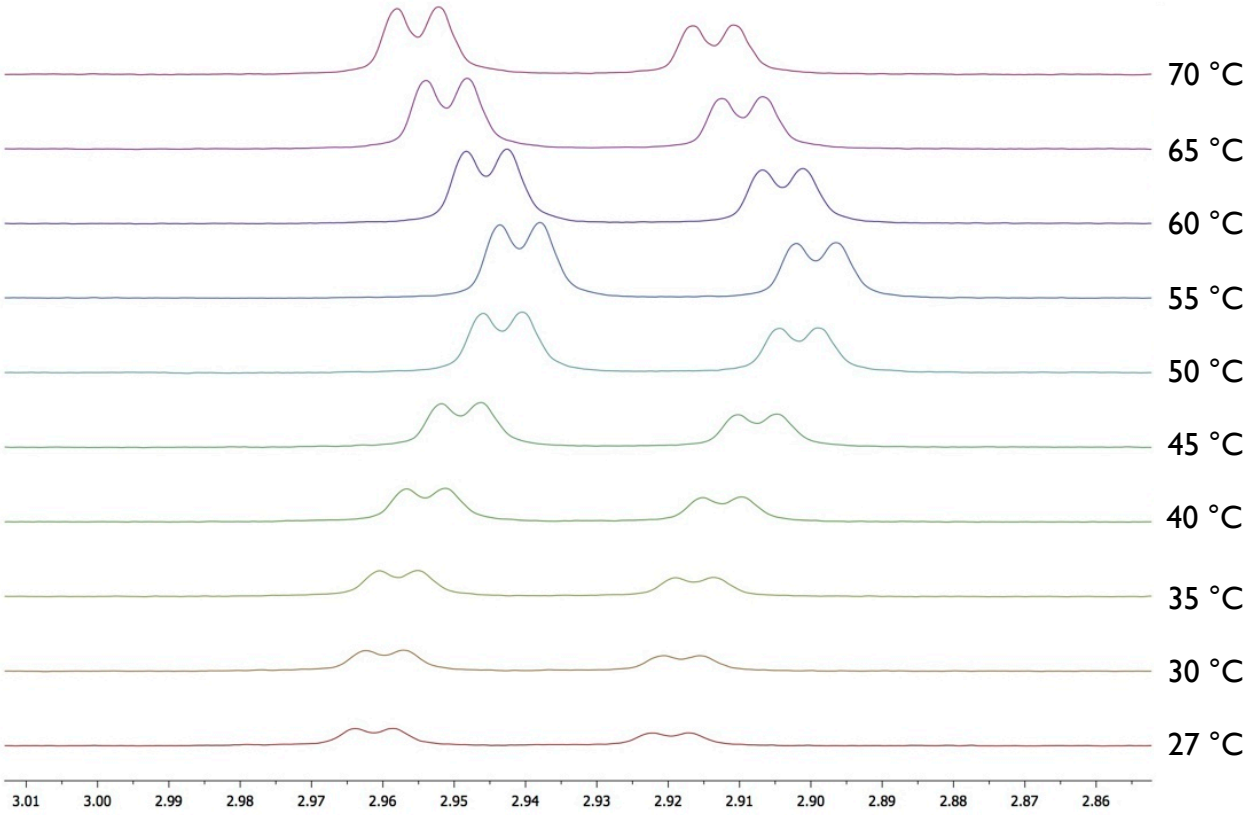

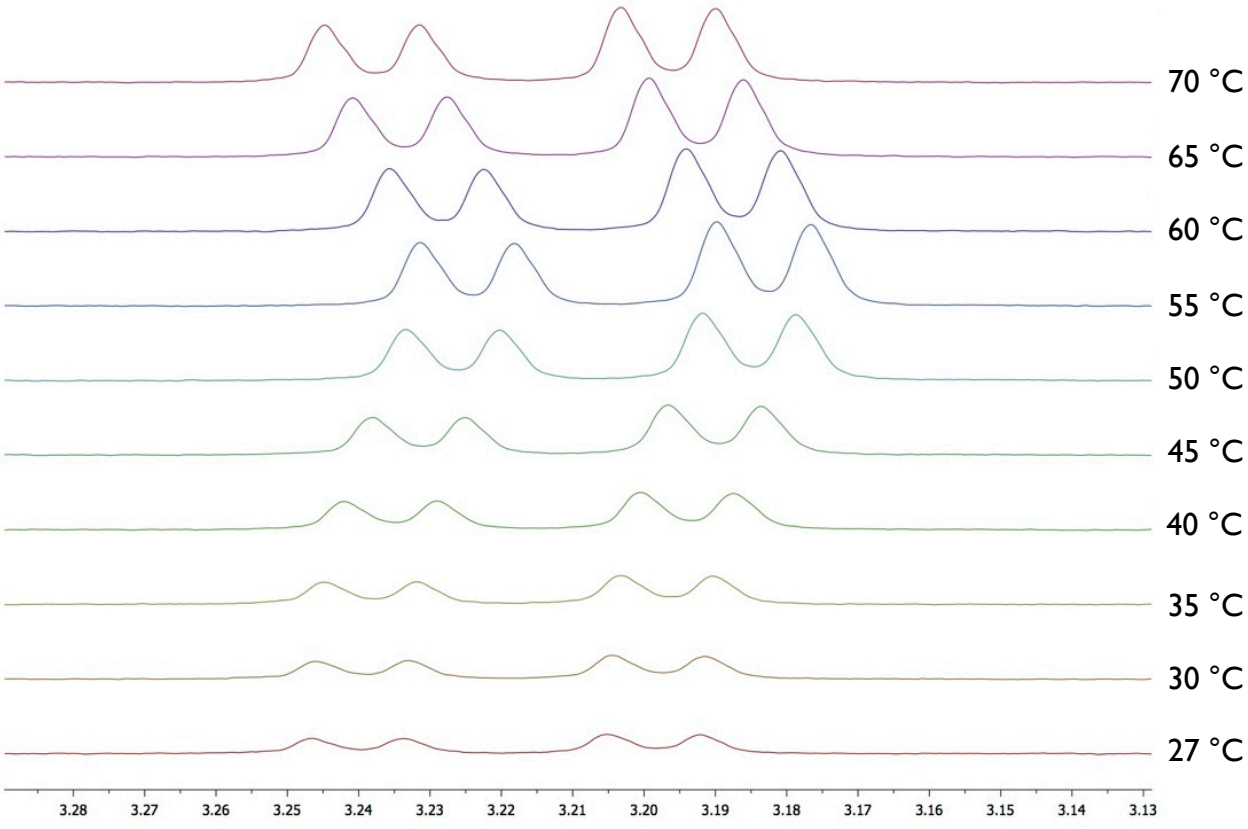

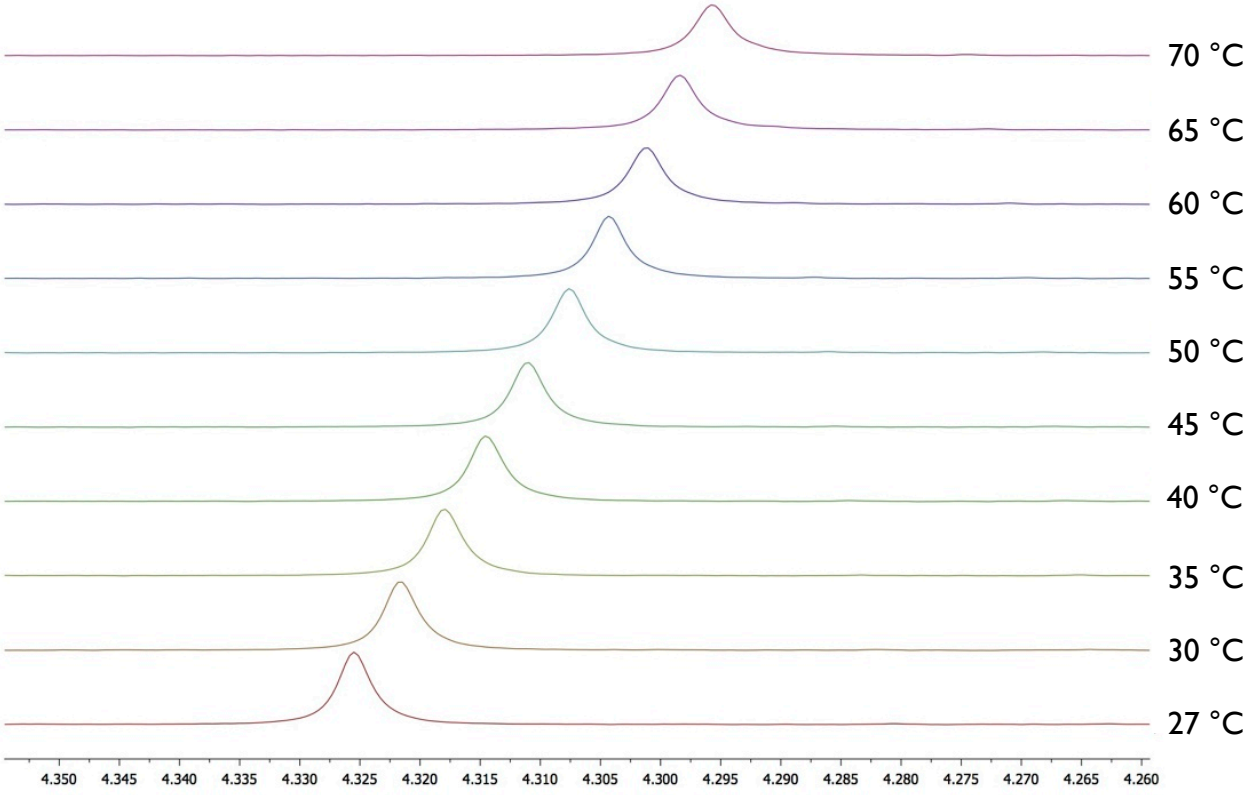
70 °C
65 °C
60 °C
55 °C
50 °C
45 °C
40 °C
35 °C
30 °C
27 °C
4.350 4.345 4.340 4.335 4.330 4.325 4.320 4.315 4.310 4.305 4.300 4.295 4.290 4.285 4.280 4.275 4.270 4.265 4.260

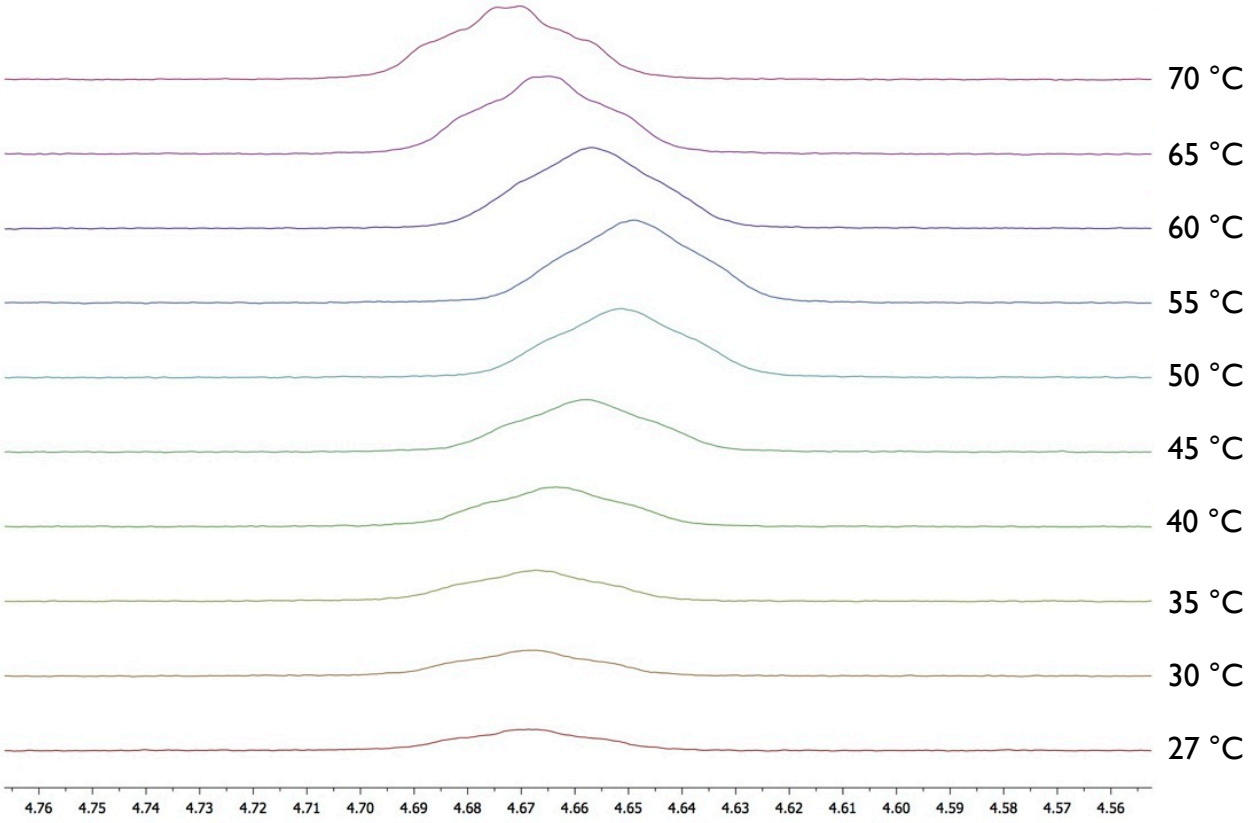
70 °C
65 °C
60 °C
55 °C
50 °C
45 °C
40 °C
35 °C
30 °C
27 °C
4.76 4.75 4.74 4.73 4.72 4.71 4.70 4.69 4.68 4.67 4.66 4.65 4.64 4.63 4.62 4.61 4.60 4.59 4.58 4.57 4.56

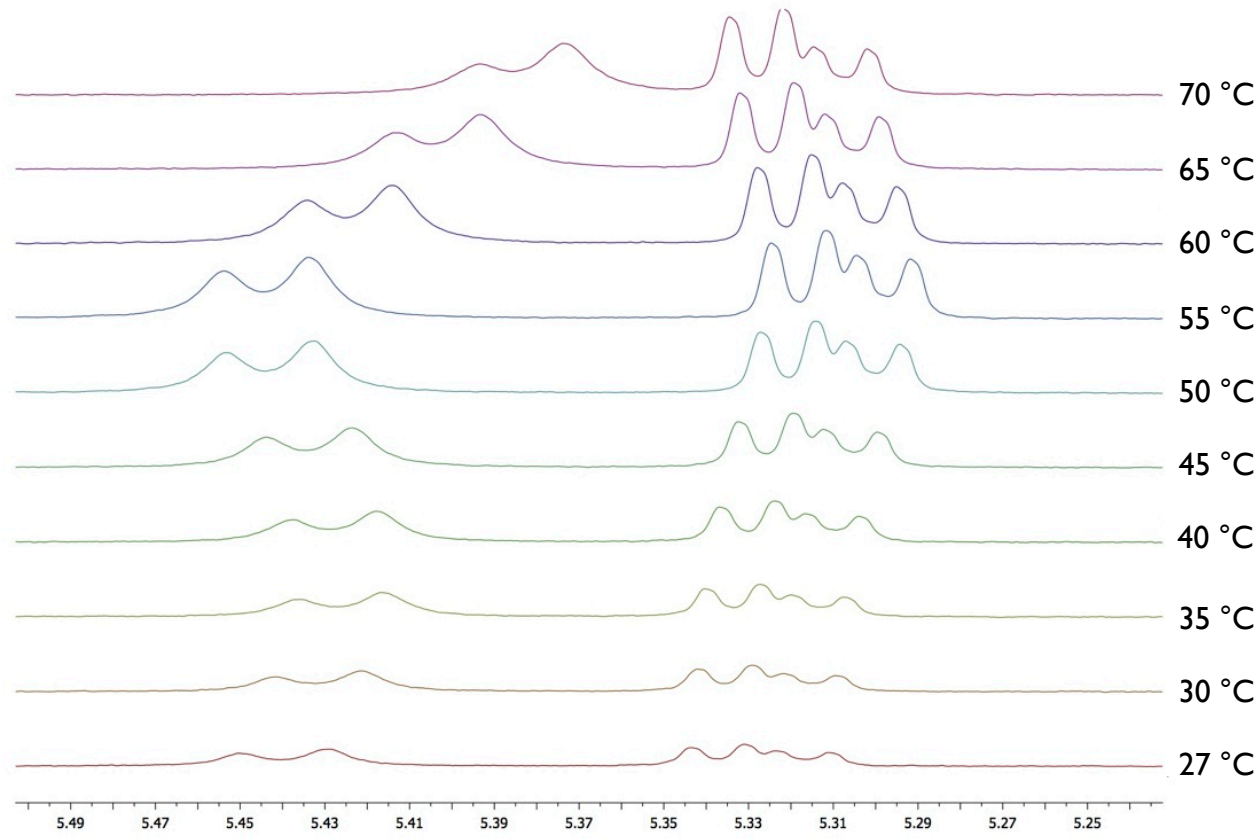
70 °C
65 °C
60 °C
55 °C
50 °C
45 °C
40 °C
35 °C
30 °C
27 °C
5.49
5.47
5.45
5.43
5.41
5.39
5.37
5.35
5.33
5.31
5.29
5.27
5.25

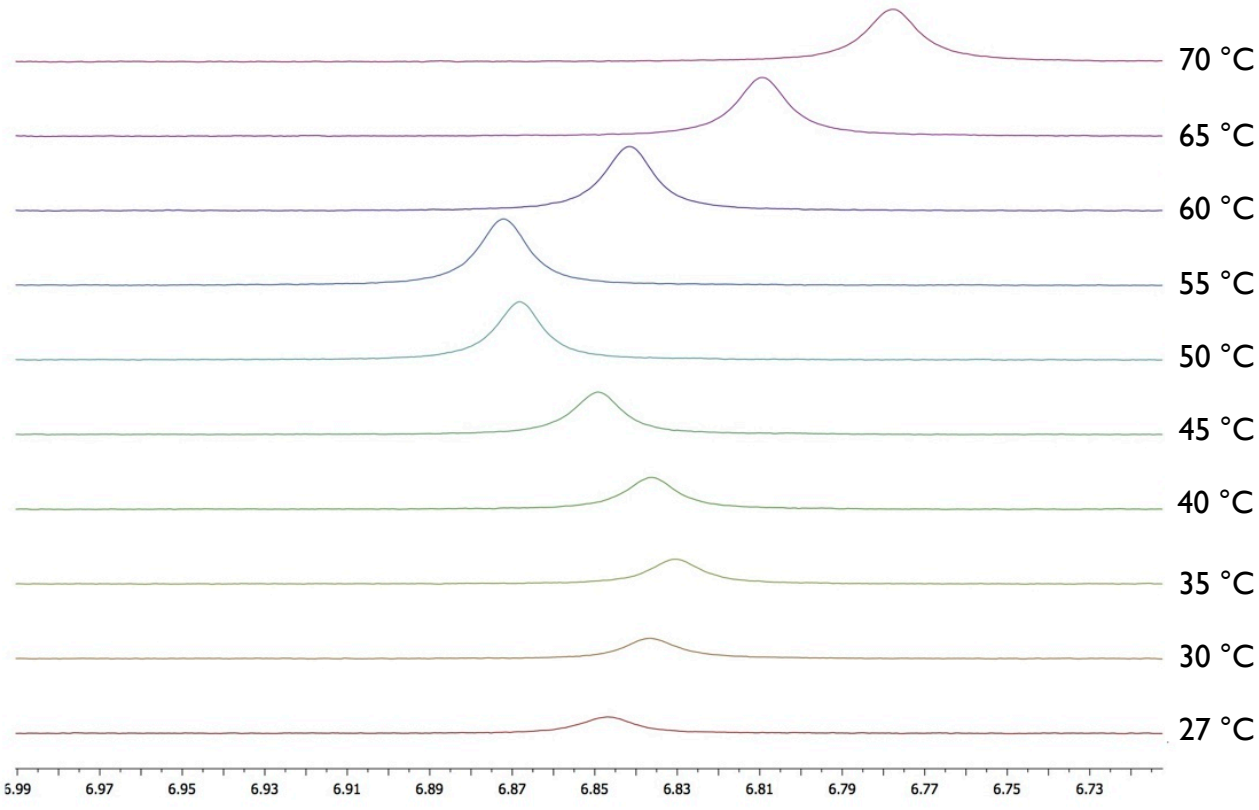
70 °C
65 °C
60 °C
55 °C
50 °C
45 °C
40 °C
35 °C
30 °C
27 °C
5.99
6.97
6.95
6.93
6.91
6.89
6.87
6.85
6.83
6.81
6.79
6.77
6.75
6.73

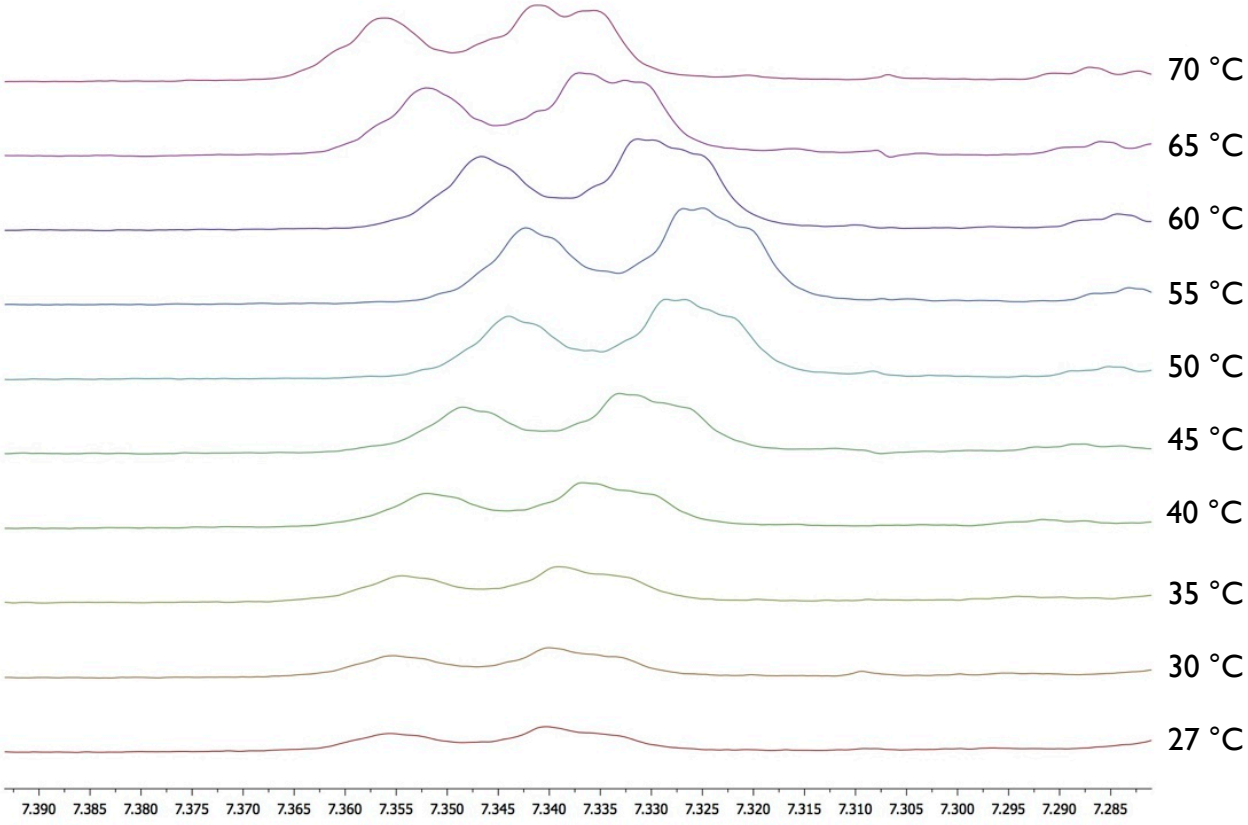
70 °C
65 °C
60 °C
55 °C
50 °C
45 °C
40 °C
35 °C
30 °C
27 °C
7.390 7.385 7.380 7.375 7.370 7.365 7.360 7.355 7.350 7.345 7.340 7.335 7.330 7.325 7.320 7.315 7.310 7.305 7.300 7.295 7.290 7.285

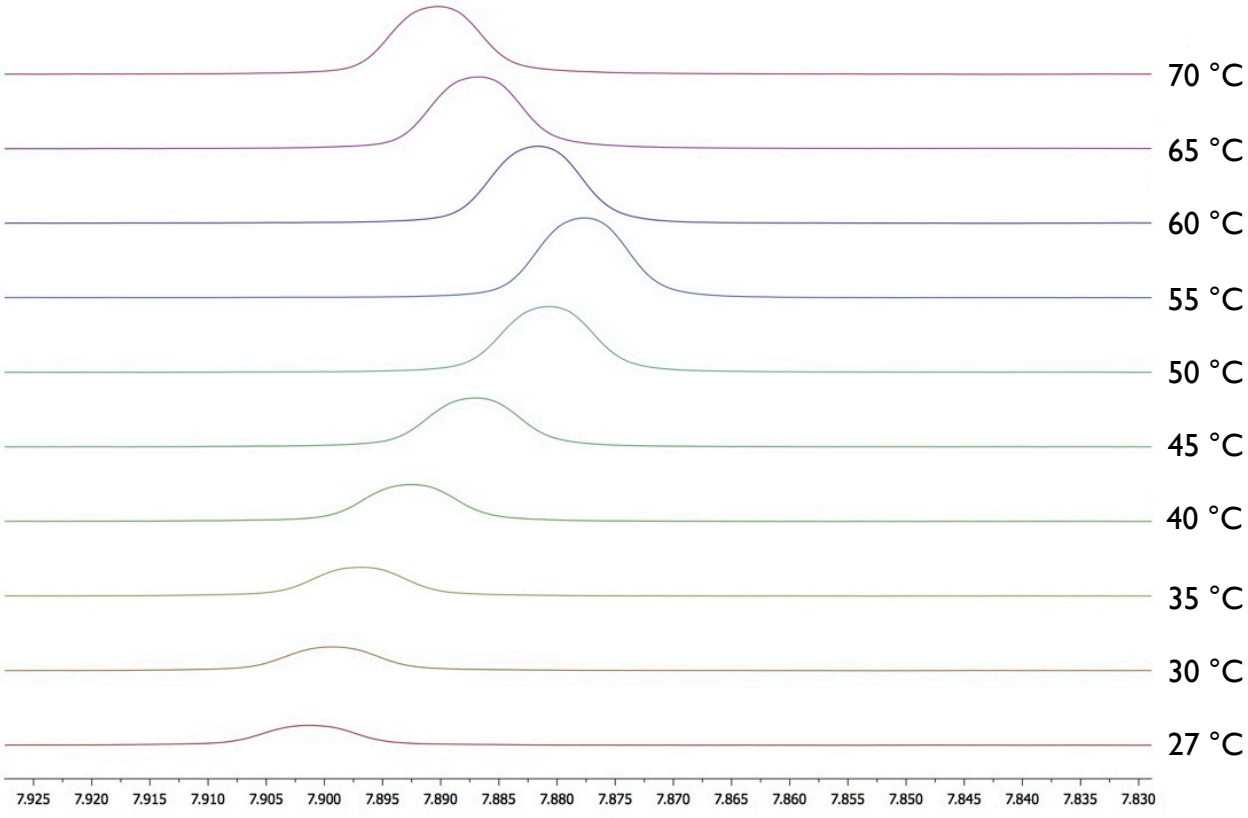
70 °C
65 °C
60 °C
55 °C
50 °C
45 °C
40 °C
35 °C
30 °C
27 °C
7.925 7.920 7.915 7.910 7.905 7.900 7.895 7.890 7.885 7.880 7.875 7.870 7.865 7.860 7.855 7.850 7.845 7.840 7.835 7.830

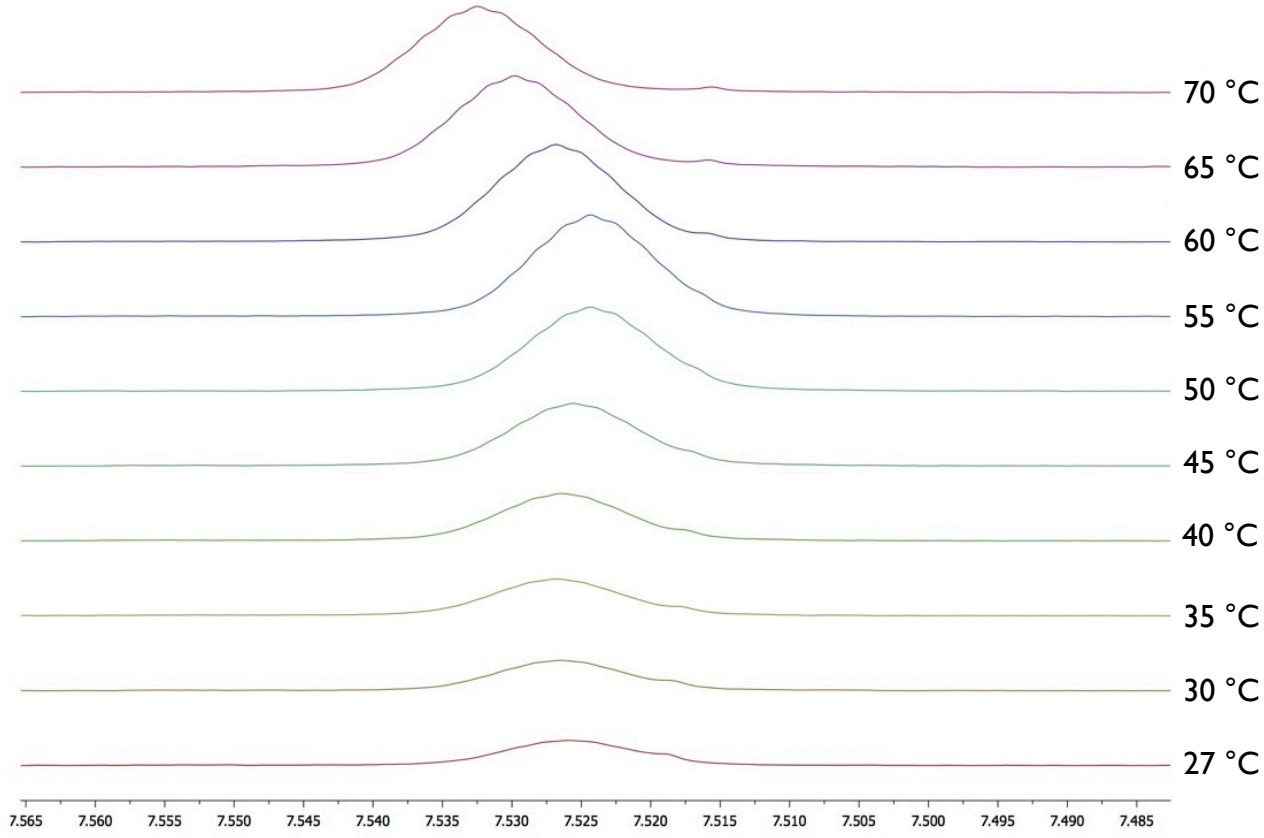
70 °C
65 °C
60 °C
55 °C
50 °C
45 °C
40 °C
35 °C
30 °C
27 °C
7.565
7.560
7.555
7.550
7.545
7.540
7.535
7.530
7.525
7.520
7.515
7.510
7.505
7.500
7.495
7.490
7.485

2. Solvent parameters

Table 14: Selection of solvent properties and parameters.[a]

Entry	Solvent	ε_r[b]	α[c]	β[d]	π*[e]	bp[f] [°C]
1	Water	80.0	1.17	0.47	1.09	100
2	DMSO	46.7	0.00	0.76	1.00	189
3	Glycerol	43.0	1.21	0.51	0.62	290
4	DMF	38.0	0.00	0.69	0.88	153
5	DMA	37.8	0.00	0.76	0.88	164-166
6	Ethylene glycol	37.0	0.90	0.52	0.92	197
7	NM	37.3	0.22	0.06	0.85	100-103
8	ACN	36.6	0.19	0.40	0.75	82
9	NMP	32.3	0.00	0.77	0.92	202-204
10	Nitrobenzene	26.3	0.00	0.30	1.01	211
11	BN	25.9	0.00	0.37	0.90	188-191
12	2-Nitropropane	25.5	NF	NF	NF	120
13	Ethanol	24.5	0.86	0.75	0.54	78
14	1-Nitropropane	23.2	0.00	0.25	0.75	131
15	ACT	21.0	0.08	0.43	0.71	56-57
16	Nitroethane	19.7	0.00	0.25	0.80	112-116
17	Cyclohexane	18.5	0.00	0.00	0.00	81
18	CHN	16.1	0.00	0.53	0.76	156
19	Pyridine	12.4	0.00	0.64	0.87	115
20	[BMIM][PF_6]	11.4	0.63	0.21	1.03	> 340 (dec.)
21	MBN	10.4	NF	NF	NF	93-95
22	1,2-Dichloroethane	10.4	0.00	0.10	0.81	84
23	DCM	9.1	0.13	0.10	0.82	40
24	1,2-Dimethoxyethane	7.3	0.00	0.41	0.53	85
25	2-Methoxyethyl ether	7.2	0.00	0.40	0.64	162
26	ETAC	6.1	0.00	0.45	0.55	77
27	THF	5.7	0.00	0.55	0.58	66

Entry	Solvent	ε_r[b]	α[c]	β[d]	π^*[e]	bp[f] [°C]
28	Chloroform	4.8	0.20	0.10	0.58	61
29	DEE	4.3	0.00	0.47	0.27	35
30	Dibutyl ether	3.1	0.00	0.46	0.27	142
31	1,2-Dichlorobenzene	2.8	0.00	0.03	0.80	181
32	Methyl *tert*-butyl ether	2.6	NF	NF	NF	55
33	Carbon disulfide	2.6	0.00	0.07	0.61	46
34	Tetrachloroethylene	2.5	0.00	0.05	0.28	121
35	Toluene	2.4	0.00	0.11	0.54	111
36	Benzene	2.3	0.00	0.10	0.59	80
37	DOX	2.2	0.00	0.37	0.55	101
38	Carbon tetrachloride	2.2	0.00	0.10	0.28	77
39	*n*-Octane	2.0	0.00	0.00	0.01	126
40	*n*-Hexane	1.9	0.00	0.00	-0.04	69

[a]Abbreviations: NF = not found, dec. = decomposes. [b]Relative permittivity (dielectric constant)[1] measured in the range of 20-25°C. [c]Kamlet-Taft parameter[2] defining the hydrogen bond donor ability. [d]Kamlet-Taft parameter defining the hydrogen bond acceptor ability. [e]Kamlet-Taft parameter defining the polarizability of the solvent. [f]Boiling point.

3. Curriculum vitae

Personal data:

Name:	Eva-Maria Schön
Date of birth:	08.09.1985
Place of birth:	Tirschenreuth, Germany
Nationality:	German
Marital status:	Single

Education:

10.2010-11.2013	**PhD thesis** under the supervision of Prof. Dr. David Díaz Díaz at University of Regensburg *Preparation, Characterization an possible Application of new low-molecular-weight Organogels*
05-08.2013	**Research project** under the supervision of Prof. Dr. Jeremiah A. Johnson at Massachusetts Institute of Technology, Cambridge, USA *Detection of loops in polymers at different M/T ratio*
09.2010	**Master of Science** graduation in chemistry
01.2010-09.2010	**Master thesis** under the supervision of Prof. Dr. David Díaz Díaz at the University of Regensburg *Synthesis, characterization and properties tuning of gels made by low-molecular-weight compounds*
10.2008-09.2010	**Studies in chemistry** at University of Regensburg
09.2008	**Bachelor of Science** graduation in chemistry
02-03.2008	**Bachelor thesis** under the supervision of Prof. Dr. Oliver Reiser at the University of Regensburg *Einsatz von Azabis(oxazolinen) in der Katalyse*
10.2005-09.2008	**Studies in chemistry** at University of Regensburg
09.2000-06.2005	**Abitur** (A-levels) Stiftlandgymnasium Tirschenreuth

Contribution to scientific meetings:

10.07.2013.	Weihnachtskolloquium des Instituts für Organische Chemie der Universität Regensburg, Talk: *Gel-based materials for biomedicine and catalysis*
06-09.01.2013	Frühjahrssymposium der Jungchemiker, Berlin. Poster presentation: *Multicomponent organogelator liquid system based organogels: A tough competition between gelation and crystallization*
07-12.07.2013	ESOC 2013, Marseille, Frankreich. Poster presentation: *MGS I & II: A tough competition between gelation & crystallization.*

Languages:

German	Native
English	Fluently

References:

Prof. Dr. David Díaz Díaz
Institut für Organische Chemie
Universität Regensburg, Universitätsstraße 31
93053 Regensburg, Germany
E-mail: david.diaz@chemie.uni-regensburg.de

Prof. Dr. Jeremiah A. Johnson
Department of Chemistry
Massachusetts Institute of Technology
77 Massachusetts Avenue
Cambridge, MA 02139-4307, USA
E-mail: jaj2109@mit.edu

4. List of publications

1. Zhou, H.; Schön, E.-M.; Wang, M.; Glassman, M.; Liu, J. Díaz, D. D.; Olsen, B. D.; Johnson, J. A. **2013**, submitted:
   Isotopic Labeling Disassembly Spectrometry (ILDaS): Crossover Experiments in Polymer Networks Reveal Cyclic Defects

2. Kühbeck, D.; Schön, E.-M.; Bachl, J.; Gotor-Fernández, V.; Díaz, D. D. *Helv. Chim. Acta* **2013**, accepted:
   Gelatin protein-mediated direct aldol reaction

3. Kühbeck, D.; Dhar, B. B.; Schön, E.-M.; Cativiela, C.; Gotor-Fernández, V.; Díaz, D. D. Beilstein J. Org. Chem. **2013**, 9, 1111-1118:
   C-C Bond Formation Catalyzed by Natural Gelatin and Collagen Proteins

4. Saha, S.; Schön, E.-M.; Cativiela, C.; Díaz, D. D.; Banerjee, R. *Chem. Eur. J.* **2013** *19*, 9562-9568:
   Proton-Conducting Supramolecular Metallogels from Lowest Molecular Weight Assembler Ligand: A Quote for Simplicity

5. Bachl, J.; Huber, T.; Kühbeck, D.; Schön, E.-M.; Brunner, G.; Kraus, B.; Heilmann, J.; Codelli, J. A.; Bertozzi, C. R.; Cativiela, C.; Díaz, D. D. *Nanosci. and Nanotech. Asia* **2012**, 2, 200-209:
   Hybrid bioactive hydrogels containing single-walled carbon nanotubes covalently integrated via strain-promoted azide-alkyne cycloaddition

6. Mallick, A.; Schön, E.-M.; Panda, T.; Sreenivas, K.; Díaz, D. D.; Banerjee, R. *J. Mater. Chem.* **2012**, *22*, 14951-14963:
   Fine-tuning the balance between crystallization and gelation and enhancement of CO_2 uptake on functionalized calcium based MOFs and metallogels

7. Kapoor, I.; Schön, E.-M.; Bachl, J.; Kühbeck, D.; Cativiela, C.; Saha, S.; Banerjee, R.; Roelens, S.; Marrero-Tellado, J. J.; Díaz, D. D. *Soft Matter* **2012**, *8*, 3446-3456:
Competition between gelation and crystallisation of a peculiar multicomponent liquid system based on ammonium salts

8. Díaz, D. D.; Morin, E.; Schön, E.-M.; Budin, G.; Wagner, A.; Remy, J.-S. *J. Mater. Chem.* **2011**, *21*, 641-644:
Tailoring drug release profile of low molecular weight hydrogels by supramolecular co-assembly and controlled thiol-ene orthogonal coupling

9. Schön, E.-M.; Díaz, D. D. *Molbank* **2010**, *3*, M689:
N-Cyclohexyl-11-(octylthio)undecanamide

5. References

[1] http://web.archive.org/web/20070529185028/http://www.asiinstr.com/technical/Dielectric%20Constants.htm (retrieved on 8th of december, 2013)

[2] http://www.stenutz.eu/chem/solv26.php (retrieved on 8th of december, 2013).

H Acknowledgements

First of all I would like to express my sincere thanks to my supervisor Prof. Dr. David Díaz Díaz for his warm welcome to his newly founded group. He not only gave me the opportunity to carry out my thesis in his laboratory, he also guided me through my research, encouraged me and spent countless hours supporting me.

I would like to say special thanks to Prof. Dr. Jeremiah Johnson, Dr. Huaxing Zhou and all members of the Johnson group at the MIT for their warm welcome, support, discussions and fun during my stay. The months I spent in Boston were definitely some of the best in my whole life, thank you!

Ich möchte mich auch bei Prof. Oliver Reiser, Prof. Dr. Werner Kunz, Prof. Dr. Göpferich und Prof. Dr. Burkhard König für die Erlaubnis bedanken, die Instrumente ihrer Arbeitskreise zu benutzen. Weiterhin möchte ich mich auch bei den Mitgliedern der Gruppen für die freundliche Zusammenarbeit, Hilfe und Rat bedanken.

Bei Peter Kreitmeier, Georg Adolin, Klaus Döring, Helena Konkel und Roxane Harteis möchte ich mich für die kleinen und großen Hilfen, die den Arbeitsalltag erleichtert haben bzw. erst möglich gemacht haben, bedanken. Insbesondere gilt mein Dank Frau Anette Schramm und Frau Georgine Stühler für die Aufnahme der NMR-Spektren.

Dasselbe gilt natürlich auch für die Sekretärinnen Young Rotermund, Hedwig Ohli und besonders Antje Weigert und Nicole Guber.

Mein besonderer Dank gilt Dr. Rainer Müller, der uns sowohl seine Geräte, als auch Laborräume zur Verfügung gestellt hat.

Danke an meine Laborkollegen Dennis und Jürgen für die freundliche Arbeitsatmosphäre und die hilfreichen Diskussionen in den letzten Jahren. Danke auch an Stefan und Thimo, die uns ein kurzes Stück des Wegs begleitet haben.

Ich möchte mich auch bei unseren Gästen am Arbeitskreis Iti, Munmun, Justin, Matthew,

Marek, Paul und Stefan für die freundliche Arbeitsatmosphäre und den Spaß, den wir hatten, bedanken.

Bei Andi E., Andi N., Auriane, Julien, Michi, Oli, Susanne, Tobi und Vroni möchte ich danke sagen für die jahrelange, gemeinsame, lustige und informative Mittagsrunde in der Cafete, auch wenn ich ihr die letzten Monate nicht mehr treu war.

Katrin Ledermüller, Michael Klossek, Susanne Dengler und Markus Hof bin ich zu großem Dank für das Korrekturlesen meiner Arbeit verpflichtet.

Ganz besonders möchte ich mich noch bei Katrin bedanken. Danke fürs Diskutieren, Zuhören und Verstehen! Für Michi und Susanne möchte ich auch noch ein extra Dankeschön aussprechen, für alle Gespräche und Diskussionen.

Meinen Freunden außerhalb der Universität, Sina und der “kloinen“ Verena, danke ich für ihre jahrelange Freundschaft. Auch wenn ihr räumlich beide weit entfernt seid, bin ich sehr dankbar, dass es euch gibt.

Lieber Markus, ich bin so dankbar, dass du in meinem Leben bist und immer an mich glaubst. Danke für deine Liebe, Hoffnung und Zuversicht, die du mir in den letzten Jahren gegeben hast.

Meiner Familie, Mama, Claudia und Sebastian, möchte ich zuletzt ein riesiges und besonderes Dankeschön aussprechen. Ihr Verständnis und der Rückhalt, den sie mir in den letzten 28 Jahren gegeben haben, waren wichtige Faktoren, die auch zum Gelingen dieser Arbeit beigetragen haben.